doi : 10.17596/0003614

# MR05-05

# Cruise Report

Ver.1.0

March, 2006

Edited by

Dr. Takeshi Kawano

Dr. Akihiko Murata

Dr. Ikuo Kaneko

Dr. Shuichi Watanabe

# 1. Cruise Narrative



# 2. Underway Measurements



# 3. Hydrography



# 4. Floats, Drifters and Moorings

# 1. Cruise Narrative

## 1.1 Highlight

| | |
|---|---|
| Cruise Code : | MR05-05 Legs 1, 2 and 3 |
| GHPO Section designation: | P03 |
| Chief Scientist : | Leg.1: Takeshi Kawano<br>Leg.2: Akihiko Murata<br>Ikuo Kaneko<br>Leg.3: Shuichi Watanabe |
| | Ocean General Circulation Observational Research Program<br>Institute of Observational Research for Global Change<br>Japan Agency for Marine-Earth Science and Technology<br>2-15, Natsushima, Yokosuka, Japan 237-0061 |
| Ship : | R/V MIRAI |
| Ports of Call : | San Diego – Honolulu – Okinawa - Sekinehama |
| Cruise Date : | October 31, 2005 – January 30, 2006<br>Leg1: October 21, 2005 – November 24, 2005<br>Leg2: November 27, 2005 – January 17, 2006<br>Leg3: January 20, 2006 – January 30, 2006 |

## 1.2 Cruise Summary

**Cruise Track**

Cruise Track and station locations are shown in Figure.1.1.

**Number of Stations**

A total of 237 stations (Leg.1:78, Leg2:129, Leg3:30) were occupied using a Sea Bird Electronics 36 bottle carousel equipped with 12 liter Niskin X water sample bottles, a SBE911plus equipped with SBE35 deep ocean standards thermometer, SBE43 oxygen sensor, AANDERAA “optode” oxgen sensor and Benthos Inc. Altimeter and RDI Monitor ADCP.

**Sampling and measurements**

1) Measurements of temperature, salinity, oxygen,current profile, fluorescence using CTD/$O_2$ with LADCP.
2) Water sampling and analysis of salinity, oxygen, nutrients, CFC11,12, 113, total alkalinity, DIC, and pH. The sampling depths in db were 10, 50, 100, 150, 200, 250, 300, 400, 500, 600, 700, 800, 900, 1000, 1200, 1400, 1600, 1800, 2000, 2200, 2400, 2600, 2800, 3000, 3250, 3500, 3750, 4000, 4250, 4500, 4750, 5000, 5250, 5500, 5750 and sea bottom (minus 10db).

Sampling layers at 25 and 75 dbs were added during Leg3.

3) Water sampling of POM, $^{14}C$, $^{13}C$, $^{15}N$, $^{137}Cs$, $N_2O$, $CH_4$ and Bacteria.
4) Underway measurements of $pCO_2$, temperature, salinity, nutrients, surface current, bathymetry and meteorological parameters

**Floats, Drifters and Moorings**

(None for Leg.1 and Leg 3)

During Leg2, one Argo float was deployed at 24-14.24N, 144-12.64E after the CTD cast at Sta.291 on January 3, 2006. Five mooring systems in the Wake Island Deep Channel were recovered during the period from December 14 to 16, 2006. The details are described in Chapter 4.

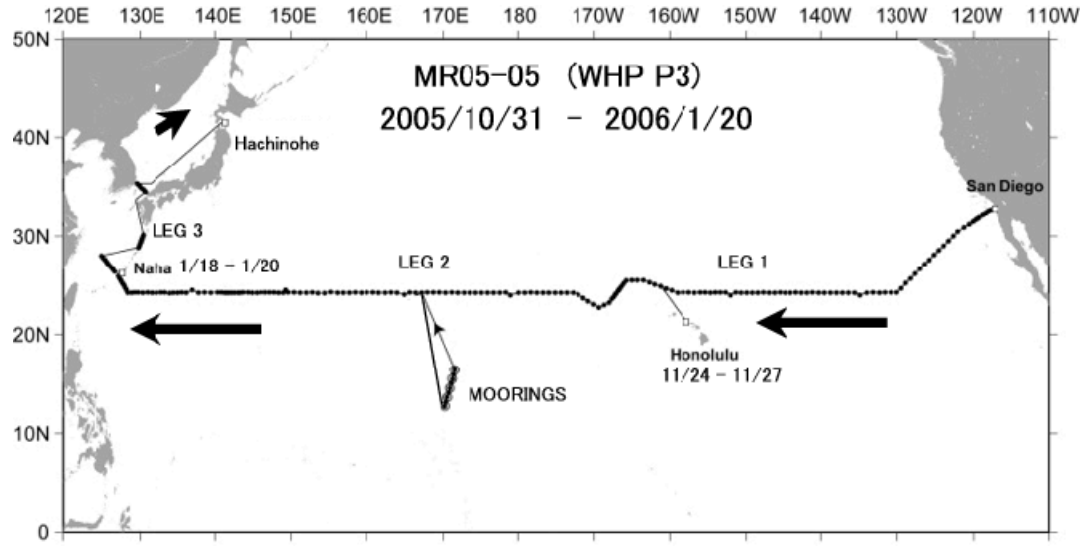


**Figure.1.1 Cruise Track**

**1.3 Responsibility**

The principal investigators responsible for major parameters are listed in Table.1.1.

## 1.4 Objective of the Cruise

### 1.4.1 Objectives

It is well known that the oceans play a central role in determining global climate. However heat and material transports in the oceans and their temporal changes have not yet been sufficiently quantified. Therefore the global climate change is not understood satisfactorily. The purposes of this research are to evaluate heat and material transports including carbon, nutrients etc, in the North Pacific and to detect their long term changes and basin-scale biogeochemical changes since the 1990s. This cruise is a reoccupation of the hydrographic section called 'WHP-P3', which was once

observed by an ocean science group of USA in 1985 and later its data have been included in the data set of the World Ocean Circulation Experiment (WOCE: 1990-2002) Hydrographic Programme (WHP). We will compare physical and chemical properties along section WHP-P3 with those obtained in 1985 to detect and evaluate long term changes of marine environment in the North Pacific.

Reoccupations of the WOCE hydrographic sections are now in progress by international cooperation among ocean science community, in the framework of CLIVAR(Climate Variability and Predictability) as part of World Climate Research Programme (WCRP) and IOCCP(International Ocean Carbon Coordination Project). Our research is planned as a contribution to these international projects supported by WMO, ICSU/SCOR and UNESCO/IOC, and its results and data will be published by 2008 for worldwide use.

The other purposes of this cruise are as follows:

1) to observe surface meteorological and hydrological parameters as a basic data of the meteorology and oceanography,
2) to observe sea bottom topography, gravity and magnetic fields along cruise track to understand the dynamics of ocean plate and the accompanying geophysical activities,

#### 1.4.2 Data Policy

Obtained data will be quality controlled and opened through GHPO and JAMSTEC within two years .

## 1.5 List of Cruise Participants

Cruise participants for each leg are listed in Table 1.2a, b and c.

## 1.6 Major Problems

(1) Position Changed

a) Leg1

Positions of stations 120, 122, 124, 126 and 128 were changed from (158º16.2'W, 24 º15.7'N), (159º0.5'W, 24 º14.5'N), (159º46.8'W, 24 º28.1'N), (160º31.9'W, 24 º40.2'N) and (161º15.4'W, 24 º53.6'N) to (158º00'W, 25º00'N), (159º0.5'W, 25 º50'N), (159º46.8'W, 25 º50'N), (160º31.9'W, 24 º50'N) and (161º15.4'W, 25º50'N), respectively, to avoid entering the training area of U.S.Navy.

b) Leg2

The position of stn. 155 was changed from (24º10.00'N, 167º06.40'W) to (24º08.82'N, 167º07.96W). This is because the water depth (2006m) at the original position recorded in the SUM file of WHP-P3 in 1985 was largely different from our value (800m) at stn. 155, whose position was accurately determined by the modern GPS system. In addition to that, the original position of stn. 155 distributes unnaturally against adjacent stations on the WHP-P3 section in 1985, therefore we presumed it wrong or inaccurate. Dr. Roemmich's (Chief scientist of WHP-P3 in 1985) reply to our enquiry on this matter is "It would seem that the ship was positioned correctly in between stns 154 and 157, but the recorded position was

erroneously taken from the dead reckoning Satnav computer".

The postion of stn. X09 (the crossover station with WHP-P09) was changed from (24º30.2'N, 136º59.1'E) to (23º59.22'N,136º59.60'E) because a fishery boat was in operation with a longline at the initial position when R/V Mirai reached there on January 6.

c)Leg3

No position of station was changed. However, TS3 was shifted about 0.3 nm from planned position because a lot of fisherman boats were operating.

(2) Misfiring and mistrip

The carousel water sampler misfired at the following stations:

Leg1: 33, 51 and 116
Leg2: X14, 201, 203, 217, 231, 322 and 351_2
Leg3: None.

Through the bottle data QC, mistrips were detected at the following stations:

Leg1: 38
Leg2: 185, WC2, WC5, 289, 357 and 351_2
Leg3: 380

(3) CTD sensor replacement

During Leg2, we encountered to several problems (drift, shift, noise) of CTD sensors and replaced them after the following stations:

Sta. X14: primary and secondary conductivity sensors
Sta. WC8: primary oxygen sensor
Sta. 285: secondary oxygen sensor

(4) Interruption of sequential occupations due to gale and bad sea condition

At Sta. 353 above the Ryukyu Trench, the first CTD cast was hindered due to bad weather and sea conditions. Because the weather forecast predicted that the gale persisted for a long time there, we abandoned the original plan of sequential occupations of the P3 stations form east to west, reached the west end station (Sta. 369), and re-start the observation form west to east toward Sta. 351, where sections were connected with the second CTD cast. Sta. 351 was occupied twice in Leg2.

The CTD observation in the East China Sea was stopped at stn. 384 due to bad sea condition for about a half day. The observation was restarted at stn. 382.

**Table 1.1 List of principal investigator and person in charge on the ship for Leg 1-3**

| | Leg 1 | Leg 2 | Leg 3 |
|---|---|---|---|
| **Chief Scientist :** | Takeshi Kawano | Akihiko Murata<br>Ikuo Kaneko | Shuichi Watanabe |
| **Chief Technologist :** | Satoshi Ozawa | Fuyuki Shibata | Minoru Kamata |

| **Item** | Principal Investigator<br>*Person in Charge on the Ship* | | |
|---|---|---|---|
| **Hydrography** | | | |
| | **Leg 1** | **Leg 2** | **Leg 3** |
| **CTDO** | Hiroshi Uchida<br>*Kentaro Oyama* | Hiroshi Uchida<br>*Satoshi Ozawa* | Hiroshi Uchida<br>*Kentaro Oyama* |
| **LADCP** | Shin'ya Kouketsu<br>*Shin'ya Kouketsu* | Shin'ya Kouketsu<br>*Hiroshi Uchida* | Shin'ya Kouketsu<br>*Shin'ya Kouketsu* |
| **BTL Salinity** | Takeshi Kawano<br>*Fujio Kobayashi* | Takeshi Kawano<br>*Fujio Kobayashi* | Takeshi Kawano<br>*Naoko Takahashi* |
| **BTL Oxygen** | Yuichiro Kumamoto<br>*Takayoshi Seike* | Yuichiro Kumamoto<br>*Takayoshi Seike* | Yuichiro Kumamoto<br>*Kimiko Nishijima* |
| **Nutrients** | Michio Aoyama<br>*Kenichiro Sato* | Michio Aoyama<br>*Junko Hamanaka* | Michio Aoyama<br>*Junko Hamanaka* |
| **DIC** | Akihiko Murata<br>*Minoru Kamata* | Akihiko Murata<br>*Mikio Kitada* | Akihiko Murata<br>*Masaki Moro* |
| **Alkalinity** | Akihiko Murata<br>*Taeko Ohama* | Akihiko Murata<br>*Fuyuki Shibata* | Akihiko Murata<br>*Taeko Ohama* |
| **pH** | Akihiko Murata<br>*Taeko Ohama* | Akihiko Murata<br>*Fuyuki Shibata* | Akihiko Murata<br>*Taeko Ohama* |
| **CFCs** | Ken'ichi Sasaki<br>*Hideki Yamamoto* | Ken'ichi Sasaki<br>*Katsunori Sagishima* | Ken'ichi Sasaki<br>*Hideki Yamamoto* |
| **$\Delta^{14}C$** | Yuichiro Kumamoto<br>*Takeshi Kawano*<br>*(collection only)* | Yuichiro Kumamoto<br>*Yuichiro Kumamoto* | Yuichiro Kumamoto<br>*Yuichiro Kumamoto* |
| **Cs** | Michio Aoyama<br>*Takeshi Kawano*<br>*(collection only)* | Michio Aoyama<br>*Akihiko Murata*<br>*Yuichiro Kumamoto* | |
| **CH4 etc,** | Osamu Yoshida<br>*Osamu Yoshida* | Osamu Yoshida<br>*Narin Boontanon* | Osamu Yoshida<br>*Narin Boontanon* |

| **Underway** | | | |
|---|---|---|---|
| | **Leg 1** | **Leg 2** | **Leg 3** |
| **ADCP** | Yasushi Yoshikawa<br>*Soichiro Sueyohi* | Yasushi Yoshikawa<br>*Shinya Okumura* | Yasushi Yoshikawa<br>*Katsuhisa Maeno* |
| **Bathymetry** | Shin'ya Kouketsu<br>*Soichiro Sueyoshi* | Shin'ya Kouketsu<br>*Shinya Okumura* | Shin'ya Kouketsu<br>*Katsuhisa Maeno* |
| **Meteorology** | Kunio Yoneyama<br>*Soichiro Sueyoshi* | Kunio Yoneyama<br>*Yasutaka Imai* | Kunio Yoneyama<br>*Katsuhisa Maeno* |
| **Thermo-salinograph** | Takeshi Kawano<br>*Takuhei Shiozaki* | Takeshi Kawano<br>*Kimiko Nishijima* | Takeshi Kawano<br>*Takuhei Shiozaki* |
| **Infrared Radiometer** | Hajime Okamoto<br>*Akihito Hirai* | Hajime Okamoto<br>*Eiji Abe* | Hajime Okamoto<br>*Katsuhisa Maeno* |
| **Sky Radiometer** | Tatsuo Endo<br>*Soichiro Sueyoshi* | Tatsuo Endo<br>*Yasutaka Imai* | Tatsuo Endo<br>*Katsuhisa Maeno* |
| **Laser Radar** | Nobuo Sugimoto<br>*Akihito Hirai* | Nobuo Sugimoto<br>*Eiji Abe* | Nobuo Sugimoto<br>*Katsuhisa Maeno*<br>*(operating only)* |
| **$pCO_2$** | Akihiko Murata<br>*Minoru Kamata* | Akihiko Murata<br>*Mikio Kitada* | Akihiko Murata<br>*Masaki Moro* |
| **Bactria** | | | Masaaki Tamayama<br>*Masaaki Tamayama* |
| **Floats, Drifters** | | | |
| | **Leg 1** | **Leg 2** | **Leg 3** |
| **Argo float** | | Nobuyuki Shikama<br>*Satoshi Ozawa* | |
| **Mooring** | | | |
| | **Leg 1** | **Leg 2** | **Leg 3** |
| **Mooring** | | Hiroshi Uchida<br>*Satoshi Ozawa* | |

**Table 1.2a List of Cruise Participants for Leg 1**

| Name | Responsibility | Affiliation |
|---|---|---|
| Ayako Fujii | CH4, N2O, N15 | Tokyo Tech. |
| Go Haruta | Water Sampling | MWJ |
| Hiroyuki Hayashi | CTD | MWJ |
| Akihito Hirai | Laser Ladar, Infrared Radiometer | Chiba Univ |
| Tetsuya Inaba | Water Sampling | MWJ |
| Yoshiko Ishikawa | Carbon Items | MWJ |
| Minoru Kamata | Carbon Items | MWJ |
| Takeshi Kawano | Chief Scientist, Salinity | IORGC/JAMSTEC |
| Mikio Kitada | Carbon Items | MWJ |
| Fujio Kobayashi | Salinity | MWJ |
| Shinya Kouketsu | LADCP, ADCP | IORGC/JAMSTEC |
| Katsuhisa Maeno | Meteorology, Geology | GODI |
| Junji Matsushita | Nutrients | MWJ |
| Takami Mori | Water Sampling | MWJ |
| Norio Nagahama | Meteorology, Geology | GODI |
| Yoshifumi Noiri | Water Sampling | MWJ |
| Taeko Ohama | Carbon Items | MWJ |
| Miwa Okino | Water Sampling | MWJ |
| Kosuke Okudaira | Water Sampling | MWJ |
| Kentaro Oyama | CTD | MWJ |
| Satoshi Ozawa | Chief Technologist, Water Sampling | MWJ |
| Kenichi Sasaki | CFCs | MIO/JAMSTEC |
| Kenichiro Sato | Nutrients | MWJ |
| Takayoshi Seike | LADCP, DO | MWJ |
| Takuhei Siozaki | DO, Thermosalinograph | MWJ |
| Yuichi Sonoyama | CFCs | MWJ |
| Soichiro Sueyoshi | Meteorology, Geology | GODI |
| Nobuhiko Tahara | Water Sampling | MWJ |
| Tomoyuki Takamori | CTD | MWJ |
| Asumi Takeuchi | Water Sampling | MWJ |
| Ayumi Takeuchi | Nutrients | MWJ |
| Tatsuya Tanaka | Salinity | MWJ |
| Hiroshi Uchida | Water Sampling, CTD | IORGC/JAMSTEC |
| Hiroki Ushiromura | CTD | MWJ |
| Masahide Wakita | CFCs | MIO/JAMSTEC |
| Keisuke Wataki | DO, Thermosalinograph | MWJ |
| Hideki Yamamoto | CFCs | MWJ |
| Osamu Yoshida | CH4, N2O, N15 | Tokyo Tech. |
| Atsushi Yoshimura | Water Sampling | MWJ |

| | |
|---|---|
| GODI | Grobal Ocean Development Inc. |
| MWJ | Marine Works Japan |
| JAMSTEC | Japan Agency for Marine-Earth Science and Technology |
| IORGC | Institute of Observational Research for Global Change |
| MIO | Mutsu Institute for Oceanography |
| Tokyo Tech. | Tokyo Institute of Technology |

**Table 1.2b List of Cruise Participants for Leg 2**

| Name | Responsibility | Affiliation |
|---|---|---|
| Eiji Abe | Laser Radar, Infrared Radiometer | Chiba Univ |
| Narin Boontanon | CH4, N2O, N15 | Tokyo Tech. |
| Masanori Enoki | CFCs | MWJ |
| Ami Fujiwara | Water Sampling | MWJ |
| Junko Hamanaka | Nutrients | MWJ |
| Yasushi Hashimoto | Water Sampling | MWJ |
| Ei Hatakeyama | Carbon Items | MWJ |
| Miyo Ikeda | Water Sampling | MWJ |
| Yasutaka Imai | Meteorology, Geology, ADCP | GODI |
| Ikuo Kaneko | Chief Scientist, LADCP | IORGC/JAMSTEC |
| Mikio Kitada | Carbon Items | MWJ |
| Fujio Kobayashi | Salinity | MWJ |
| Misato Koide | Water Sampling | MWJ |
| Hiroshi Komura | Water Sampling | MWJ |
| Yuichiro Kumamoto | Water Sampling, DO | IORGC/JAMSTEC |
| Kouhei Miura | Nutrients | MWJ |
| Takami Mori | Water Sampling | MWJ |
| Masaki Moro | Carbon Items | MWJ |
| Akihiko Murata | Chief Scientist, Carbon Items | IORGC/JAMSTEC |
| Akinori Murata | CTD, Water Sampling | MWJ |
| Kimiko Nishijima | DO, Thermosalinograph | MWJ |
| Ryo Ohyama | Meteorology, Geology, ADCP | GODI |
| Shinya Okumura | Meteorology, Geology, ADCP | GODI |
| Asako Onda | Water Sampling | MWJ |
| Satoshi Ozawa | CTD, Argo Float | MWJ |
| Katsunori Sagishima | CFCs | MWJ |
| Ken'ichi Sasaki | CFCs | MIO/JAMSTEC |
| Ken'ichiro Sato | Water Sampling | MWJ |
| Takayoshi Seike | DO | MWJ |
| Fuyuki Shibata | Chief Technologist, Carbon Items | MWJ |
| Naoko Takahashi | Salinity | MWJ |
| Tomoyuki Takamori | CTD, Water Sampling | MWJ |
| Ayumi Takeuchi | Nutrients | MWJ |
| Shinsuke Toyoda | CTD, Water Sampling | MWJ |
| Hiroshi Uchida | LADCP, Mooring, CTD | IORGC/JAMSTEC |
| Hirokatsu Uno | CTD | MWJ |
| Hiroki Ushiromura | CTD, Water Sampling | MWJ |
| Keisuke Wataki | CFCs | MWJ |

| | |
|---|---|
| GODI | Grobal Ocean Development Inc. |
| MWJ | Marine Works Japan |
| JAMSTEC | Japan Agency for Marine-Earth Science and Technology |
| IORGC | Institute of Observational Research for Global Change |
| MIO | Mutsu Institute for Oceanography |
| Tokyo Tech. | Tokyo Institute of Technology |

**Table 1.2c List of Cruise Participants for Leg 3**

| Name | Responsibility | Affiliation |
|---|---|---|
| Yukiko Aoyagi | Water Sampling | MWJ |
| Narin Boontanon | $CH_4$, $N_2O$, $^{15}N$ | Tokyo Tech. |
| Masanori Enoki | CFCs | MWJ |
| Ami Fujiwara | Water Sampling | MWJ |
| Chusei Fujiwara | Laser Radar, Infrared Radiometer | GODI |
| Yoko Fukuda | Water Sampling | MWJ |
| Junko Hamanaka | Nutrients | MWJ |
| Miyo Ikeda | Water Sampling | MWJ |
| Yoshiko Ishikawa | Carbon Items | MWJ |
| Minoru Kamata | Chief Technologist, Carbon Items | MWJ |
| Misato Koide | Water Sampling | MWJ |
| Shinya Koketsu | LADCP, ADCP, Bathymetry | IORGC/JAMSTEC |
| Yuichiro Kumamoto | Water Sampling, DO | IORGC/JAMSTEC |
| Hiroshi Komura | Water Sampling | MWJ |
| Masaaki Maekawa | Water Sampling | MWJ |
| Katsuhisa Maeno | Meteorology, Geology, ADCP | GODI |
| Junji Matsushita | Nutrients | MWJ |
| Hiroshi Matsunaga | CTD | MWJ |
| Kohei Miura | Nutrients | MWJ |
| Masaki Moro | Carbon Items | MWJ |
| Kimiko Nishijima | DO | MWJ |
| Tomohide Noguchi | CTD, Water Sampling | MWJ |
| Taeko Ohama | Carbon Items | MWJ |
| Asako Onda | Water Sampling | MWJ |
| Kentaro Oyama | CTD | MWJ |
| Ryo Oyama | Meteorology, Geology, ADCP | GODI |
| Takuhei Shiozaki | DO | MWJ |
| Yuichi Sonoyama | CFCs | MWJ |
| Naoko Takahashi | Salinity | MWJ |
| Masaaki Tamayama | Bacteria | JAMES |
| Tatsuya Tanaka | Salinity | MWJ |
| Hiroshi Uchida | Water Sampling, CTD | IORGC/JAMSTEC |
| Masahide Wakita | CFCs | MIO/JAMSTEC |
| Shuichi Watanabe | Chief Scientist, LADCP, Water Sampling | MIO/JAMSTEC |
| Makito Yokota | CTD, Water Sampling | MWJ |
| Hideki Yamamoto | CFCs | MWJ |

| | |
|---|---|
| GODI | Grobal Ocean Development Inc. |
| MWJ | Marine Works Japan |
| JAMSTEC | Japan Agency for Marine-Earth Science and Technology |
| IORGC | Institute of Observational Research for Global Change |
| MIO | Mutsu Institute for Oceanography |
| Tokyo Tech. | Tokyo Institute of Technology |
| JAMES | Japan Macro-Engineers' Society |

## 2.1 Meteorological observation

### 2.1.1 Surface Meteorological Observation

| | | |
|---|---|---|
| *Kunio Yoneyama* | *(JAMSTEC) Principal Investigator / Not on-board* | |
| *Souichro Sueyoshi* | *(Global Ocean Development Inc.)* | *-Leg1* |
| *Yasutaka Imai* | *(Global Ocean Development Inc.)* | *-Leg2* |
| *Shinya Okumura* | *(Global Ocean Development Inc.)* | *-Leg2* |
| *Katsuhisa Maeno* | *(Global Ocean Development Inc.)* | *-Leg1,3* |
| *Norio Nagahama* | *(Global Ocean Development Inc.)* | *-Leg1* |
| *Ryo Ohyama* | *(Global Ocean Development Inc.)* | *-Leg2,3* |

(1) Objectives

The surface meteorological parameters are observed as a basic dataset of the meteorology. These parameters bring us the information about the temporal variation of the meteorological condition surrounding the ship.

(2) Methods

The surface meteorological parameters were observed throughout the MR05-05 Leg-1 cruise departed from San Diego on 31 Oct. 2005 and arrived at Honolulu on 24 Nov. 2005, Leg-2 cruise departed from Honolulu on 27 Nov. 2005 and arrived at Nakagusuku on 17 Jan. 2006, Leg-3 cruise departed from from Nakagusuku on 20 Jan. 2006 and arrived Sekinehama on 30 Jan. 2006. During this cruise, we used two systems for the observation.

1) MIRAI Surface Meteorological observation (SMET) system
2) Shipboard Oceanographic and Atmospheric Radiation (SOAR) system

1) MIRAI Surface Meteorological observation (SMET) system

Instruments of SMET system are listed in Table 2.1.1-1 and measured parameters are listed in Table 2.1.1-2. Data was collected and processed by KOAC-7800 weather data processor made by Koshin-Denki, Japan. The data set consists of 6-second averaged data.

2) Shipboard Oceanographic and Atmospheric Radiation (SOAR) system

SOAR system designed by BNL (Brookhaven National Laboratory, USA) consists of major three parts.

i) Portable Radiation Package (PRP) designed by BNL – short and long wave downward radiation.

ii) Zeno Meteorological (Zeno/Met) system designed by BNL – wind, air temperature, relative humidity, pressure, and rainfall measurement.

iii) Scientific Computer System (SCS) designed by NOAA (National Oceanic and Atmospheric Administration, USA) – centralized data acquisition and logging of all data sets.

SCS recorded PRP data every 6 seconds, Zeno/Met data every 10 seconds. Instruments and their locations are listed in Table2.1.1-3 and measured parameters are listed in Table 2.1.1-4.

We have checked the following sensors before and after the cruise for quality control as post processing.

a) Young Rain gauge (SMET and SOAR)

Inspecting the linearity of output value from the rain gauge sensor to change input value by adding fixed quantity of test water.

b) Barometer (SMET and SOAR)

Comparing with the portable barometer value, PTB220CASE, VAISALA.

c) Thermometer (air temperature and relative humidity) (SMET and SOAR)
Comparing with the portable thermometer value, HMP41/45, VAISALA.

(3) Preliminary results

Figures 2.1.1-1 ,2.1.1-2 and 2.1.1-3 show the time series of the following parameters;
Wind (SOAR)
Air temperature (SOAR)
Relative humidity (SOAR)
Precipitation (SOAR, ORG)
Short/long wave radiation (SOAR)
Pressure (SOAR)
Sea surface temperature (SMET)
Significant wave height (SMET)

(4) Data archives

The raw data obtained during this cruise will be submitted to JAMSTEC Data Management Office. Corrected data sets will also be available from K. Yoneyama of JAMSTEC.

(5) Remarks

MR05-05Leg1

1. Sea surface temperature is not acquired from the departure to 12:30 UTC of 31 October and from 23:00 UTC of 23 November the arrival, because we stopped pumping up surface water.

MR05-05Leg2

1. Sea surface temperature is not acquired from the departure to 04:00 UTC of 29 November and from 05:12 UTC of 15 January to the arrival, because we stopped pumping up surface water.

2. PRP data acquisition stopped from the 05:10 UTC of 25 December to 06:41 UTC of 25 December, because of PC trouble.

MR05-05Leg3

1. Sea surface temperature is not acquired from the departure to 04:32 UTC of 20 January and from 23:28 UTC of 27 January the arrival, because we stopped pumping up surface water.

Table 2.1.1-1 Instruments and installations of MIRAI Surface Meteorological observation system

| Sensors | Type | Manufacturer | Location (altitude from surface) |
|---|---|---|---|
| Anemometer | KE-500 | Koshin Denki, Japan | foremast (24 m) |
| Tair/RH | HMP45A | Vaisala, Finland | |
| with 43408 Gill aspirated radiation shield | | R.M. Young, USA | compass deck (21 m) |
| starboard side and port side | | | |
| Thermometer: SST RFN1-0 | | Koshin Denki, Japan | 4th deck (-1m, inlet -5m) |
| Barometer | F-451 | Yokogawa, Japan | captain deck (13 m) |
| weather observation room | | | |
| Rain gauge | 50202 | R. M. Young, USA | compass deck (19 m) |
| Optical rain gauge | ORG-815DR | Osi, USA | compass deck (19 m) |
| Radiometer (short wave) | MS-801 | Eiko Seiki, Japan | radar mast (28 m) |
| Radiometer (long wave) | MS-202 | Eiko Seiki, Japan | radar mast (28 m) |
| Wave height meter | MW-2 | Tsurumi-seiki, Japan | bow (10 m) |

Table 2.1.1-2 Parameters of MIRAI Surface Meteorological observation system

| | Parmeter | Units | Remarks |
|---|---|---|---|
| 1 | Latitude | degree | |
| 2 | Longitude | degree | |
| 3 | Ship's speed | knot | Mirai log, DS-30 Furuno |
| 4 | Ship's heading | degree | Mirai gyro, TG-6000, Tokimec |
| 5 | Relative wind speed | m/s | 6sec./10min. averaged |
| 6 | Relative wind direction | degree | 6sec./10min. averaged |
| 7 | True wind speed | m/s | 6sec./10min. averaged |
| 8 | True wind direction | degree | 6sec./10min. averaged |
| 9 | Barometric pressure | hPa | adjusted to sea surface level |
| | 6sec. averaged | | |
| 10 | Air temperature (starboard side) | degC | 6sec. averaged |
| 11 | Air temperature (port side) | degC | 6sec. averaged |
| 12 | Dewpoint temperature (starboard side) | degC | 6sec. averaged |
| 13 | Dewpoint temperature (port side) | degC | 6sec. averaged |
| 14 | Relative humidity (starboard side) | % | 6sec. averaged |
| 15 | Relative humidity (port side) | % | 6sec. averaged |
| 16 | Sea surface temperature | degC | 6sec. averaged |
| 17 | Rain rate (optical rain gauge) | mm/hr | hourly accumulation |
| 18 | Rain rate (capacitive rain gauge) | mm/hr | hourly accumulation |
| 19 | Down welling shortwave radiation | $W/m^2$ | 6sec. averaged |
| 20 | Down welling infra-red radiation | $W/m^2$ | 6sec. averaged |
| 21 | Significant wave height (bow) | m | hourly |
| 22 | Significant wave height (aft) | m | hourly |
| 23 | Significant wave period (bow) | second | hourly |
| 24 | Significant wave period (aft) | second | hourly |

Table 2.1.1-3 Instrument and installation locations of SOAR system

| Sensors (*Zeno/Met*) | Type | Manufacturer | Location (altitude from surface) |
|---|---|---|---|
| Anemometer | 05106 | R.M. Young, USA | foremast (25 m) |
| Tair/RH | HMP45A | Vaisala, Finland | |
| with 43408 Gill aspirated radiation shield | | R.M. Young, USA | foremast (24 m) |
| Barometer | 61201 | R.M. Young, USA | |
| with 61002 Gill pressure port | | R.M. Young, USA | foremast (24 m) |
| Rain gauge | 50202 | R. M. Young, USA | foremast (24 m) |
| Optical rain gauge | ORG-815DA | Osi, USA | foremast (24 m) |

| Sensors (*PRP*) | Type | Manufacturer | Location (altitude from surface) |
|---|---|---|---|
| Radiometer (short wave) | PSP | Epply Labs, USA | foremast (25 m) |
| Radiometer (long wave) | PIR | Epply Labs, USA | foremast (25 m) |
| Fast rotating shadowband radiometer | | Yankee, USA | foremast (25 m) |

Table 2.1.1-4 Parameters of SOAR system

| | Parmeter | Units | Remarks |
|---|---|---|---|
| 1 | Latitude | degree | |
| 2 | Longitude | degree | |
| 3 | SOG | knot | |
| 4 | COG | degree | |
| 5 | Relative wind speed | m/s | |
| 6 | Relative wind direction | degree | |
| 7 | Barometric pressure | hPa | |
| 8 | Air temperature | degC | |
| 9 | Relative humidity | % | |
| 10 | Rain rate (optical rain gauge) | mm/hr | |
| 11 | Precipitation (capacitive rain gauge) | mm | reset at 50 mm |
| 12 | Down welling shortwave radiation | $W/m^2$ | |
| 13 | Down welling infra-red radiation | $W/m^2$ | |
| 14 | Defuse irradiance | $W/m^2$ | |

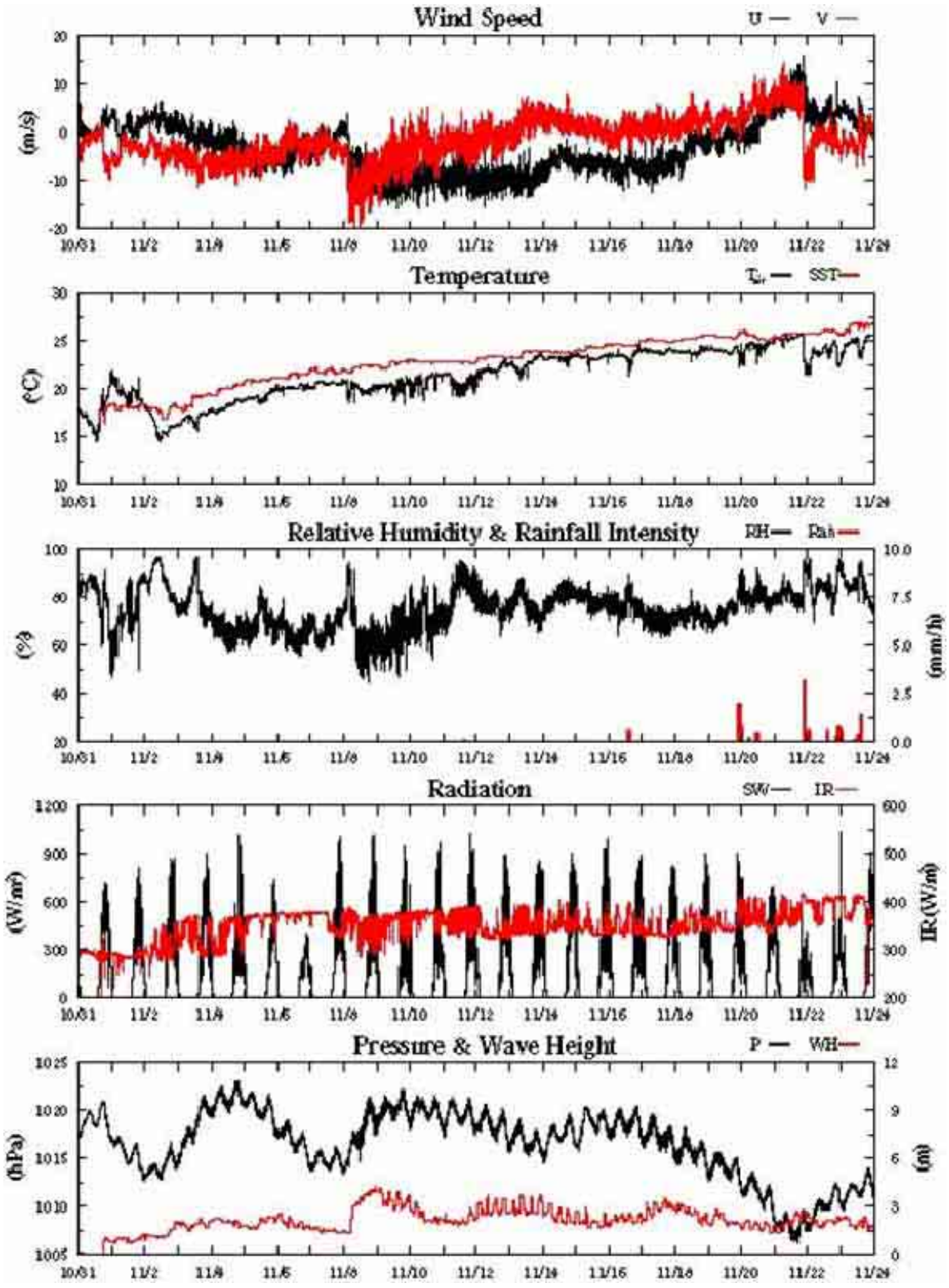


Fig.2.1.1-1 Time series of surface meteorological parameters during the MR05-05Leg1 cruise

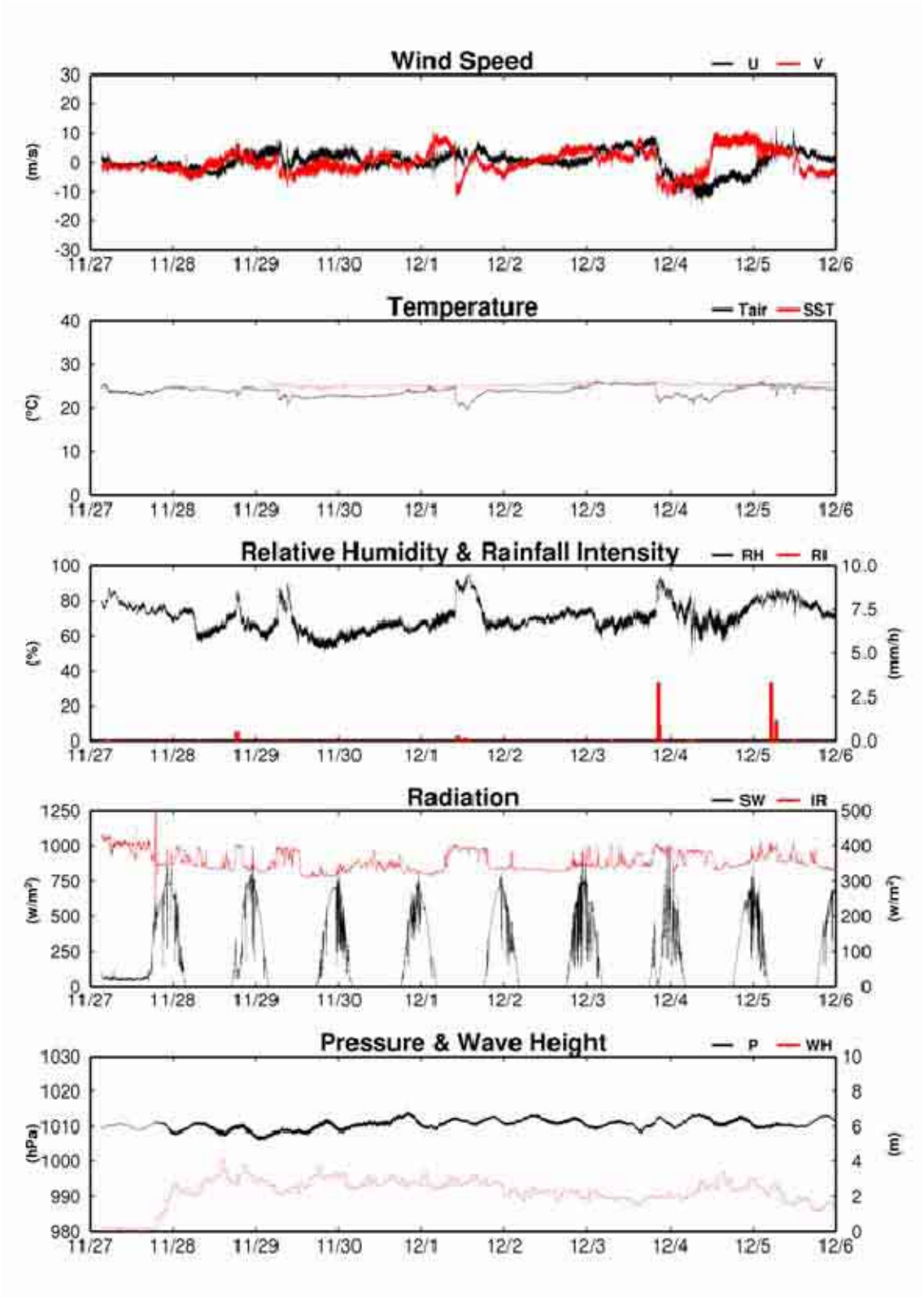


Fig.2.1.1-2 Time series of surface meteorological parameters during the MR05-05Leg2

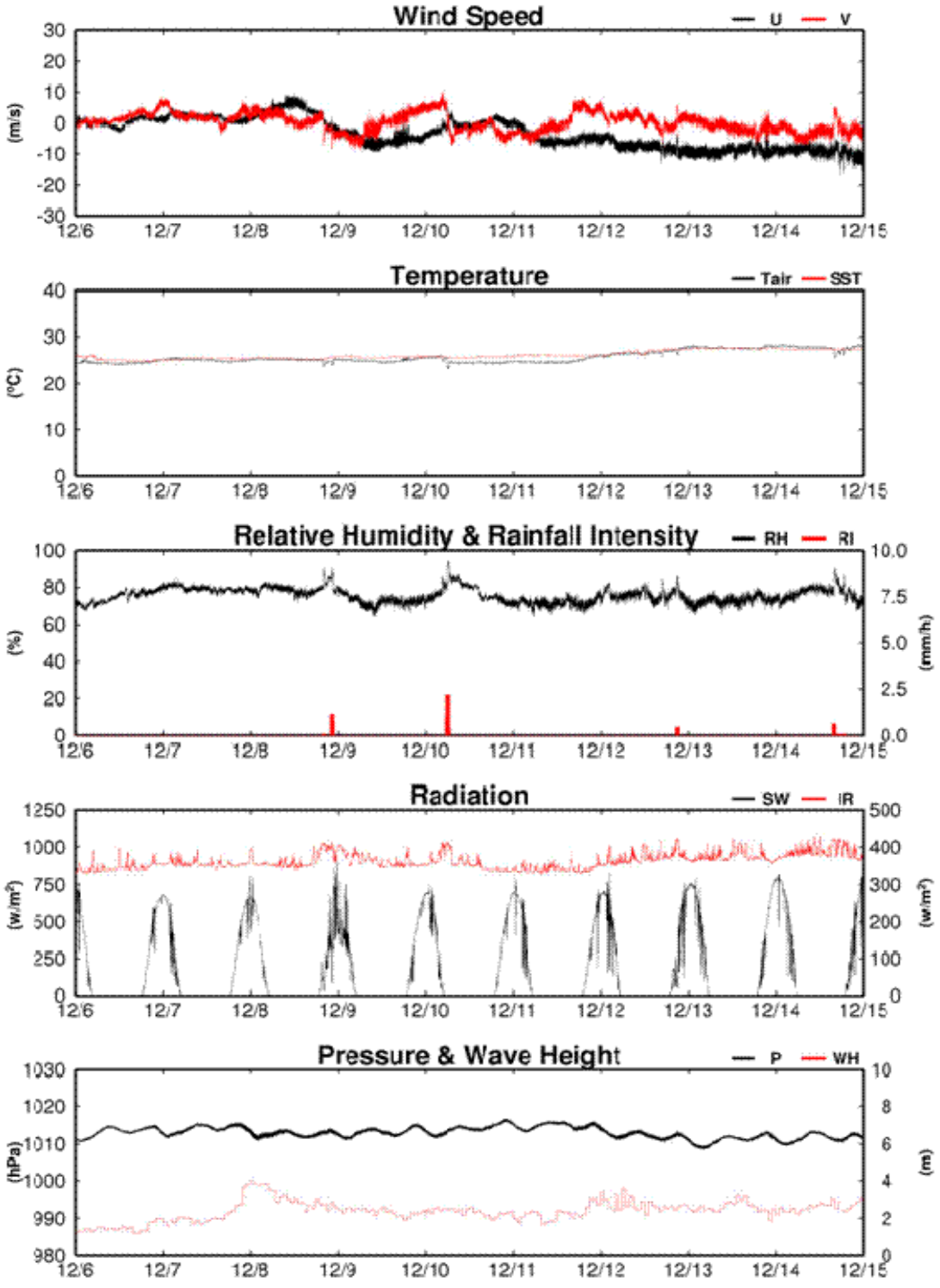


Fig.2.1.1-2 Continued

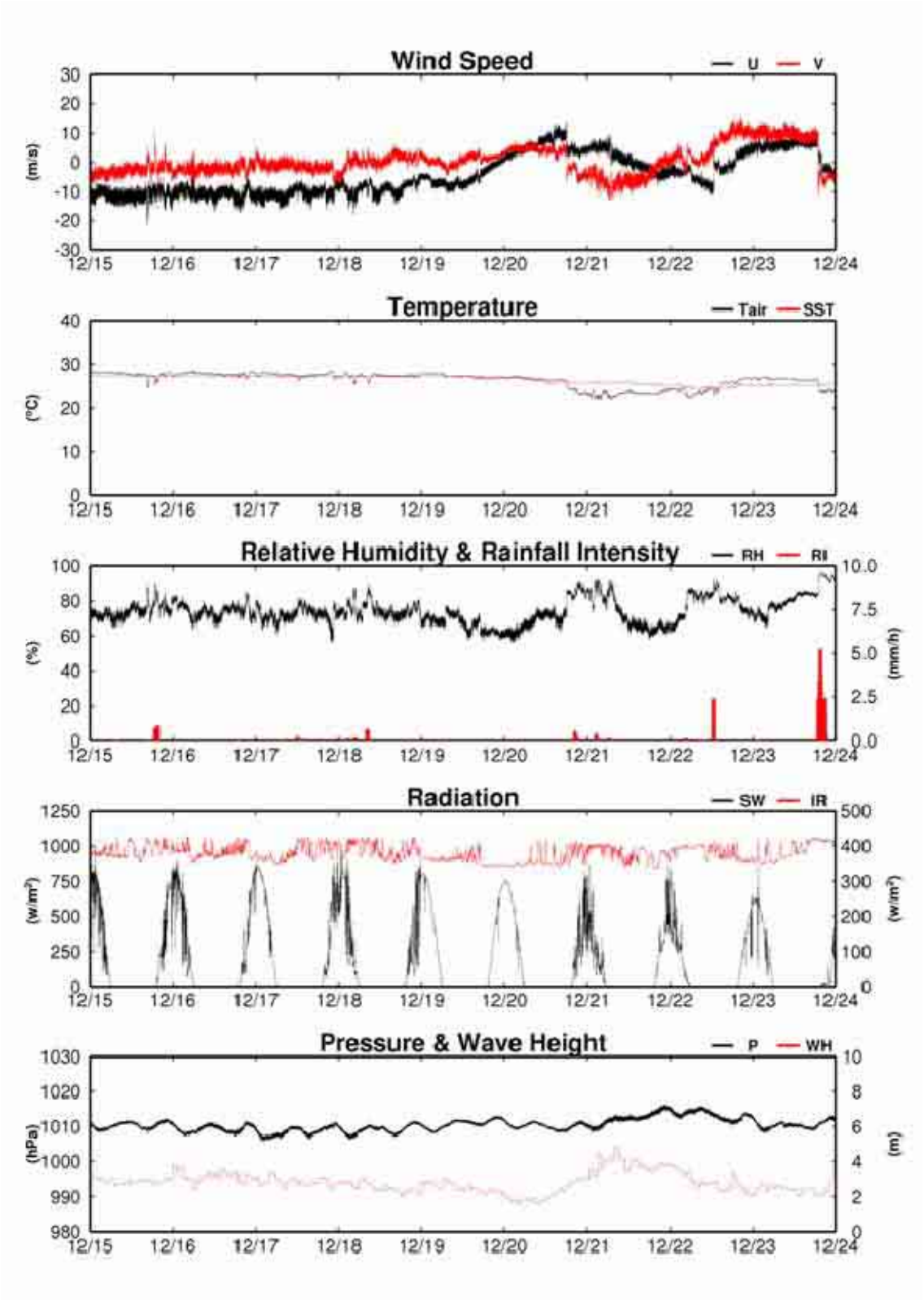


Fig.2.1.1-2 Continued

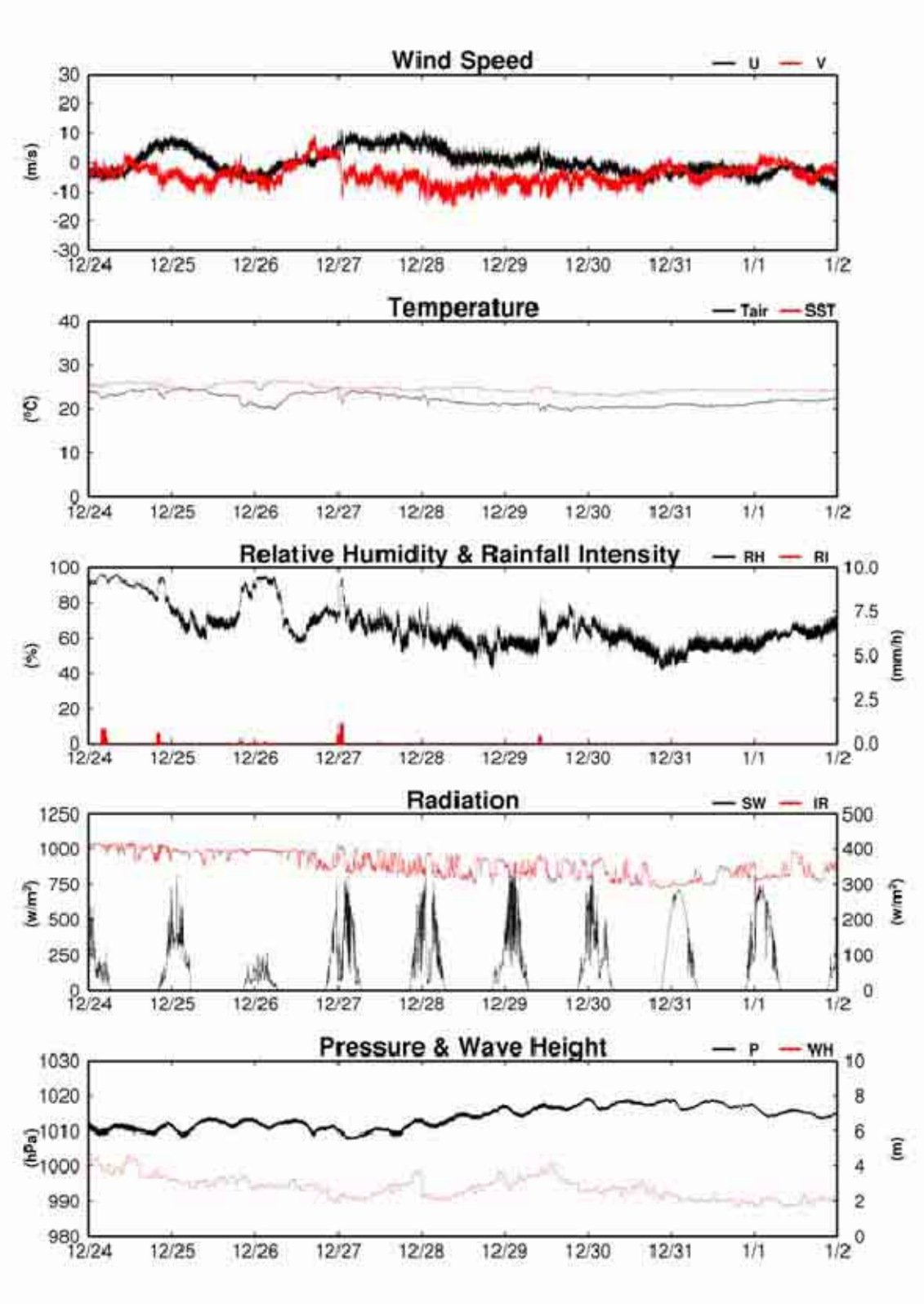


Fig.2.1.1-2 Continued

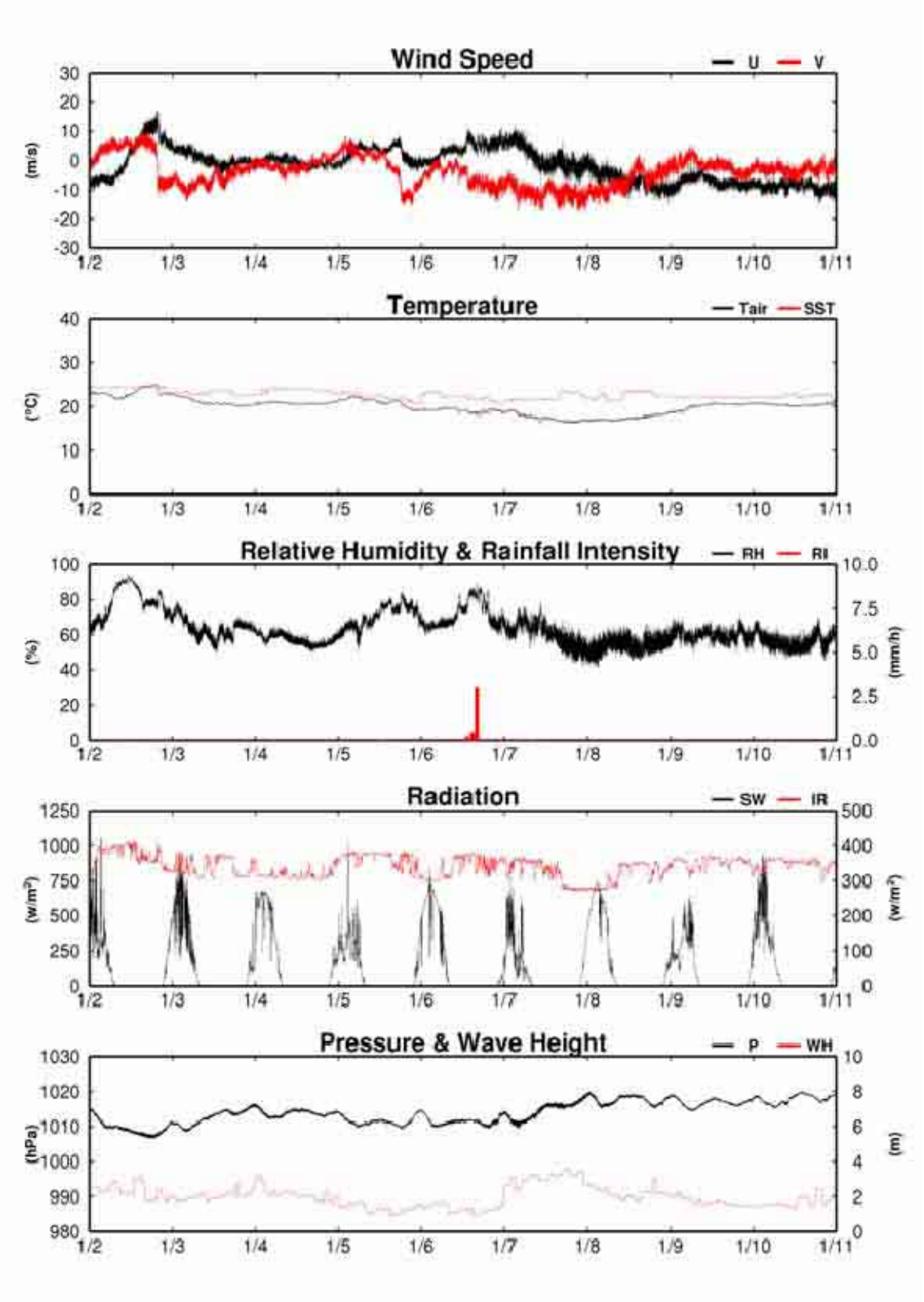


Fig.2.1.1-2 Continued

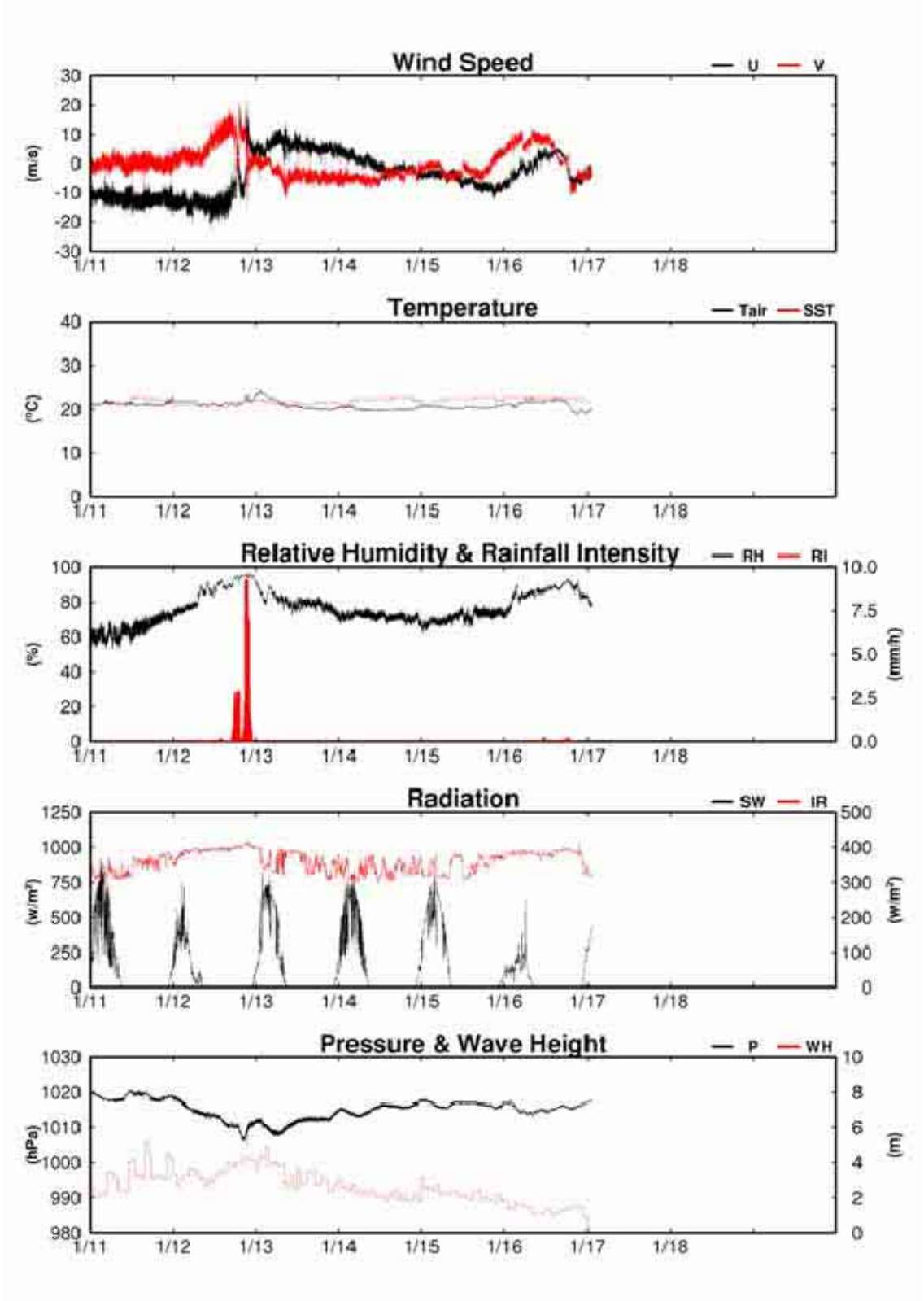


Fig.2.1.1-2 Continued

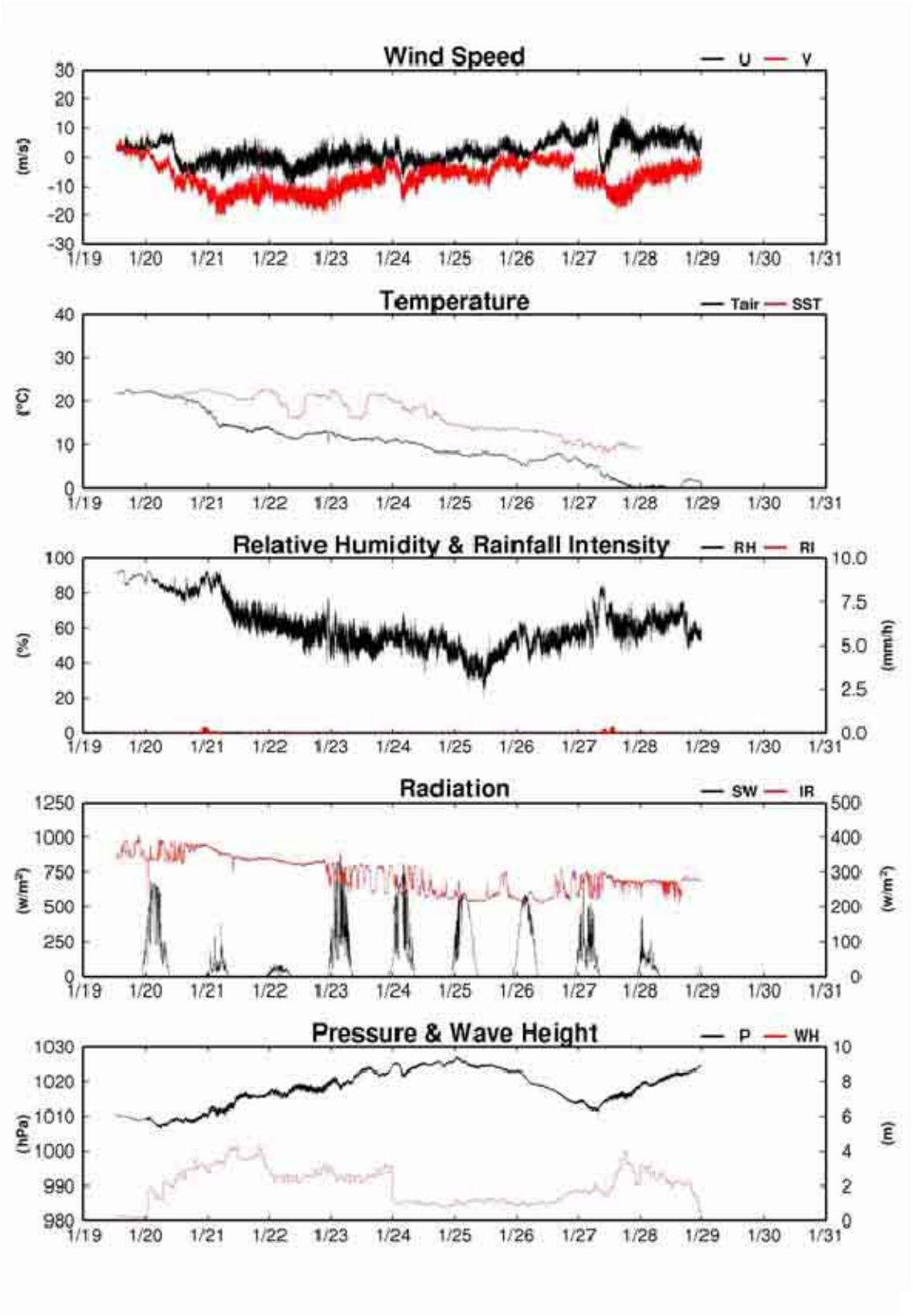


Fig.2.1.1-3 Time series of surface meteorological parameters during the MR05-05Leg3cruise

### 2.1.2 Ceilometer Observation


| | | |
|---|---|---|
| ***Kunio Yoneyama*** | ***(JAMSTEC) Principal Investigator / Not on-board*** | |
| ***Souichro Sueyoshi*** | ***(Global Ocean Development Inc.)*** | ***-Leg1*** |
| ***Yasutaka Imai*** | ***(Global Ocean Development Inc.)*** | ***-Leg2*** |
| ***Shinya Okumura*** | ***(Global Ocean Development Inc.)*** | ***-Leg2*** |
| ***Katsuhisa Maeno*** | ***(Global Ocean Development Inc.)*** | ***-Leg1,3*** |
| ***Norio Nagahama*** | ***(Global Ocean Development Inc.)*** | ***-Leg1*** |
| ***Ryo Ohyama*** | ***(Global Ocean Development Inc.)*** | ***-Leg2,3*** |


Objectives

The information of cloud base height and liquid water amount around the cloud base is important to understand the process on formation of cloud. As one of the methods to measure them, the ceilometer observation was carried out.

Methods

We measured cloud base height and backscatter profile using ceilometer (CT-25K, VAISALA, Finland) throughout the MR05-05 leg1 cruise from San Diego departed on 31 Oct. 2005 to Honolulu arrived on 24 Nov. 2005, leg2 cruise from Honolulu departed on 27 Nov. 2005 to Nakagusuku arrived on 17 Jan. 2006, leg3 cruise from Nakagusuku departed on 20 Jan. 2006 to Sekinehama arrived on 30 Jan. 2006. Major parameters to be measured are 1) cloud base height in meters, 2) backscatter profiles, and 3) estimated cloud amount in octas.

Specifications of the system are as follows.

| | |
|---|---|
| Laser source: | Indium Gallium Arsenide Diode |
| Transmitting wavelength: | 905±5 mm at 25 degC |
| Transmitting average power: | 8.9 mW |
| Repetition rate: | 5.57 kHz |
| Detector: | Silicon avalanche photodiode (APD) |
| Responsibility at 905 nm: | 65 A/W |
| Measurement range: | 0 ~ 7.5 km |
| Resolution: | 50 ft in full range |
| Sampling rate: | 60 sec |
| Sky Condition: | 0, 1, 3, 5, 7, 8 oktas (9: Vertical Visibility) |
| | (0: Sky Clear, 1:Few, 3:Scattered, 5-7: Broken, 8: Overcast) |

On the archive dataset, cloud base height and backscatter profile are recorded with the resolution of 30 m (100 ft).

Preliminary results

Figure 2.1.2-1 and Figure 2.1.2-2 show the time series of the first and second lowest cloud base height during the Cruise.

Data archives

The raw data obtained during this cruise will be submitted to JAMSTEC Data Management Division. Also it is available from K. Yoneyama of JAMSTEC.

Remarks

Window cleaning：

28 Oct. 2005 23:02 UTC
12 Nov. 2005 22:53 UTC
4 Dec. 2005 02:48 UTC
10 Dec. 2005 20:48 UTC
18 Dec. 2005 21:40 UTC

24 Dec. 2005 21:58 UTC
30 Dec. 2005 22:57 UTC
08 Jan. 2006 22:36 UTC
28 Jun. 2006 23:07 UTC

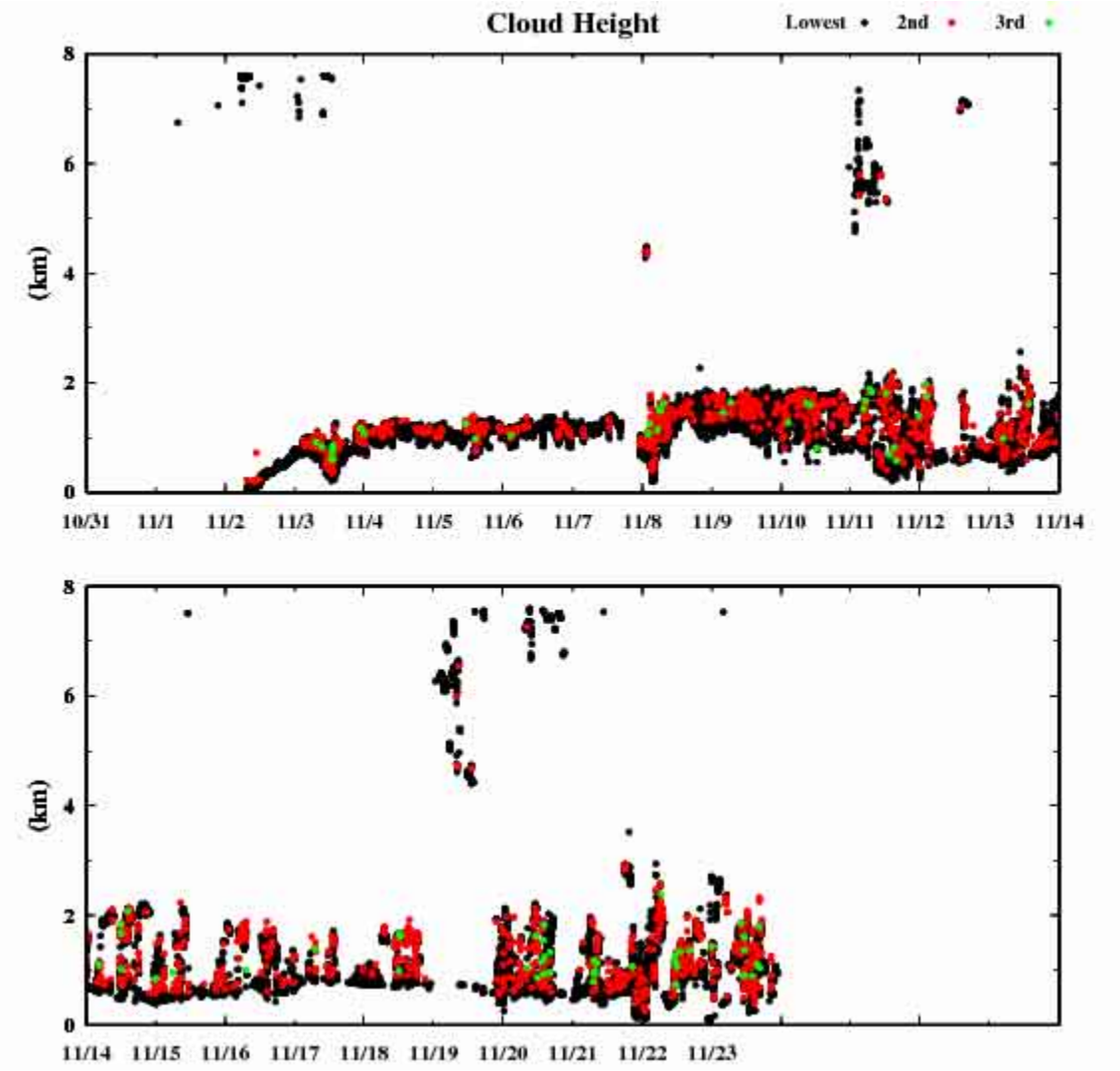


**Fig.2.1.2-1 1st, 2nd and 3rd lowest cloud base height during MR05-05Leg1 cruise.**

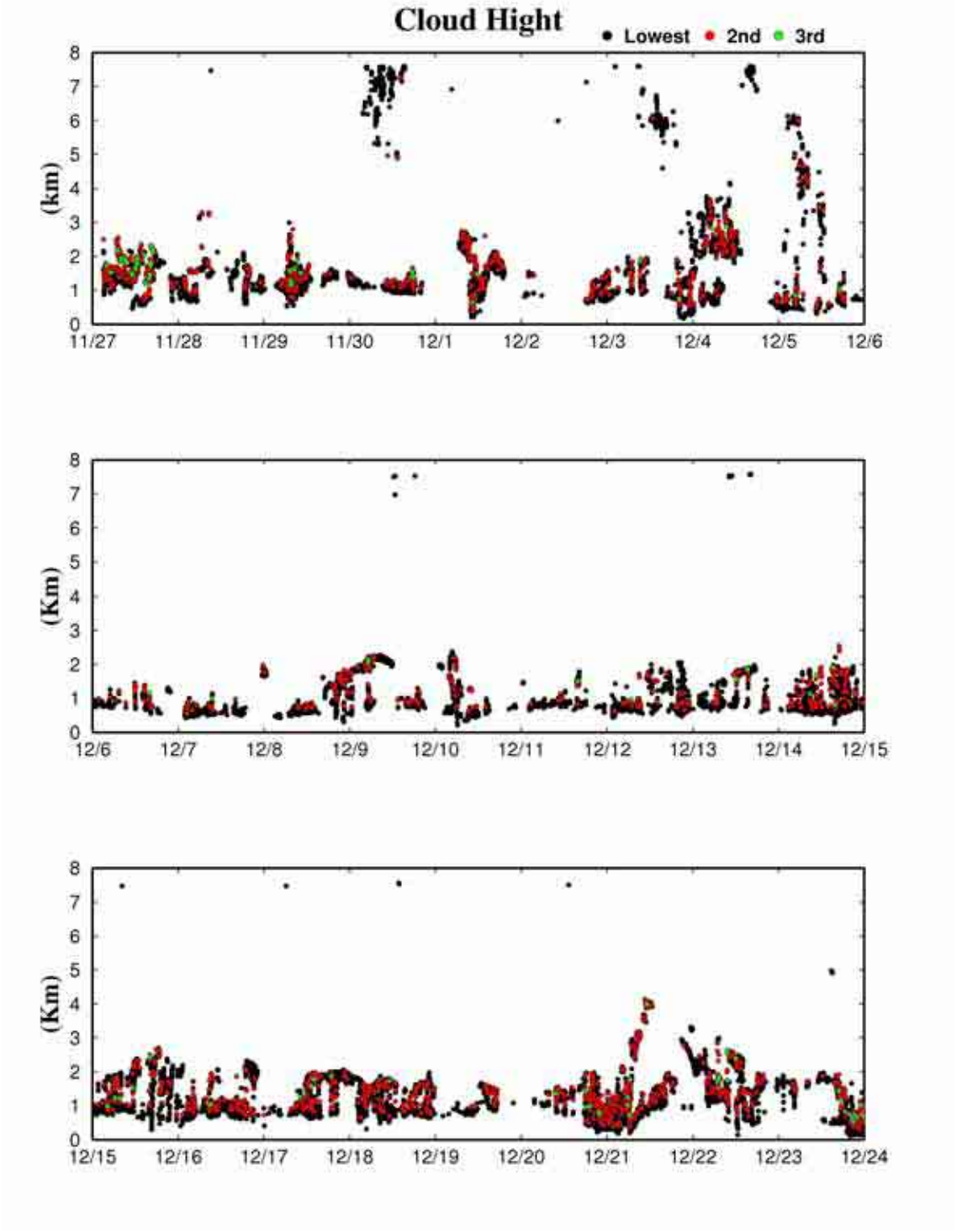


**Fig.2.1.2-2 1st, 2nd and 3rd lowest cloud base height during MR05-05Leg2 cruise.**

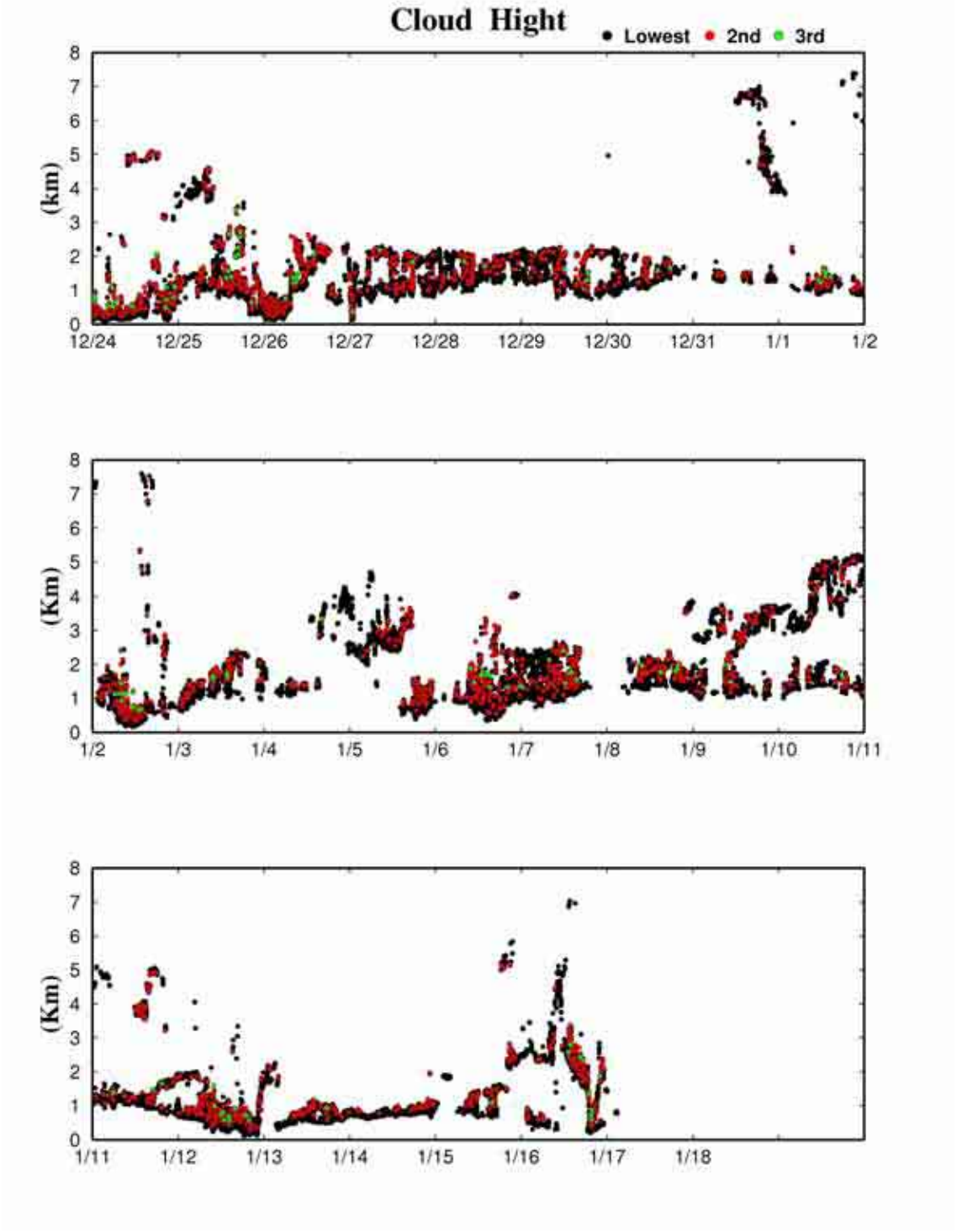


**Fig.2.1.2-2 Continued**

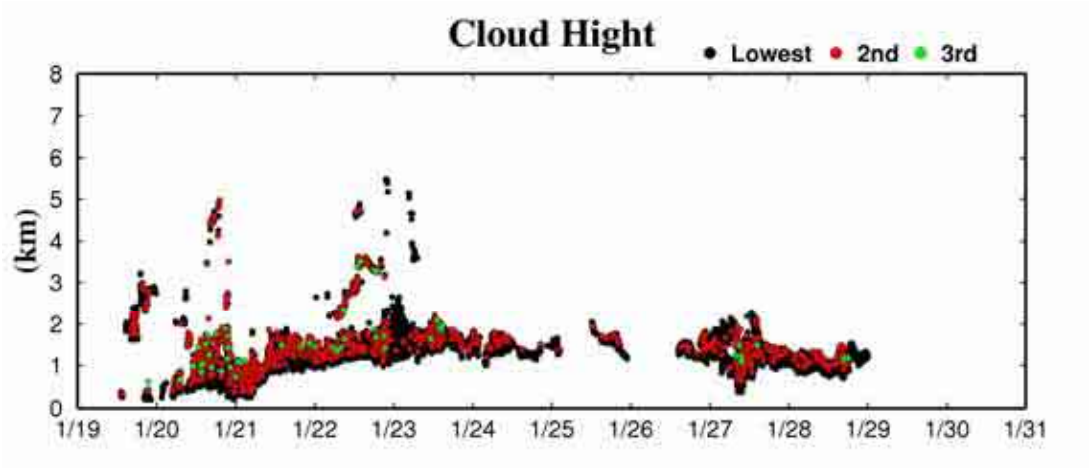


**Fig.2.1.2-3 1st, 2nd and 3rd lowest cloud base height during MR05-05 Leg3 cruise.**

### 2.1.3 Surface Atmospheric Turbulent Flux Measurement

Personnel

| | |
|---|---|
| Kunio Yoneyama | (JAMSTEC) Principal Investigator / Not-onboard |
| Osamu Tsukamoto | (Okayama University) Not-onboard |
| Souichiro Sueyoshi | (Global Ocean Development Inc.) Leg-1 |
| Katsuhisa Maeno | (Global Ocean Development Inc.) Leg-1 and Leg-3 |
| Norio Nagahama | (Global Ocean Development Inc.) Leg-1 |
| Yasutaka Imai | (Global Ocean Development Inc.) Leg-2 |
| Shinya Okumura | (Global Ocean Development Inc.) Leg-2 |
| Ryo Ohyama | (Global Ocean Development Inc.) Leg-2 and Leg-3 |

Objective

To better understand the air-sea interaction, accurate measurements of surface heat and fresh water budgets are necessary, as well as momentum exchange through the sea surface. In addition, the evaluation of surface flux of carbon dioxide is also indispensable for the study of global warming. Sea surface turbulent fluxes of momentum, sensible heat, latent heat, and carbon dioxide were measured by using the eddy correlation method that is thought to be the most accurate method and free from assumptions. These surface heat flux data are combined with radiation fluxes and water temperature profiles to derive surface energy budget.

Methods

The surface turbulent flux measurement system (Fig. 2.1.3-1) consists of turbulence instruments (Kaijo Co., Ltd.) and ship motion sensors (Kanto Aircraft Instrument Co., Ltd.). The turbulence sensors include a three-dimensional sonic anemometer-thermometer (Kaijo, DA-600) and an infrared hygrometer (LICOR, LI-7500). The sonic anemometer measures three-dimensional wind components relative to the ship. The ship motion sensors include a two-axis inclinometer (Applied Geomechanics, MD-900-T), a three-axis accelerometer (Applied Signal Inc., QA-700-020), and a

three-axis rate gyro (Systron Donner, QRS-0050-100). LI7500 is a CO2/H2O turbulence sensor that measures turbulent signals of carbon dioxide and water vapor simultaneously.

These signals are sampled at 10 Hz by a PC-based data logging system (Labview, National Instruments Co., Ltd.). By obtaining the ship speed and heading information through the Mirai network system it yields the absolute wind components relative to the ground. Combining wind data with the turbulence data, turbulent fluxes and statistics are calculated on a real-time basis. These data are also saved in digital files every 0.1 second for raw data and every 1 minute for statistic data.

Fig. 2.1.3-1 Turbulent flux measurement system on the top deck of the foremast.

Preliminary results

Data will be processed after the cruise at Okayama University.

Data Archive

All data are archived at Okayama University, and will be open to public after quality checks and corrections by K. Yoneyama and/or O. Tsukamoto. Corrected data will be submitted to JAMSTEC Data Management Office.

Remarks

After the cruise, we found that the processing trouble for wind data occurred on 8 November 2005. Therefore, most of data would not be available.

### 2.1.4 Infrared radiometer

#### (1) Personnel

Hajime Okamoto (CAOS, Tohoku University): Principal Investigator
Shinichi Otake (CAOS, Tohoku University): Student
Nobuo Sugimoto (National Institute for Environmental Studies)
Ichiro Matsui (National Institute for Environmental Studies)
Akihide Kamei (National Institute for Environmental Studies)
Toshiaki Takano (Chiba University)

#### (2) Objective

The infrared radiometer (hereafter IR) is used to derive the temperature of the cloud base and emissivity of the thin clouds. Main objective is to use study clouds and climate system in tropics by the combination of IR with active sensors such as lidar and 95GHz cloud radar. From these integrated approaches, it is expected to extend our knowledge of clouds and climate system. Special emphasis is made to retrieve cloud microphysics in upper part of clouds, including sub-visual clouds that is recognized to be a key component for the exchange of water amount between troposphere and stratosphere.

#### (3) Method

IR instrument directly provides broadband infrared temperature (9.6-10.5μm).
General specifications of IR system (KT 19II, HEITRONICS)

| | |
|---|---|
| Temperature range | -100 to 100$^{o}$C |
| Accuracy | 0.5 $^{o}$C |
| Mode | 24hours |
| Time resolution | 1 min. |
| Field of view | Less than 1$^{o}$ (will be estimated later) |
| Spectral region | 9.6-10.5μm |

This is converted to broadband radiance around the wavelength region. This is further combined with the lidar or the radar for retrieval of cloud microphysics such as optical thickness at visible wavelength, effective particle size. The applicability of the retrieval technique of the synergetic use of radar/IR or lidar/IR is so far limited to ice clouds. The microphysics of clouds from these techniques will be compared with other retrieval technique such as radar/lidar one or radar with multi-parameter.

#### (4) Data archive

The data archive server is set inside Tohoku University and the original data and the results of the analyses will be available from us.

#### (5) Operations.

Basically the IRT is operated for 24 hours. In order to avoid direct sun light entering the lens of the IRT, we asked to the staffs in MIRAI to use a shutter (cover) on the top of the lens. And we also asked to use

the shutter when precipitation was expected.

(6) Condition of measurements

Surface condition of the lens used as a receiver for IRT measurements may be changing during the cruise due to the precipitation attached on the lens, and the damage of the lens affects the accuracy of the measurements. We recorded the surface of the lens to count the area where color changed from the original one. It is found the area has slightly increased from leg. 1to leg.2 and this may lead to slight increase of the observed value for temperature. The correction scheme for the radiances in IRT is currently developed by us for accurate estimation of the temperature by using the temperature at the cloud-base of low-level clouds.

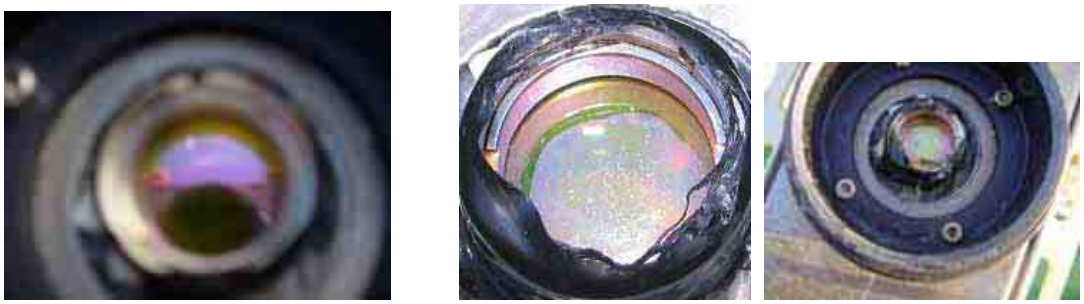

(a) (b) (c)

Fig.2.1.4 Photos of the surface of the lens in Infrared radiometer for cirrus cloud studies. (a) Nov. 13, 2005, during the leg.1 cruise. (b) Dec. 17, 2005 during leg.2 cruise. (c) Jan. 25 during leg.3 cruise.

**2.1.5.2 95GHz cloud profiling radar**

**(1) Personnel**

Hajime Okamoto (CAOS, Tohoku University): Principal Investigator
Toshiaki Takano (Chiba University)
Nobuo Sugimoto (National Institute for Environmental Studies)

**(2) Objective**

Main objective for the 95GHz cloud radar is to detect vertical structure of cloud and precipitation in the observed region. Combinational use of the radar and lidar is recognized to be a powerful tool to study vertical distribution of cloud microphysics, i.e., particle size and liquid/ice water content (LWC/IWC).

**(3) Method**

Basic output from data is cloud occurrence, radar reflectivity factor and cloud microphysics. In order to derive reliable cloud amount and cloud occurrence, we need to have radar and lidar for the same record.

Radar / lidar retrieval algorithm has been developed in Tohoku University. The algorithm is applied to water cloud in low level and also cirrus cloud in high altitude. In order to analyze the

radar data, it is first necessary to calibrate the signal to convert the received power to radar reflectivity factor, which is proportional to backscattering coefficient in the frequency of interest. Then we can interpolate radar and lidar data to match the same time and vertical resolution. Finally we can apply radar/lidar algorithm to infer cloud microphysics.

**(4) Data archive**

The data archive server is set inside Tohoku University and the original data and the results of the analyses will be available from us.

**(5) Operations**

The cloud radar is operated for 24 hours.

**(6) Preliminary data**

The time height cross section of radar signal obtained in Oct 12, 2005 during leg.1 cruise, Jan. 13 during leg.2 cruise and Jan.29 during leg.3 are shown in Fig.2.1.5.2.1(a), (b) and (c), respectively. Vertical extent is 20km. The frequent convective activities are seen.

The time-height cross section of clouds and precipitation.

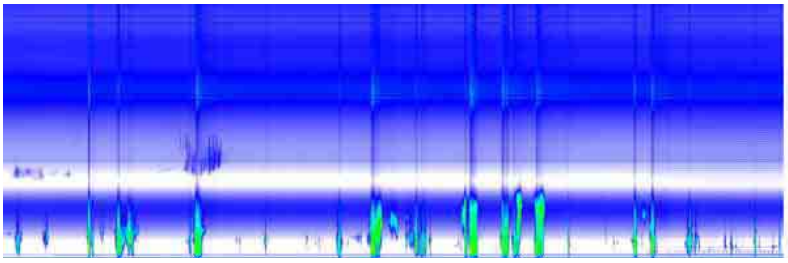

(a)

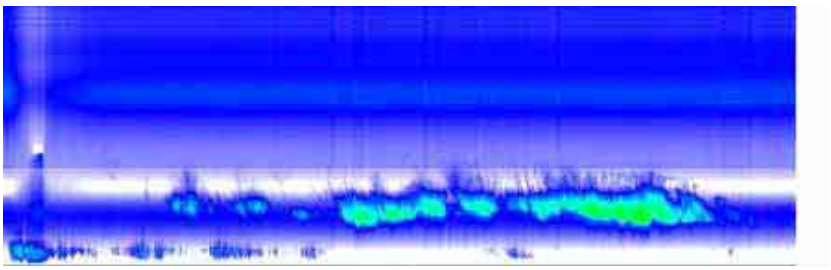

(b)

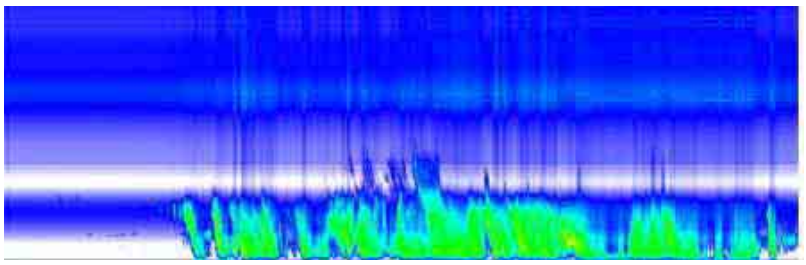

(c)

Fig 2.1.5.2.1 Time height cross section of radar reflectivity in (a) Oct.12, (b) Jan.13 and (c) Jan. 29 obtained by the 95GHZ FMCW radar during leg. 1,2 and 3 cruises

## 2.1.6 Sky Radiometer

**MR05-05 Leg1, 2 and 3 Cruise and Observation Report of the R/V Mirai**

**Special Observation:**

**Studies on behaviors and climate influence of atmospheric aerosols over the ocean**

**2.1.6.1.1 Name of research cruise**: Observational Research on transportation and fluctuations of heat and substance by oceanic circulation / Observational Research to Understanding on Chemical Variation in Oceanic Environment over Central area of Northern Pacific Ocean, East China Sea and Tsusima Strait

**2.1.6.1.2 Observational duration**: From 31 October 2005-18 February 2006 ( 101 days )

**2.1.6.1.3 Area of ocean**: Central area of Northern Pacific Ocean, East China Seas and Tsusima Strait

**2.6.1.2.1. Objective theme**:

Investigation of horizontal distribution on the concentration and size distribution and optical properties of atmospheric aerosols at the surface and optical thickness of columnar aerosol over the ocean.

**2.6.1.2.2. Objects**:

To clear and solve the problems of horizontal distribution and optical properties of aerosols, some observations were carried out over the western North Pacific Ocean. Furthermore, collections of the data for calibration and validation to the remote sensing data were performed simultaneously

**2.6.1.3. Summery**: To obtain the data for calibration and validation between remote sensing and surface measurements over the ocean, a series of simultaneous observations has been carried out about optical properties such as scattering and absorption coefficients and radiative properties as optical properties of atmospheric aerosols, the concentration and size distribution of surface aerosols over the Central area of Northern Pacific Ocean, East China Seas and Tsusima Strait for 101 days from 31 October 2005-18 February 2006 ( 101 days ). In addition to that, a sky radiometer was examined for to a fully automated ship-borne instrument and improved to the practical usage on same board.

**2.6.1.4. Personnel**

**2.6.1.4. 1 Principal Investigator not on board**

Tatsuo ENDOH (Tottori University of Environmental Studies) Professor

**2.6.1.4.2 On board scientists**

Shuichi WATANABE ( JAMSTEC ) Chief Scientist
Ikuo KANEKO ( JAMSTEC ) Chief Scientist

**2.6.1.4.3 Co-workers not on board**

Sachio OHTA (Engineering environmental resource laboratory, Graduate school of engineering, Hokkaido University) Professor
Tamio TAKAMURA (Center of environmental remote sensing science, Chiba University) Professor
Teruyuki NAKAJIMA (Center of climate system research, University of Tokyo) Professor
Nobuo SUGIMOTO (National Institute for Environmental Studies, Japan) Chief Research Scientist

**2.6.1.5.1 Objects/Introduction**

One of the most important objects is the collection of calibration and validation data from the surface (Nakajima et al.1996, 1997 and 1999). It may be considered for the observation over the widely opening of the huge ocean to be desired ideally because of horizontal homogeneity. Furthermore, the back ground values of aerosol concentration are easily obtained over there (Ohta et al.1996, Miura et al. 1997 and Takahashi et al. 1996) and vertical profile of aerosol concentration are obtained by means of extrapolation up to the scale height. It is desired to compare the integrated value of these profile of aerosol concentration with optical thickness observed by the optical and radiative measurement (Hayasaka et al. 1998, Takamura et al.1994). Facing this object, the optical and radiative observations were carried out by mean of the Sky Radiometer providing more precise radiation data as the radiative forcing for global warming.

**2.6.1.5.2 Measuring parameters**

Atmospheric optical thickness, Ångström coefficient of wave length efficiencies,
Direct irradiating intensity of solar, and forward up to back scattering intensity with scattering angles of 2-140degree and seven different wave lengths
GPS provides the position with longitude and latitude and heading direction of the vessel, and azimuth and elevation angle of sun. Horizon sensor provides rolling and pitching angles.

**2.6.1.5.3 Methods**

The instruments used in this work are shown as following in Table-1.

Sky Radiometer was measuring irradiating intensities of solar radiation through seven different filters with the scanning angle of 2-140 degree. These data will provide finally optical thickness, Ångström exponent, single scattering albado and size distribution of atmospheric aerosols with a kind of retrieval method.

Optical Particle Counter was measuring the size of large aerosol particle and counting the number concentration with laser light scattering method and providing the size distribution in 0.3,0.5,1.0,2.0 and 5.0 micron of diameter with real time series display graphically.

**2.6.1.5.4 Results**

Information of data and sample obtained are summarized in Table-2. The sky radiometer has been going well owing to more calm and silent condition and circumstances about shivering problems provided

by the R/V Mirai whose engines are supported by well defined cushions. Therefore, measured values will be expected to be considerably stable and to provide good calculated parameters in higher quality. However, some noise waves were found to interfere the 16,13 and 12channel marine bands of VHF from the sky radiometer. Fortunately the origin and source were identified by using VHF wide band receiver and the interference waves were kept by fairly separating from two VHF antennae and decreased to recovery of 100%.

Aerosols size distribution of number concentration have been measured by the Particle Counter and data obtained are displayed in real time by a kind of time series *in situ* with 5stages of size range of 0.3, 0.5, 1.0, 2.0, and 5.0 micron in diameter.

**2.6.1.5.5 Data archive**

This aerosol data by the Particle Counter will be able to be archived soon and anytime. However, the data of other kind of aerosol measurements are not archived so soon and developed, examined , arranged and finally provided as available data after a certain duration. All data will be archived at TUES (Endoh),Tottori University of Environmental Studies, CCSR(Nakajima), University of Tokyo and CEReS (Takamura), Chiba University after quality check and submitted to JAMSTEC within 3-year.

**References**

Takamura, T., et al., 1994: Tropospheric aerosol optical properties derived from lidar, sun photometer and prtical counter measurements. Applied Optics, Vol. 33, No. 30,7132-7140.

Hayasaka, T., T. Takamura, et al., 1998: Stratification and size distribution of aerosols retrieved from simultaneous measurements with lidar, a sunphotometer, and an aureolemeter. Applied Optics, 37(1998), No 6, 961-970.

Nakajima, T., T. Endoh and others(7 parsons) 1999: Early phase analysis of OCTS radiance data for aerosol remote sensing., IEEE Transactions on Geoscience and Remote Sensing, Vol. 37, No. 2, 1575-1585.

Nakajima, T., et al., 1997: The current status of the ADEOS- Ⅱ /GLI mission. Advanced and Next-generation Satellites Ⅱ , eds. H. Fujisada, G . Calamai, M. N. Sweeting, SPIE 2957, 183-190.

Nakajima, T., and A. Higurashi, 1996: AVHRR remote sensing of aerosol optical properties in the Persian Gulf region, the summer 1991. J . Geophys. Res., 102, 16935-16946.

Ohta, S., et al., 1997: Variation of atmospheric turbidity in the area around Japan. Journal of Global Environment Engineering, Vol.3, 9-21.

Ohta, S., et al., 1996: Chemical and optical properties of lower tropospheric aerosols measured at Mt. Lemmon in Arizona, Journal of Global Environment Engineering,
Vol.2,67-78.

Takahashi, T., T. Endoh, et al., 1996: Influence of the growth mechanism of snow particles on their chemical composition. Atmospheric Environment, Vol.30, No. 10/11, 1683-1692.

Miura, K., S. Nakae, et al.,: Optical properties of aerosol particles over the Western Pacific Ocean, Proc. Int. Sym. Remote Sensing, 275-280, 1997.

### 2.1.7 Laser Radar

(1) Personnel

Nobuo Sugimoto, Ichiro Matsui, Atsushi Shimizu and Akihide Kamei (National Institute for Environmental Studies, not on board). Operation was supported by Akihito Hirai (Leg 1, Chiba University), Hideji Abe (Leg 2, Chiba University), and Chusei Fujiwara (Leg3, GODI).

(2) Objectives

Objectives of the observations in this cruise is to study distribution and optical characteristics of ice/water clouds and marine aerosols using a two-wavelength lidar.

(3) Measured parameters

- Vertical profiles of backscattering coefficient at 532 nm
- Vertical profiles of backscattering coefficient at 1064 nm
- Depolarization ratio at 532 nm

(4) Method

Vertical profiles of aerosols and clouds were measured with a two-wavelength lidar. The lidar employs a Nd:YAG laser as a light source which generates the fundamental output at 1064 nm and the second harmonic at 532 nm. Transmitted laser energy is typically 100 mJ per pulse at 1064 nm and 50 mJ per pulse at 532 nm. The pulse repetition rate is 10 Hz. The receiver telescope has a diameter of 20 cm. The receiver has three detection channels to receive the lidar signals at 1064 nm and the parallel and perpendicular polarization components at 532 nm. An analog-mode avalanche photo diode (APD) is used as a detector for 1064 nm, and photomultiplier tubes (PMTs) are used for 532 nm. The detected signals are recorded with a transient-recorder and stored on a hard disk with a computer. The lidar system was installed in the radiosonde container on the compass deck. The container has a glass window on the roof, and the lidar was operated continuously regardless of weather.

(5) Results

Data obtained in this cruise has not been analyzed. Quick-look figures of backscattering intensity at 532 nm, which were generated on board, on November 7, 2005 (Leg 1), January 7, 2006 (Leg 2), and January 20, 2006 (Leg 3) are shown below. On November 7, lower clouds and a marine boundary aerosol layer were detected at 1.5 km altitude. Cirrus clouds were located between 6.5 km and 11.5 km on this day. On January 7, a floating aerosol layer which is considered as an outflow from Eurasia continent was detected at around 4 km after 1630UTC. Other continental aerosol layers were observed on January 20. In this case, the highest layer was located around 7 km. Multi aerosol layers were clearly seen at around 1200UTC.

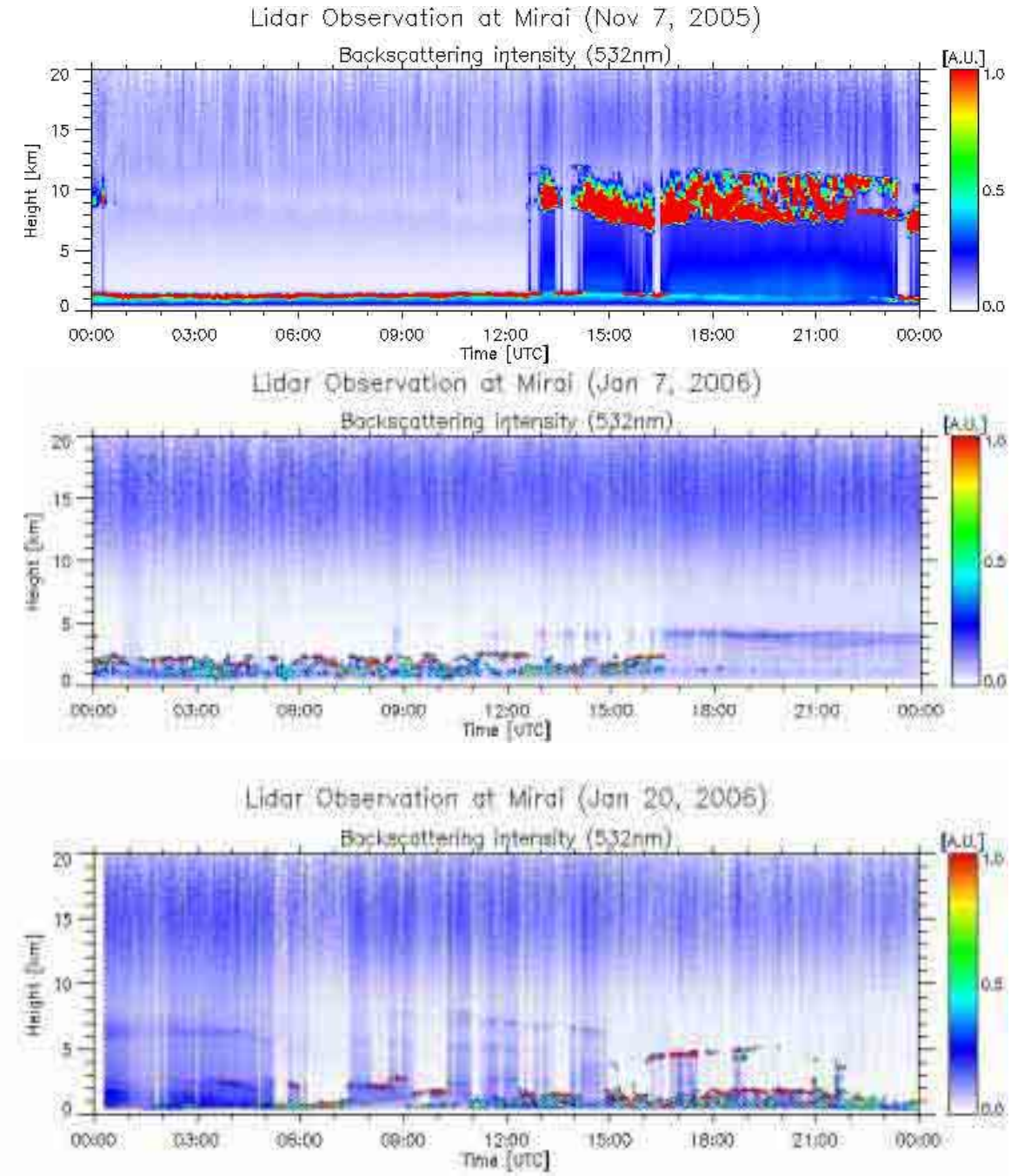


Figure 1. Examples of time-height indication of backscattering intensity at 532 nm on November 7, 2005 (upper), January 6, 2006 (middle), and January 20, 2006 (bottom).

(6) Data archive

- raw data

lidar signal at 532 nm
lidar signal at 1064 nm
depolarization ratio at 532 nm
temporal resolution 15 min.
vertical resolution 6 m.

data period : Oct 31, 2005 – Jan 18, 2006

- processed data

cloud base height, apparent cloud top height
phase of clouds (ice/water)
cloud fraction
boundary layer height (aerosol layer upper boundary height)
backscatter coefficient of aerosols
particle depolarization ratio of aerosols

### 2.1.8 Rain Sampling for Stable Isotopes

(1) Personnel

Kimpei Ichiyanagi (JAMSTEC) (Not on board)

(2) Objective

To determine the spatial distribution of isotopic composition of rainfall on the Ocean

(3) Method

Rainfall samples are collected in 6cc glass bottle with plastic cap. Isotopic compositions for hydrogen and oxygen in rainfall are determined by the Isotope Ratio Mass Spectrometry (IRMS).

(4) Preliminary results

During this cruise, we collected 22 samples in total. Table 2.1.7-1 lists the date and location of rainfall samples. Analysis will be done after the cruise.

(5) Data archive

Original samples will be analyzed by IORGC. Inventory and analyzed digital data will be submitted to JAMSTEC Data Management Office.

Table 2.1.7-1 Dates and locations to show when and where rain water were sampled.

| Sample No. | Date (UTC) | Location (lat/lon) | Rain (mm) |
|---|---|---|---|
| 001 | 03:00, November 8 | 24-14.20N, 134-00.30W | 0.3 |
| 002 | 21:06, November 11 | 24-15.51N, 141-51.17W | 0.6 |
| 003 | 16:20, November 16 | 24-14.13N, 154-37.59W | 1.6 |
| 004 | 22:32, November 19 | 25-09.84N, 161-58.56W | 1.5 |
| 005 | 01:10, November 20 | 25-08.08N, 162-01.74W | 1.3 |
| 006 | 05:51, November 22 | 24-28.74N, 168-52.84W | 1.4 |
| 007 | 16:32, November 22 | 22-47.77N, 166-29.47W | 1.2 |
| 008 | 23:26, November 22 | 22-17.33N, 165-14.83W | 1.2 |
| 009 | 02:35, November 23 | 22-02.35N, 164-36.79W | 0.3 |
| 010 | 16:15, November 23 | 21-00.80N, 162-07.74W | 3.8 |
| 011 | 15:10, December 1 | 24-01.27N, 167-14.52W | 0.9 |
| 012 | 22:25, December 3 | 23-41.85N, 171-23.87W | 1.5 |
| 013 | 06:13, December 5 | 24-14.64N, 174-49.05W | 1.4 |
| 014 | 22:50, December 8 | 24-13.63N, 178-27.18E | 0.7 |

| | | | |
|---|---|---|---|
| 015 | 07:51, December10 | 24-15.17N, 175-10.05E | 1.8 |
| 016 | 21:00, December23 | 24-02.70N, 164-59.09E | 38 |
| 017 | 05:07, December24 | 24-12.65N, 164-10.92E | 2.4 |
| 018 | 22:50, December25 | 24-16.28N, 160-04.37E | 0.5 |
| 019 | 04:44, December26 | 24-14.16N, 159-15.22E | 0.2 |
| 020 | 03:40, December27 | 24-13.36N, 156-50.47E | 0.6 |
| 021 | 00:30, January 7 | 24-13.93N, 136-11.10E | 1.5 |
| 022 | 00:57, January13 | 24-48.77N, 128-01.59E | 55 |

### 2.2.1 Navigation

| | |
|---|---|
| ***Souichiro Sueyoshi*** | *(Global Ocean Development Inc.)* |
| ***Katsuhisa Maeno*** | *(Global Ocean Development Inc.)* |
| ***Norio Nagahama*** | *(Global Ocean Development Inc.)* |
| ***Yasutaka Imai*** | *(Global Ocean Development Inc.)* |
| ***Shinya Okumura*** | *(Global Ocean Development Inc.)* |
| ***Ryo Ohyama*** | *(Global Ocean Development Inc.)* |

Navigation: Ship's position was measured by navigation system, made by Sena Co. Ltd, Japan. The system has two 12-channel GPS receivers (Leica MX9400N) and two 9-channel GPS receivers (Trimble DS-4000). GPS antennas located at Navigation deck, offset to starboard and portside, respectively. We switched them to choose better state of receiving when the number of GPS satellites decreased or HDOP increased. But the system sometimes lost the position while the receiving status became worse. The system also integrates gyro heading (Tokimec TG-6000), log speed (Furuno DS-30) and other navigation devices data on HP workstation. The workstation keeps accurate time using GPS Time server (Datum Tymserv2100) via NTP(Network Time Protocol). Navigation data was recorded as "SOJ" data every 60 seconds. The periods of losing the position are described in "Readme" file attached to SOJ data.

### 2.2.2 Bathymetry

| | |
|---|---|
| ***Tsuyoshi Matsumoto*** | *(Ryukyu Univ.) Principal Investigator / Not on-board:* |
| ***Souichiro Sueyoshi*** | *(Global Ocean Development Inc.)* |
| ***Katsuhisa Maeno*** | *(Global Ocean Development Inc.)* |
| ***Norio Nagahama*** | *(Global Ocean Development Inc.)* |
| ***Yasutaka Imai*** | *(Global Ocean Development Inc.)* |
| ***Shinya Okumura*** | *(Global Ocean Development Inc.)* |
| ***Ryo Ohyama*** | *(Global Ocean Development Inc.)* |

Bathymetry: R/V MIRAI equipped a Multi Narrow Beam Echo Sounding system (MNBES), SEABEAM 2112.004 (SeaBeam Instruments Inc.) The main objective of MNBES survey is collecting continuous bathymetry data along ship's track to make a contribution to geological and geophysical investigations and global datasets. We carried out bathymetric survey during the MR05-05 Leg1 cruise from CTD station P03-001c on 31 Oct 2005 to CTD station P03-146 on 22 Oct. 2005, Leg2 cruise from CTD station P03-146 on 30 Nov 2005 to CTD station P03-351 on 15 Jan 2006, Leg3 cruise from CTD station P03-370 on 20 Jan 2006 to

CTD station TS-1 on 26 Jan 2006. Data interval along ship's track was max 17 seconds at 6,000 m. To get accurate sound velocity of water column for ray-path correction of acoustic multibeam, we used Surface Sound Velocimeter (SSV) data at the surface (6.2m) sound velocity, and the others depth sound velocity was calculated using temperature and salinity profiles from the nearest CTD data by the equation in Mackenzie (1981).

System configuration and performance of SEABEAM 2112.004,

| | |
|---|---|
| Frequency: | 12 kHz |
| Transmit beam width: | 2 degree |
| Transmit power: | 20 kW |
| Transmit pulse length: | 3 to 20 msec. |
| Depth range: | 100 to 11,000 m |
| Beam spacing: | 1 degree athwart ship |
| Swath width: | 150 degree (max)<br>120 degree to 4,500 m<br>100 degree to 6,000 m<br>90 degree to 11,000 m |
| Depth accuracy: | Within < 0.5% of depth or +/-1m, whichever is greater, over the entire swath.<br>(Nadir beam has greater accuracy; typically within < 0.2% of depth or +/-1m, whichever is greater) |

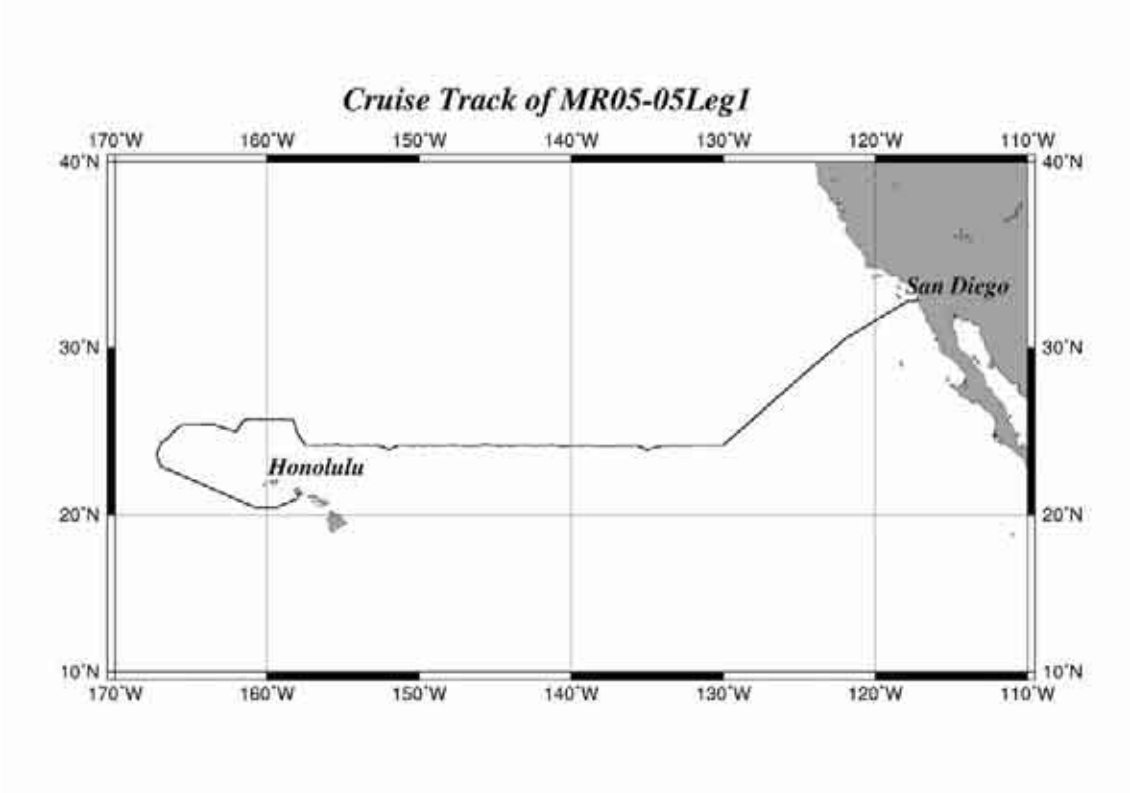


Figure 2.2.1-1 Cruise Track of MR05-05Leg1

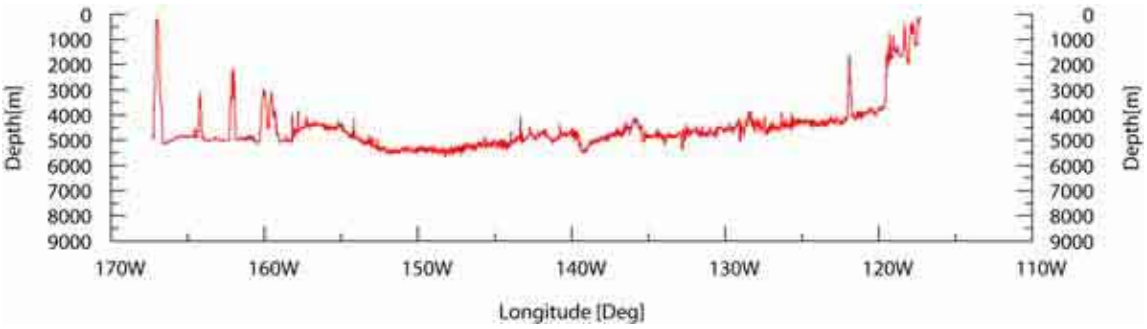


Figure 2.2.2-1 Depth of CTD line MR05-05Leg1

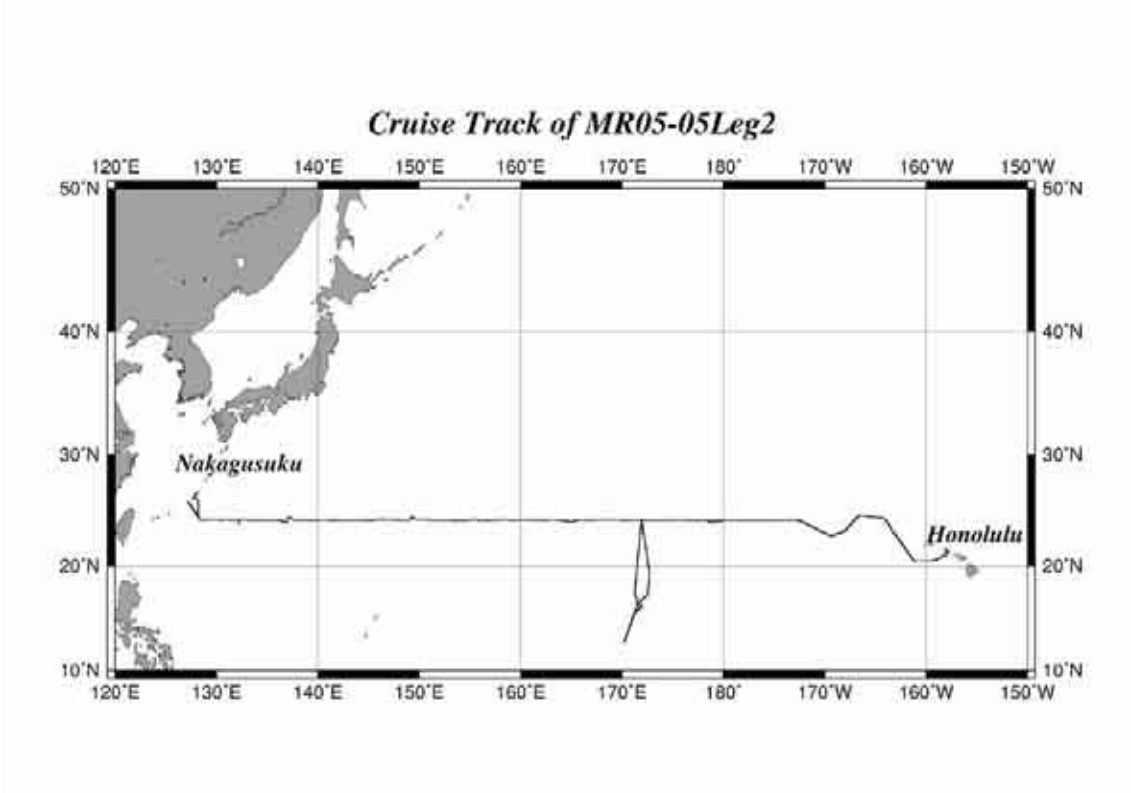


Figure 2.2.1-2 Cruise Track of MR05-05Leg2

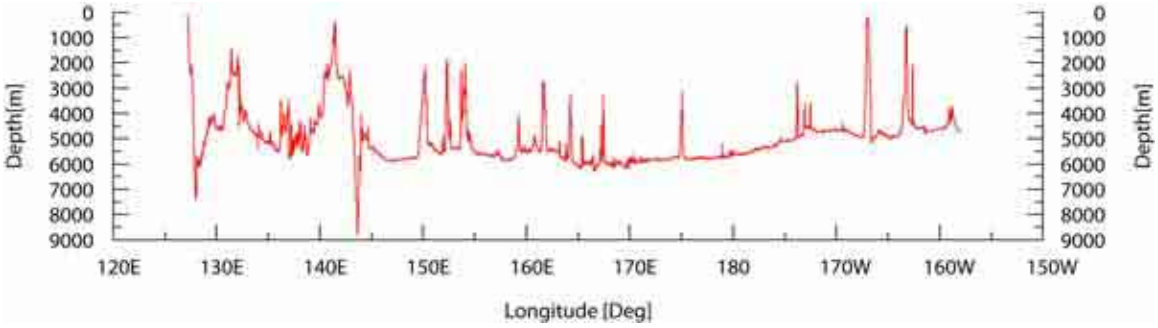


Figure 2.2.2-2 Depth of CTD line MR05-05Leg2

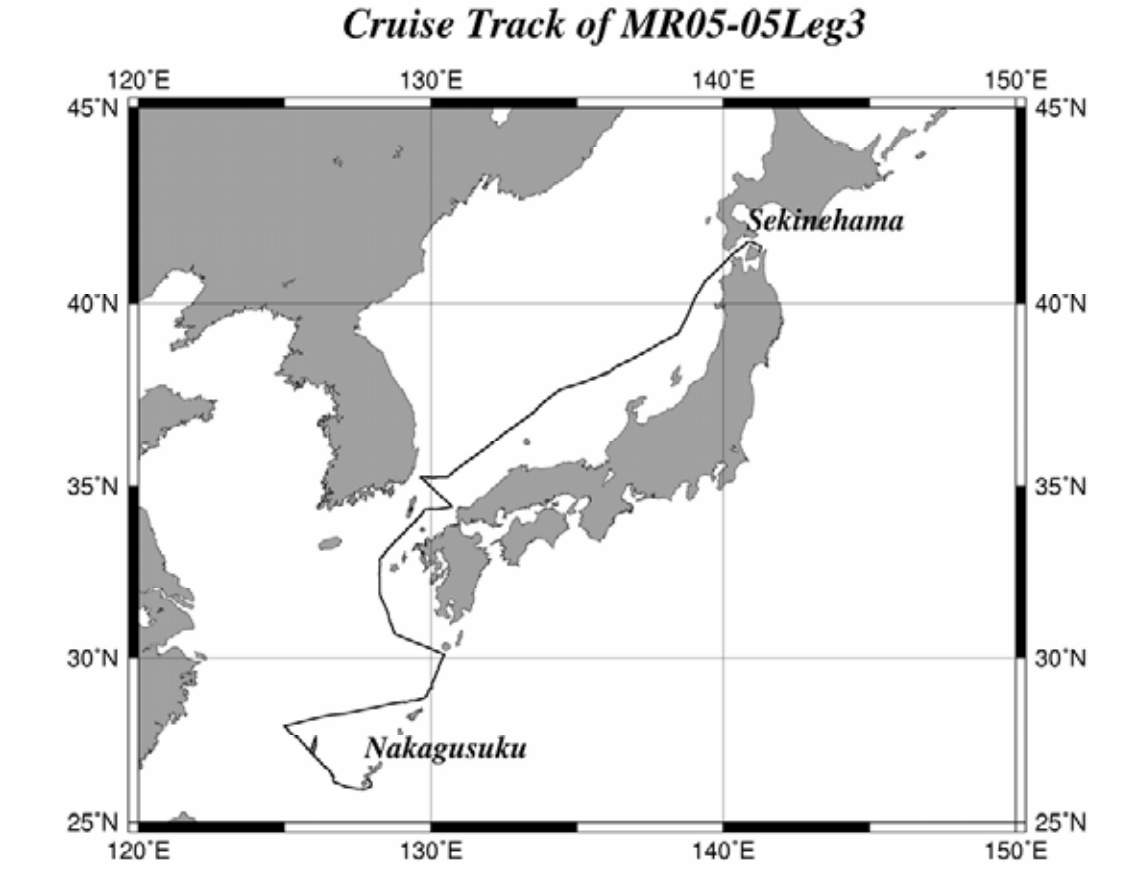


Figure 2.2.1-3 Cruise Track of MR05-05 Leg3

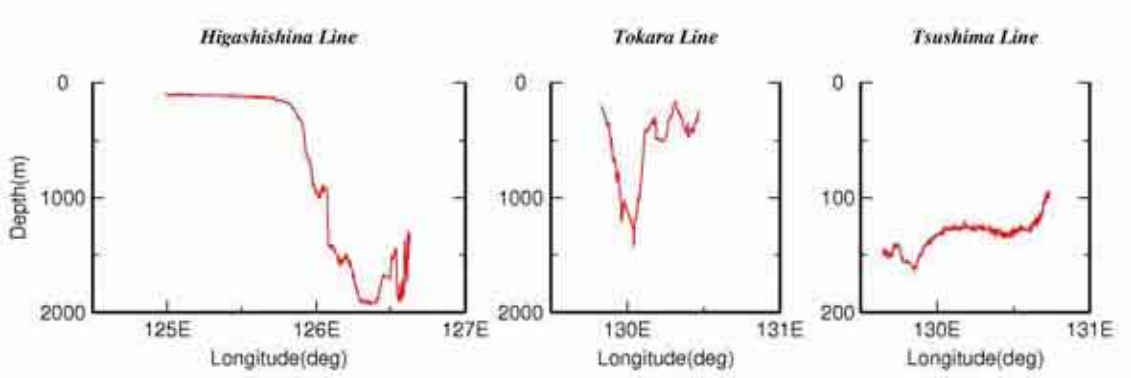


Figure 2.2.2-3 Depth of CTD line MR05-05 Leg3

### 2.2.3 Sea surface gravity

**Personnel**

*Tsuyoshi Matsumoto (Ryukyu Univ.) Principal Investigator / Not on-board:*
*Souichiro Sueyoshi (Global Ocean Development Inc.)*
*Katsuhisa Maeno (Global Ocean Development Inc.)*
*Norio Nagahama (Global Ocean Development Inc.)*
*Yasutaka Imai (Global Ocean Development Inc.)*
*Shinya Okumura (Global Ocean Development Inc.)*
*Ryo Ohyama (Global Ocean Development Inc.)*

**Introduction**

The difference of local gravity is an important parameter in geophysics and geodesy. We collected gravity data at the sea surface during MR05-05 Leg1 cruise from 31 Oct. 2005 to 24 Nov. 2005, Leg2 cruise from 27 Nov. 2005 to 17 Jan. 2006, Leg3 cruise from 20 Jan. 2005 to 30 Jan. 2006.

**Parameters**

Relative Gravity [mGal]

**Data Acquisition**

We have measured relative gravity using LaCoste and Romberg air-sea gravity system Ⅱ (LaCosat and Romberg Gravity Meters, Inc.) during this cruise. To convert the relative gravity to absolute one, we measured gravity, using portable gravity meter (Scintrex gravity meter CG-3), at Honolulu and Nakagusuku as reference points.

**Preliminary Results**

Absolute gravity shown in Table 2.2.3-1

| No. | Date | UTC | Port | Absolute Gravity (mGal) | Sea Level (cm) | Draft (cm) | Gravity at Sensor (mGal) | L&R (mGal) |
|---|---|---|---|---|---|---|---|---|
| 1 | 2005/Oct/31 | 14:23 | SanDiego | - | 240 | 636 | - | 11853.74 |
| 2 | 2005/Nov/25 | 21:59 | Honolulu | 978927.57 | 154 | 655 | 978928.10 | 11266.15 |
| 3 | 2006/Jan/19 | 01:53 | Nakagusuku | 979114.12 *3 | 219 | 622 | 979114.84 | 11456.52 |
| 4 | 2006/Jan/19 | 23:03 | Nakagusuku | 979114.12 *3 | 237 | 605 | 979114.88 | 11456.67 |

Table 2.2.3-1

*1: Gravity at Sensor= Absolute Gravity + Sea Level*0.3086/100 + (Draft-530)/100*0.0431

*2: LaCoste and Romberg air-sea gravity system Ⅱ

*3: It was measured at June 20, 2003.

**Data Archives**

Gravity data obtained during this cruise will be submitted to the JAMSTEC Data Management Division, and archived there.

**Remarks**

1. We did not collect data from 18:55UTC to 19:10UTC of 18 Nov. 2005, due to reboot the meter.
2. Long Accelerometer did not work normally from 31 Oct. 2005 to 18 Nov. 19:10. Therefore, Gravity, VCC and AL were not correct value.

### 2.2.4 On-board geomagnetic measurement

Personnel

| | |
|---|---|
| ***Tsuyoshi Matsumoto*** | ***(Ryukyu Univ.) Principal Investigator / Not on-board:*** |
| ***Souichiro Sueyoshi*** | ***(Global Ocean Development Inc.)*** |
| ***Katsuhisa Maeno*** | ***(Global Ocean Development Inc.)*** |
| ***Norio Nagahama*** | ***(Global Ocean Development Inc.)*** |
| ***Yasutaka Imai*** | ***(Global Ocean Development Inc.)*** |
| ***Shinya Okumura*** | ***(Global Ocean Development Inc.)*** |
| ***Ryo Ohyama*** | ***(Global Ocean Development Inc.)*** |

**Introduction**

Measurements of magnetic force on the sea are required for the geophysical investigations of marine magnetic anomaly caused by magnetization in upper crustal structure. We measured geomagnetic field using a three-component magnetometer during MR05-05 Leg1 cruise from 31 Oct. 2005 to 24 Nov. 2005, Leg2 cruise from 27. Nov 2005 to 17 Jan. 2006, Leg3 cruise from 20 Jan. 2006 to 30 Jan. 2006.

**Instruments on R/V Mirai**

A shipboard three-component magnetometer system (Tierra Tecnica SFG1214) is equipped on-board R/V Mirai. Three-axis flux-gate sensors with ring-cored coils are fixed on the fore mast. Outputs of the sensors are digitized by a 20-bit A/D converter (1 nT/LSB), and sampled at 8 times per second. Ship's heading, pitch and roll are measured utilizing a ring-laser gyro installed for controlling attitude of a Doppler radar. Ship's position (GPS) and speed data are taken from LAN every second.

**Data Archives**

Magnetic force data obtained during this cruise will be submitted to the JAMSTEC Data Management Division, and archived there.

## Remarks

1. We collected the data for calibration following period.
   11 Oct. 2005 00:00 – 00:23 (Leg1)
   08 Dec. 2005 05:58 – 06:22 (Leg2)
   01 Jan. 2006 03:55 – 04:21 (Leg2)
   28 Jan. 2006 08:25 – 08:50 (Leg3)

## 2.3 Acoustic Doppler Current Profiler

Yasushi Yoshikawa, Shinya Kouketsu (JAMSTEC), Souichiro Sueyoshi, Shinya Okumura, Katsuhisa Maeno, and Norio Nagahama (GODI)

(1) Instruments and method

The instrument used was an RDI 76.8kHz unit, hull-mounted on the centerline and approximately 23m aft of the bow at the water line. The firmware version was 5.59 and the data acquisition software was the RDI VMDAS Version. 1.4. The Operation was made from the first CTD station to the last CTD station in each leg. It was continued to the Sekine port in Leg3. The instrument was used in the water-tracking mode during the most of operations, recording each ping raw data in 8m x 90bin from about 23m to 735m in deep. Typical sampling interval was 3.5 seconds. Bottom track mode was added in the easternmost shallow water region. GPS gave the

navigation data. Two kinds of compass data were recorded. One was the ship's gyrocompass, which is connected the ADCP system directory, were stored with the ADCP data. Current field based on the gyrocompass was used to check the operation and the performance on board. Another compass used was the Inertial Navigation Unit (INU), DRU-H, Honeywell Inc. Its accuracy is 1.0mile (about 0.056 degree) and had already set on zero bias before the beginning of the cruise. The INU compass data were stored independently, and were combined with the ADCP data after the cruise.

(2) Performance of the ADCP data

The performance of the ADCP instrument was generally good: on streaming, profiles usually reached to about 600m. Profiles were rather bad on CTD station. The profiles were sometimes obtained from 200m to 500m. In these cases the ADCP signal was weak typically at about 350m in depth. It is probably due to the babbles from the bow-thruster. The performance of the ADCP was bad on streaming around 130 W because of the less reflection of the sound. The NMEA data from the GPS was changed from the GPS2 to the SKYFIX2 on 00:20 November 7 because of higher HDOP.

(3) Data processing

We processed ADCP data as described below. ADCP-coordinate velocities were converted to the earth-coordinate velocities using the ship heading from the INU. The earth-coordinate currents were obtained by subtracting ship velocities from the earth-coordinate velocities. Corrections of the misalignment and scale factors were made by using the bottom track data obtained during the engineering test cruise carried out in May 2005. The misalignment angle was calculated to be 0.05 degree and the scale factor was 0.975. These parameters were similar to those calculated in August 2003. Criteria for the correlation less than 64 and error velocity more than 20 mm/s are removed here. Therefore the error is estimated at 20 mm/s.

The flow measured the shipboard ADCP along the ship track is shown in the Figure. 2.3.1. The data when the ship was moving are used to plot. Eddy-like structures were seen in the mid ocean. A Strong current associated with the Kuroshio was seen in the western boundary region. The flow in the 400-meter in depth was somewhat southward along 24.5 N. It might be due to incomplete correction of the misalignment. We would make further check after the cruise by using the data obtained during the CTD operation and also the bottom track data during the cruise. The flow in the leg 3 is shown in Figure 2.3.2. The strong current of the Kuroshio was observed clearly.

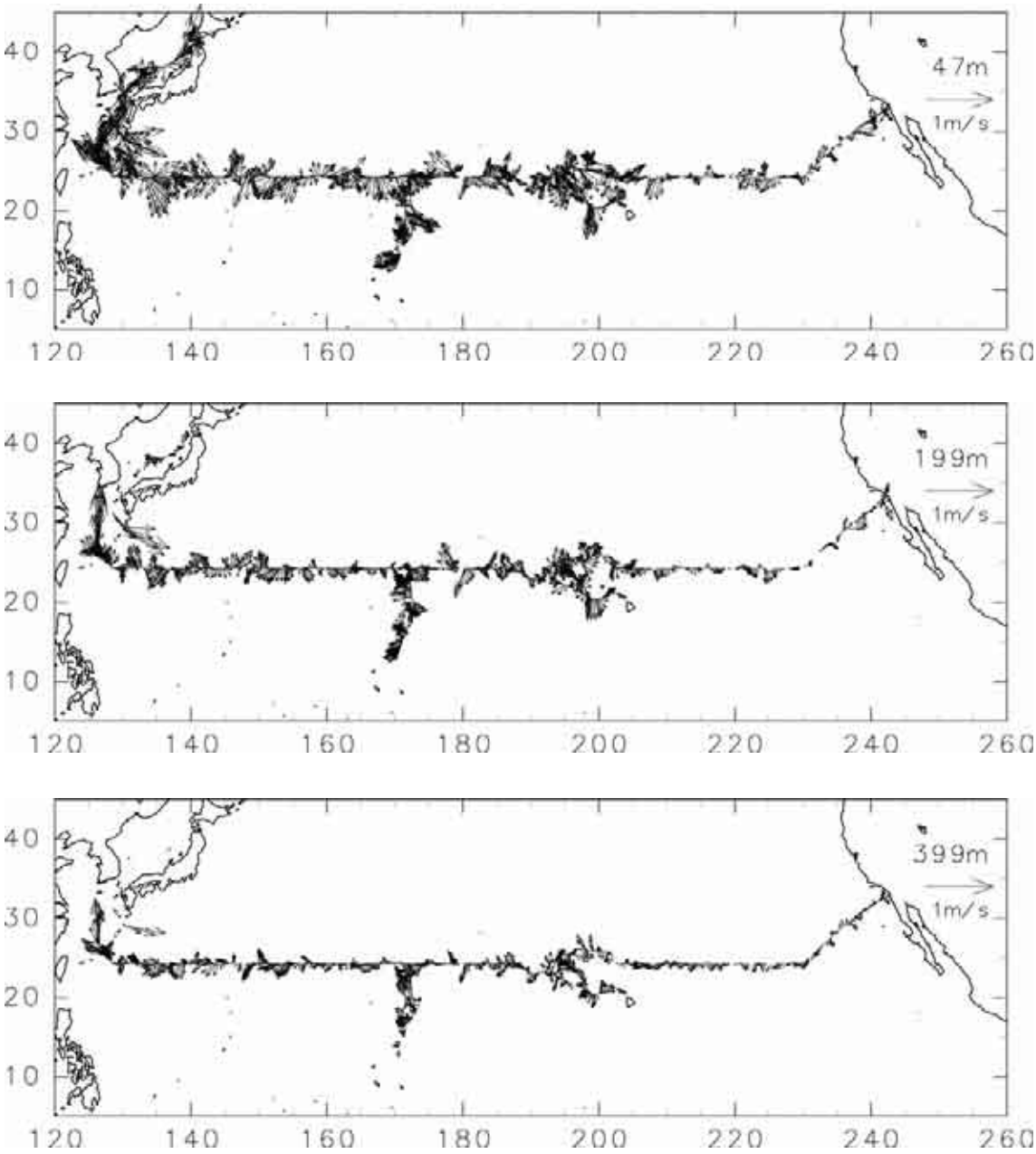


Figure 2.3.1. Flow distribution measured by the shipboard ADCP. The depths are about 50m (top), 200m (middle), and 400m (bottom), respectively.

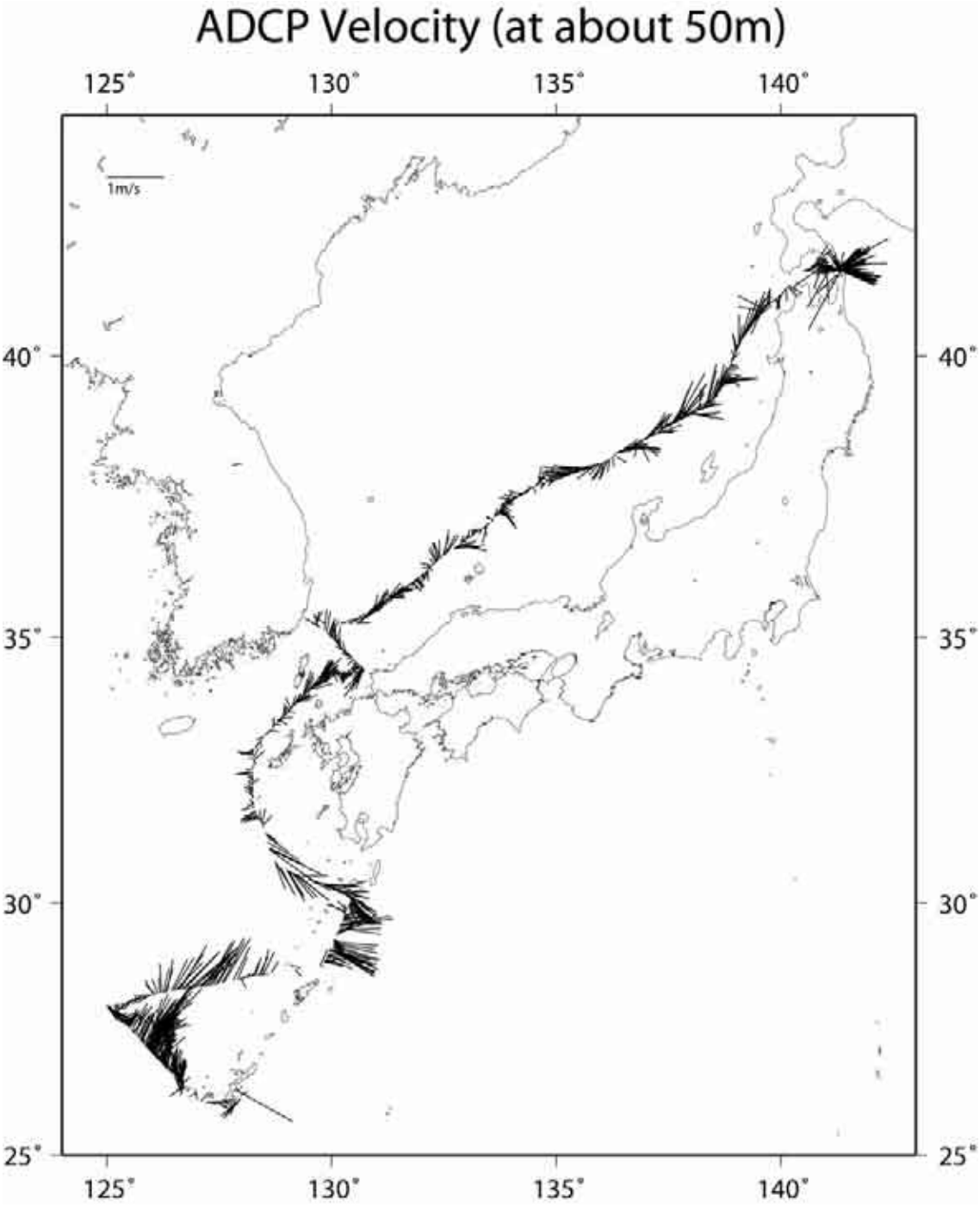


Figure 2.3.2. Flow distribution measured by the shipboard ADCP in Leg.3. The depth is 50 meters. There were three sections across the Kuroshio.

Raw data are filtered by using the median filter every 3 minutes. There are about 90 data in one ensemble. In vertical direction 3 bins data are used, which would mean 24 m averaging in the filtering process. Time series of upper 25 bins average flow are calculated using the 3 minutes sub set. The continuity of the series is examined in order to use each to average on the CTD site and on streaming between the sites.

Cross-sections of the velocity field are shown in Fig. 2.3.3. The quality controls of the data set should be made after the cruise. The flow around 400-meter in depth, where the questionable peak appears, should be examined in the next procedure.

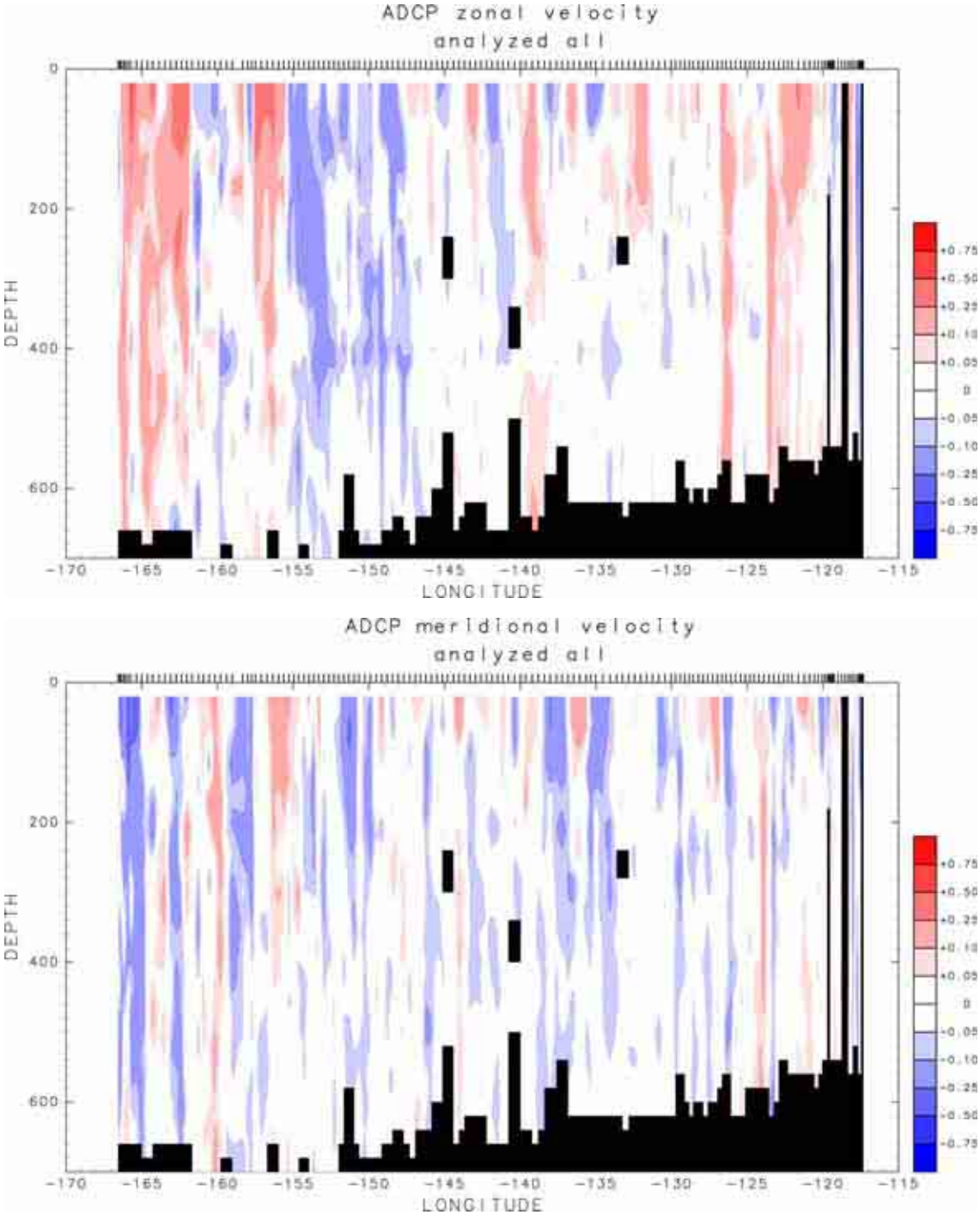


Figure 2.3.3. Cross-sections of the flow measured by the ADCP; the zonal component (top) and the meridional component (bottom). Shadows area indicates the non-available in the first process.

## 2.4 Thermo-salinograph

30-Jan.-2006

### 2.4.1 Personnel

Yuichiro KUMAMOTO [1)], Takeshi KAWANO[1)], Takuhei SHIOZAKI [2)], Keisuke WATAKI [2)], Kimiko NISHIJIMA [2)], Takayoshi SEIKE [2)], Osamu YOSHIDA[3)]

1) Japan Agency for Marine Earth Science and Technology

2) Marine Works Japan Co. Ltd.

3) Tokyo Institute of Technology

### 2.4.2 Objective

Our purpose is to measure salinity, temperature, dissolved oxygen, fluorescence, and particle size and number in near-sea surface water during MR05-05 cruise.

### 2.4.3 Methods

The Continuous Sea Surface Water Monitoring System (Nippon Kaiyo Co. Ltd.), including the thermo-salinograph, has six kind of sensors and can automatically measure salinity, temperature, dissolved oxygen, fluorescence and particle size and number in near-sea surface water every one minute. This system is located in the sea surface monitoring laboratory on R/V MIRAI and connected to shipboard LAN system. Measured data, time, and location of the ship were displayed on a monitor and then stored in a data management PC (IBM NetVista 6826-CBJ).

Near-surface water was continuously pumped up to the laboratory from about 4 m water depth and flowed into the system through a vinyl-chloride pipe. The flow rate of the surface seawater was controlled by several valves and adjusted to be 12 L/min except for a fluorometer (about 0.3 L/min). The flow rate was measured by two flow meters.

During this cruise, the data management PC had a problem in data acquisition of dissolved oxygen and particle counting and sizing. Thus, we connected another computer (IBM ThinkPad T41) to the system for data storage.

Specifications of the each sensor in this system are listed below.

a) Temperature and salinity sensors*

SEACAT THERMOSALINOGRAPH

| | | |
|---|---|---|
| Model: | SBE-21, SEA-BIRD ELECTRONICS, INC. | |
| Serial number: | 2118859-3126 | |
| Measurement range: | Temperature -5 to +35℃, | Salinity 0 to 6.5 S $m^{-1}$ |
| Accuracy: | Temperature 0.01 ℃ 6$month^{-1}$, | Salinity 0.001 S $m^{-1}$ $month^{-1}$ |
| Resolution: | Temperatures 0.001℃, | Salinity0.0001 S $m^{-1}$ |

b) Bottom of ship thermometer

| | |
|---|---|
| Model: | SBE 3S, SEA-BIRD ELECTRONICS, INC. |
| Serial number: | 032607 |
| Measurement range: | -5 to +35℃ |
| Resolution: | ±0.001℃ |
| Stability: | 0.002 ℃ $year^{-1}$ |

c) Dissolved oxygen sensor

Model: 2127A, HACH ULTRA ANALYTICS JAPAN, INC.
Serial number: 47477
Measurement range: 0 to 14 ppm
Accuracy: ±1% at 5 ℃ of correction range
Stability: 1% $month^{-1}$

d) Fluorometer

Model: 10-AU-005, TURNER DESIGNS
Serial number: 5562 FRXX
Detection limit: 5 ppt or less for chlorophyll a
Stability: 0.5% month-1 of full scale

e) Particle Size sensor

Model: P-05, Nippon Kaiyo LTD.
Serial number: P5024
Measurement range: 0.2681 mm to 6.666 mm
Accuracy: ±10% of range
Reproducibility: ±5%
Stability: 5% $week^{-1}$

f) Flow meter

Model: EMARG2W, Aichi Watch Electronics LTD.
Serial number: 8672
Measurement range: 0 to 30 l $min^{-1}$
Accuracy: ±1%
Stability: ±1% $day^{-1}$

*During the past cruises, an antifoulant (antibiotic) device including TBTO (tributyltin oxide) was attached to the salinity sensor to control growth of aquatic organisms in electronic conductivity sensors. TBTO is one of endocrine disrupting chemicals and restricted its use in the environments by law. Consequently, we did not use the antifoulant device during this cruise. After Leg-2, we found biogenic stains on the temperature and salinity sensors that had not been found at the end of Leg-1 cruise. Effectiveness of the antibiotic device is uncertain, however the device should be attached to the temperature and salinity sensors in cruises more than one month.

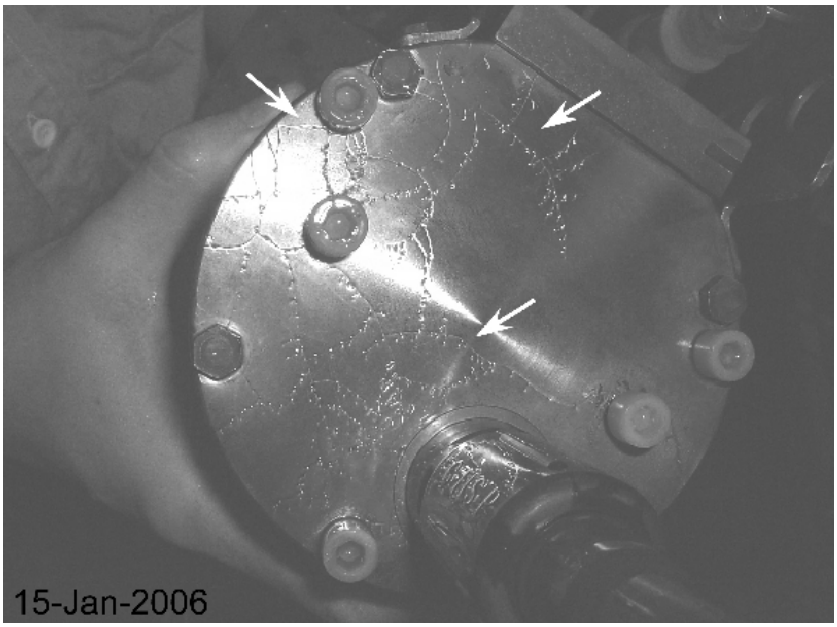


Photo 2.4-1

**2.4.4 Measurments**

Periods of measurement, maintenance, and problems during MR05-05 are listed in Table 2.4-1.

Table 2.4-1 Events list of the thermo-salinograph

| Date [UTC] | Time [UTC] | Event | Remarks |
|---|---|---|---|
| 31-Oct-05 | 18:13 | All the measurements started. | Leg-1 start |
| 11-Nov-05 | 02:45～03:46 | The fluorescence measurement stopped for cell cleaning. | |
| 23-Nov-05 | 22:57 | All the measurements stopped. | Leg-1 end |
| 29-Nov-05 | 06:53 | All the measurements started. | Leg-2 start |
| 14-Dec-05 | 20:23～21:50 | The fluorescence measurement stopped for cell cleaning. | |
| 15-Jan-06 | 05:12 | All the measurements stopped. | Leg-2 end |
| 20-Jan-06 | 04:32 | All the measurements started. | Leg-3 start |
| 25-Jan-06 | 05:48～07:14 | Failure of data storage for T, S, Flu, location due to problems of the PC. | |
| 26-Jan-06 | 07:58～09:04<br>09:13～09:39 | Failure of data storage for T, S, Flu, location due to problems of the PC. | |
| 26-Jan-06 | 09:13～09:28 | Failure of data storage for oxygen and particle size due to problems of the PC. | |
| 27-Jan-06 | 23:27 | All the measurements stopped. | Leg-3 end |

**2.4.5 Calibrations**

We collected the surface seawater samples approximately twice a day from the outlet equipped in the middle of water line of the system for salinity sensor calibration. A 250ml brown grass bottle with plastic inner stopper and screw cap was used to collect the samples. The sample bottles were

stored in the sea surface monitoring laboratory. The samples were measured using the Guildline 8400B at the end of the legs after all the measurements of hydrocast bottle samples. The measurement technique was almost same as that for bottle salinity measurement. The results are shown in Table 2.4-2.

In order to calibrate the fluorescence sensor, Tokyo Institute of Technology group collected the surface seawater at noon and ~4 hours after the sunset for measurement of chlorophyll-*a*. 500 ml of the seawater sample was gently filtrated by low vacuum pressure (<15 cmHg) through Whatman GF/F filter (diameter 25 mm) in a dark room. The filter was immediately transferred into 7 ml of N,N-dimethylformamide (DMF) and then the bottle of DMF was stored at –20℃ under the dark condition to extract chlorophyll-*a* for more than 24 hours. Concentrations of chlorophyll-*a* were measured by a fluorometer (10-AU-005, TURNER DESIGNS) that was previously calibrated against a pure chlorophyll-*a* (Sigma chemical Co.). We carried out "Non-acidification method" (Welschmeyer, 1994) for chlorophyll-*a* measurements. The results of the measurements of chlorophyll-*a* are shown in Table 2.4-3.

Sensors of dissolved oxygen and particle size were not calibrated during this cruise.

**2.4.6 Date archive**

The data were stored on a magnetic optical disk. The disk will be submitted to the Data Management Office (DMO) of JAMSTEC and public via R/V MIRAI Data Web Page in the JAMSTEC web page.

Table 2.4-2 Comparison of the sensor salinity and the bottle salinity.

| Date [UTC] | Time [UTC] | Sensor salinity [PSS-78] | Bottle salinity [PSS-78] | Quality Flag for bottle salinity |
|---|---|---|---|---|
| 2-Nov-05 | 6:50 | 33.5700 | 33.5695 | 2 |
| 3-Nov-05 | 8:22 | 33.1737 | 33.1713 | 2 |
| 4-Nov-05 | 6:13 | 33.6508 | 33.6571 | 3 |
| 5-Nov-05 | 5:17 | 34.2141 | 34.2115 | 2 |
| 6-Nov-05 | 8:26 | 34.5818 | 34.5795 | 2 |
| 7-Nov-05 | 8:00 | 34.8829 | 34.8789 | 2 |
| 8-Nov-05 | 7:46 | 35.0396 | 35.0376 | 2 |
| 9-Nov-05 | 5:59 | 35.2435 | 35.2407 | 2 |
| 10-Nov-05 | 7:10 | 35.1329 | 35.1297 | 2 |
| 11-Nov-05 | 2:40 | 35.1480 | 35.1459 | 2 |
| 12-Nov-05 | 8:16 | 35.1758 | 35.1731 | 2 |
| 13-Nov-05 | 8:21 | 35.2669 | 35.2644 | 2 |
| 14-Nov-05 | 10:58 | 35.3217 | 35.3188 | 2 |
| 15-Nov-05 | 8:14 | 35.3293 | 35.3255 | 2 |
| 16-Nov-05 | 8:27 | 35.0564 | 35.0519 | 2 |
| 17-Nov-05 | 7:00 | 35.2159 | 35.2122 | 2 |
| 18-Nov-05 | 10:12 | 35.3360 | 35.3320 | 2 |
| 18-Nov-05 | 22:25 | 35.3442 | 35.3403 | 2 |
| 19-Nov-05 | 8:52 | 35.3532 | 35.3484 | 2 |
| 19-Nov-05 | 21:20 | 35.3188 | 35.3158 | 2 |
| 20-Nov-05 | 11:25 | 35.3493 | 35.3466 | 2 |
| 20-Nov-05 | 23:29 | 35.3597 | 35.3548 | 2 |
| 21-Nov-05 | 12:05 | 35.1876 | 35.1860 | 2 |
| 21-Nov-05 | 18:09 | 35.2402 | 35.2369 | 2 |
| 29-Nov-05 | 20:08 | 35.2438 | 35.2462 | 2 |
| 29-Nov-05 | 23:17 | 35.1937 | 35.1943 | 2 |
| 30-Nov-05 | 15:46 | 35.2185 | 35.2217 | 2 |
| 1-Dec-05 | 1:25 | 35.2297 | 35.2325 | 2 |
| 1-Dec-05 | 14:25 | 35.2561 | 35.2590 | 2 |
| 2-Dec-05 | 8:07 | 35.2581 | 35.2605 | 2 |
| 2-Dec-05 | 13:21 | 35.2560 | 35.2573 | 2 |
| 3-Dec-05 | 0:41 | 35.1905 | 35.1972 | 2 |

Table 2.4-2 continued.

| Date [UTC] | Time [UTC] | Sensor salinity [PSS-78] | Bottle salinity [PSS-78] | Quality Flag for bottle salinity |
|---|---|---|---|---|
| 3-Dec-05 | 15:12 | 35.1715 | 35.1738 | 2 |
| 4-Dec-05 | 0:44 | 35.2197 | 35.2220 | 2 |
| 4-Dec-05 | 13:59 | 35.2867 | 35.2874 | 2 |
| 5-Dec-05 | 0:47 | 35.3573 | 35.3594 | 2 |
| 5-Dec-05 | 13:36 | 35.2448 | 35.2460 | 2 |
| 6-Dec-05 | 1:25 | 35.2640 | 35.2658 | 2 |
| 6-Dec-05 | 13:33 | 35.2607 | 35.2663 | 2 |
| 7-Dec-05 | 1:00 | 35.2957 | 35.2981 | 2 |
| 7-Dec-05 | 13:28 | 35.3609 | 35.3635 | 2 |
| 8-Dec-05 | 1:00 | 35.3706 | 35.3732 | 2 |
| 9-Dec-05 | 1:38 | 35.3573 | 35.3590 | 2 |
| 9-Dec-05 | 9:02 | 35.3492 | 35.3494 | 2 |
| 9-Dec-05 | 14:28 | 35.3398 | 35.3414 | 2 |
| 10-Dec-05 | 1:56 | 35.3514 | 35.3536 | 2 |
| 10-Dec-05 | 14:25 | 35.2974 | 35.2998 | 2 |
| 11-Dec-05 | 2:10 | 35.2485 | 35.2508 | 2 |
| 11-Dec-05 | 14:30 | 35.2312 | 35.2333 | 2 |
| 12-Dec-05 | 2:18 | 35.2767 | 35.2751 | 2 |
| 12-Dec-05 | 19:46 | 34.9113 | 34.9100 | 2 |
| 13-Dec-05 | 5:32 | 34.8525 | 34.8533 | 2 |
| 13-Dec-05 | 20:55 | 34.8668 | 34.8662 | 2 |
| 14-Dec-05 | 9:51 | 34.8070 | 34.8062 | 2 |
| 14-Dec-05 | 21:32 | 34.8108 | 34.8095 | 2 |
| 15-Dec-05 | 13:57 | 34.7460 | 34.7482 | 2 |
| 15-Dec-05 | 20:08 | 34.7251 | 34.7255 | 2 |
| 16-Dec-05 | 13:48 | 34.7450 | 34.7477 | 2 |
| 16-Dec-05 | 18:51 | 34.7879 | 34.7876 | 2 |
| 17-Dec-05 | 1:58 | 34.7641 | 34.7631 | 2 |
| 17-Dec-05 | 14:40 | 34.7886 | 34.7886 | 2 |
| 18-Dec-05 | 11:02 | 34.7928 | 34.7894 | 2 |
| 18-Dec-05 | 14:27 | 34.8002 | 34.8000 | 2 |
| 19-Dec-05 | 8:39 | 34.8347 | 34.8312 | 2 |

Table 2.4-2 continued.

| Date [UTC] | Time [UTC] | Sensor salinity [PSS-78] | Bottle salinity [PSS-78] | Quality Flag for bottle salinity |
|---|---|---|---|---|
| 19-Dec-05 | 21:15 | 35.0004 | 35.0000 | 2 |
| 20-Dec-05 | 2:25 | 34.9669 | 34.9672 | 2 |
| 21-Dec-05 | 10:24 | 35.2600 | 35.2600 | 2 |
| 21-Dec-05 | 15:05 | 35.3098 | 35.3092 | 2 |
| 22-Dec-05 | 10:32 | 35.2453 | 35.2428 | 2 |
| 22-Dec-05 | 15:32 | 35.1821 | 35.1809 | 2 |
| 23-Dec-05 | 5:49 | 35.2539 | 35.2529 | 2 |
| 23-Dec-05 | 15:20 | 35.2687 | 35.2681 | 2 |
| 24-Dec-05 | 4:17 | 35.1506 | 35.1516 | 2 |
| 24-Dec-05 | 15:21 | 35.1108 | 35.1093 | 2 |
| 25-Dec-05 | 3:02 | 35.1697 | 35.1665 | 2 |
| 25-Dec-05 | 15:17 | 35.0202 | 35.0187 | 2 |
| 26-Dec-05 | 3:56 | 34.9861 | 34.9841 | 2 |
| 26-Dec-05 | 15:30 | 35.0344 | 35.0326 | 2 |
| 27-Dec-05 | 3:16 | 35.1956 | 35.1938 | 2 |
| 27-Dec-05 | 15:19 | 35.0220 | 35.0204 | 2 |
| 28-Dec-05 | 3:23 | 35.0168 | 35.0160 | 2 |
| 28-Dec-05 | 15:25 | 35.1121 | 35.1052 | 2 |
| 29-Dec-05 | 3:17 | 35.1368 | 35.1358 | 2 |
| 29-Dec-05 | 15:40 | 34.8900 | 34.8895 | 2 |
| 30-Dec-05 | 4:15 | 34.9790 | 34.9782 | 2 |
| 30-Dec-05 | 15:31 | 35.0010 | 35.0015 | 2 |
| 31-Dec-05 | 4:26 | 34.9686 | 34.9685 | 2 |
| 01-Jan-06 | 5:45 | 34.9579 | 34.9565 | 2 |
| 01-Jan-06 | 15:39 | 34.9594 | 34.9580 | 2 |
| 02-Jan-06 | 6:23 | 34.9835 | 34.9818 | 2 |
| 02-Jan-06 | 15:29 | 34.9401 | 34.9392 | 2 |
| 02-Jan-06 | 17:25 | 34.9542 | 34.9542 | 2 |
| 03-Jan-06 | 13:12 | 34.8194 | 34.8195 | 2 |
| 03-Jan-06 | 17:53 | 34.8762 | 34.8715 | 2 |
| 04-Jan-06 | 5:14 | 34.7966 | 34.7961 | 2 |
| 04-Jan-06 | 17:30 | 34.8093 | 34.8091 | 2 |

Table 2.4-2 continued.

| Date [UTC] | Time [UTC] | Sensor salinity [PSS-78] | Bottle salinity [PSS-78] | Quality Flag for bottle salinity |
|---|---|---|---|---|
| 05-Jan-06 | 6:43 | 34.8998 | 34.8989 | 2 |
| 05-Jan-06 | 17:38 | 34.9090 | 34.9085 | 2 |
| 06-Jan-06 | 6:47 | 34.8450 | 34.8434 | 2 |
| 06-Jan-06 | 17:51 | 34.8190 | 34.8180 | 2 |
| 07-Jan-06 | 7:59 | 34.8109 | 34.8101 | 2 |
| 07-Jan-06 | 17:42 | 34.6597 | 34.6584 | 2 |
| 08-Jan-06 | 8:01 | 34.7983 | 34.7971 | 2 |
| 08-Jan-06 | 18:20 | 34.6684 | 34.6674 | 2 |
| 09-Jan-06 | 20:46 | 34.7581 | 34.7569 | 2 |
| 10-Jan-06 | 13:37 | 34.7615 | 34.7667 | 2 |
| 10-Jan-06 | 17:45 | 34.6906 | 34.6897 | 2 |
| 11-Jan-06 | 6:11 | 34.8660 | 34.8650 | 2 |
| 11-Jan-06 | 17:47 | 34.7070 | 34.7076 | 2 |
| 12-Jan-06 | 8:57 | 34.7660 | 34.7654 | 2 |
| 12-Jan-06 | 17:34 | 34.7228 | 34.7217 | 2 |
| 13-Jan-06 | 6:46 | 34.7033 | 34.7006 | 2 |
| 13-Jan-06 | 17:37 | 34.7052 | 34.7038 | 2 |
| 14-Jan-06 | 7:31 | 34.6351 | 34.6353 | 2 |
| 14-Jan-06 | 17:44 | 34.6562 | 34.6549 | 2 |
| 20-Jan-06 | 5:50 | 34.7968 | 34.7928 | 2 |
| 20-Jan-06 | 18:35 | 34.6766 | 34.6693 | 2 |
| 21-Jan-06 | 5:36 | 34.6326 | 34.6265 | 2 |
| 21-Jan-06 | 17:57 | 34.5974 | 34.5979 | 2 |
| 22-Jan-06 | 5:46 | 34.5873 | 34.5817 | 2 |
| 22-Jan-06 | 17:20 | 34.6853 | 34.6788 | 2 |
| 23-Jan-06 | 5:42 | 34.7726 | 34.7714 | 2 |
| 23-Jan-06 | 18:06 | 34.6577 | 34.6525 | 2 |
| 24-Jan-06 | 5:44 | 34.6295 | 34.6273 | 2 |
| 24-Jan-06 | 18:07 | 34.6144 | 34.6033 | 2 |
| 25-Jan-06 | 5:46 | 34.5806 | 34.5724 | 2 |
| 25-Jan-06 | 17:52 | 34.5397 | 34.5399 | 2 |
| 26-Jan-06 | 5:41 | 34.5224 | 34.5162 | 2 |
| 26-Jan-06 | 18:14 | 34.2362 | 34.2482 | 2 |

Table 2.4-3 Comparison of sensor fluorescence and bottle chlorophyll-a.

| Date [UTC] | Time [UTC] | Sensor Fluorescence | Chlorophyll-a ( $\mu$ g/L) |
|---|---|---|---|
| 1-Nov-05 | 6:20 | 15.791 | 0.37 |
| 1-Nov-05 | 20:00 | 15.266 | 0.44 |
| 2-Nov-05 | 6:03 | 16.915 | 0.30 |
| 2-Nov-05 | 20:29 | 14.017 | 0.17 |
| 3-Nov-05 | 6:02 | 14.768 | 0.13 |
| 3-Nov-05 | 20:13 | 13.192 | 0.12 |
| 4-Nov-05 | 6:13 | 13.394 | 0.08 |
| 4-Nov-05 | 20:05 | 12.899 | 0.08 |
| 5-Nov-05 | 6:00 | 12.971 | 0.08 |
| 5-Nov-05 | 20:08 | 12.469 | 0.10 |
| 6-Nov-05 | 6:11 | 13.063 | 0.09 |
| 6-Nov-05 | 20:08 | 12.755 | 0.12 |
| 7-Nov-05 | 6:03 | 13.085 | 0.10 |
| 7-Nov-05 | 20:59 | 12.587 | 0.08 |
| 8-Nov-05 | 7:05 | 12.750 | 0.10 |
| 8-Nov-05 | 21:15 | 12.280 | 0.12 |
| 9-Nov-05 | 7:10 | 12.815 | 0.12 |
| 9-Nov-05 | 23:34 | 12.659 | 0.15 |
| 10-Nov-05 | 7:19 | 12.784 | 0.13 |
| 10-Nov-05 | 21:08 | 12.427 | 0.12 |
| 11-Nov-05 | 7:19 | 13.846 | 0.12 |
| 11-Nov-05 | 22:10 | 12.609 | 0.12 |
| 12-Nov-05 | 8:10 | 13.467 | 0.13 |
| 12-Nov-05 | 22:08 | 12.914 | 0.11 |
| 13-Nov-05 | 8:33 | 13.169 | 0.10 |
| 13-Nov-05 | 22:10 | 12.733 | 0.11 |
| 14-Nov-05 | 8:12 | 13.103 | 0.10 |
| 14-Nov-05 | 22:00 | 12.639 | 0.12 |
| 15-Nov-05 | 8:12 | 12.977 | 0.11 |
| 15-Nov-05 | 22:03 | 12.357 | 0.08 |
| 16-Nov-05 | 9:22 | 12.768 | 0.09 |
| 16-Nov-05 | 22:00 | 12.361 | 0.09 |

Table 2.4-3 continued.

| Date [UTC] | Time [UTC] | Sensor Fluorescence | Chlorophyll a ( $\mu$ g/L) |
|---|---|---|---|
| 17-Nov-05 | 8:07 | 12.623 | 0.11 |
| 17-Nov-05 | 22:35 | 12.353 | 0.11 |
| 18-Nov-05 | 8:25 | 12.652 | 0.12 |
| 18-Nov-05 | 22:15 | 12.260 | 0.11 |
| 19-Nov-05 | 8:52 | 12.803 | 0.08 |
| 19-Nov-05 | 22:10 | 12.305 | 0.08 |
| 20-Nov-05 | 8:06 | 12.589 | 0.08 |
| 20-Nov-05 | 22:15 | 12.542 | 0.09 |
| 21-Nov-05 | 8:10 | 13.062 | 0.12 |
| 21-Nov-05 | 22:15 | 12.828 | 0.13 |
| 21-Nov-05 | 22:15 | 12.828 | 0.13 |
| 22-Nov-05 | 8:11 | 13.125 | 0.16 |
| 22-Nov-05 | 22:10 | 13.035 | 0.15 |
| 22-Nov-05 | 22:10 | 13.035 | 0.18 |
| 29-Nov-05 | 23:27 | 13.936 | 0.14 |
| 30-Nov-05 | 9:00 | 13.722 | 0.14 |
| 30-Nov-05 | 9:00 | 13.722 | 0.15 |
| 30-Nov-05 | 23:22 | 12.934 | 0.13 |
| 30-Nov-05 | 23:22 | 12.934 | 0.13 |
| 01-Dec-05 | 9:01 | 13.479 | 0.12 |
| 02-Dec-05 | 1:45 | 13.153 | 0.13 |
| 02-Dec-05 | 10:08 | 13.229 | 0.08 |
| 02-Dec-05 | 10:08 | 13.229 | 0.08 |
| 02-Dec-05 | 23:50 | 12.193 | 0.10 |
| 02-Dec-05 | 23:50 | 12.193 | 0.10 |
| 03-Dec-05 | 9:01 | 12.679 | 0.08 |
| 03-Dec-05 | 23:29 | 12.356 | 0.14 |
| 04-Dec-05 | 9:00 | 12.600 | 0.12 |
| 04-Dec-05 | 9:00 | 12.600 | 0.12 |
| 04-Dec-05 | 23:28 | 11.957 | 0.10 |
| 04-Dec-05 | 23:28 | 11.957 | 0.10 |
| 05-Dec-05 | 9:39 | 12.214 | 0.10 |

Table 2.4-3 continued.

| Date [UTC] | Time [UTC] | Sensor Fluorescence | Chlorophyll a ( $\mu$ g/L) |
|---|---|---|---|
| 06-Dec-05 | 2:01 | 11.869 | 0.09 |
| 06-Dec-05 | 8:56 | 11.974 | 0.08 |
| 06-Dec-05 | 8:56 | 11.974 | 0.08 |
| 07-Dec-05 | 0:22 | 11.713 | 0.09 |
| 07-Dec-05 | 0:22 | 11.713 | 0.09 |
| 07-Dec-05 | 9:01 | 11.932 | 0.07 |
| 07-Dec-05 | 23:41 | 11.669 | 0.08 |
| 08-Dec-05 | 8:47 | 11.884 | 0.07 |
| 08-Dec-05 | 8:47 | 11.884 | 0.07 |
| 09-Dec-05 | 1:05 | 11.760 | 0.08 |
| 09-Dec-05 | 1:05 | 11.760 | 0.08 |
| 09-Dec-05 | 10:07 | 12.234 | 0.08 |
| 10-Dec-05 | 0:59 | 11.767 | 0.12 |
| 10-Dec-05 | 10:05 | 12.198 | 0.08 |
| 10-Dec-05 | 10:05 | 12.198 | 0.08 |
| 11-Dec-05 | 1:18 | 11.926 | 0.08 |
| 11-Dec-05 | 1:18 | 11.926 | 0.08 |
| 11-Dec-05 | 10:09 | 12.172 | 0.07 |
| 21-Dec-05 | 2:21 | 11.858 | 0.09 |
| 21-Dec-05 | 12:12 | 12.124 | 0.09 |
| 21-Dec-05 | 12:12 | 12.124 | 0.08 |
| 22-Dec-05 | 1:38 | 12.132 | 0.08 |
| 22-Dec-05 | 1:38 | 12.132 | 0.08 |
| 22-Dec-05 | 11:58 | 12.556 | 0.10 |
| 23-Dec-05 | 1:38 | 12.560 | 0.11 |
| 23-Dec-05 | 12:20 | 12.649 | 0.10 |
| 23-Dec-05 | 12:20 | 12.649 | 0.10 |
| 24-Dec-05 | 1:31 | 13.030 | 0.09 |
| 24-Dec-05 | 1:31 | 13.030 | 0.09 |
| 24-Dec-05 | 12:39 | 13.108 | 0.10 |
| 25-Dec-05 | 2:08 | 13.015 | 0.09 |
| 25-Dec-05 | 11:17 | 13.893 | 0.09 |

Table 2.4-3 continued.

| Date [UTC] | Time [UTC] | Sensor Fluorescence | Chlorophyll a ( $\mu$ g/L) |
|---|---|---|---|
| 26-Dec-05 | 1:23 | 13.137 | 0.12 |
| 26-Dec-05 | 1:23 | 13.137 | 0.12 |
| 26-Dec-05 | 10:35 | 13.459 | 0.12 |
| 27-Dec-05 | 1:34 | 13.209 | 0.14 |
| 27-Dec-05 | 11:51 | 13.308 | 0.11 |
| 27-Dec-05 | 11:51 | 13.308 | 0.12 |
| 28-Dec-05 | 1:42 | 13.408 | 0.11 |
| 28-Dec-05 | 1:42 | 13.408 | 0.11 |
| 28-Dec-05 | 10:53 | 14.309 | 0.13 |
| 29-Dec-05 | 1:47 | 13.215 | 0.13 |
| 29-Dec-05 | 11:08 | 13.639 | 0.10 |
| 29-Dec-05 | 11:08 | 13.639 | 0.09 |
| 30-Dec-05 | 1:35 | 13.246 | 0.14 |
| 30-Dec-05 | 1:35 | 13.246 | 0.13 |
| 30-Dec-05 | 11:12 | 14.087 | 0.13 |
| 31-Dec-05 | 1:42 | 12.956 | 0.13 |
| 31-Dec-05 | 10:57 | 13.773 | 0.15 |
| 31-Dec-05 | 10:57 | 13.773 | 0.15 |
| 02-Jan-06 | 2:44 | 12.987 | 0.15 |
| 02-Jan-06 | 2:44 | 12.987 | 0.15 |
| 02-Jan-06 | 13:07 | 13.275 | 0.13 |
| 03-Jan-06 | 3:29 | 12.960 | 0.10 |
| 03-Jan-06 | 13:46 | 13.116 | 0.10 |
| 03-Jan-06 | 13:46 | 13.116 | 0.10 |
| 04-Jan-06 | 3:20 | 13.127 | 0.12 |
| 04-Jan-06 | 3:20 | 13.127 | 0.12 |
| 04-Jan-06 | 12:22 | 13.009 | 0.12 |
| 05-Jan-06 | 3:37 | 13.136 | 0.10 |
| 05-Jan-06 | 14:03 | 13.950 | 0.13 |
| 05-Jan-06 | 14:03 | 13.950 | 0.13 |
| 06-Jan-06 | 3:40 | 13.146 | 0.22 |
| 06-Jan-06 | 12:25 | 14.240 | 0.25 |

Table 2.4-3 continued.

| Date [UTC] | Time [UTC] | Sensor Fluorescence | Chlorophyll a ( $\mu$ g/L) |
|---|---|---|---|
| 07-Jan-06 | 3:40 | 13.948 | 0.25 |
| 07-Jan-06 | 12:30 | 14.208 | 0.27 |
| 07-Jan-06 | 12:30 | 14.208 | 0.26 |
| 08-Jan-06 | 3:40 | 13.427 | 0.27 |
| 08-Jan-06 | 3:40 | 13.427 | 0.27 |
| 08-Jan-06 | 13:02 | 13.625 | 0.25 |
| 10-Jan-06 | 13:10 | 13.954 | 0.25 |
| 11-Jan-06 | 3:40 | 13.387 | 0.23 |
| 11-Jan-06 | 3:40 | 13.387 | 0.23 |
| 11-Jan-06 | 13:34 | 14.446 | 0.45 |
| 11-Jan-06 | 13:34 | 14.446 | 0.44 |
| 12-Jan-06 | 3:20 | 15.650 | 0.74 |
| 12-Jan-06 | 14:34 | 15.012 | 0.48 |
| 12-Jan-06 | 14:34 | 15.012 | 0.49 |
| 13-Jan-06 | 3:18 | 14.052 | 0.54 |
| 13-Jan-06 | 3:18 | 14.052 | 0.55 |
| 13-Jan-06 | 13:22 | 14.403 | 0.35 |
| 14-Jan-06 | 3:43 | 14.164 | 0.44 |
| 14-Jan-06 | 13:53 | 14.134 | 0.36 |
| 14-Jan-06 | 13:53 | 14.134 | 0.37 |
| 15-Jan-06 | 3:40 | 13.333 | 0.24 |
| 15-Jan-06 | 3:40 | 13.333 | 0.25 |
| 20-Jan-06 | 13:27 | 15.864 | 0.18 |
| 20-Jan-06 | 13:27 | 15.864 | 0.18 |
| 21-Jan-06 | 4:56 | 19.848 | 1.57 |
| 21-Jan-06 | 4:56 | 19.848 | 1.62 |
| 21-Jan-06 | 13:10 | 21.013 | 2.40 |
| 22-Jan-06 | 3:47 | 19.055 | 1.54 |
| 22-Jan-06 | 13:18 | 18.849 | 0.49 |
| 22-Jan-06 | 13:18 | 18.849 | 0.48 |
| 23-Jan-06 | 2:43 | 14.727 | 0.33 |
| 23-Jan-06 | 2:43 | 14.727 | 0.32 |

Table 2.4-3 continued.

| Date [UTC] | Time [UTC] | Sensor Fluorescence | Chlorophyll a ( $\mu$ g/L) |
|---|---|---|---|
| 23-Jan-06 | 12:34 | 16.606 | 0.47 |
| 24-Jan-06 | 3:42 | 16.021 | 0.63 |
| 24-Jan-06 | 12:36 | 19.706 | 0.83 |
| 24-Jan-06 | 12:36 | 19.706 | 0.88 |
| 25-Jan-06 | 3:45 | 20.538 | 2.20 |
| 25-Jan-06 | 3:45 | 20.538 | 2.16 |
| 25-Jan-06 | 13:22 | 25.41 | 3.02 |
| 26-Jan-06 | 6:17 | 21.289 | 1.34 |
| 26-Jan-06 | 14:03 | 23.116 | 0.56 |
| 26-Jan-06 | 14:03 | 23.116 | 0.55 |

## 2.5. $pCO_2$

***Akihiko Murata (JAMSTEC)***
***Fuyuki Shibata (MWJ)***
***Mikio Kitada (MWJ)***
***Minoru Kamata (MWJ)***
***Taeko Ohama (MWJ)***
***Masaki Moro (MWJ)***
***Yoshiko Ishikawa (MWJ)***

### 2.5.1 Objective

Concentrations of $CO_2$ in the atmosphere are now increasing at a rate of 1.5 ppmv $y^{-1}$ owing to human activities such as burning of fossil fuels, deforestation, and cement production. It is an urgent task to estimate the absorption capacity of the oceans against the increased atmospheric $CO_2$ as accurately as possible and to clarify the mechanism of the $CO_2$ absorption, because the magnitude of the anticipated global warming depends on the levels of $CO_2$ in the atmosphere, and because the ocean currently absorbs 1/3 of the 6 Gt of carbon emitted into the atmosphere each year by human activities.

In this cruise, we wee aimed at quantifying how much anthropogenic $CO_2$ is absorbed in the surface ocean in the North Pacific. For the purpose, we measured $pCO_2$ (partial pressures of $CO_2$) in the atmosphere and surface seawater.

### 2.5.2 Apparatus and performance

Concentrations of $CO_2$ in the atmosphere and the sea surface were measured continuously during the cruise using an automated system with a non-dispersive infrared (NDIR) analyzer (BINOS$^{TM}$). The automated system was operated on one and a half hour cycle. In one cycle, standard gases, marine air and an air in a headspace of an equilibrator were analyzed subsequently. The concentrations of the standard gases were 262.95, 320.44, 381.03 and 420.75 ppm. The standard

gases will be recalibrated after the cruise.

The marine air taken from the bow is introduced into the NDIR by passing through a mass flow controller which controls the air flow rate at about 0.5 L/min, a cooling unit, a perma-pure dryer (GL Sciences Inc.) and a desiccant holder containing $Mg(ClO_4)_2$.

A fixed volume of the marine air taken from the bow is equilibrated with a stream of seawater that flows at a rate of 5-6L/min in the equilibrator. The air in the equilibrator is circulated with a pump at 0.7-0.8L/min in a closed loop passing through two cooling units, a perma-pure dryer (GL Science Inc.) and a desiccant holder containing $Mg(ClO_4)_2$.

### 2.5.3 Results

Concentrations of $CO_2$ ($xCO_2$) of marine air and surface seawater during Leg 1 are shown in Figure 1. From this figure, it is found that the ocean acted as a source for atmospheric $CO_2$ during the former period of the cruise. However, it acted as a sink for atmospheric $CO_2$ during the latter period.

Concentrations of $CO_2$ ($xCO_2$) of marine air and surface seawater during Leg 2 are shown in Figure 2. From this figure, it is found that the ocean acted as a sink for atmospheric $CO_2$ during the Leg 2.

Concentrations of $CO_2$ ($xCO_2$) of marine air and surface seawater during Leg 3 are shown in Figure 3. From this figure, it is found that the ocean acted as a sink for atmospheric $CO_2$ during the Leg 3.

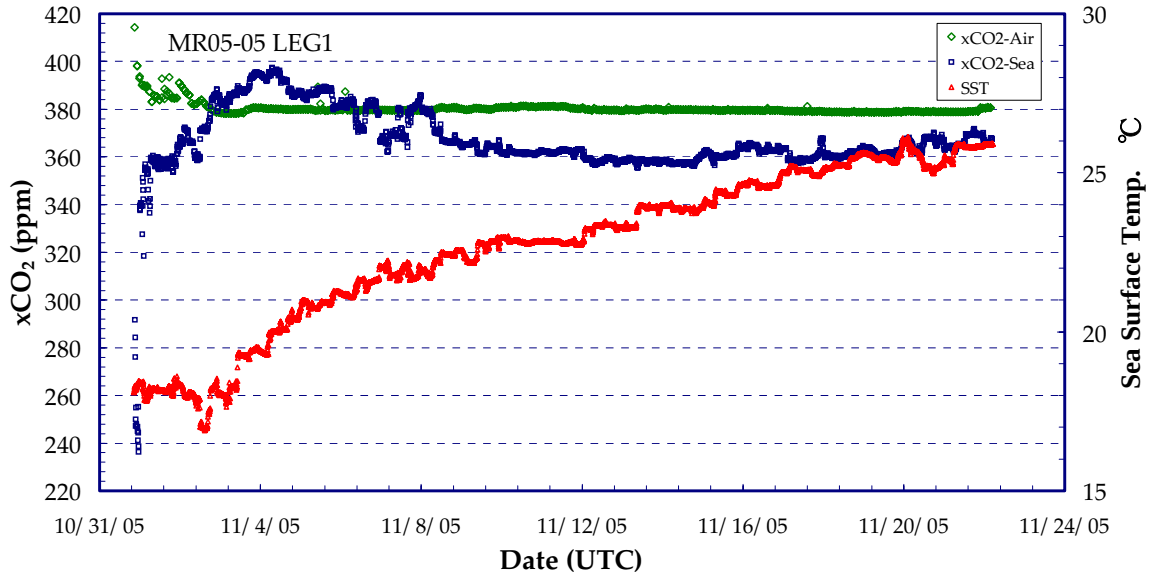


Figure 1. Temporal changes of concentrations of CO2 (xCO2) in atmosphere (green) and surface seawater (blue), and SST (red) during leg 1.

.

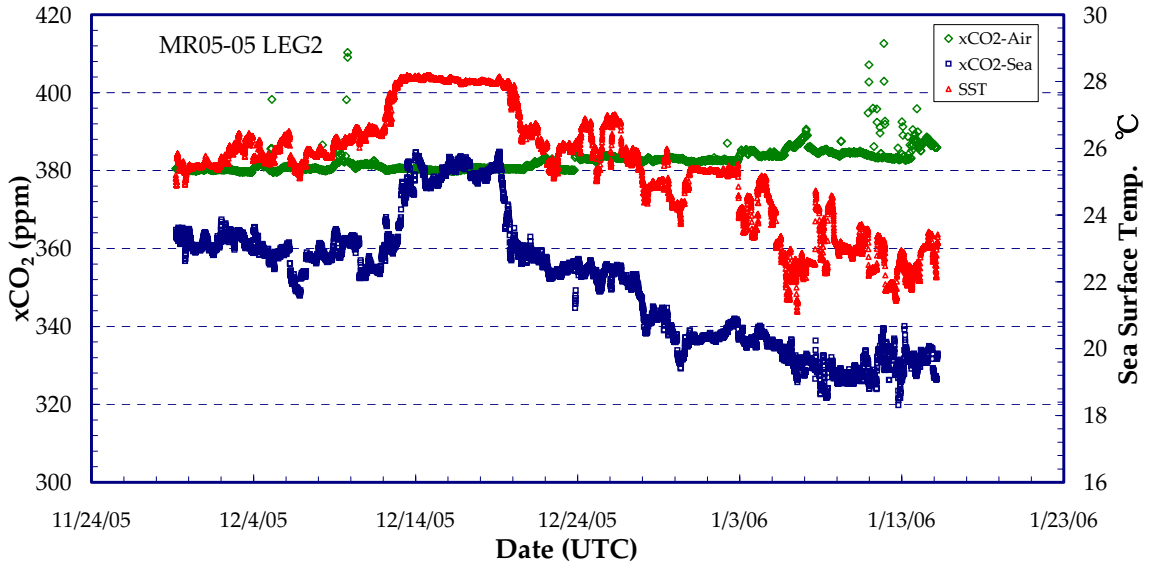


**Figure 2. Temporal changes of concentrations of $CO_2$ ($xCO_2$) in atmosphere (green) and surface seawater (blue), and SST (red) during leg2.**

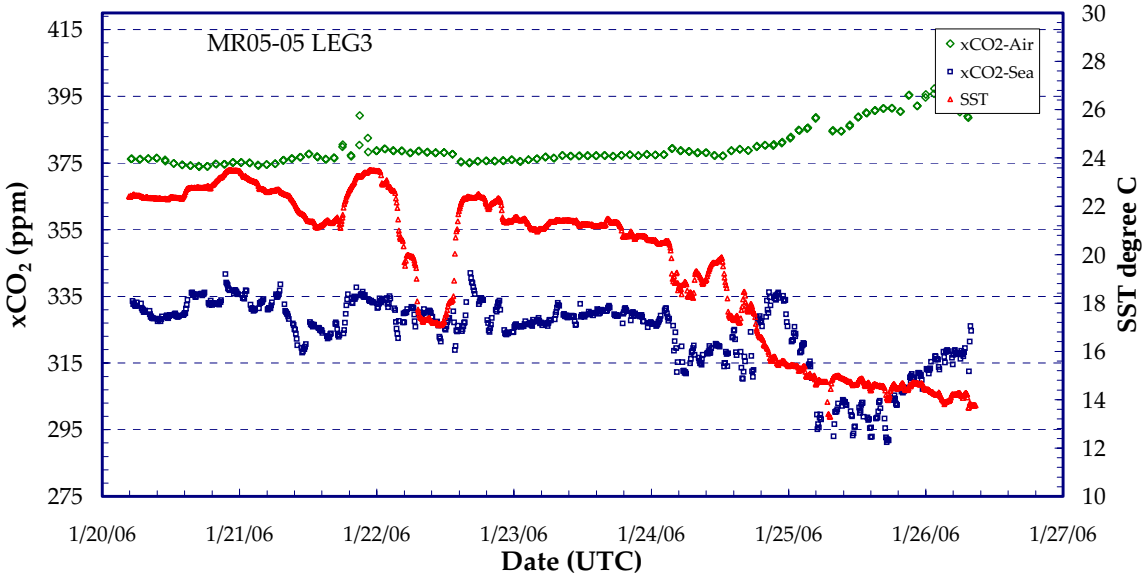


**Figure 3. Temporal changes of concentrations of $CO_2$ ($xCO_2$) in atmosphere (green) and surface seawater (blue), and SST (red) during leg 3.**

# 3. Hydrography

## 3.1 CTD/$O_2$ Measurements (*16 February 2006)*

***Hiroshi Uchida, Masao Fukasawa (JAMSTEC),***
***Satoshi Ozawa, Tomoyuki Takamori, Kentaro Oyama, Hiroki Ushiromura, Hiroyuki Hayashi, Hirokatsu Uno, Akinori Murata, Shinsuke Toyoda, Hiroshi Matsunaga, Tomohide Noguchi and Makito Yokota (MWJ)***

### 3.1.1 Winch arrangements

A CTD package was deployed by using 4.5 Ton Traction Winch System (Dynacon, Inc., USA), which was installed on the R/V Mirai in April 2001. The CTD Traction Winch System with the Heave Compensation Systems (Dynacon, Inc., USA) is designed to reduce cable stress resulting from load variation caused by wave or vessel motion. The system is operated passively by providing a nodding boom crane that moves up or down in response to line tension variations. Primary system components include a complete CTD Traction Winch System with up to 10 km of 9.53 mm armored cable (Ocean Cable and Communication Co.), cable rocker and Electro-Hydraulic Power Unit, nodding-boom crane assembly, two hydraulic cylinders and two hydraulic oil/nitrogen accumulators mounted within a single frame assembly. The system also contains related electronic hardware interface and a heave compensation computer control program.

### 3.1.2 Overview of the equipment

The CTD system, SBE 911plus system (Sea-Bird Electronics, Inc., USA), is a real time data system with the CTD data transmitted from a SBE 9plus underwater unit via a conducting cable to the SBE 11plus deck unit. The SBE 11plus deck unit is a rack-mountable interface which supplies DC power to the underwater unit, decodes the serial data stream, formats the data under microprocessor control, and passes the data to a companion computer. The serial data from the underwater unit is sent to the deck unit in RS-232 NRZ format using a 34,560 Hz carrier-modulated differential-phase-shift-keying (DPSK) telemetry link. The deck unit decodes the serial data and sends them to a personal computer to display, at the same time, to storage in a disk file using SBE SEASOFT software.

The SBE 911plus system acquires data from primary, secondary and auxiliary sensors in the form of binary numbers corresponding to the frequency or voltage outputs from those sensors at 24 samples per second. The calculations required to convert from raw data to engineering units of the parameters are performed by the SBE SEASOFT in real-time. The same calculations can be carried out after the observation using data stored in a disk file.

The SBE 911plus system controls the 36-position SBE 32 Carousel Water Sampler. The Carousel accepts 12-litre water sample bottles. Bottles were fired through the RS-232C modem connector on the back of the SBE 11plus deck unit while acquiring real time data. The 12-litre Niskin-X water sample bottle (General Oceanics, Inc., USA) is equipped externally with two stainless steel springs. The external springs are ideal for applications such as the trace metal analysis because the inside of the sampler is free from contaminants from springs.

SBE's temperature (SBE 3) and conductivity (SBE 4) sensor modules were used with the SBE 9plus underwater unit fixed by a single clamp and "L" bracket to the lower end cap. The conductivity cell entrance is co-planar with the tip of the temperature sensor's protective steel sheath. The pressure

sensor is mounted in the main housing of the underwater unit and is ported to outside through the oil-filled plastic capillary tube. A compact, modular unit consisting of a centrifugal pump head and a brushless DC ball bearing motor contained in an aluminum underwater housing pump (SBE 5T) flushes water through sensor tubing at a constant rate independent of the CTD's motion. Motor speed and pumping rate (3,000 rpm) remain nearly constant over the entire input voltage range of 12-18 volts DC. Flow speed of pumped water in standard TC duct is about 2.4 m/s. A SBE's dissolved oxygen sensor (SBE 43) was placed between the conductivity sensor module and the pump. Auxiliary sensors, a Deep Ocean Standards Thermometer (SBE 35), an altimeter and an oxygen optode were also used with the SBE 9plus underwater unit. The SBE 35 position in regard to the SBE 3 is shown in Figure 3.1.2.1.

It is known that CTD temperature data is influenced by the motion (pitching and rolling) of the CTD package. In order to reduce the motion of the CTD package, a heavy stainless frame (total weight of the CTD package without sea water in the bottles is about 1,000 kg) was used and an aluminum plate (54 x 90 cm) was attached to the frame (Figure 3.1.2.1).

**Summary of the system used in this cruise**

Deck unit:

SBE, Inc., SBE 11plus, S/N 0344

Under water unit:

SBE, Inc., SBE 9plus, S/N 79511 (Pressure sensor: S/N 0677)

Temperature sensor:

SBE, Inc., SBE 3, S/N 1464 (Leg 1: primary)
SBE, Inc., SBE 3, S/N 4216 (Leg 1: secondary, Leg 2, 3: primary)
SBE, Inc., SBE 3, S/N 1525 (Leg 2, 3: secondary)

Conductivity sensor:

SBE, Inc., SBE 4, S/N 1203 (Leg 1: primary)
SBE, Inc., SBE 4, S/N 2854 (Leg 1: secondary)
SBE, Inc., SBE 4, S/N 3124 (Leg 2: primary from 146_2 to 197_1)
SBE, Inc., SBE 4, S/N 3036 (Leg 2: secondary from 146_2 to 197_1)
SBE, Inc., SBE 4, S/N 2854 (Leg 2, 3: primary from X14_1 to TS_1)
SBE, Inc., SBE 4, S/N 3116 (Leg 2, 3: secondary from X14_1 to TS_1)

Oxygen sensor:

SBE, Inc., SBE 43, S/N 0391 (Leg 1: primary, Leg 2: primary from 146_2 to WC7)
SBE, Inc., SBE 43, S/N 0488 (Leg 1: secondary)
SBE, Inc., SBE 43, S/N 0390 (Leg 2, 3: primary from WC8 to TS1)
SBE, Inc., SBE 43, S/N 0394 (Leg 2: secondary from 146_2 to 283_1, Leg 3: secondary)
SBE, Inc., SBE 43, S/N 0205 (Leg 2: secondary from 285_1 to 351_2)
AANDERAA, Oxygen Optode 3830, S/N 612 (Leg 1, 2, 3: pilot)

Pump:

SBE, Inc., SBE 5T, S/N 3293 (Leg 1: primary)
SBE, Inc., SBE 5T, S/N 3118 (Leg 1: secondary)
SBE, Inc., SBE 5T, S/N 0984 (Leg 2, 3: primary)
SBE, Inc., SBE 5T, S/N 2627 (Leg 2, 3: secondary)

Altimeter:

Benthos Inc., PSA-916T, S/N 1100 (Leg 1)

Benthos Inc., PSA-916T, S/N 1157 (Leg 2, 3)

Deep Ocean Standards Thermometer:

SBE, Inc., SBE 35, S/N 0022 (Leg 1, 2)

SBE, Inc., SBE 35, S/N 0045 (Leg 3)

Carousel Water Sampler:

SBE, Inc., SBE 32, S/N 0391 (Leg 1, 2, 3)

Water sample bottle:

General Oceanics, Inc., 12-litre Niskin-X (no TEFLON coating)

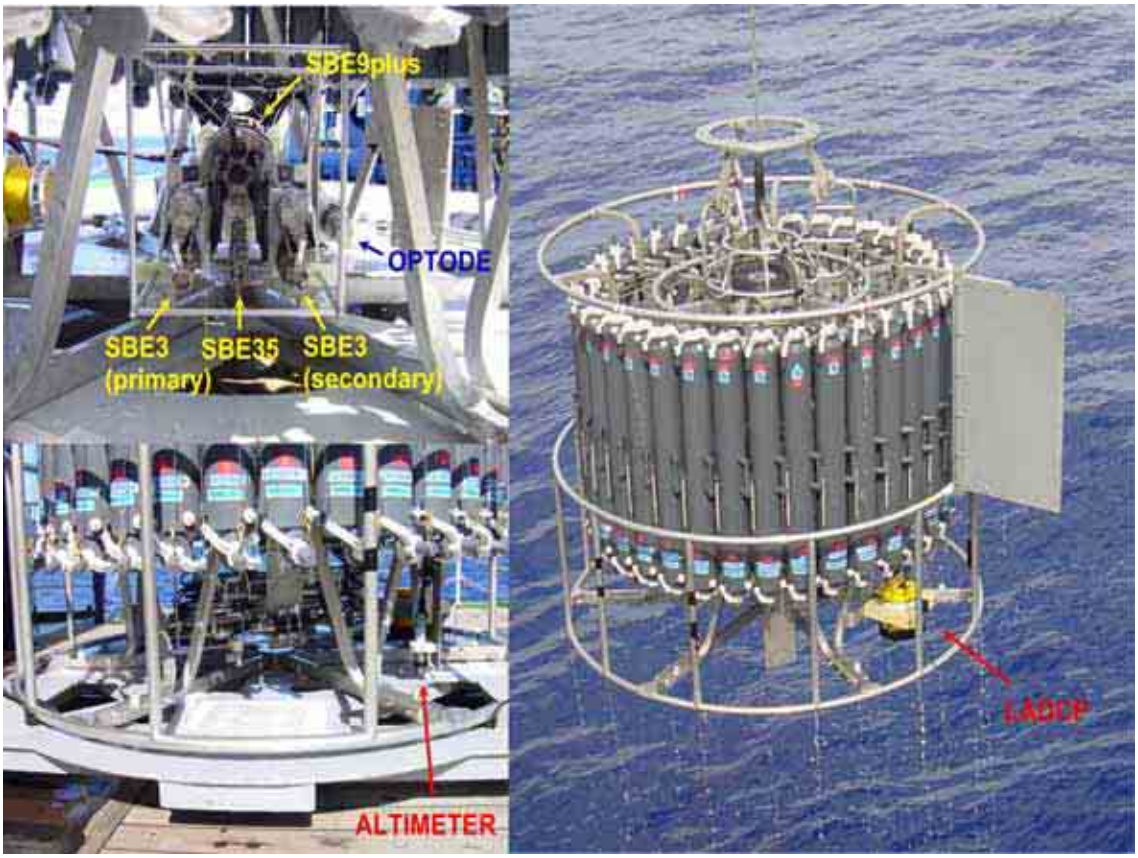


**Figure 3.1.2.1. CTD package (right) and the SBE 35 position in regard to the SBE 3 temperature sensors (left).**

### 3.1.3 Pre-cruise calibration

**(1) Pressure**

Paroscientific series 4000 Digiquartz high pressure transducer (Paroscientific, Inc., USA) uses a quartz crystal resonator whose frequency of oscillation varies with pressure induced stress with 0.01 per million of resolution over the absolute pressure range of 0 to 15,000 psia (0 to 10,332 dbar). Also, a quartz crystal temperature signal is used to compensate a wide range of temperature changes at the time of an observation. The pressure sensor (MODEL 415K-187) has a nominal accuracy of 0.015 % FS (1.5 dbar), typical stability of 0.0015 % FS/month (0.15 dbar/month) and resolution of 0.001 % FS (0.1 dbar).

Pre-cruise sensor calibrations were performed at SBE, Inc., USA. The following coefficients were used in the SEASOFT:

*S/N 0677, 2 July 2002*

$c_1$ = –62072.94
$c_2$ = –1.176956
$c_3$ = 1.954420e–02
$d_1$ = 0.027386
$d_2$ = 0.0
$t_1$ = 30.05031
$t_2$ = –4.744833e–04
$t_3$ = 3.757590e–06
$t_4$ = 3.810700e–09
$t_5$ = 0.0

Pressure coefficients are first formulated into

$$c = c_1 + c_2 * U + c_3 * U^2$$
$$d = d_1 + d_2 * U$$
$$t_0 = t_1 + t_2 * U + t_3 * U^2 + t_4 * U^3 + t_5 * U^4$$

where U is temperature in degrees Celsius. The pressure temperature, U, is determined according to

$$U\ (°C) = M * (12\ \text{bit pressure temperature compensation word}) – B$$

The following coefficients were used in SEASOFT:

*S/N 0677*

M = 0.0128041
B = –9.324136
(in the underwater unit system configuration sheet dated on 22 February 2002)

Finally, pressure is computed as

$$P\ (psi) = c * [1 – (t_0^2 / t^2)] * \{1 – d * [1 – (t_0^2 / t^2)]\}$$

where t is pressure period (μsec). Since the pressure sensor measures the absolute value, it inherently includes atmospheric pressure (about 14.7 psi). SEASOFT subtracts 14.7 psi from computed pressure above automatically.

Pressure sensor calibrations against a dead-weight piston gauge (Bundenberg Gauge Co. Ltd., UK; Model 480DA, S/N 23906) are performed at JAMSTEC (Yokosuka, Kanagawa, JAPAN) by Marine Works Japan Ltd. (MWJ), usually once in a year in order to monitor sensor time drift and linearity. The pressure sensor drift is known to be primarily an offset drift at all pressures rather than a change of span slope. The pressure sensor hysterisis is typically 0.2 dbar. The following coefficients for the sensor drift correction were also used in SEASOFT:

*S/N 0677, 8 September 2005*

slope = 0.9998495

offset = –0.49595

The drift-corrected pressure is computed as

Drift-corrected pressure (dbar) = slope * (computed pressure in dbar) + offset

Result of the pressure sensor calibration against the dead weight piston gauge is shown in Figure 3.1.3.1. Time drift of the pressure sensor based on the offset and the slope of the calibrations is also shown in Figure 3.1.3.2.

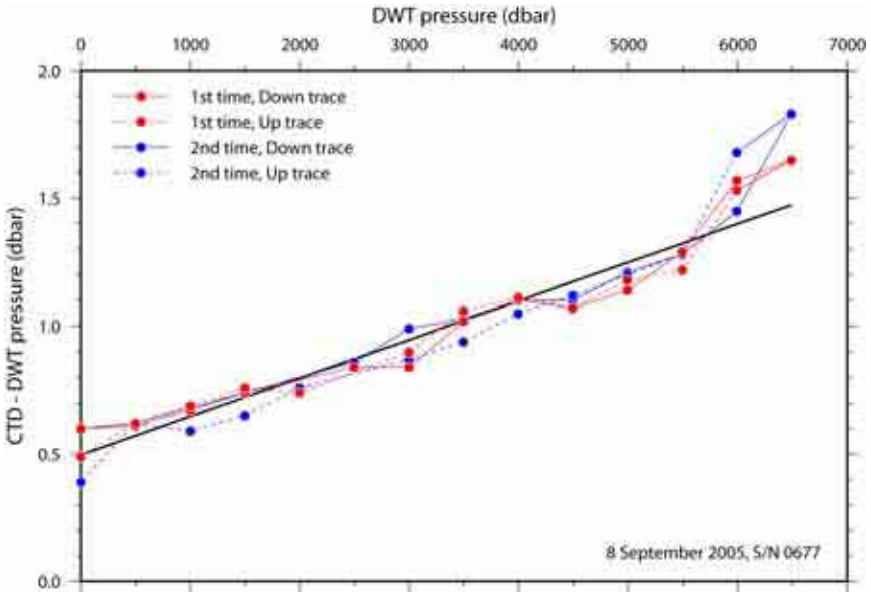


**Figure 3.1.3.1. The residual pressures between the dead weight piston gauge and the CTD pressure (S/N 0677). The calibration line (black line) is also shown.**

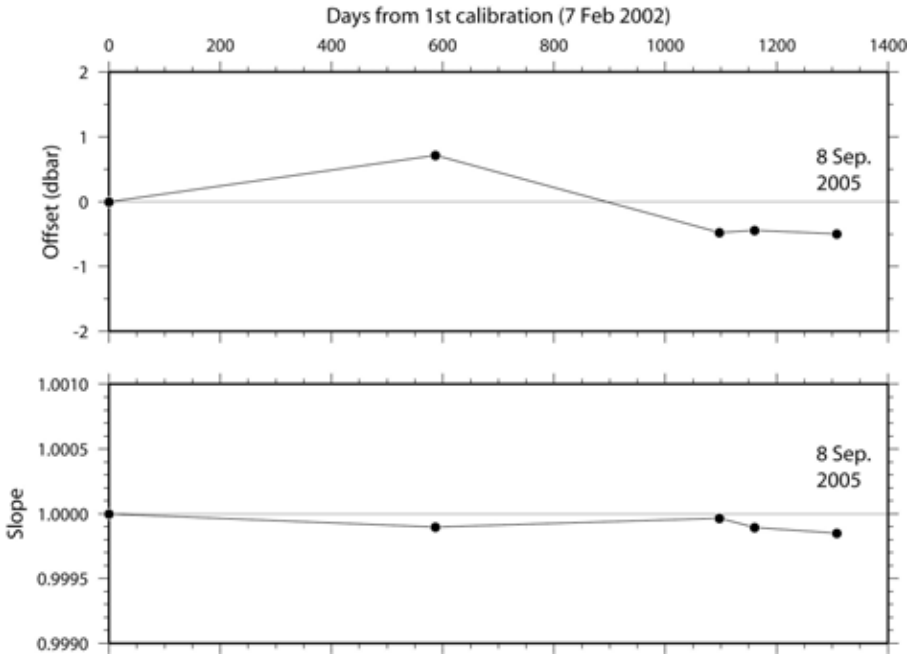


**Figure 3.1.3.2. Pressure sensor (S/N 0677) time drift of offset (upper panel) and slope (lower panel) based on laboratory calibrations.**

**(2) Temperature (SBE 3)**

The temperature sensing element is a glass-coated thermistor bead in a stainless steel tube, providing a pressure-free measurement at depths up to 10,500 (6,800) meters by titanium (aluminum) housing. The sensor output frequency ranges from approximately 5 to 13 kHz corresponding to temperature from –5 to 35 °C. The output frequency is inversely proportional to the square root of the thermistor resistance, which controls the output of a patented Wien Bridge circuit. The thermistor resistance is exponentially related to temperature. The SBE 3 thermometer has nominal accuracy of 0.001 °C, typical stability of 0.0002 °C/month and resolution of 0.0002 °C at 24 samples per second. The premium temperature sensor, SBE 3plus, is a more rigorously tested and calibrated version of standard temperature sensor (SBE 3). A sensor is designated as an SBE 3plus only after demonstrating drift of less than 0.001 °C during a six-month screening period. In addition, the time response is carefully measured and verified to be 0.065 ± 0.010 seconds.

Pre-cruise sensor calibrations were performed at SBE, Inc., USA. The following coefficients were used in SEASOFT:

*S/N 1464 (Leg 1: primary), 14 September 2005*

g = 4.84384166e–03
h = 6.80721378e–04
i = 2.69562893e–05
j = 2.12657768e–06
$f_0$ = 1000.000

*S/N 4216 (Leg 1: secondary, Leg 2 and 3: primary), 20 September 2005*

g = 4.35983643e–03
h = 6.46128037e–04
i = 2.28907910e–05
j = 1.94862297e–06
$f_0$ = 1000.000

*S/N 1525 (Leg 2 and 3: secondary), 14 September 2005*

g = 4.84604175e–03
h = 6.75287460e–04
i = 2.65140918e–05
j = 2.12921574e–06
$f_0$ = 1000.000

Temperature (ITS-90) is computed according to

Temperature (ITS-90) =

$$1 / \{g + h * [\ln(f0 / f)] + i * [\ln^2(f0 / f)] + j * [\ln^3(f_0 / f)]\} - 273.15$$

where f is the instrument frequency (kHz).

Time drift of the SBE 3 temperature sensors based on the laboratory calibrations is shown in Figure 3.1.3.3.

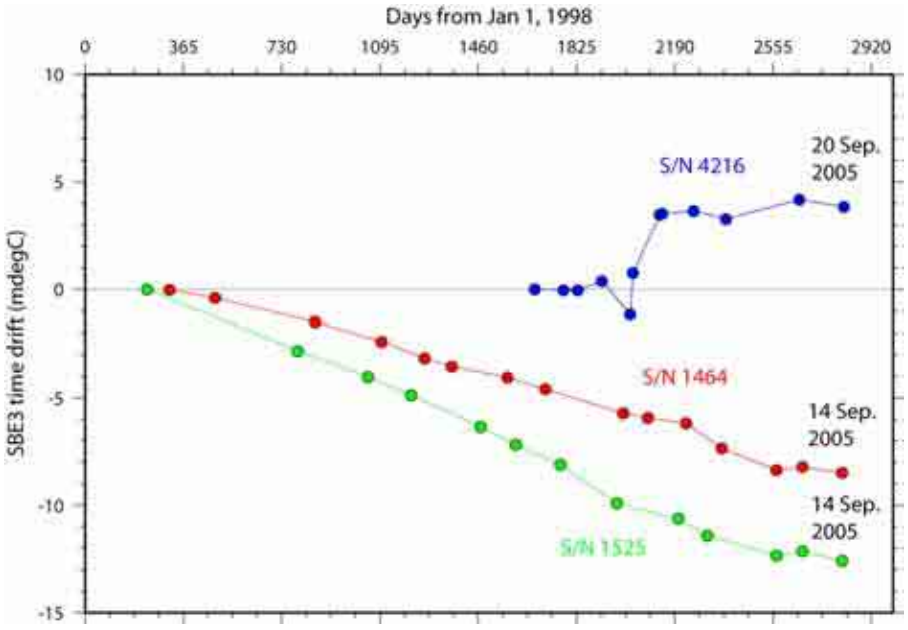


**Figure 3.1.3.3. Time drift of SBE 3 temperature sensors (S/N 1464, S/N 4216 and S/N 1525) based on laboratory calibrations performed by SBE, Inc.**

**(3) Conductivity (SBE 4)**

The flow-through conductivity sensing element is a glass tube (cell) with three platinum electrodes to provide in-situ measurements at depths up to 10,500 meters. The impedance between the center and the end electrodes is determined by the cell geometry and the specific conductance of the fluid within the cell. The conductivity cell composes a Wien Bridge circuit with other electric elements of which frequency output is approximately 3 to 12 kHz corresponding to conductivity of the fluid of 0 to 7 S/m. The SBE 4 has nominal accuracy of 0.0003 S/m, typical stability of 0.0003 S/m/month and resolution of 0.00004 S/m at 24 samples per second. Pre-cruise sensor calibrations were performed at SBE, Inc., USA. The following coefficients were used in SEASOFT:

*S/N 1203 (Leg 1: primary), 15 September 2005*

g = –4.05182265e+00
h = 4.93483365e–01
i = 9.77451923e–05
j = 2.18599851e–05
CPcor = –9.57e–08 (nominal)
CTcor = 3.25e–06 (nominal)

*S/N 2854 (Leg 1: secondary, Leg 2: primary from X14_1 to 351_2, Leg 3: primary), 15 September 2005*

g = –1.02631821e+01
h = 1.41526600e+00
i = –9.49444425e–06
j = 5.73270605e–05
CPcor = –9.57e-08 (nominal)
CTcor = 3.25e–06 (nominal)

*S/N 3124 (Leg 2: primary from 146_2 to 197_1), 8 November 2005*

g = –1.02907974e+01

h = 1.38692851e+00
i = –8.89254353e–05
j = 8.59164344e–05
CPcor = –9.57e–08 (nominal)
CTcor = 3.25e–06 (nominal)

*S/N 3036 (Leg 2: secondary from 146_2 to 197_1), 23 September 2005*

g = –1.03246469e+01
h = 1.42860596e+00
i = 3.40735271e–04
j = 4.76172694e–05
CPcor = –9.57e-08 (nominal)
CTcor = 3.25e–06 (nominal)

*S/N 3116 (Leg 2: secondary from X14_1 to 351_2, Leg 3: secondary), 8 November 2005*

g = –1.04289250e+01
h = 1.43335621e+00
i = 4.35984135e–04
j = 3.98255096e–05
CPcor = –9.57e-08 (nominal)
CTcor = 3.25e–06 (nominal)

Conductivity of a fluid in the cell is expressed as:

$$C\ (S/m) = (g + h * f^2 + i * f^3 + j * f^4) / [10 ( 1 + CTcor * t + CPcor * p)]$$

where f is the instrument frequency (kHz), t is the water temperature (°C) and p is the water pressure (dbar). The value of conductivity at salinity of 35, temperature of 15 °C (IPTS-68) and pressure of 0 dbar is 4.2914 S/m.

**(4) Oxygen (SBE 43)**

The SBE 43 oxygen sensor uses a Clark polarographic element to provide in-situ measurements at depths up to 7,000 meters. Calibration stability is improved by an order of magnitude and pressure hysterisis is largely eliminated in the upper ocean (1,000 m) compared with the previous oxygen sensor (SBE 13). Continuous polarization eliminates wait-time for stabilization after power-up. Signal resolution is increased by on-board temperature compensation. The oxygen sensor is also included in the path of pumped sea water. The oxygen sensor determines the dissolved oxygen concentration by counting the number of oxygen molecules per second (flux) that diffuse through a membrane, where the permeability of the membrane to oxygen is a function of temperature and ambient pressure. Computation of dissolved oxygen in engineering units is done in SEASOFT software. The range for dissolved oxygen is 120 % of surface saturation in all natural waters; nominal accuracy is 2 % of saturation; typical stability is 2 % per 1,000 hours.

Pre-cruise sensor calibrations were performed at SBE, Inc., USA. The following coefficients were used in SEASOFT:

*S/N 0391 (Leg 1: primary, Leg 2: primary from 146_2 to WC7), 18 October 2005*

Soc = 0.35440
Offset = –0.4919
TCor = 0.0013
PCor = 1.350e–04

*S/N 0488 (Leg 1: secondary), 11 October 2005*

Soc = 0.58120

Offset = –0.6959

TCor = –0.0004

PCor = 1.350e–04

*S/N 0390 (Leg 2: primary from WC8 to 351_2, Leg 3: primary), 18 October 2005*

Soc = 0.3877

Offset = –0.5151

TCor = 0.0012

PCor = 1.350e–04

*S/N 0394 (Leg 2: secondary from 146_2 to 283_1, Leg 3: secondary), 1 July 2005*

Soc = 0.3629

Offset = –0.5220

TCor = 0.0020

PCor = 1.350e–04

*S/N 0205 (Leg 2: secondary from 285_1 to 351_2), 10 May 2005*

Soc = 0.4131

Offset = –0.4688

TCor = –0.0009

PCor = 1.350e–04

Oxygen (ml/l) is computed as

Oxygen (ml/l) = {Soc * (v + Offset)} * exp(TCor * t + PCor * p) * Oxsat(t, s)

$Oxsat(t, s) = \exp[A_1 + A_2 * (100 / t) + A_3 * \ln(t / 100) + A_4 * (t / 100) + s * \{B_1 + B_2 * (t / 100) + B_3 * (t / 100) * (t / 100)\}]$

$A_1 = -173.4292$

$A_2 = 249.6339$

$A_3 = 143.3483$

$A_4 = -21.8482$

$B_1 = -0.033096$

$B_2 = -0.00170$

where p is pressure in dbar, t is absolute temperature and s is salinity in psu. Oxsat is oxygen saturation value minus the volume of oxygen gas (STP) absorbed from humidity-saturated air.

Serial number 0488 is used in SBE's research for oxygen sensor membranes. This sensor has a membrane that is thicker than standard SBE 43s. This thicker membrane will cause the sensor slower response than standard SBE 43s but it may be more stable. The field performance of this sensor is examined in the Leg 1.

**(5) Deep Ocean Standards Thermometer**

Deep Ocean Standards Thermometer (SBE 35) is an accurate, ocean-range temperature sensor that can be standardized against Triple Point of Water and Gallium Melt Point cells and is also capable of measuring temperature in the ocean to depths of 6,800 m.

Temperature is determined by applying an AC excitation to reference resistances and an ultrastable aged thermistor with a drift rate of less than 0.001 °C/year. Each of the resulting outputs is digitized by a 20-bit A/D converter. The reference resistor is a hermetically sealed, temperature-controlled VISHAY.

The switches are mercury wetted reed relays with a stable contact resistance. AC excitation and ratiometric comparison using a common processing channel removes measurement errors due to parasitic thermocouples, offset voltages, leakage currents, and gain errors. Maximum power dissipated in the thermistor is 0.5 µwatts, and contributes less than 200 µK of overheat error.

The SBE 35 communicates via a standard RS-232 interface at 300 baud, 8 bits, no parity. The SBE 35 can be used with the SBE 32 Carousel Water Sampler and SBE 911plus CTD system. The SBE 35 makes a temperature measurement each time when a bottle fire confirmation is received, and stores the value in EEPROM. Calibration coefficients stored in EEPROM allow the SBE 35 to transmit data in engineering units. Commands can be sent to SBE 35 to provide status display, data acquisition setup, data retrieval, and diagnostic test using terminal software.

By following the methodology used for standards-grade platinum resistance thermometers (SPRT), the calibration of the SBE 35 is accomplished in two steps. The first step is to characterize and capture the non-linear resistance vs temperature response of the sensor. The SBE 35 calibrations are performed at SBE, Inc., in a low-gradient temperature bath and against ITS-90 certified SPRTs maintained at Sea-Bird's primary temperature metrology laboratory. The second step is frequent certification of the sensor by measurements in thermodynamic fixed-point cells. Triple point of water (TPW) and gallium melt point (GaMP) cells are appropriate for the SBE 35. The SBE 35 resolves temperature in the fixed-point cells to approximately 25 µK. Like SPRTs, the slow time drift of the SBE 35 is adjusted by a slope and offset correction to the basic non-linear calibration equation.

Pre-cruise sensor calibrations were performed at SBE, Inc., USA. The following coefficients were stored in EEPROM:

*S/N 0022 (Leg 1 and 2), 12 October 1999 (1st step: linearization)*

$a_0$ = 4.320725498e-3
$a_1$ = -1.189839279e-3
$a_2$ = 1.836299593e-3
$a_3$ = -1.032916769e-5
$a_4$ = 2.225491125e-7

*S/N 0045 (Leg 3), 27 October 2002 (1st step: linearization)*

$a_0$ = 5.84093815e–03
$a_1$ = –1.65529280e–03
$a_2$ = 2.37944937e–04
$a_3$ = –1.32611385e–05
$a_4$ = 2.83355203e–07

Linearized temperature (ITS-90) is computed according to

Linearized temperature (ITS-90) =

$$1 / \{a_0 + a_1 * [\ln(n)] + a_2 * [\ln^2(n)] + a_3 * [\ln^3(n)] + a_4 * [\ln^4(n)]\} - 273.15$$

where n is the instrument output. Then the SBE 35 is certified by measurements in thermodynamic fixed-point cells of the TPW (0.0100 °C) and GaMP (29.7646 °C). Like SPRTs, the slow time drift of the SBE 35 is adjusted by periodic recertification corrections.

*S/N 0022 (Leg 1 and 2), 30 September 2005 (2nd step: fixed point calibration)*

Slope = 1.000036
Offset = 0.000151

*S/N 0045 (Leg 3), 3 October 2005 (2nd step: fixed point calibration)*

Slope = 1.000013

Offset = –0.001084

Temperature (ITS-90) is calibrated according to

Temperature (ITS-90) = Slope * Linearized temperature + Offset

The SBE 35 has a time constant of 0.5 seconds. The time required per sample = 1.1 * NCYCLES + 2.7 seconds. The 1.1 seconds is total time per an acquisition cycle. NCYCLES is the number of acquisition cycles per sample. The 2.7 seconds is required for converting the measured values to temperature and storing average in EEPROM. Root mean square (rms) temperature noise for a SBE 35 in a Triple Point of Water cell is typically expressed as 82 / NCYCLES$^{1/2}$ in µK. In this cruise NCYCLES was set to 4 and the rms noise is estimated to be 0.04 m°C.

When using the SBE 911 system with SBE 35, the deck unit receives incorrect signal from the under water unit for confirmation of firing bottle #16. In order to correct the signal, a module (Yoshi Ver. 1, EMS Co. Ltd., JAPAN) was used between the under water unit and the deck unit.

Time drift of the SBE 35 based on the fixed point calibrations is shown in Figure 3.1.3.4.

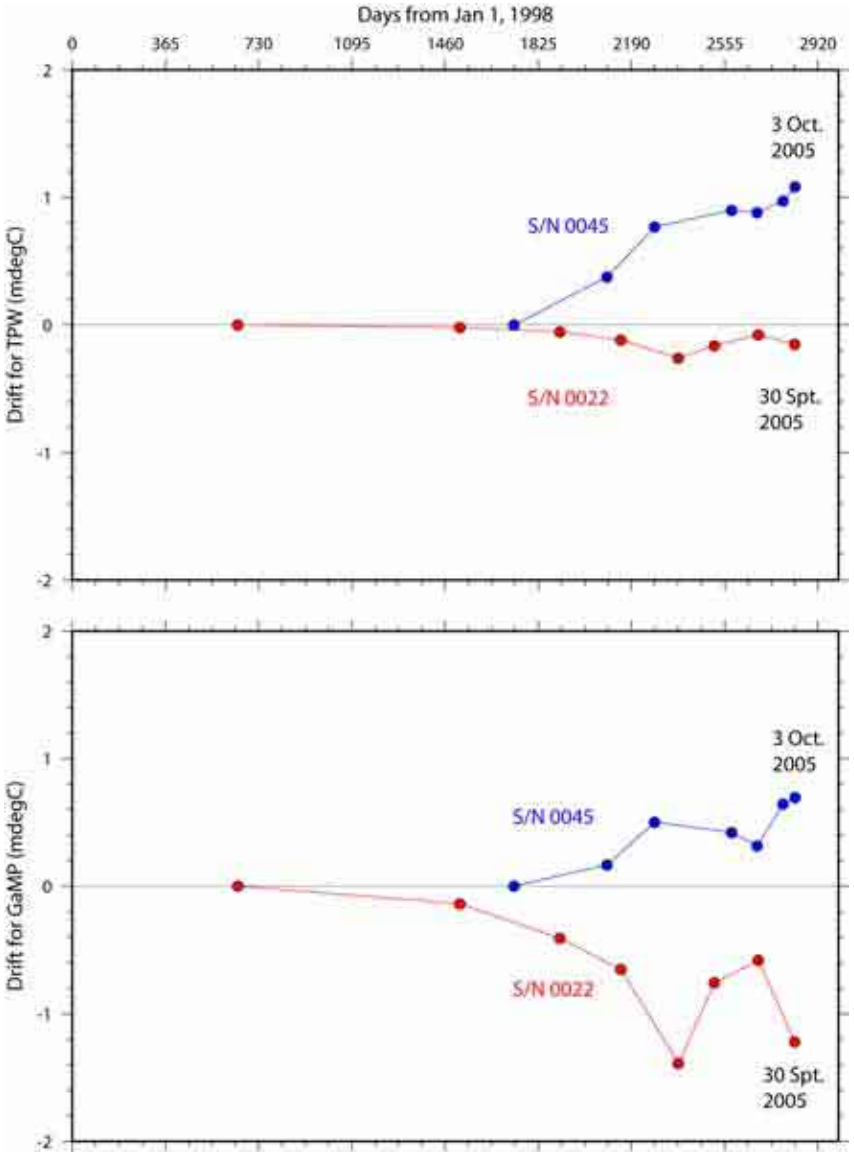


**Figure 3.1.3.4. SBE35 time drift based on laboratory fixed point calibrations (triple point of water, TPW and gallium melt point, GaMP) performed by SBE, Inc.**

**(6) Altimeter**

Benthos PSA-916T Sonar Altimeter (Benthos, Inc., USA) determines the distance of the target from the unit by generating a narrow beam acoustic pulse and measuring the travel time for the pulse to bounce back from the target surface. The PSA-916T is the same as the standard PSA-916 Sonar Altimeter except that it is housed in a corrosion-resistant titanium pressure case. It is O-ring-sealed and rated for operation in water depths up to 10,000 meters. In this unit, a 250 microseconds pulse at 200 kHz is transmitted 5 times in a second. The PSA-916T uses the nominal speed of sound of 1,500 m/s. Thus the unit itself, neglecting variations in the speed of sound, can be considered accurate to 5 % or 0.1 meter, whichever is greater. In the PSA-916T the jitter of the detectors is approximately 5 microseconds or +/– 0.4 cm total distance. Since the total travel time is divided by two, the jitter error is +/– 0.2 cm.

The following scale factors were used in SEASOFT:

*S/N 1100, S/N 1157*

FSVolt * 300 / FSRange = 15

Offset = 0.0

**(7) Oxygen Optode**

The Aanderaa Oxygen Optode 3830 (Aanderaa Instruments AS, NORWAY) is based on the ability of selected substances to act as dynamic fluorescence quenchers. The fluorescent indicator is a special platinum porphyrin complex embedded in a gas permeable foil that is exposed to the surrounding water. A black optical isolation coating protects the complex from sunlight and fluorescent particles in the water. This sensing foil is attached to a sapphire window providing optical access for the measuring system from inside a watertight titanium housing. The foil is excited by modulated blue light, and the phase of a returned red light is measured. By linearizing and temperature compensating, with an incorporated temperature sensor, the absolute $O_2$ concentration can be determined.

In order to use with the SBE 911plus CTD system, an analog adaptor (3966) is connected to the oxygen optode (3830). The analog adaptor is packed into titanium housing made by Alec Electronics Co. Ltd., JAPAN (Figure 3.1.3.5). The sensor is designed to operate down to 6,000 meters and the titanium housing for the analog adaptor is designed to operate down to 7,000 meters. The range for dissolved oxygen is 120 % of surface saturation in all natural waters; nominal accuracy is less than 5 % of saturation; setting time (68%) is shorter than 25 seconds.

The following scale factors were used in SEASOFT:

*S/N 612*

Phase shift (degrees) = $V_p$ * 12 + 10

Temperature (°C) = $V_t$ * 9 – 5

where $V_p$ and $V_t$ are voltage output (V) of phase shift and temperature, respectively.

Each batch of sensing foils is delivered with calibration data describing the behavior with respect to oxygen concentration and temperature.

*Foil batch No. 4104 (S/N 612), 13 November 2004*

$C0Coef_0$ = 3.199840e+3

$C0Coef_1$ = –1.119634e+2

$C0Coef_2$ = 2.408296

$C0Coef_3$ = –2.248740e–2

$C1Coef_0$ = –1.744936e+2

$C1Coef_1$ = 5.462500
$C1Coef_2$ = –1.244084e–1
$C1Coef_3$ = 1.239153e–3
$C2Coef_0$ = 3.941711
$C2Coef_1$ = –1.086677e–1
$C2Coef_2$ = 2.719394e–3
$C2Coef_3$ = –2.906343e–5
$C3Coef_0$ = –4.220910e–2
$C3Coef_1$ = 1.018155e–3
$C3Coef_2$ = –2.905609e–5
$C3Coef_3$ = 3.306610e–7
$C4Coef_0$ = 1.738870e–4
$C4Coef_1$ = –3.637668e–6
$C4Coef_2$ = 1.227403e–7
$C4Coef_3$ = –1.468399e–9

Temperature dependent coefficients are calculated as follows.

$$C0Coef = C0Coef_0 + C0Coef_1 * t + C0Coef_2 * t^2 + C0Coef_3 * t^3$$
$$C1Coef = C1Coef_0 + C1Coef_1 * t + C1Coef_2 * t^2 + C1Coef_3 * t^3$$
$$C2Coef = C2Coef_0 + C2Coef_1 * t + C2Coef_2 * t^2 + C2Coef_3 * t^3$$
$$C3Coef = C3Coef_0 + C3Coef_1 * t + C3Coef_2 * t^2 + C3Coef_3 * t^3$$
$$C4Coef = C4Coef_0 + C4Coef_1 * t + C4Coef_2 * t^2 + C4Coef_3 * t^3$$

where t is temperature (°C). The oxygen concentration can be calculated by use of the following formula.

$$O_2\ (\mu mol/l) = C0Coef + C1Coef * P + C2Coef * P^2 + C3Coef * P^3 + C4Coef * P^4$$

where P is phase shift (degrees) measured by the Optode. In addition to the above mentioned coefficient, phase measurement is calibrated for individual sensor and foil variations by a two point calibration (one in air saturated water and one in a zero-oxygen solution).

$$P = A + B * P_b$$

where P is a calibrated phase shift (degrees) and $P_b$ is a raw phase measurement. The coefficients A and B can be calculated by ordinary linear curve fitting and is delivered.

*S/N 612, 20 September 2005*

A = –3.00536
B = 1.11847

Outputs from the sensor are the raw phase shift (P) and temperature. The raw phase data was calibrated using above coefficients after data acquisition. The oxygen concentration was calculated using temperature data from the first responding CTD temperature sensor instead of temperature data from slow responding optode temperature sensor.


**Figure 3.1.3.5. Aanderaa Oxygen Optode (3830) with analog adaptor (3966). The analog adaptor is packed into titanium housing made by Alec Electronics, Japan.**

### 3.1.4 Data collection and processing

**(1) Data collection**

CTD measurements were made using a SBE 9plus equipped with two pumped temperature-conductivity (TC) sensors. The TC pairs were monitored to check drift and shifts by examining the differences between the two pairs. Dissolved oxygen sensor was placed between the conductivity sensor module and the pump. Auxiliary sensors included Deep Ocean Standards Thermometer, altimeter and oxygen optode. The SBE 9plus (sampling rate of 24 Hz) was mounted horizontally in a 36-position carousel frame.

CTD system was powered on at least 30 minutes in advance of the data acquisition and was powered off at least two minutes after the operation in order to acquire pressure data on ship's deck.

The package was lowered into the water from the starboard side and held 10 m beneath the surface for about one minute in order to activate the pump. After the pump was activated the package was lifted to the surface and lowered at a rate of 1.0 m/s to 200 m (or 300 m) then the package was stopped in order to operate the heave compensator of the crane. The package was lowered again at a rate of 1.2 m/s to the bottom. The position of the package relative to the bottom was monitored by the altimeter reading. Also the bottom depth was monitored by the SEABEAM multi-narrow beam sounder on board. For the up cast, the package was lifted at a rate of 1.1 m/s except for bottle firing stops. At each bottle firing stops, the bottle was fired after waiting 30 seconds and the package was stayed at least 5 seconds for measurement of the Deep Ocean Standards Thermometer. At 200 m (or 300 m) from the surface, the package was stopped in order to stop the heave compensator of the crane.

Water samples were collected using a 36-bottle SBE 32 Carousel Water Sampler with 12-litre Nisken-X bottles. Before a cast for taking water for CFCs, the 36-bottle frame and Niskin-X bottles were wiped with acetone.

The SBE 11plus deck unit received the data signal from the CTD. Digitized data were forwarded to a personal computer running the SEASAVE data acquisition software. Temperature, conductivity, salinity, oxygen and descent rate profiles were displayed in real-time with the package depth and altimeter reading. Temperature, salinity and oxygen difference between primary and secondary sensor were also displayed in order to monitor the status of the sensors.

*Data acquisition software*

SBE, Inc., SEASAVE-Win32, version 5.27b

**(2) Data collection problems**

*Leg 1:*

At following stations, the trigger of the bottle was not released. Therefore the latch assembly was replaced after the cast.

33_1 (#12), 51_1 (#28), 116_1 (#36)

At following station, the bottle did not trip correctly. It was found by temperature reading at dissolved oxygen sampling. Therefore the latch assembly was replaced after the cast.

38_1 (#19)

At station 51_1, bottle #26 was not fired by missed operation.

After station 51_1, Niskin bottle #15 was changed from S/N X12006 to S/N X12009 due to frequent leak.

At following stations, output from the sensor showed abnormal values.

94_1, secondary sensors, 32-96 dbar (down cast)

114_1, secondary conductivity, 1,192-2,546 dbar (down cast)

118_1, primary conductivity, 1,391-1,438 dbar (down cast)

*Leg 2:*

At following stations, the trigger of the bottle was not released. Therefore the latch assembly was replaced after the cast.

X14_1 (#17), 201_1 (#17), 203_1 (#10), 217_2 (#28), 231_1 (#26), 322_1 (#18), 351_2 (#14)

At following stations, the bottle did not trip correctly. It was found by temperature reading at dissolved oxygen sampling. Therefore the latch assembly was replaced after the cast.

WC5_1 (#8), 291_1 (#20), 351_2 (21)

At following stations, the bottle did not trip correctly. It was found by sampled water analysis.

185_1 (#17): The latch assembly was replaced after station 195_1.

WC2_1 (#1): The latch assembly was replaced after station WC5_1.

357_1 (#17): The bottle tripped before firing the bottle.

At station 217_2, bottle #36 was not fired due to missed operation.

After station 267_1, Niskin bottle #23 was changed from S/N X12043 to S/N X12005.

At following stations, output from the sensor showed abnormal values.

146_2, secondary sensors

148_1, secondary sensors

WC7_1, primary sensors

328_1, primary sensors, 0-1,106 dbar (up cast), Jellyfish in primary TC duct

At station 299_1, the deck unit fuzed at 2,790 dbar of up cast. The system was re-started at the depth. At station 347_1, system error occurred at 2,743-2,744 dbar of up cast by unknown reason.

For primary oxygen sensor S/N 0391, noise became large near surface (0-400 dbar) compared to the data obtained from the same sensor in leg 1. The sensor was bleached after stations 171_1, 209_1 and WC6_1. Noise became large again although it was improved after bleaching.

After station 197_1, the primary conductivity sensor was changed from S/N 3124 to S/N 2854 due to large time drift. After station 197_1, the secondary conductivity sensor was also changed from S/N 3036 to S/N 3116 due to large time drift. After station WC7_1, the primary oxygen sensor was changed from S/N 0391 to S/N 0390 due to shift and noise.

After station 283_1, the secondary oxygen sensor was changed from S/N 0394 to S/N 0205 due to small noise. But the noise was found in the secondary oxygen data after the sensor change as well. So the connecting cable for the secondary oxygen sensor after station 285_1. But the noise was found as well. At station 333_1, the connecting port was changed from AUX3 to AUX2 and the noise disappeared after that.

*Leg 3:*

At following station, the bottle was not trip correctly. It was found by temperature reading at dissolved oxygen sampling. Therefore the latch assembly was replaced after the cast.

380_1 (#23)

**(3) Data processing**

SEASOFT consists of modular menu driven routines for acquisition, display, processing, and archiving of oceanographic data acquired with SBE equipment, and is designed to work with a compatible personal computer. Raw data are acquired from instruments and are stored as unmodified

data. The conversion module DATCNV uses the instrument configuration and calibration coefficients to create a converted engineering unit data file that is operated on by all SEASOFT post processing modules. Each SEASOFT module that modifies the converted data file adds proper information to the header of the converted file permitting tracking of how the various oceanographic parameters were obtained. The converted data is stored in rows and columns of ascii numbers. The last data column is a flag field used to mark scans as good or bad.

The following are the SEASOFT data processing module sequence and specifications used in the reduction of CTD data in this cruise.

*Data processing software*

SBE, Inc., SEASOFT-Win32, version 5.27b

DATCNV converted the raw data to scan number, pressure, depth, temperatures, conductivities, oxygen voltage, descent rate, altitude and fluorescence. DATCNV also extracted bottle information where scans were marked with the bottle confirm bit during acquisition. The duration was set to 4.4 seconds, and the offset was set to 0.0 seconds.

ROSSUM created a summary of the bottle data. The bottle position, date and time were output as the first two columns. Scan number, pressure, depth, temperatures, conductivities, oxygen voltage, descent rate, altitude and optode phase shift were averaged over 4.4 seconds. And salinity, potential temperature, density ($\sigma_\theta$) and oxygen were computed.

ALIGNCTD converted the time-sequence of conductivity and oxygen sensor outputs into the pressure sequence to ensure that all calculations were made using measurements from the same parcel of water. For a SBE 9plus CTD with the ducted temperature and conductivity sensors and a 3,000-rpm pump, the typical net advance of the conductivity relative to the temperature is 0.073 seconds. So, the SBE 11plus deck unit was set to advance the primary and the secondary conductivity for 1.73 scans (1.75/24 = 0.073 seconds). Oxygen data are also systematically delayed with respect to depth mainly because of the long time constant of the oxygen sensor and of an additional delay from the transit time of water in the pumped plumbing line. This delay was compensated by 6 seconds advancing oxygen sensor output (oxygen voltage) relative to the temperature. For the serial number 0488 that have thicker membrane than standard SBE 43s, the delay was compensated by 14 seconds. Oxygen optode data are also delayed by relatively slow response time of the sensor. The delay was compensated by 8 seconds advancing optode sensor output (phase shift and optode temperature) relative to the CTD temperature.

WILDEDIT marked extreme outliers in the data files. The first pass of WILDEDIT obtained an accurate estimate of the true standard deviation of the data. The data were read in blocks of 1,000 scans. Data greater than 10 standard deviations were flagged. The second pass computed a standard deviation over the same 1,000 scans excluding the flagged values. Values greater than 20 standard deviations were marked bad. This process was applied to all variables.

CELLTM used a recursive filter to remove conductivity cell thermal mass effects from the measured conductivity. Typical values used were thermal anomaly amplitude alpha = 0.03 and the time constant 1/beta = 7.0.

FILTER performed a low pass filter on pressure with a time constant of 0.15 seconds. In order to produce zero phase lag (no time shift) the filter runs forward first then backwards.

SECTION selected a time span of data based on scan number in order to reduce a file size. The minimum number was set to be the start time when the CTD package was beneath the sea-surface after

activation of the pump. The maximum number was set to be the end time when the package came up from the surface. Data for estimation of the CTD pressure drift were prepared before SECTION.

LOOPEDIT marked scans where the CTD was moving less than the minimum velocity of 0.0 m/s (traveling backwards due to ship roll).

DERIVE was used to compute oxygen.

BINAVG averaged the data into 1-dbar pressure bins. The center value of the first bin was set equal to the bin size. The bin minimum and maximum values are the center value plus and minus half the bin size. Scans with pressures greater than the minimum and less than or equal to the maximum were averaged. Scans were interpolated so that a data record exists every dbar.

DERIVE was re-used to compute salinity, potential temperature, and density ($\sigma_\theta$).

SPLIT was used to split data into the down cast and the up cast.

For stations from 146_2 to 331_1 in leg 2, small noise was found in the secondary oxygen data because the sensor connected to the port of AUX3. Therefore the sensor output (voltage) was low-pass filtered with a time constant of 1 second at the same time of the low-pass filtering for the pressure data mentioned above. At following stations, the noise could not be removed completely from down cast profile data.

X14_1: 5,650-5,800 dbar
201_1: 5,600-5,760 dbar
203_1: 5,710-5,850 dbar
205_1: 5,760-5,820 dbar
207_1: 5,660-5,860 dbar
213_1: 5,840-5,880 dbar
215_1: 5,750-5,920 dbar
217_1: 5,730-5,880 dbar

Remaining spikes in salinity or oxygen data were manually eliminated from the raw data or the 1-dbar-averaged data. When number of data in the 1-dbar-pressure bin was less than 10, the data of the bin was not used. The data gap over 1-dbar was linearly interpolated with a quality flag of 6.

For the oxygen optode data, the delay due to the long time constant was compensated by 8 seconds using the software module ALIGNCTD mentioned above. However it was found that the delay was dependent on temperature after the cruise. So the delay was compensated advancing optode sensor output relative to the CTD temperature as a following function of temperature.

$$\text{align (sec)} = 25 * \exp(-0.13 * t)$$

where t is CTD temperature (°C). The delay is estimated as 25 seconds when temperature is 0 °C, 8 seconds when 8.8 °C and 0.5 seconds when 30 °C.

### 3.1.5 Post-cruise calibration

Post-cruise calibration is basically performed for each leg. However the cruise period of leg 2 is longer than usual (53 days). Thus, the data of leg 2 is divided into two periods for the post-cruise calibration. In this section the two periods are called as leg 2a (from station 146_2 to WC10_1) and leg 2b (from station 217_2 to 351_2).

**(1) Pressure**

The CTD pressure sensor offset in the period of the cruise is estimated from the pressure readings on the ship deck. For best results the Paroscientific sensor has to be powered for at least 10 minutes before the operation and carefully temperature equilibrated. Therefore CTD system was powered on at least 30 minutes in advance of the data acquisition (from 55_1, Leg 1). It is very important to obtain stable pressure data. In order to get the calibration data for the pre- and post-cast pressure sensor drift, the CTD deck pressure is averaged over first and last one minute, respectively. Then the atmospheric pressure deviation from a standard atmospheric pressure (14.7 psi) is subtracted from the CTD deck pressure. The atmospheric pressure was measured at the captain deck (20 m high from the base line) and sub-sampled one-minute interval as a meteorological data. Time series of the CTD deck pressure is shown in from Figure 3.1.5.1 to Figure 3.1.5.4.

The CTD pressure sensor offset is estimated from the deck pressure obtained above. Mean of the pre- and the post-casts data over the whole period gave an estimation of the pressure sensor offset from the pre-cruise calibration. Mean residual pressure between the dead weight piston gauge and the calibrated CTD data at 0 dbar of the pre-cruise calibration is subtracted from the mean deck pressure. Estimated offset of the pressure data is summarized in Table 3.1.5.1. The post-cruise correction of the pressure data is not deemed necessary for the pressure sensor.

**Table 3.1.5.1. Offset of the pressure data. Mean and standard deviation are calculated from time series of the average of the pre- and the post-cast deck pressures.**

| Leg | S/N | Mean deck Pressure (dbar) | Standard deviation (dbar) | Residual pressure (dbar) | Estimated offset (dbar) |
|---|---|---|---|---|---|
| Leg1 | 0677 | –0.53 | 0.03 | 0.03 | –0.56 |
| Leg 2a | 0677 | –0.54 | 0.03 | 0.03 | –0.57 |
| Leg 2b | 0677 | –0.53 | 0.02 | 0.03 | –0.56 |
| Leg 3 | 0677 | –0.49 | 0.02 | 0.03 | –0.52 |

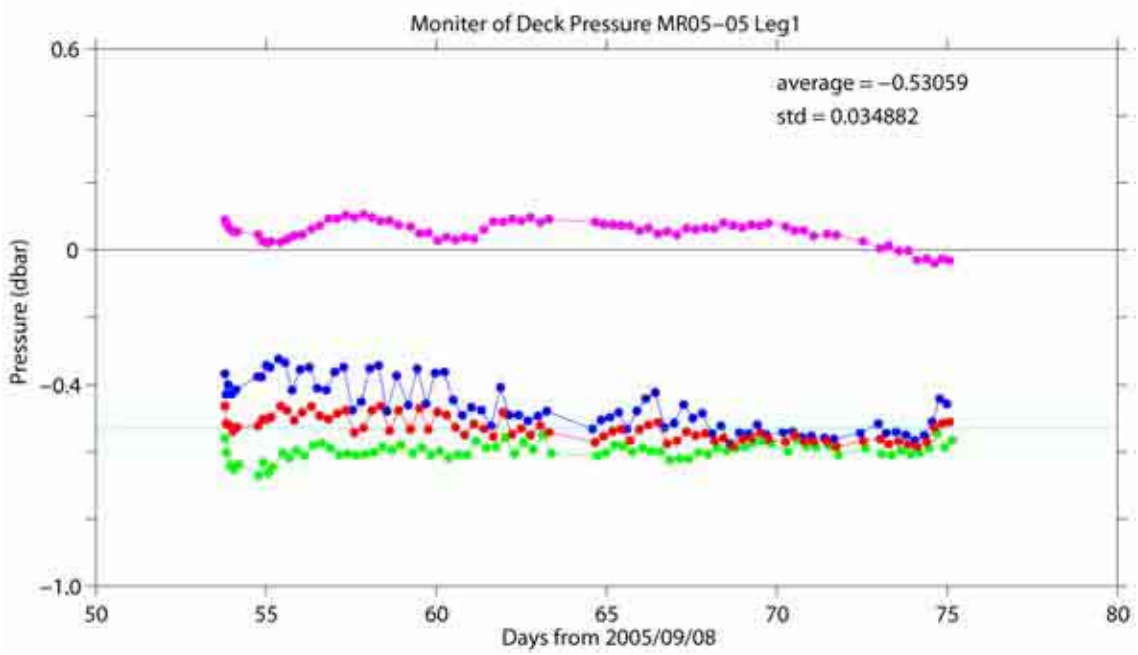


**Figure 3.1.5.1. Time series of the CTD deck pressure for leg 1. Pink dot indicates atmospheric pressure anomaly. Blue and green dots indicate pre- and post-cast deck pressures, respectively. Red dot indicates an average of the pre- and the post-cast deck pressures.**

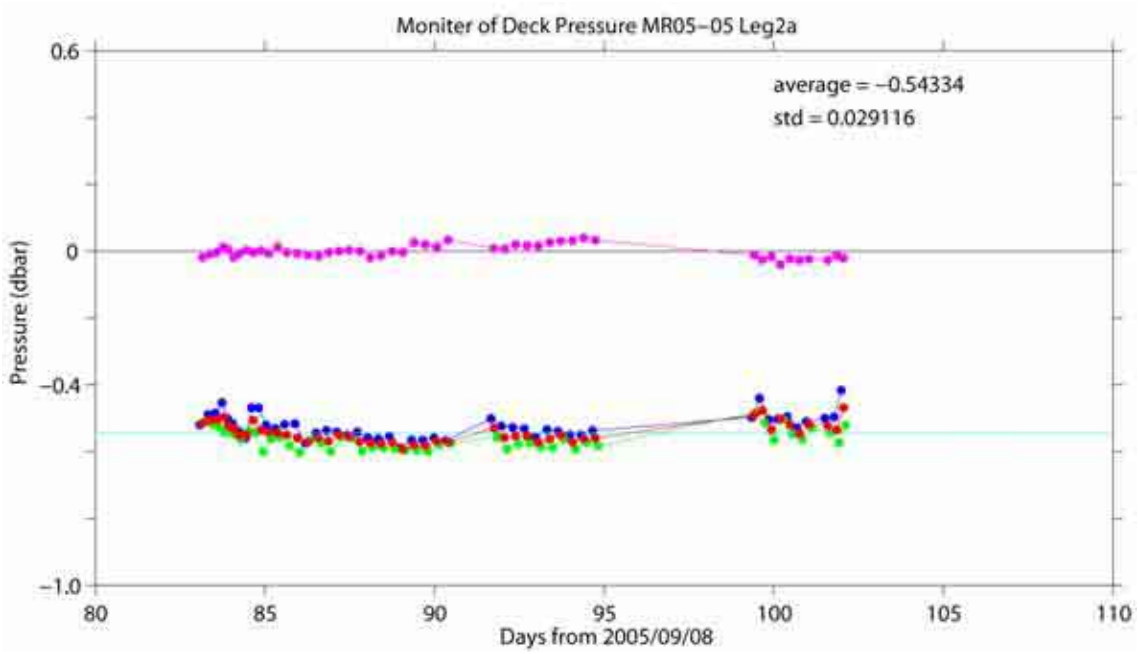


**Figure 3.1.5.2. Same as Figure 3.1.5.1, but for leg 2a.**

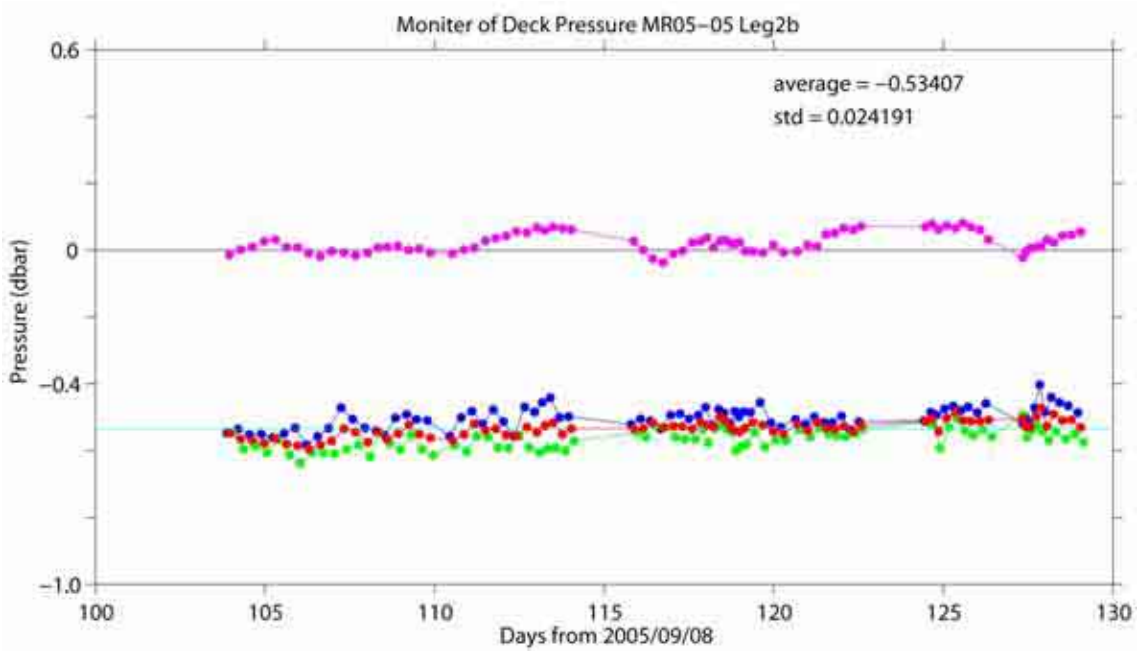


**Figure 3.1.5.3. Same as Figure 3.1.5.1, but for leg 2b.**

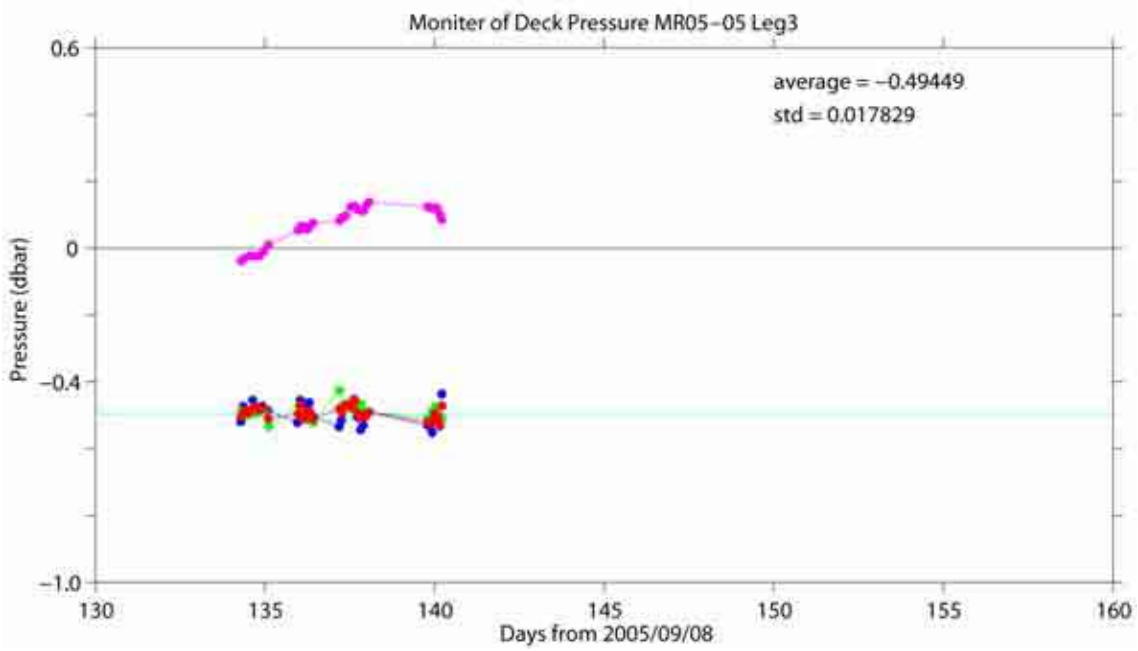


**Figure 3.1.5.4. Same as Figure 3.1.5.1, but for leg 3.**

**(2) Temperature**

The CTD temperature sensor (SBE 3) is made with a glass encased thermistor bead inside a needle. The needle protects the thermistor from seawater. If the thermistor bead is slightly large of specification it receives mechanical stress when the needle is compressed at high pressure (Budeus and Schneider, 1998). The pressure sensitivity for a SBE 3 sensor is usually less than +2 m°C / 6000 dbar. It is somewhat difficult to measure this effect in laboratory and it is one of the primary reasons to use the SBE 35 at sea for critical work. Also SBE 3 measurements may be affected by viscous heating (about +0.5 m°C) that occurs in a TC duct and does not occur for un-pumped SBE 35 measurements (Larson and Pederson, 1996). Furthermore the SBE 35 calibrations have some uncertainty about 0.2 m°C and SBE 3 calibrations have some uncertainty about 1 m°C. So the practical corrections for CTD temperature data can be made by using a SBE 35, correcting the SBE 3 to agree with the SBE 35 (a linear pressure correction, a time drift correction and an offset for viscous heating and/or calibration uncertainty).

Post-cruise sensor calibrations for the SBE 35 were performed at SBE, Inc., USA.

*S/N 0022, 1 February 2006 (2nd step: fixed point calibration)*

Slope = 1.000034

Offset = 0.000038

Offset of the SBE 35 (S/N 0022) data from the pre-cruise calibration is estimated to be 0.1 m°C for temperature less than 4 °C. Thus the post-cruise correction of the SBE 35 temperature data is not deemed necessary for the SBE 35.

The discrepancy between the CTD temperature and the SBE 35 is considered to be a function of pressure and time. Effect of the viscous heating is assumed to be constant in depth and time. Since the pressure sensitivity is thought to be constant in time at least during observation period, the CTD temperature is calibrated as

$$\text{Calibrated temperature} = T - (c_0 * P + c_1 * t + c_2)$$

where T is CTD temperature in °C, P is pressure in dbar, t is time in days from pre-cruise calibration date of CTD temperature and $c_0$, $c_1$, and $c_2$ are calibration coefficients. The best fit sets of coefficients are determined by minimizing the sum of absolute deviation from the SBE 35 data. The MATLAB® function FMINSEARCH is used to determine the sets. The FMINSEARCH uses the simplex search method (Lagarias et al., 1998). This is a direct search method that does not use numerical or analytic gradients.

The calibration is performed for the CTD data created by the software module ROSSUM. The deviation of CTD temperature from the SBE 35 temperature at depth shallower than 2,000 dbar is large for determining the coefficients with sufficient accuracy since the vertical temperature gradient is too large in the regions. Thus the coefficients are determined using the data for the depth deeper than 1,950 dbar. For leg 3 the calibration coefficients determined for leg 2b are used for the calibration because the maximum pressure of the CTD casts is shallower than 2,000 dbar in leg 3.

Finally following temperature data are used for the data set in consideration for the data quality.

Leg 1: secondary (S/N 4216) except for 94_1 and 114_1
primary (S/N 1464) for 94_1 and 114_1

Leg 2: primary (S/N 4216) except for WC7_1 and 328_1
secondary (S/N 1525) for WC7_1 and 328_1

Leg 3: primary (S/N 4216)

The number of data used for the calibration and the mean absolute deviation from the SBE 35 are listed in Table 3.1.5.2 and the calibration coefficients are listed in Table 3.1.5.3. The results of

the post-cruise calibration for the CTD temperature are summarized in Table 3.1.5.4 and shown in from Figure 3.1.5.5 to Figure 3.1.5.11.

**Table 3.1.5.2. Number of data used for the calibration (pressure >= 1,950 dbar) and mean absolute deviation (ADEV) between the CTD temperature and the SBE 35.**

| Leg | S/N | Number of data | ADEV (m°C) | Note |
|---|---|---|---|---|
| Leg 1 | 1464 | 976 | 0.10 | for 94_1, 114_1 |
| | 4216 | 976 | 0.10 | |
| Leg 2a | 4216 | 672 | 0.12 | |
| | 1525 | 661 | 0.10 | for WC7_1 |
| Leg 2b | 4216 | 1070 | 0.14 | |
| | 1525 | 1070 | 0.11 | for 328_1 |

**Table 3.1.5.3. Calibration coefficients for the CTD temperature sensors.**

| Leg | S/N | $c_0$ (°C/dbar) | $c_1$ (°C/day) | $c_2$ (°C) |
|---|---|---|---|---|
| Leg1 | 1464 | –1.090e–7 | 1.3833e–5 | –0.34e–3 |
| | 4216 | 1.8917e–8 | –4.1245e–6 | 0.55e–3 |
| Leg 2a | 4216 | –3.9923e–9 | –1.1221e–6 | 0.70e–3 |
| | 1525 | 1.0202e–9 | –5.4892e–6 | 0.84e–3 |
| Leg 2b | 4216 | –7.2153e–9 | 1.0834e–5 | –0.65e–3 |
| | 1525 | 2.7008e–9 | 1.8342e–6 | –0.07e–3 |
| Leg 3 | 4216 | Same as Leg 2b | Same as Leg 2b | Same as Leg 2b |

**Table 3.1.5.4. Difference between the CTD temperature and the SBE 35 after the post-cruise calibration. Mean and standard deviation (Sdev) are calculated for the data below and above 1,950 dbar. Number of data (Num) used is also shown.**

| Leg | S/N | Pressure >= 1,950 dbar | | | Pressure < 1,950 dbar | | |
|---|---|---|---|---|---|---|---|
| | | Num | Mean (m°C) | Sdev (m°C) | Num | Mean (m°C) | Sdev (m°C) |
| Leg 1 | 1464 | 976 | –0.01 | 0.14 | 1392 | –0.57 | 4.3 |
| | 4216 | 976 | –0.01 | 0.14 | 1392 | –0.13 | 4.0 |
| Leg 2a | 4216 | 672 | 0.02 | 0.17 | 888 | –0.04 | 4.6 |
| | 1525 | 661 | –0.00 | 0.17 | 872 | 0.16 | 5.5 |
| Leg 2b | 4216 | 1070 | –0.00 | 0.18 | 1407 | –0.11 | 4.3 |
| | 1525 | 1070 | –0.01 | 0.15 | 1421 | –0.21 | 4.4 |
| Leg 3 | 4216 | – | – | – | 332 | –0.59 | 5.5 |

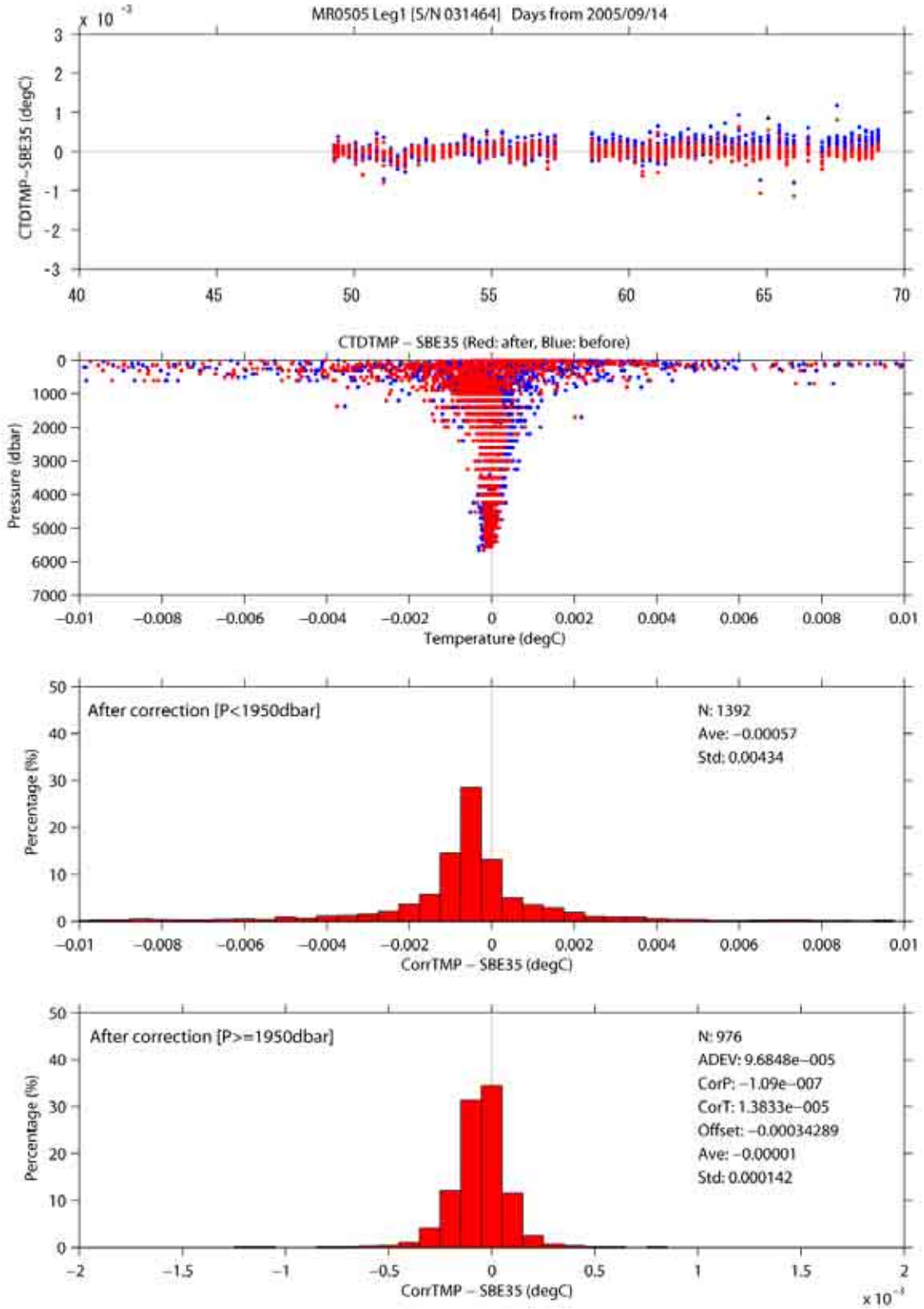


**Figure 3.1.5.5. Difference between the CTD temperature (primary) and the Deep Ocean Standards thermometer (SBE 35) for Leg 1. Blue and red dots indicate before and after the post-cruise calibration using the SBE 35 data, respectively. Top panel shows for P >= 1950 dbar. Lower two panels show histogram of the difference after the calibration.**

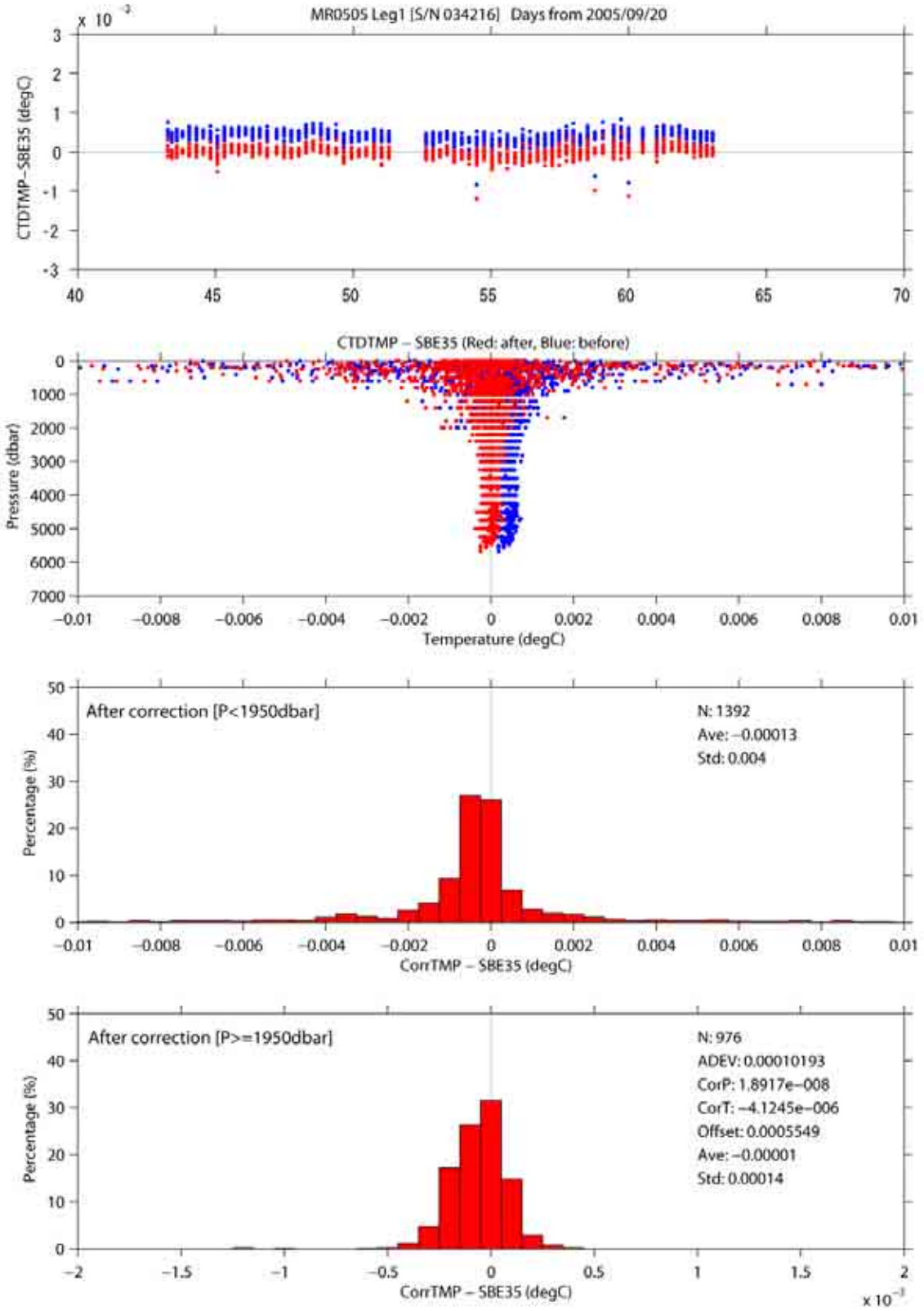


**Figure 3.1.5.6. Same as Figure 3.1.5.5, but for the secondary CTD temperature for Leg 1.**

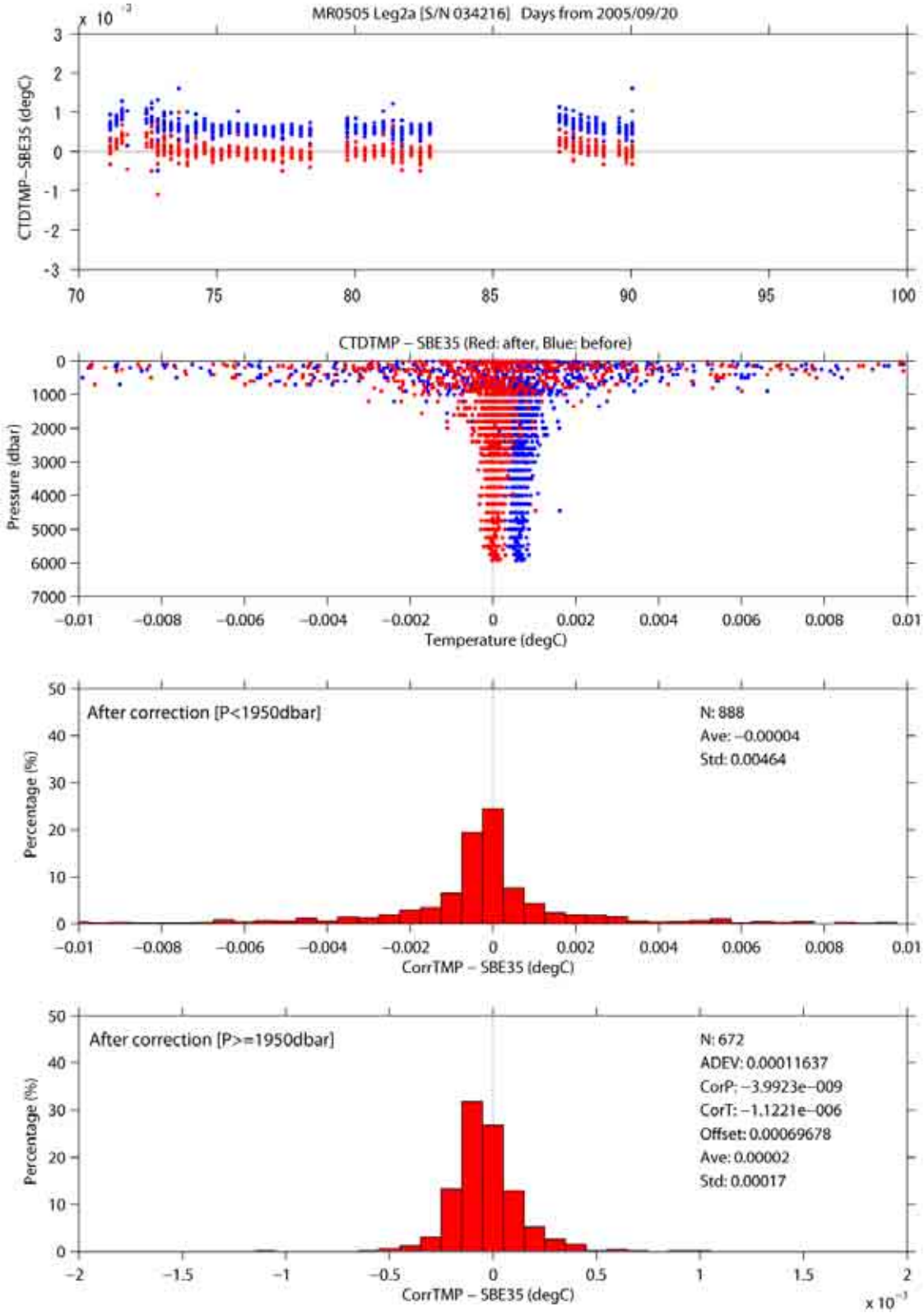


**Figure 3.1.5.7. Same as Figure 3.1.5.5, but for the primary CTD temperature for Leg 2a.**

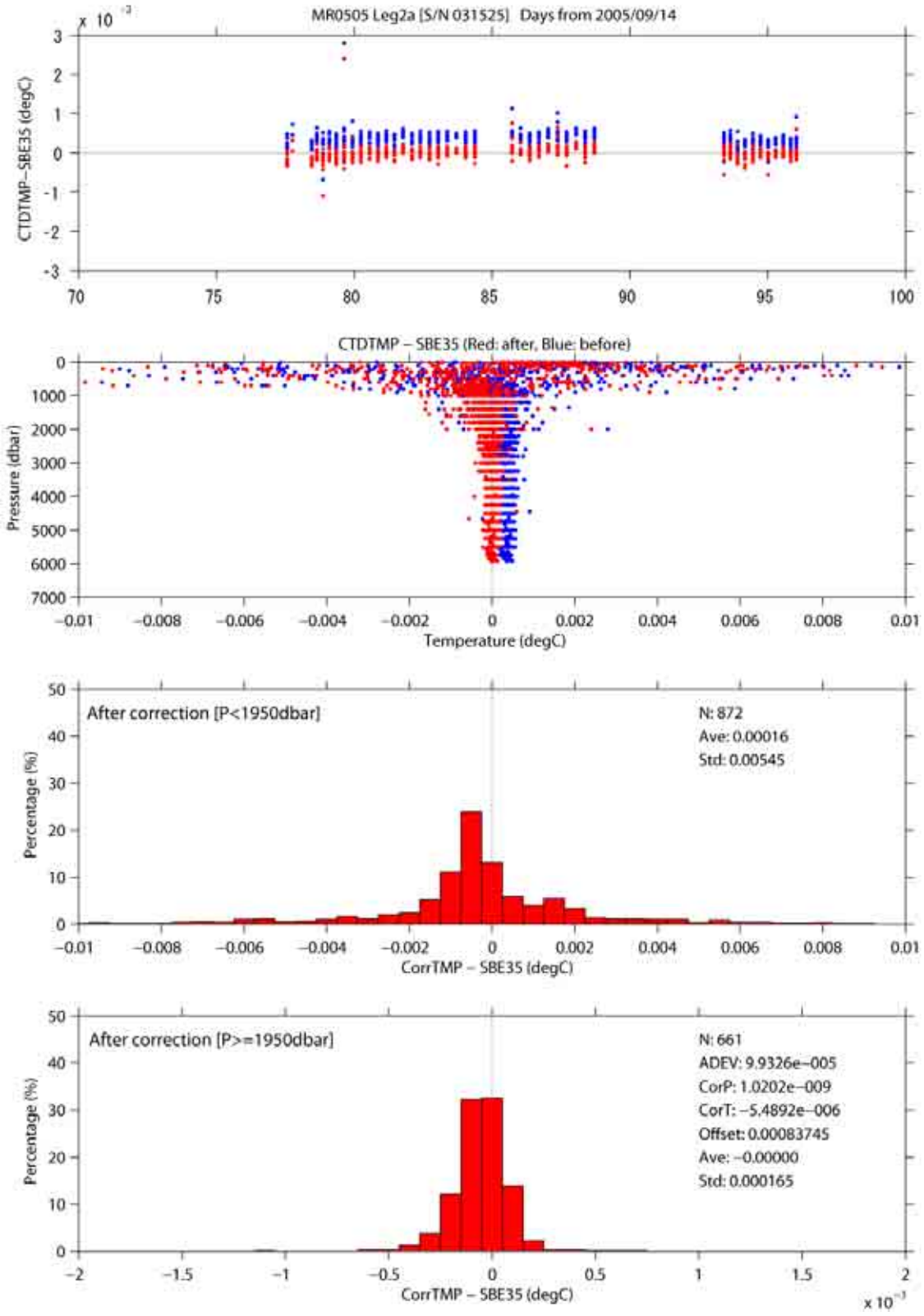


**Figure 3.1.5.8. Same as Figure 3.1.5.5, but for the secondary CTD temperature for Leg 2a.**

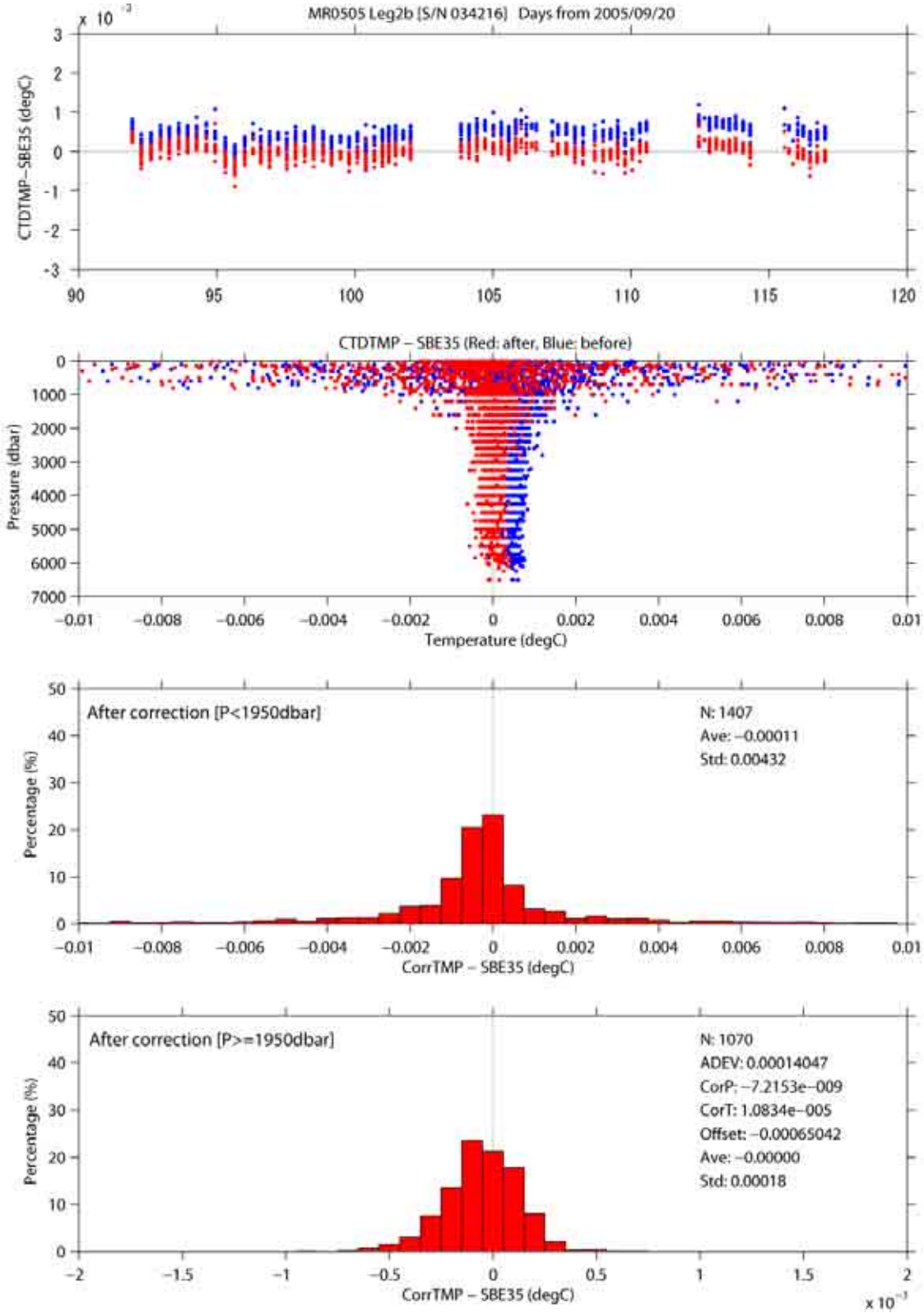


**Figure 3.1.5.9. Same as Figure 3.1.5.5, but for the primary CTD temperature for Leg 2b.**

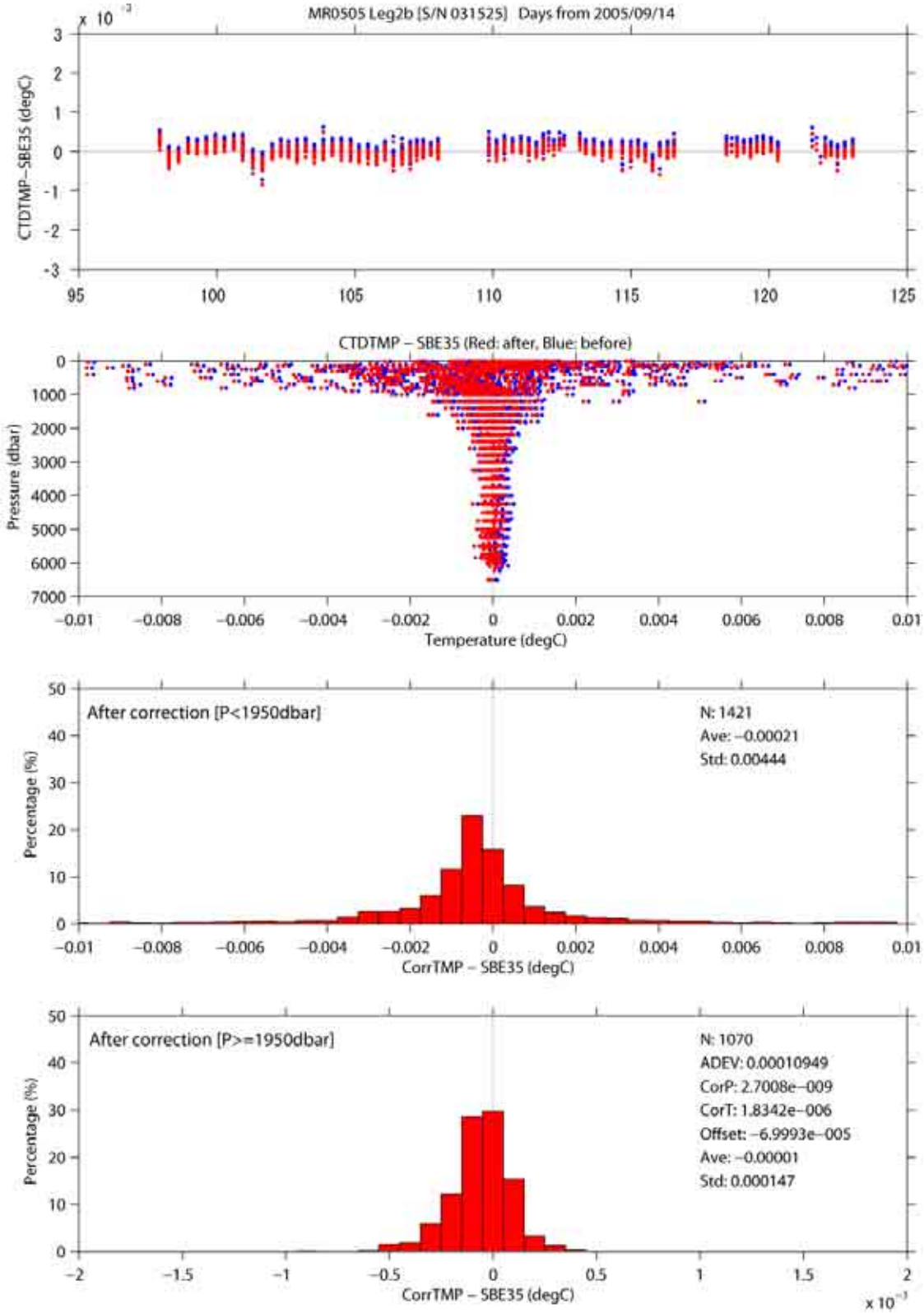


**Figure 3.1.5.10. Same as Figure 3.1.5.5, but for the secondary CTD temperature for Leg 2b.**

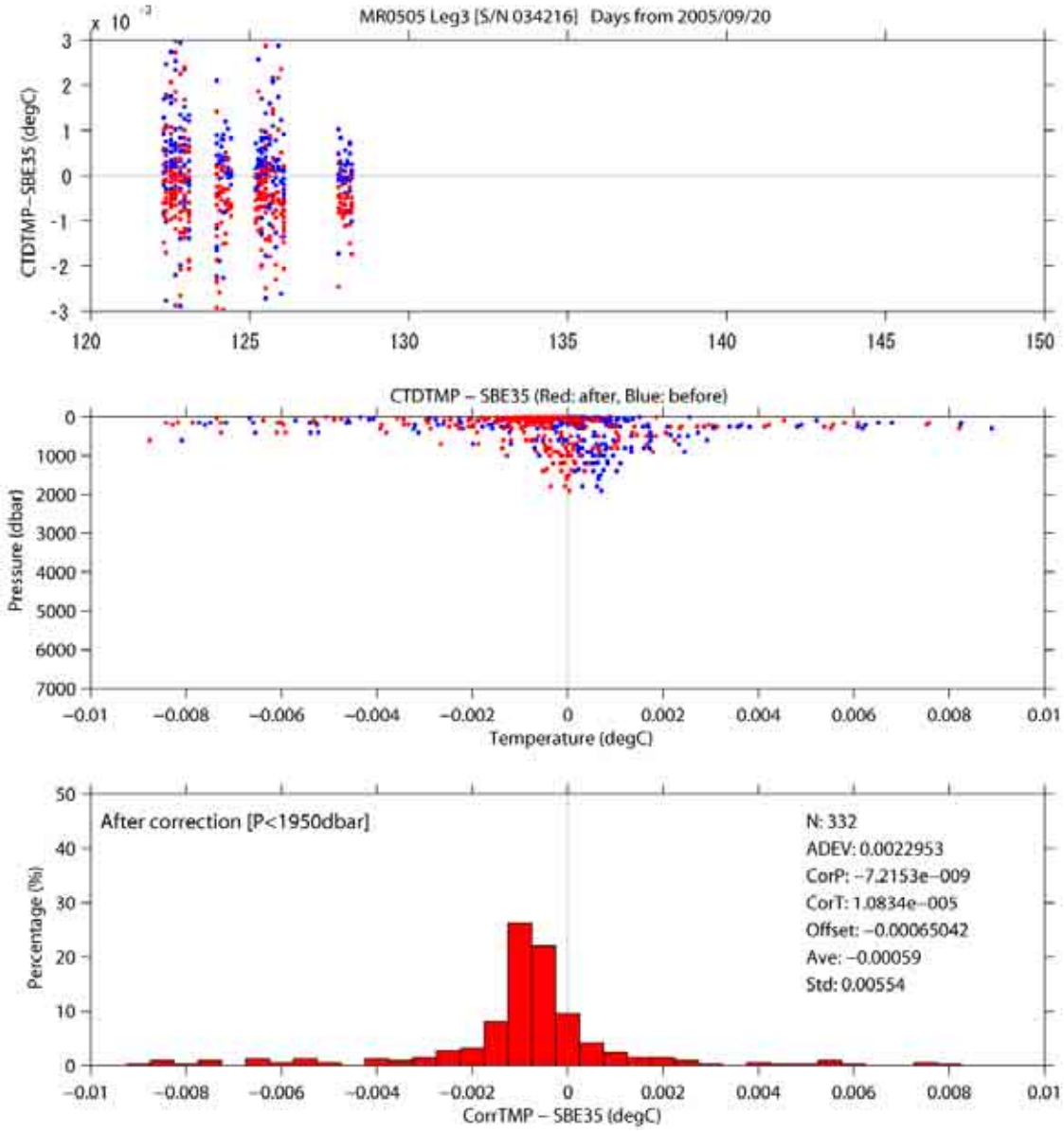


**Figure 3.1.5.11. Same as Figure 3.1.5.5, but for the primary CTD temperature for Leg 3. Top and bottom panels show full pressure range.**

**(3) Salinity**

The discrepancy between the CTD salinity and the bottle salinity is considered to be a function of conductivity and pressure. The CTD salinity is calibrated as

Calibrated salinity = $S - (c_0 * P + c_1 * C + c_2 * C * P + c_3)$

where S is CTD salinity, P is pressure in dbar, C is conductivity in S/m and $c_0$, $c_1$, $c_2$ and $c_3$ are calibration coefficients. The best fit sets of coefficients are determined by minimizing the sum of absolute deviation with a weight from the bottle salinity data. The MATLAB® function FMINSEARCH is used to determine the sets. The weight is given as a function of vertical salinity gradient and pressure as

Weight = $\min[4, \exp\{\log(4) * Gr / Grad\}] * \min[4, \exp\{\log(4) * P^2 / PR^2\}]$

where Grad is vertical salinity gradient in PSU $dbar^{-1}$, P is pressure in dbar. Gr and PR are threshold of the salinity gradient (0.5 mPSU $dbar^{-1}$) and pressure (1,000 dbar), respectively. When salinity gradient is small (large) and pressure is large (small), the weight is large (small) at maximum (minimum) value of 16 (1). The salinity gradient is calculated using up-cast CTD salinity data. The up-cast CTD salinity data is low-pass filtered with a 3-point (weights are 1/4, 1/2, 1/4) triangle filter before the calculation.

Finally salinity data derived from following conductivity sensor are used for the data set in consideration for the data quality.

Leg 1: secondary (S/N 2854) except for 94_1 and 114_1
primary (S/N 1203) for 94_1 and 114_1
Leg 2: primary (S/N 3124 and S/N 2854) except for WC7_1 and 328_1
secondary (S/N 3116) for WC7_1 and 328_1
Leg 3: primary (S/N 2854)

The CTD data created by the software module ROSSUM are used after the post-cruise calibration for the CTD temperature.

The coefficients are determined for some groups of the CTD stations. The results of the post-cruise calibration of the CTD salinity are summarized in Table 3.1.5.5 and shown in from Figure 3.1.5.12 to Figure 3.1.5.15. In addition the calibration coefficients and the number of the data used for the calibration are listed in Table 3.1.6.

**Table 3.1.5.5. Difference between the CTD salinity and the bottle salinity after the post-cruise calibration. Mean and standard deviation (Sdev) are calculated for the data below and above 950 dbar. Number of data (Num) used is also shown.**

| Leg | Pressure >= 950 dbar | | | Pressure < 950 dbar | | |
|---|---|---|---|---|---|---|
| | Num | Mean (mPSU) | Sdev (mPSU) | Num | Mean (mPSU) | Sdev (mPSU) |
| Leg 1 | 1320 | 0.01 | 0.32 | 1002 | 0.06 | 6.36 |
| Leg 2a | 920 | –0.02 | 0.34 | 656 | 0.72 | 5.89 |
| Leg 2b | 1422 | –0.02 | 0.36 | 1025 | 0.67 | 3.16 |
| Leg 3 | 25 | –0.04 | 0.41 | 296 | –0.17 | 1.86 |

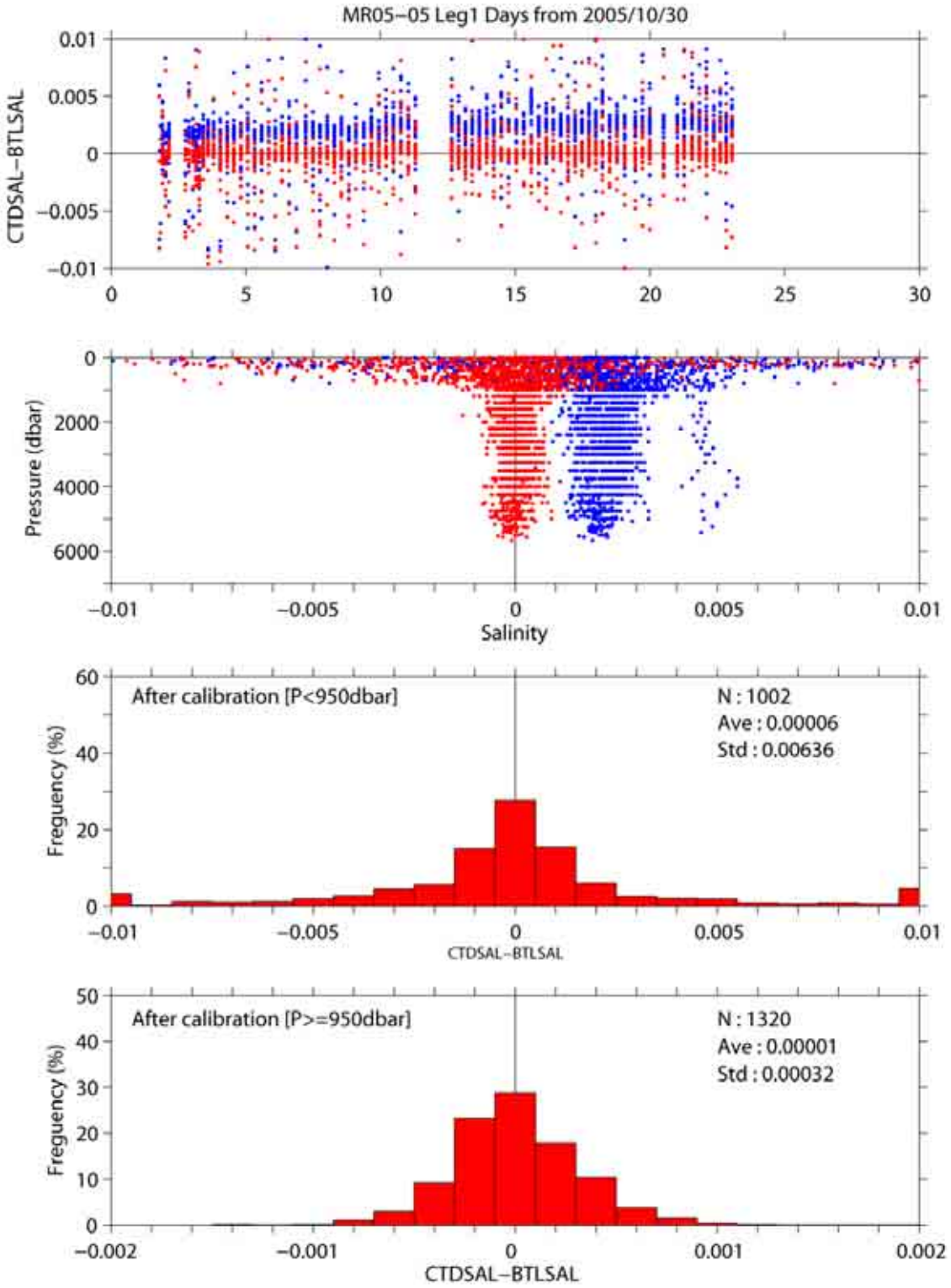


**Figure 3.1.5.12. Difference between the CTD salinity and the bottle salinity for Leg 1. Blue and red dots indicate before and after the post-cruise calibration using the bottle salinity data, respectively. Top panel shows P >= 950 dbar. Lower two panels show histogram of the difference after the calibration.**

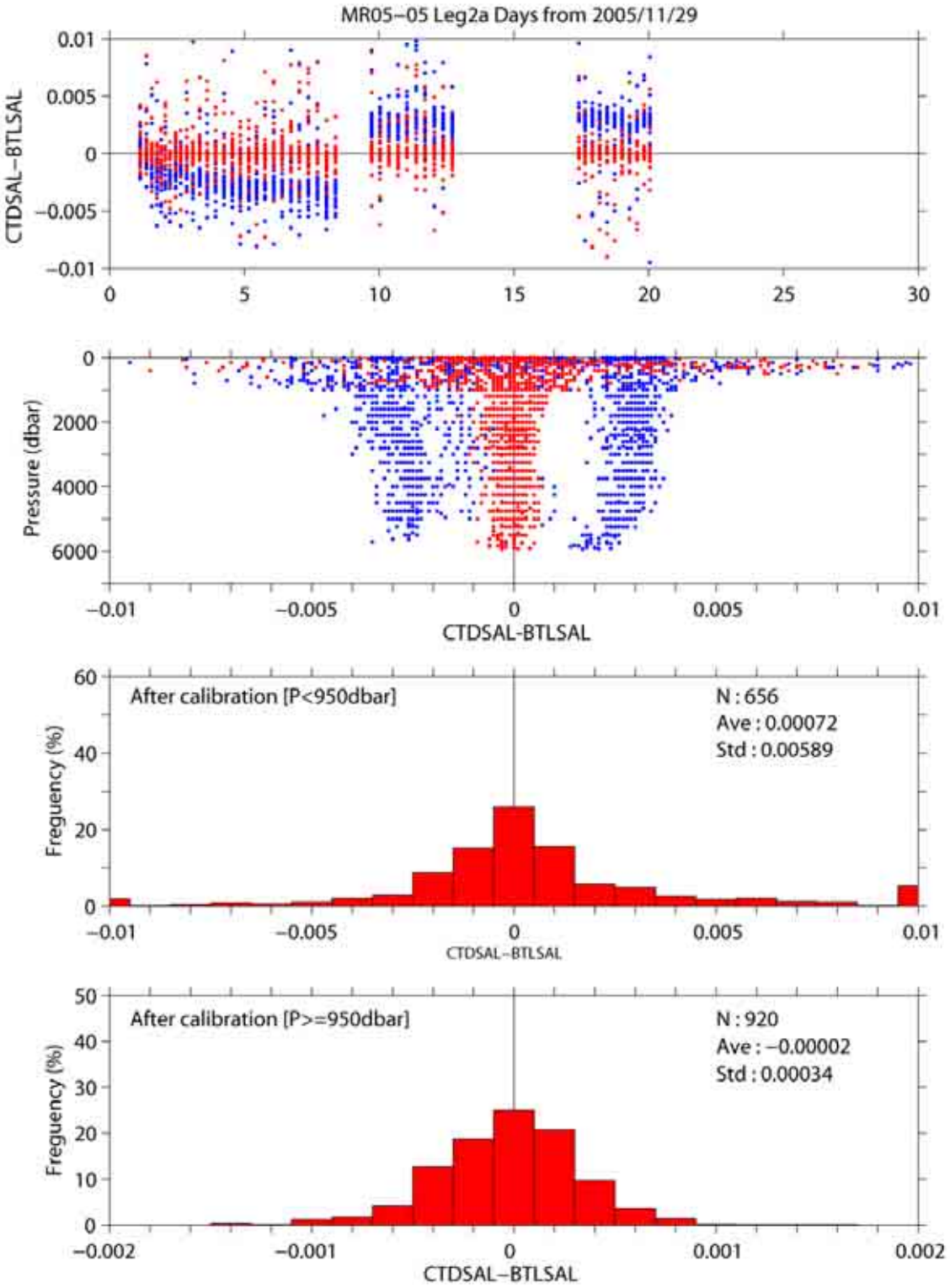


**Figure 3.1.5.13. Same as Figure 3.1.5.12, but for Leg 2a.**

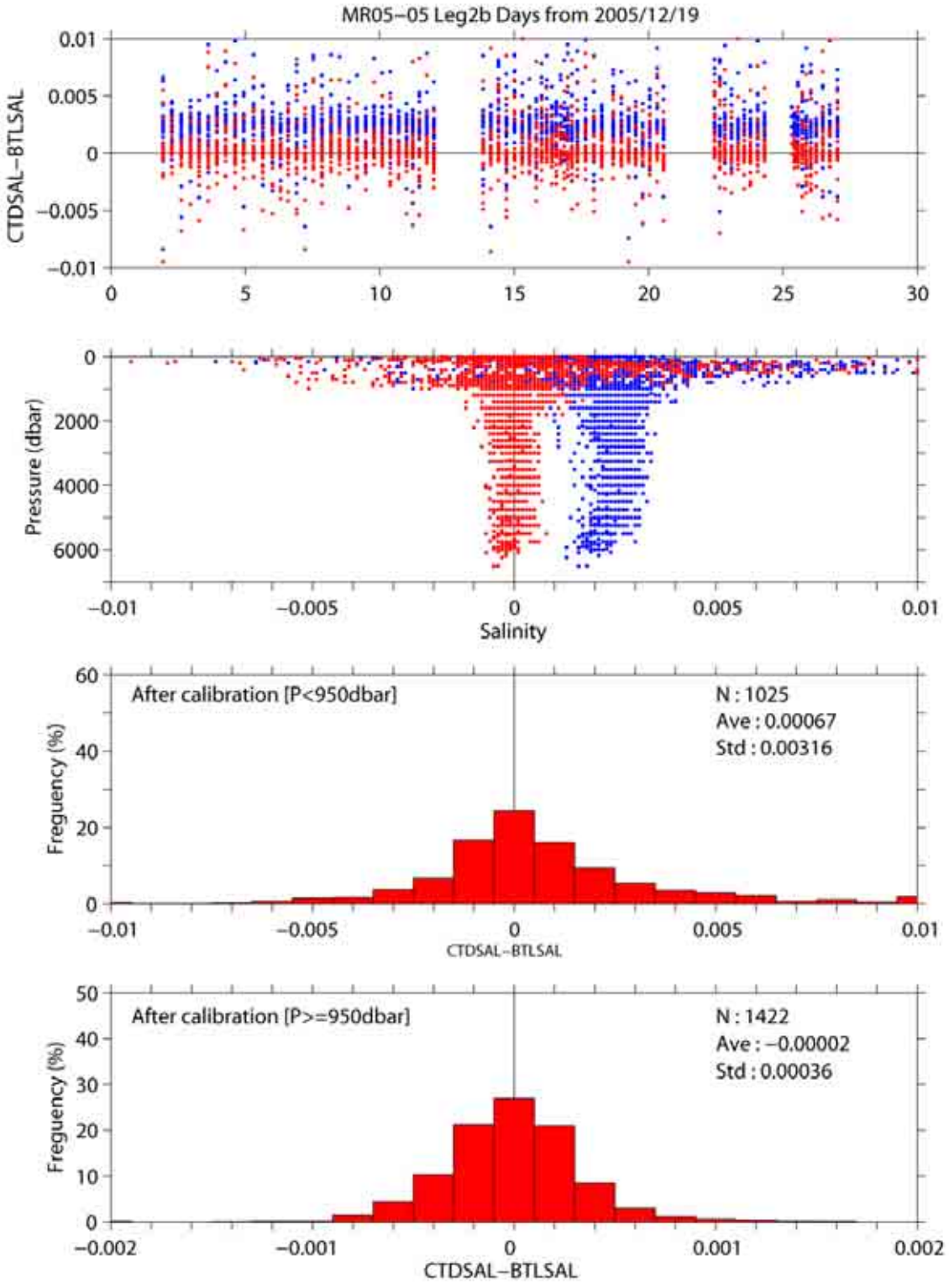


**Figure 3.1.5.14. Same as Figure 3.1.5.12, but for Leg 2b.**

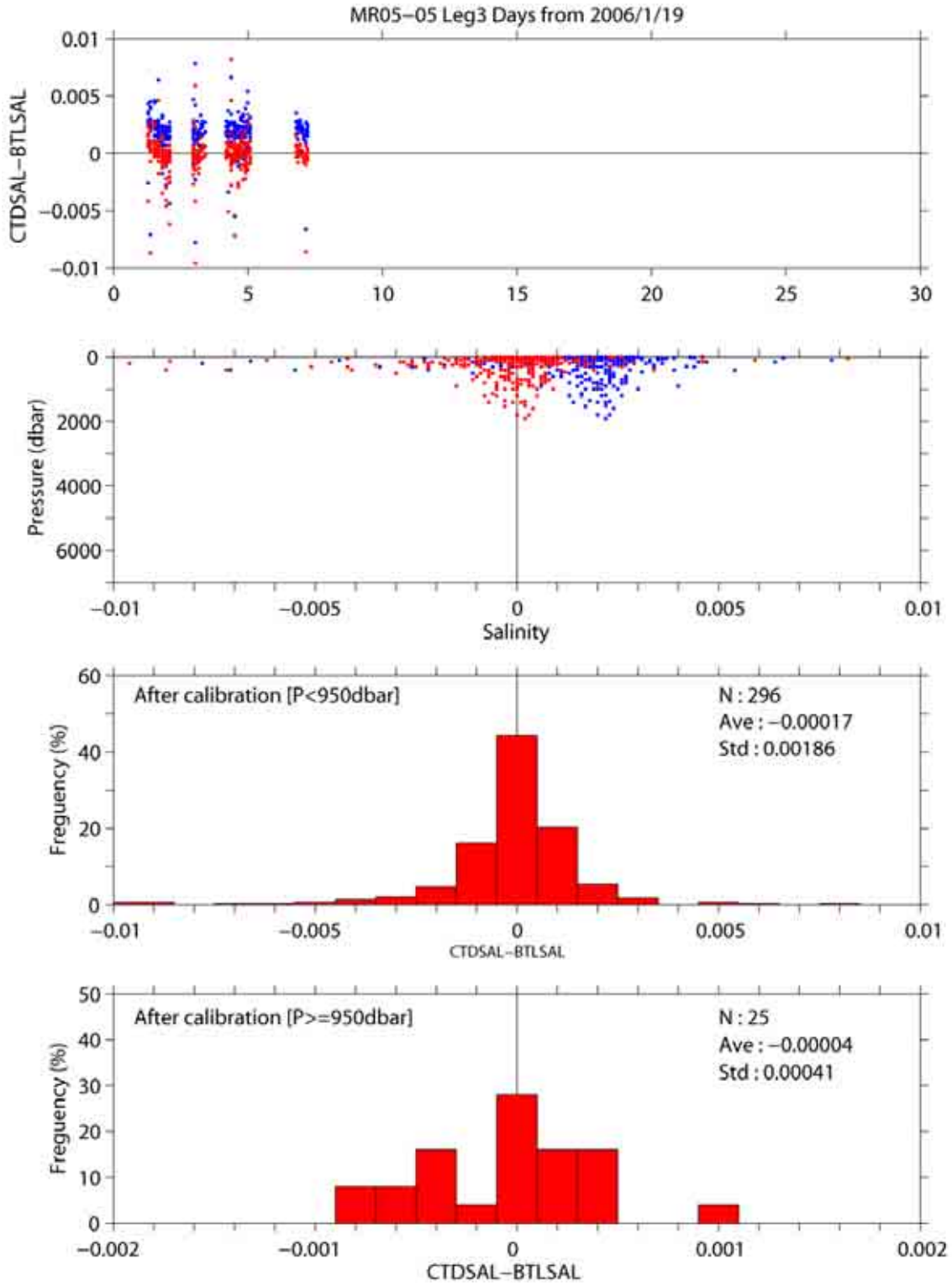


**Figure 3.1.5.15. Same as Figure 3.1.5.12, but for Leg 3. Top panel shows full pressure range.**

**Table 3.1.5.6. Calibration coefficients for the CTD salinity. Number of data (Num) used is also shown.**

| Stations | (Num) | C0 | C1 | C2 | C3 |
|---|---|---|---|---|---|
| Leg 1: | | | | | |
| 1_1-26_1 | (275) | -6.9332569403e-6 | -1.7406138415e-3 | 2.1616864848e-6 | 7.4450762843e-3 |
| 28_1-44_1 | (298) | -1.2804422689e-6 | -9.1223600910e-4 | 3.6879791066e-7 | 5.1074521112e-3 |
| 46_1-73_1 | (512) | 3.6529672450e-7 | -2.3847830676e-4 | -1.4495159805e-7 | 3.1629438129e-3 |
| 94_1,114_1 | (65) | 2.7703624740e-6 | 6.1243709126e-5 | -8.2572575661e-7 | 4.0659912660e-3 |
| 74_1-104_1 | (543) | 1.8730171701e-6 | -1.4227773847e-4 | -6.2019187422e-7 | 3.2067999773e-3 |
| 106_1-146_1 | (629) | -6.1266343657e-7 | -3.3024724989e-4 | 1.6374587979e-7 | 3.8794661715e-3 |
| Leg 2a: | | | | | |
| 146_2 | (32) | -1.3534051256e-6 | 2.6822634099e-4 | 4.8090447234e-7 | -1.7023616632e-3 |
| 148_1 | (30) | 2.8648089621e-6 | 7.9162918294e-4 | -8.5229000985e-7 | -4.1877005940e-3 |
| 150_1 | (27) | -6.3263920182e-6 | 5.6172052014e-4 | 2.1176194280e-6 | -4.0658193232e-3 |
| 152_1-157_1 | (96) | -1.3932496449e-6 | 5.0002444812e-4 | 4.6572414581e-7 | -4.3072082193e-3 |
| 159_1,161_1 | (62) | 2.6431715417e-6 | 6.2244409716e-4 | -8.1258089784e-7 | -4.1441691258e-3 |
| 163_1-171_1 | (161) | 8.2248815256e-7 | 5.4513664671e-4 | -2.1423403281e-7 | -5.1979263905e-3 |
| 173_1-197_1 | (437) | 4.6490157041e-6 | 7.1901447939e-4 | -1.4095235922e-6 | -6.4071128225e-3 |
| X14_1-217_1 | (355) | 4.5636737732e-6 | -2.0954365226e-4 | -1.4886356365e-6 | 3.3521757553e-3 |
| WC7_1 | (36) | 2.3388948512e-6 | -2.5405823909e-4 | -6.8264841424e-7 | 2.6121348754e-3 |
| WC0_1-WC10_1 | (345) | 4.4734717282e-6 | -1.0524927421e-4 | -1.4726908749e-6 | 3.5284312593e-3 |
| Leg 2b: | | | | | |
| 217_2-223_1 | (141) | 8.1232759178e-6 | -4.1703838739e-4 | -2.5464247645e-6 | 3.8110914876e-3 |
| 225_1-241_1 | (318) | 3.1775413340e-6 | -2.7641170222e-4 | -9.9523713450e-7 | 3.5148018313e-3 |
| 243_1 | (25) | -5.5463302053e-6 | -6.6347509786e-4 | 1.7271918177e-6 | 4.5585473787e-3 |
| 245_1-279_1 | (660) | 2.8847022900e-6 | -3.3899298844e-4 | -9.2783398683e-7 | 3.7937826601e-3 |
| 281_1-295_1 | (271) | 3.0443912104e-6 | -1.5733314930e-4 | -9.6264878196e-7 | 3.1990129886e-3 |
| 297_1-312_1 | (184) | -9.3159288381e-6 | -4.9418235747e-4 | 2.9682608422e-6 | 3.7280395807e-3 |
| 328_1 | (33) | -1.5232103653e-6 | -6.0491327964e-4 | 5.1646883670e-7 | 2.9111918302e-3 |
| 314_1-333_1 | (315) | 1.2037381315e-6 | -2.1752035380e-4 | -3.8674041433e-7 | 3.2959858445e-3 |
| 335_1-343_1 | (130) | -2.0392893584e-7 | -1.8946836643e-4 | 6.4501351565e-8 | 2.7992069617e-3 |
| 345_1-351_1 | (134) | 2.7238042547e-6 | -2.3311048294e-5 | -8.6986291755e-7 | 2.5838371732e-3 |
| 369_1-357_1 | (136) | 8.7957026329e-7 | 1.1423193230e-4 | -2.8274598494e-7 | 1.8615333187e-3 |
| 355_1-351_2 | (105) | 3.6018768105e-6 | -1.6276726098e-4 | -1.1078997582e-6 | 2.8866166830e-3 |
| Leg 3: | | | | | |
| 370_1-TS1_1 | (321) | 3.6800065006e-6 | -6.9694450581e-5 | -1.1545267726e-6 | 2.4027579868e-3 |

**(4) Oxygen (SBE 43)**

The CTD oxygen is calibrated using the oxygen model (see 3.1.3(4)) as

Calibrated oxygen (ml/l)

= {(Soc+dSoc) * {v+offset+doffset} * exp{(TCor+dTCor) * t + (PCor+dPCor) * p}} * Oxsat(t, s)

where p is pressure in dbar, t is absolute temperature and s is salinity in psu. Oxsat is oxygen saturation value minus the volume of oxygen gas (STP) absorbed from humidity-saturated air (see 3.1.3(4)). Soc, offset, TCor and PCor are the pre-cruise calibration coefficients (see 3.1.3(4)) and dSoc, doffset, dTCor and dPCor are calibration coefficients. The best fit sets of coefficients are determined by minimizing the sum of absolute deviation with a weight from the bottle oxygen data. The MATLAB® function FMINSEARCH is used to determine the sets. The weight is given as a function of vertical oxygen gradient and pressure as

Weight = min[4, exp{log(4) * Gr / Grad}] * min[4, exp{log(4) * $P^2$ / $PR^2$}]

where Grad is vertical oxygen gradient in μmol $kg^{-1}$ $dbar^{-1}$, P is pressure in dbar. Gr and PR are threshold of the oxygen gradient (0.3 μmol $kg^{-1}$ $dbar^{-1}$) and pressure (1,000 dbar), respectively. When oxygen gradient is small (large) and pressure is large (small), the weight is large (small) at maximum (minimum) value of 16 (1). The oxygen gradient is calculated using down-cast CTD oxygen data. The down-cast CTD oxygen data is low-pass filtered with a 3-point (weights are 1/4, 1/2, 1/4) triangle filter before the calculation.

Finally oxygen data derived from following oxygen sensor are used for the data set in consideration for the data quality.

Leg 1: primary (S/N 0391)
Leg 2: primary (S/N 0391) for 146_2 and 148_1
secondary (S/N 0394) from 150_1 to WC8_1
primary (S/N 0390) from WC9_1 to 351_2
Leg 3: primary (S/N 0390)

The down-cast CTD data sampled at same density of the up-cast CTD data created by the software module ROSSUM are used after the post-cruise calibration for the CTD temperature and salinity.

The coefficients are basically determined for each station. Some stations, especially for shallow stations, are grouped for determining the calibration coefficients. The results of the post-cruise calibration for the CTD oxygen are summarized in Table 3.1.5.7 and shown in from Figure 3.1.5.16 to Figure 3.1.5.19. And the calibration coefficients and number of the data used for the calibration are listed in Table 3.1.5.8.

**Table 3.1.5.7. Difference between the CTD oxygen and the bottle oxygen after the post-cruise calibration. Mean and standard deviation (Sdev) are calculated for the data below and above 950 dbar. Number of data used is also shown.**

| Leg | Pressure >= 950 dbar | | | Pressure < 950 dbar | | |
|---|---|---|---|---|---|---|
| | Num | Mean (μmol/kg) | Sdev (μmol/kg) | Num | Mean (μmol/kg) | Sdev (μmol/kg) |
| Leg 1 | 1326 | –0.04 | 0.66 | 1006 | 0.03 | 3.59 |
| Leg 2a | 925 | 0.03 | 0.67 | 643 | 0.08 | 2.94 |
| Leg 2b | 1419 | –0.03 | 0.91 | 1012 | 0.05 | 2.53 |
| Leg 3 | 25 | –0.05 | 0.33 | 295 | –0.02 | 2.23 |

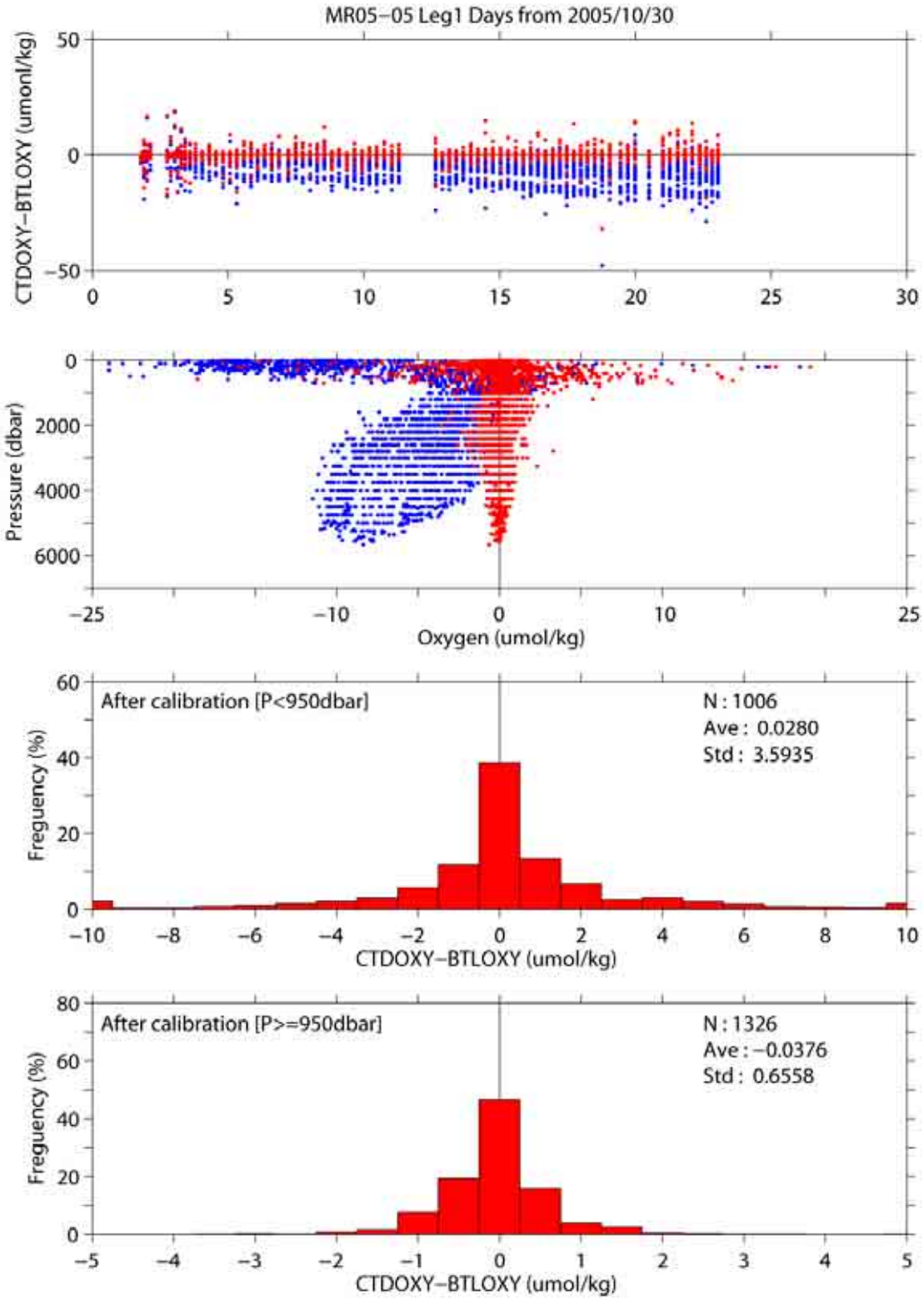


**Figure 3.1.5.16. Difference between the CTD oxygen and the bottle oxygen for Leg 1. Blue and red dots indicate before and after the post-cruise calibration using the bottle oxygen data, respectively. Top panel shows P >= 950 dbar. Lower two panels show histogram of the difference after the calibration.**

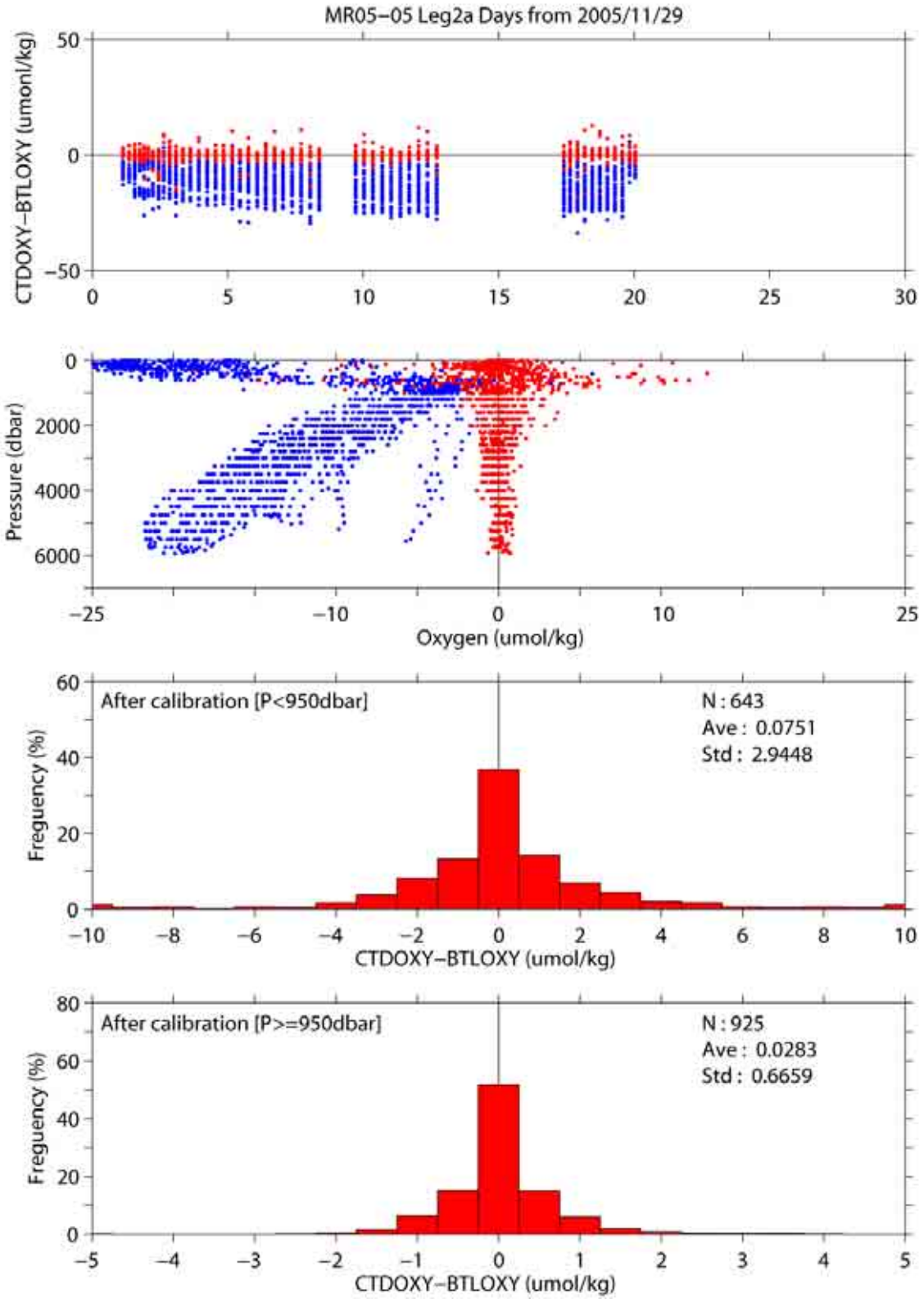


**Figure 3.1.5.17. Same as Figure 3.1.5.16, but for Leg 2a.**

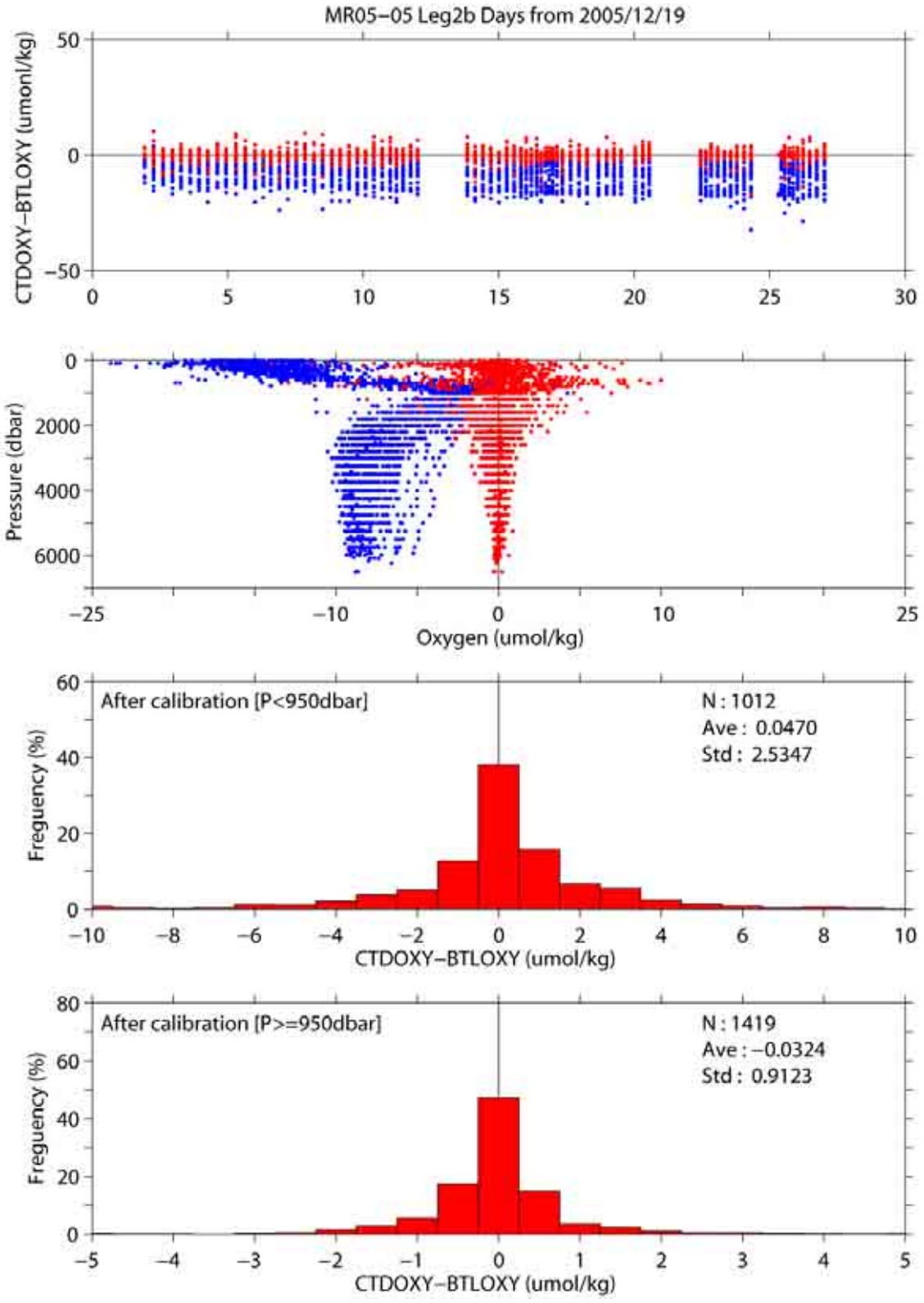


**Figure 3.1.5.18. Same as Figure 3.1.5.16, but for Leg 2b.**

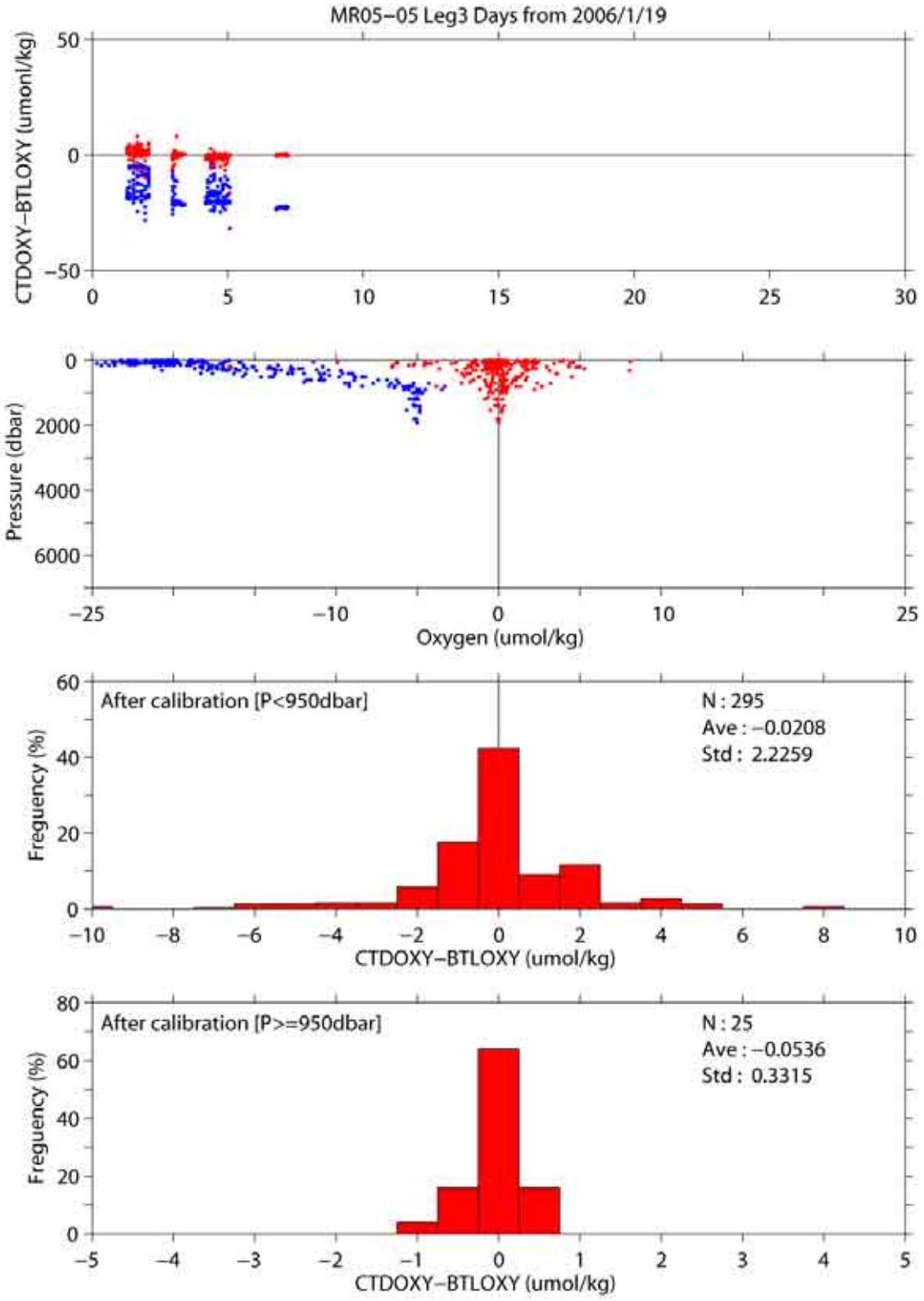


**Figure 3.1.5.19. Same as Figure 3.1.5.16, but for Leg 3. Top panel shows full pressure range.**

**Table 3.1.5.8. Calibration coefficients for the CTD oxygen. Number of data (Num) used is also shown.**

| Stations | (Num) | dSoc | dTCor | dPCor | doffset |
|---|---|---|---|---|---|
| Leg1: | | | | | |
| 1_1-16_1 | (136) | -4.7030795530e-4 | 1.2216502504e-3 | 3.5806042880e-6 | -1.1228673185e-3 |
| 18_1 | (28) | 1.6534399050e-3 | 1.0099064828e-3 | -8.3447124446e-7 | 2.4218143184e-3 |
| 20_1 | (27) | 6.7411343894e-3 | 4.4948747210e-4 | -4.6287556278e-7 | -4.6342779017e-3 |
| 22_1 | (28) | 1.5126805902e-2 | -7.0643214403e-4 | -4.6039465153e-6 | -7.7115069439e-3 |
| 24_1 | (28) | 1.8958132896e-2 | -1.1837775418e-3 | -7.7128522345e-6 | -5.9919173181e-3 |
| 26_1 | (28) | 2.7481439993e-3 | 1.7048745406e-3 | 3.3014999254e-6 | -2.9922615709e-3 |
| 28_1 | (31) | 2.4708834982e-3 | 1.3890243427e-3 | 2.1505225175e-6 | -1.3316766616e-3 |
| 30_1 | (30) | 4.1455607447e-3 | 1.0914675896e-3 | 1.1508612526e-6 | 2.0840053303e-4 |
| 31_1,33_1 | (58) | 1.3193511928e-2 | 1.6877783130e-4 | -3.0524102847e-7 | -1.1003744120e-2 |
| 34_1 | (30) | 1.8013943471e-2 | -1.4829061133e-4 | -5.3783979798e-6 | -4.4753538564e-3 |
| 36_1 | (30) | 1.0711956259e-2 | 7.9743152520e-4 | -1.9408684910e-6 | -9.8181152457e-4 |
| 38_1 | (29) | 1.6165303858e-2 | -1.0438711248e-4 | -1.1516000318e-6 | -9.8402720806e-3 |
| 40_1 | (31) | 1.1622316137e-2 | 4.8172714615e-4 | -1.8779415303e-6 | -2.7796157451e-4 |
| 42_1 | (32) | 1.3978702079e-2 | 3.5265534153e-4 | 4.0624981687e-7 | -1.1013015148e-2 |
| 44_1 | (30) | 1.5512408093e-2 | 4.3263372727e-4 | 1.2966946497e-6 | -1.4699750472e-2 |
| 46_1 | (32) | 4.3641287878e-3 | 1.4975164083e-3 | 2.4243192480e-6 | 1.5993735231e-3 |
| 48_1 | (32) | 1.0892244717e-2 | 5.2384737607e-4 | -1.4967639768e-6 | 1.5722413475e-3 |
| 50_1 | (31) | 8.0274967458e-3 | 1.1446891822e-3 | 1.1511865865e-6 | -2.9211628153e-4 |
| 51_1 | (32) | 1.6102252789e-2 | 1.2789571011e-4 | -3.0443844006e-6 | -1.1665814908e-3 |
| 53_1 | (32) | 1.3061298445e-2 | 4.2341040985e-4 | -1.0133590643e-6 | -1.5493363228e-3 |
| 55_1 | (32) | 5.6961166324e-3 | 1.2723228582e-3 | -1.8749572610e-6 | 1.2998524597e-2 |
| 56_1 | (33) | 1.1950103381e-2 | 9.5568415538e-4 | 7.9578976576e-7 | -4.9555782059e-3 |
| 58_1 | (33) | 1.6739688059e-2 | 3.4353735948e-4 | -1.1572297151e-6 | -7.0671602654e-3 |
| X17_1 | (33) | 1.6937558673e-2 | 2.3468098971e-4 | -7.6233019077e-7 | -7.6296078744e-3 |
| 62_1 | (31) | 1.8724229093e-2 | 7.0641380267e-5 | -7.1680907741e-7 | -1.0138160504e-2 |
| 64_1 | (30) | 2.1034093742e-2 | -6.9954451837e-5 | -2.9252266507e-7 | -1.2413939684e-2 |
| 66_1 | (32) | 1.1324045971e-2 | 8.8618646035e-4 | -2.6678599759e-8 | 1.5017628464e-3 |
| 67_1 | (33) | 1.5847113629e-2 | 5.5327556139e-4 | 4.5059875041e-7 | -7.8497901010e-3 |
| 69_1 | (34) | 1.4309282193e-2 | 5.8938389146e-4 | -1.2388342751e-6 | 1.0782466884e-3 |
| 71_1 | (31) | 1.7050450252e-2 | 3.9059865144e-4 | -2.6222013590e-6 | 4.1891625261e-4 |
| 73_1 | (33) | 2.0744146158e-2 | 2.1811279208e-5 | -2.0549892979e-7 | -1.2477041137e-2 |
| 74_1 | (34) | 2.5928743641e-2 | -7.3501458894e-4 | -3.9062843231e-6 | -9.6824211478e-3 |
| 76_1 | (32) | 1.9832210017e-2 | 8.6757629464e-5 | -1.4312829344e-6 | -6.0902181712e-3 |
| 77_1 | (33) | 2.6518246243e-2 | -5.7858206314e-4 | -4.5023441041e-6 | -8.6938561018e-3 |
| 79_1 | (31) | 1.8929951155e-2 | 2.3188201860e-4 | -9.4217892618e-7 | -6.4374237570e-3 |
| 81_1 | (34) | 1.0526377944e-2 | 1.0754938456e-3 | 3.6584111282e-6 | -6.3754686271e-3 |
| 83_1 | (34) | 9.4781027191e-3 | 1.2351479219e-3 | -5.8718637658e-7 | 1.2145988997e-2 |
| 84_1 | (35) | 1.5289571008e-2 | 8.8658420203e-4 | 5.2648777266e-7 | -1.5518057125e-3 |
| 86_1 | (35) | 3.5016018312e-2 | -1.1813726785e-3 | -4.2845014316e-6 | -1.6200362856e-2 |
| 88_1 | (34) | 1.8416343105e-2 | 7.9059432252e-4 | 2.7145104489e-7 | -5.7375270780e-3 |
| 90_1 | (35) | 2.4584869357e-2 | 1.0555651612e-4 | -1.3672358988e-6 | -7.7015242904e-3 |
| 92_1 | (36) | 2.6704145357e-2 | -2.6206945224e-4 | -2.2034634972e-6 | -7.8337395786e-3 |
| 94_1 | (34) | 1.9970369375e-2 | 5.0871610478e-4 | -9.7834330721e-8 | -2.0595188652e-3 |
| 96_1 | (34) | 1.7634878941e-2 | 9.5043247314e-4 | 5.2713529641e-7 | 1.6472618321e-4 |
| 98_1 | (34) | 2.3328408963e-2 | 3.5365839272e-4 | -8.6465505110e-7 | -4.4859507330e-3 |
| 100_1 | (35) | 1.9743046348e-2 | 8.0109022717e-4 | 9.6062483248e-7 | -4.1293242675e-3 |
| X16_1 | (34) | 2.3859402087e-2 | 2.5034886173e-4 | -1.7635714127e-6 | 1.2487906975e-3 |
| 104_1 | (34) | 1.9301677794e-2 | 9.9716591389e-4 | 1.1293228331e-6 | 4.4483436534e-4 |
| 106_1 | (33) | 3.7075179244e-2 | -7.0421142323e-4 | -2.2512069599e-6 | -1.7512692836e-2 |
| 108_1 | (32) | 3.1381730648e-2 | -2.6022098343e-4 | -3.3289196375e-6 | -4.4506707340e-3 |
| 110_1 | (31) | 4.0786234444e-2 | -9.3220337388e-4 | -2.5248992574e-6 | -2.2327285676e-2 |
| 112_1 | (31) | 2.9851343344e-2 | 1.3176980732e-4 | 2.3429241248e-6 | -1.7478888940e-2 |
| 114_1 | (31) | 2.4012875755e-2 | 4.9210563724e-4 | -1.0312775634e-6 | 6.4768265096e-4 |
| 116_1 | (29) | 2.6393732530e-2 | 8.0062366886e-4 | -2.5685312984e-7 | -5.6542815135e-3 |
| 118_1 | (29) | 3.0727843484e-2 | -1.2197155723e-4 | -4.4247598809e-6 | 9.0956503362e-4 |
| 120_1 | (31) | 3.6553917712e-2 | -5.0218965554e-4 | -1.4982730280e-6 | -1.6108563625e-2 |
| 122_1 | (33) | 2.4220711952e-2 | 6.2361811338e-4 | 8.3271137444e-8 | -1.6332391163e-3 |
| 124_1 | (31) | 3.0022849212e-2 | -7.5303548929e-5 | -3.7910724364e-6 | 1.5742825318e-3 |
| 126_1 | (33) | 1.9627772037e-2 | 1.0747655389e-3 | -1.1455309895e-7 | 6.8614333372e-3 |
| 128_1 | (33) | 3.1448485957e-2 | 2.9607916027e-4 | 1.3607527961e-6 | -1.7352446099e-2 |
| 130_1,132_1 | (59) | 2.4583723984e-2 | 5.0736691054e-4 | -1.2762940757e-6 | 1.0704642208e-3 |
| 134_1 | (33) | 3.4335256895e-2 | -4.9480474424e-4 | -4.8192140772e-6 | -8.5484342546e-4 |
| 136_1 | (29) | 2.0365730703e-2 | 1.2968294124e-3 | 1.1796185243e-6 | 6.2962100557e-3 |
| 138_1 | (32) | 2.6426521919e-2 | 3.6137695398e-4 | -2.4935058759e-6 | 4.4793452615e-3 |
| 140_1 | (32) | 3.1801441427e-2 | 1.7352803853e-4 | -6.0247731984e-7 | -8.6993469530e-3 |
| 142_1 | (33) | 3.8472980020e-2 | -5.6654785011e-4 | -5.2539596629e-6 | -5.1713569623e-3 |
| 144_1 | (33) | 3.2353296623e-2 | -2.2258595772e-5 | -3.0874610976e-6 | -6.0313715952e-4 |
| 146_1 | (33) | 2.2067613214e-2 | 9.4538485154e-4 | -1.4151085628e-6 | 1.1516746472e-2 |
| Leg 2a: | | | | | |
| 146_2 | (25) | 3.4831974424e-2 | -1.0489027362e-3 | -5.3458812546e-6 | -1.7794691271e-3 |
| 148_1 | (22) | 3.2913244928e-2 | -1.9172209647e-3 | -3.4275208825e-6 | -2.9609432437e-3 |
| 150_1-153_1 | (64) | 2.6216842203e-2 | 5.5063114638e-4 | 2.4225385514e-6 | 2.5351479382e-4 |
| 154_1-157_1 | (58) | 2.8792970734e-2 | 4.3269078450e-4 | 6.2331531003e-7 | -3.7430726943e-3 |
| 159_1 | (29) | 2.3780435869e-2 | 6.2041203270e-4 | 5.7286691375e-7 | 6.5676847439e-3 |
| 161_1 | (33) | 1.8811279483e-2 | 1.3376685549e-3 | 4.5932697007e-6 | 2.9595153138e-3 |
| 163_1 | (32) | 3.3070023339e-2 | 2.6527293911e-4 | 2.3344209444e-6 | -9.2043367505e-3 |
| 165_1 | (33) | 3.4940255968e-2 | 6.5069177021e-5 | -8.4926434631e-7 | 1.3316149127e-4 |

| | | | | | |
|---|---|---|---|---|---|
| 167_1 | (33) | 3.5596879935e-2 | 1.2601577349e-4 | 3.3242118063e-7 | -3.0788163161e-3 |
| 169_1 | (32) | 2.7107012759e-2 | 1.1700396704e-3 | 2.7099851088e-6 | 3.5925807067e-3 |
| 171_1 | (30) | 3.2724127309e-2 | 7.9804863297e-4 | 2.5781296329e-6 | -5.7031637195e-3 |
| 173_1 | (32) | 3.7039333806e-2 | 1.2174168773e-4 | 4.8618371003e-7 | -4.3531154911e-3 |
| 175_1 | (33) | 3.7758061787e-2 | -2.0876240963e-6 | 3.3943843796e-7 | -3.9528320902e-3 |
| 177_1 | (32) | 4.6006413719e-2 | -6.5564921676e-4 | -3.6155380214e-6 | -4.5235459974e-3 |
| 179_1 | (32) | 4.7923560328e-2 | -6.6576356566e-4 | -3.5220804069e-6 | -6.9640760215e-3 |
| 181_1 | (33) | 3.1564378306e-2 | 9.1848859794e-4 | 1.3890784446e-6 | 5.2520070228e-3 |
| 183_1 | (33) | 3.3229636456e-2 | 6.8157661465e-4 | 1.6986037449e-6 | 6.3203553002e-4 |
| 185_1 | (33) | 3.7050480674e-2 | 4.7133402533e-4 | 1.6820241219e-6 | -1.9006739062e-3 |
| 187_1 | (33) | 4.2333369446e-2 | -5.7048659015e-5 | -2.9240715205e-7 | -2.7621364798e-3 |
| 189_1 | (35) | 4.1151817291e-2 | -2.3224227347e-4 | -1.0004222362e-6 | 1.0042395055e-3 |
| 191_1 | (35) | 4.3527506894e-2 | 6.0464325495e-5 | -8.0386909126e-7 | -3.4867164045e-3 |
| 193_1 | (36) | 3.9211907311e-2 | 3.7241399742e-4 | 2.2891278242e-7 | 2.5897489051e-3 |
| 195_1 | (35) | 4.0217569824e-2 | 4.0256278320e-4 | -1.8149155112e-9 | 1.6847765006e-3 |
| 197_1 | (35) | 5.7569354039e-2 | -1.0937631335e-3 | -2.0386520217e-6 | -1.4848936627e-2 |
| X14_1 | (35) | 4.9117672620e-2 | -2.7152899309e-4 | 1.0663861851e-6 | -1.2985783638e-2 |
| 201_1 | (35) | 4.5554969562e-2 | -1.0109605411e-4 | -6.4235048912e-7 | -1.0116775825e-3 |
| 203_1 | (35) | 4.7596861818e-2 | -4.2095075119e-5 | 1.7226955299e-6 | -1.0950226113e-2 |
| 205_1 | (36) | 4.0709337977e-2 | 4.9075394345e-4 | -6.3035459021e-7 | 6.8806923598e-3 |
| 207_1 | (36) | 5.7209636999e-2 | -8.4717641480e-4 | -3.0228546427e-6 | -7.2626568386e-3 |
| 209_1 | (35) | 5.3695073179e-2 | -4.5478997260e-4 | -4.6081909759e-7 | -1.0619840678e-2 |
| 211_1 | (35) | 5.2659467705e-2 | -5.7075655586e-4 | -2.4941532402e-6 | -2.0690832062e-3 |
| 213_1 | (36) | 4.4778808286e-2 | 1.4004201835e-4 | -2.1558527316e-7 | 1.6529693648e-3 |
| 215_1 | (36) | 5.5075938071e-2 | -5.1623009898e-4 | -1.2383319773e-6 | -8.7853229993e-3 |
| 217_1 | (36) | 4.4522844237e-2 | 8.0460766747e-4 | 2.1436991555e-6 | -4.7990831298e-3 |
| WC0_1 | (32) | 5.5319732590e-2 | -4.8817470694e-4 | -3.3538811155e-6 | -5.6698363844e-4 |
| WC1_1 | (35) | 6.8240483913e-2 | -1.3349267643e-3 | -2.6649280675e-6 | -2.3309341066e-2 |
| WC2_1 | (34) | 5.3661240345e-2 | -4.6334773368e-4 | -3.3538899103e-6 | 4.5377153062e-4 |
| WC3_1 | (36) | 7.4088142499e-2 | -1.8727723335e-3 | -4.1610648702e-6 | -2.4871084261e-2 |
| WC4_1 | (36) | 5.3019689585e-2 | -4.1280590488e-4 | -1.7521594231e-6 | -4.3265311430e-3 |
| WC5_1 | (35) | 5.6732201572e-2 | -5.9427855802e-4 | -1.1840944992e-6 | -9.6799808630e-3 |
| WC6_1 | (36) | 6.6656196503e-2 | -1.3170061794e-3 | -3.6439008055e-6 | -1.5552018907e-2 |
| WC7_1 | (36) | 5.8826887868e-2 | -8.0023956530e-4 | -2.2249645423e-6 | -9.1439300874e-3 |
| WC8_1 | (36) | 6.1846470761e-2 | -9.5944449868e-4 | -2.5245608879e-6 | -1.2050988126e-2 |
| WC9_1 | (36) | 5.2401748963e-3 | 1.1391998475e-3 | 4.0307349553e-6 | -5.0300891899e-3 |
| WC10_1 | (32) | 1.7172432370e-2 | 1.8259367307e-4 | -1.4989332052e-6 | -5.7847844127e-3 |
| | | | | | |
| Leg 2b: | | | | | |
| 217_2 | (34) | 1.4044503684e-2 | 8.5319143485e-4 | 2.0836083479e-6 | -1.2283286940e-2 |
| 219_1 | (36) | 1.2903496219e-2 | 8.3339684677e-4 | 1.5327540302e-6 | -5.2061900725e-3 |
| 221_1 | (36) | 1.7242230197e-2 | 3.5515732778e-4 | -5.6688057756e-8 | -5.2863346166e-3 |
| 223_1 | (36) | 2.2633296595e-2 | 5.3249516080e-5 | -2.2889283128e-6 | -3.4908967864e-3 |
| 225_1 | (36) | 2.0948113208e-2 | 2.9462144997e-4 | -2.4480774835e-6 | 6.1334606574e-4 |
| 227_1 | (36) | 3.1207896191e-2 | -6.0545711843e-4 | -2.7014069747e-6 | -1.1225391763e-2 |
| 229_1,231_1 | (70) | 2.4711857929e-2 | 1.8894001381e-4 | -3.4842460278e-7 | -9.3369817558e-3 |
| 233_1 | (36) | 2.5678101185e-2 | 3.7903955311e-5 | -2.2023441618e-6 | -3.9491025617e-3 |
| X13_1 | (36) | 2.1995559475e-2 | 4.4308928974e-4 | 5.0692043623e-7 | -7.7479389194e-3 |
| 237_1 | (36) | 1.4725948563e-2 | 6.0848274242e-4 | -3.2711667539e-6 | 1.7285111162e-2 |
| 239_1 | (36) | 1.9521233739e-2 | 5.0101913124e-4 | -1.5721826210e-6 | 3.8509995433e-3 |
| 241_1 | (34) | 1.9245781987e-2 | 7.2459624020e-4 | -5.1587177472e-7 | 2.0403756854e-3 |
| 243_1 | (25) | 2.7223270806e-2 | 2.4667611134e-5 | -1.9322802292e-6 | -7.1292085786e-3 |
| 245_1 | (33) | 2.5061634305e-2 | 2.9916321734e-4 | -9.0261797105e-7 | -7.2048173548e-3 |
| 247_1 | (35) | 2.4125137439e-2 | 1.6605068919e-4 | -1.3465496269e-6 | -3.3260387821e-3 |
| 249_1 | (30) | 2.3634479233e-2 | 2.0566189547e-4 | -1.0481121695e-6 | -2.4851171400e-3 |
| 251_1 | (36) | 3.4870553358e-2 | -4.4186197111e-4 | 1.0595258179e-6 | -2.4738155341e-2 |
| 253_1 | (36) | 2.9373039476e-2 | -3.0741231783e-4 | -3.0282154875e-6 | -4.4339089411e-3 |
| 255_1 | (36) | 2.5697827356e-2 | 1.7397293863e-4 | -1.7100952752e-6 | -3.3125494296e-3 |
| 257_1 | (35) | 2.8415311612e-2 | 1.2761582780e-4 | 9.8660926822e-7 | -1.5172371661e-2 |
| 259_1 | (35) | 2.6162001520e-2 | 2.5851545885e-4 | -8.9142029346e-7 | -6.1630389151e-3 |
| 261_1 | (32) | 2.1040093981e-2 | 8.9015596547e-4 | -8.9761354158e-8 | -6.3261295532e-4 |
| 263_1 | (34) | 2.6892771463e-2 | -4.7288346494e-5 | -4.3205227498e-6 | 4.8353411718e-3 |
| 265_1 | (35) | 2.4981095754e-2 | 2.6617301975e-4 | -3.6785729369e-6 | 5.0096809704e-3 |
| 267_1 | (36) | 2.9501020118e-2 | 1.3963038758e-5 | 1.8429376949e-7 | -1.3313864903e-2 |
| 269_1 | (35) | 2.4163931070e-2 | 3.6695898037e-4 | -8.9552076560e-7 | -1.5947667751e-3 |
| 271_1 | (34) | 3.2056883108e-2 | -3.3254327791e-4 | -4.4366324317e-6 | -9.0218759816e-4 |
| 273_1 | (33) | 2.4533966823e-2 | 7.3143113801e-4 | 1.3069822800e-6 | -9.1455005471e-3 |
| X10_1 | (36) | 3.0841517490e-2 | 3.4865354558e-4 | 1.8616817983e-7 | -1.4775452885e-2 |
| 275_1 | (36) | 2.9861477155e-2 | 2.5434189325e-4 | 3.6511746979e-7 | -1.3895964006e-2 |
| 277_1 | (36) | 3.3049173807e-2 | -1.6960618826e-4 | -3.0105534966e-6 | -5.9897564706e-3 |
| 279_1 | (36) | 2.8565845594e-2 | 3.2187702886e-4 | -1.3469388078e-6 | -5.8492610315e-3 |
| 281_1 | (36) | 2.8442774254e-2 | 2.0774807708e-4 | -3.4107547293e-6 | 8.8087672366e-5 |
| 283_1 | (36) | 3.3246132418e-2 | 1.4503134347e-5 | -1.3371172408e-6 | -1.0644518129e-2 |
| 285_1 | (35) | 4.0931368011e-2 | -7.4412822938e-4 | -3.4694156847e-6 | -1.4355925046e-2 |
| 287_1 | (35) | 2.6434524781e-2 | 4.5542865584e-4 | -1.8761713915e-6 | 2.6105219833e-6 |
| 289_1 | (33) | 3.0746558840e-2 | 1.7639883286e-4 | -2.6382708460e-6 | -4.2066268967e-3 |
| 291_1 | (32) | 1.9143956201e-2 | 1.1271438790e-3 | 6.8944217027e-7 | 3.8876140788e-3 |
| 293_1 | (36) | 2.7333749353e-2 | 5.1941094250e-4 | -2.0997349447e-7 | -7.1734566551e-3 |
| 295_1 | (31) | 2.2078235894e-2 | 8.0943626879e-4 | -4.0888782436e-6 | 1.3755183174e-2 |
| 297_1-305_1 | (105) | 2.6466581138e-2 | 6.7521561774e-4 | 2.6560705923e-6 | -5.9923122652e-3 |
| 306_1-312_1 | (82) | 2.8781435894e-2 | 4.1244679218e-4 | -1.4990033254e-6 | -2.8395048528e-3 |
| 314_1 | (32) | 2.8148647316e-2 | 5.4287014769e-4 | -1.1650594271e-6 | -4.1847030831e-3 |

```
316_1          (33)   2.8215898497e-2  1.0709435136e-3  2.6863192013e-6 -1.5958965824e-2
318_1          (33)   3.2120430399e-2  7.6380812308e-5 -4.6745007594e-6  1.0047986624e-4
X09_1          (29)   3.7712610610e-2 -3.8475256983e-4 -2.8551495937e-6 -1.1712974810e-2
322_1          (28)   3.1880622390e-2  3.3806533907e-4 -7.9540724311e-7 -9.9254764334e-3
324_1          (34)   3.0660905835e-2  8.5067781679e-5 -3.9683619044e-6  4.2564785335e-5
326_1          (32)   3.5745349948e-2 -1.1288548584e-4 -3.1487803932e-6 -8.9475988336e-3
328_1          (33)   3.5511712382e-2 -7.2081089274e-7 -2.5450641548e-6 -9.1691446523e-3
329_1          (32)   4.3274625921e-2 -7.6172567723e-4 -3.9862580571e-6 -1.6547927646e-2
331_1          (31)   4.4207988758e-2 -8.4326066969e-4 -1.5317521038e-6 -2.2905035656e-2
333_1          (29)   2.9089812435e-2  5.4573837692e-4 -1.7284024871e-6 -2.6414355998e-3
335_1-339_1    (72)   2.8274588195e-2  7.2203394358e-4  1.8244281486e-7 -3.8249091980e-3
341_1          (31)   2.8467598768e-2  6.5872171686e-4 -1.9137099117e-8 -5.2788889870e-3
343_1          (29)   3.1804710994e-2  3.4190948069e-4 -1.4373513149e-6 -6.8952906563e-3
345_1          (30)   4.0897193625e-2 -5.2104047963e-4 -5.9349003645e-6 -8.9078094183e-3
347_1          (33)   3.6963291046e-2 -3.9493403657e-4 -2.9574013462e-6 -1.0765271175e-2
349_1          (36)   3.5632891264e-2  4.0865310881e-4 -2.7127931470e-6 -9.1060634012e-3
351_1          (36)   4.0372319773e-2 -5.3299863953e-4 -3.3631400775e-6 -1.2463550877e-2
369_1-359_1    (105)  2.9723341223e-2  4.9802937084e-4 -1.1326902672e-6 -4.2131110567e-3
357_1          (32)   3.3966225562e-2 -2.9368637931e-4 -3.2642945433e-6 -5.3473446623e-3
355_1          (36)   3.4811351883e-2  6.8239868011e-5 -1.1991743432e-6 -1.0910137627e-2
353_1,351_2    (69)   3.7032052644e-2  4.2309864070e-5 -1.2303697967e-6 -1.2631820781e-2

Leg 3:
370_1-TS1_1    (320)  3.7969098741e-2  4.4095362607e-4 -1.3937449266e-6 -1.0325558187e-2
--------------------------------------------------------------------------------
```

**(5) Oxygen optode**

The CTD oxygen is calibrated using linear time drift compensation of the uncalibrated phase measurement (Pb) and 4th degree polynomial of oxygen calculation equation (see 3.1.3(7)) as

$$P = Pb + CT_1 * T + CT_0$$

$$O_2\ (\mu mol/l) = C0Coef + C1Coef * P + C2Coef * P^2 + C3Coef * P^3 + C4Coef * P^4$$

where T is time, P is time drift compensated phase (deg), and $CT_0$ and $CT_1$ are calibration coefficients. The temperature dependent coefficients are as follows.

$$C0Coef = C0Coef_0 + C0Coef_1 * t + C0Coef_2 * t^2 + C0Coef_3 * t^3$$

$$C1Coef = C1Coef_0 + C1Coef_1 * t + C1Coef_2 * t^2 + C1Coef_3 * t^3$$

$$C2Coef = C2Coef_0 + C2Coef_1 * t + C2Coef_2 * t^2 + C2Coef_3 * t^3$$

$$C3Coef = C3Coef_0 + C3Coef_1 * t + C3Coef_2 * t^2 + C3Coef_3 * t^3$$

$$C4Coef = C4Coef_0 + C4Coef_1 * t + C4Coef_2 * t^2 + C4Coef_3 * t^3$$

where t is CTD temperature (°C). Effective 6 coefficients ($C0Coef_0$, $C0Coef_1$, $C0Coef_2$, $C1Coef_0$, $C1Coef_1$, $C2Coef_0$) with the coefficients of time drift compensation are determined for post-cruise calibration. The other temperature dependent coefficients are not changed from the value of pre-cruise calibration. The best fit sets of coefficients are determined by minimizing the sum of absolute deviation from the bottle oxygen data. The fortran subroutine DMINF1 of the Scientific Subroutine Library II (Fujitsu Ltd., JAPAN) is used to determine the sets. The DMINF1 uses the revised quasi-Newton method.

The calibration is performed for the up-cast phase data created by the software module ROSSUM after the post-cruise calibration for the CTD temperature and salinity.

The calibration coefficients are basically determined for each leg. The results of the post-cruise calibration for optode oxygen are summarized in Table 3.1.5.9 and shown in from Figure 3.1.5.20 to Figure 3.1.5.23. And the calibration coefficients and number of the data used for the calibration are listed in Table 3.1.5.10.

**Table 3.1.5.9. Difference between the optode oxygen and the bottle oxygen after the post-cruise calibration. Mean and standard deviation (Sdev) are calculated for the data below and above 950 dbar. Number of data (Num) used is also shown.**

| Leg | Pressure >= 950 dbar | | | Pressure < 950 dbar | | |
|---|---|---|---|---|---|---|
| | Num | Mean (µmol/kg) | Sdev (µmol/kg) | Num | Mean (µmol/kg) | Sdev (µmol/kg) |
| Leg 1 | 1319 | –0.04 | 0.32 | 1013 | 0.07 | 0.90 |
| Leg 2a | 919 | –0.02 | 0.21 | 665 | 0.05 | 0.79 |
| Leg 2b | 1422 | –0.00 | 0.29 | 1042 | –0.06 | 0.78 |
| Leg 3 | 24 | 0.01 | 0.37 | 297 | 0.04 | 0.63 |

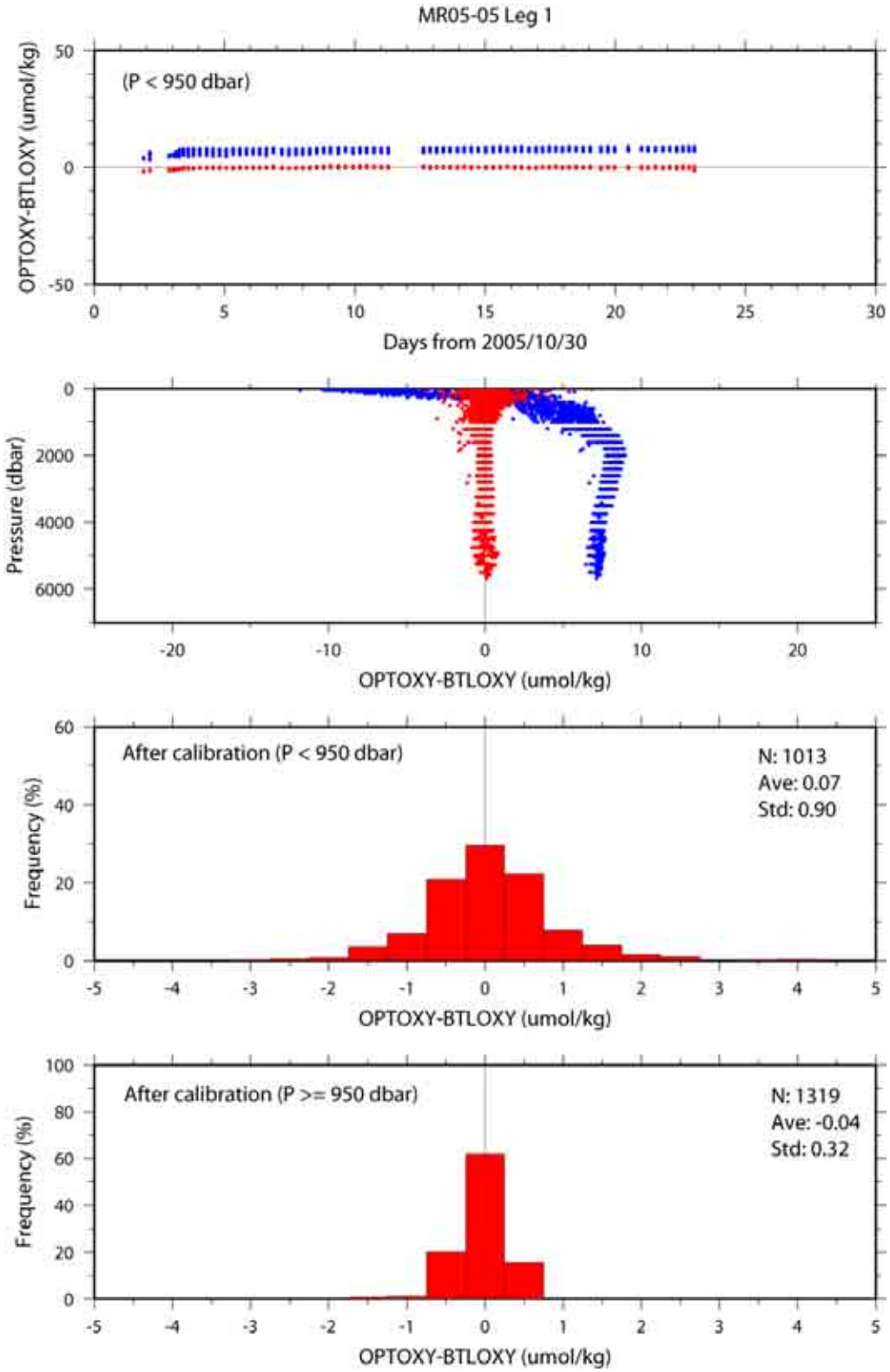


**Figure 3.1.5.20. Difference between the optode oxygen and the bottle oxygen for Leg 1. Blue and red dots indicate before and after the post-cruise calibration using the bottle oxygen data, respectively. Top panel shows P >= 950 dbar. Lower two panels show histogram of the difference after the calibration.**

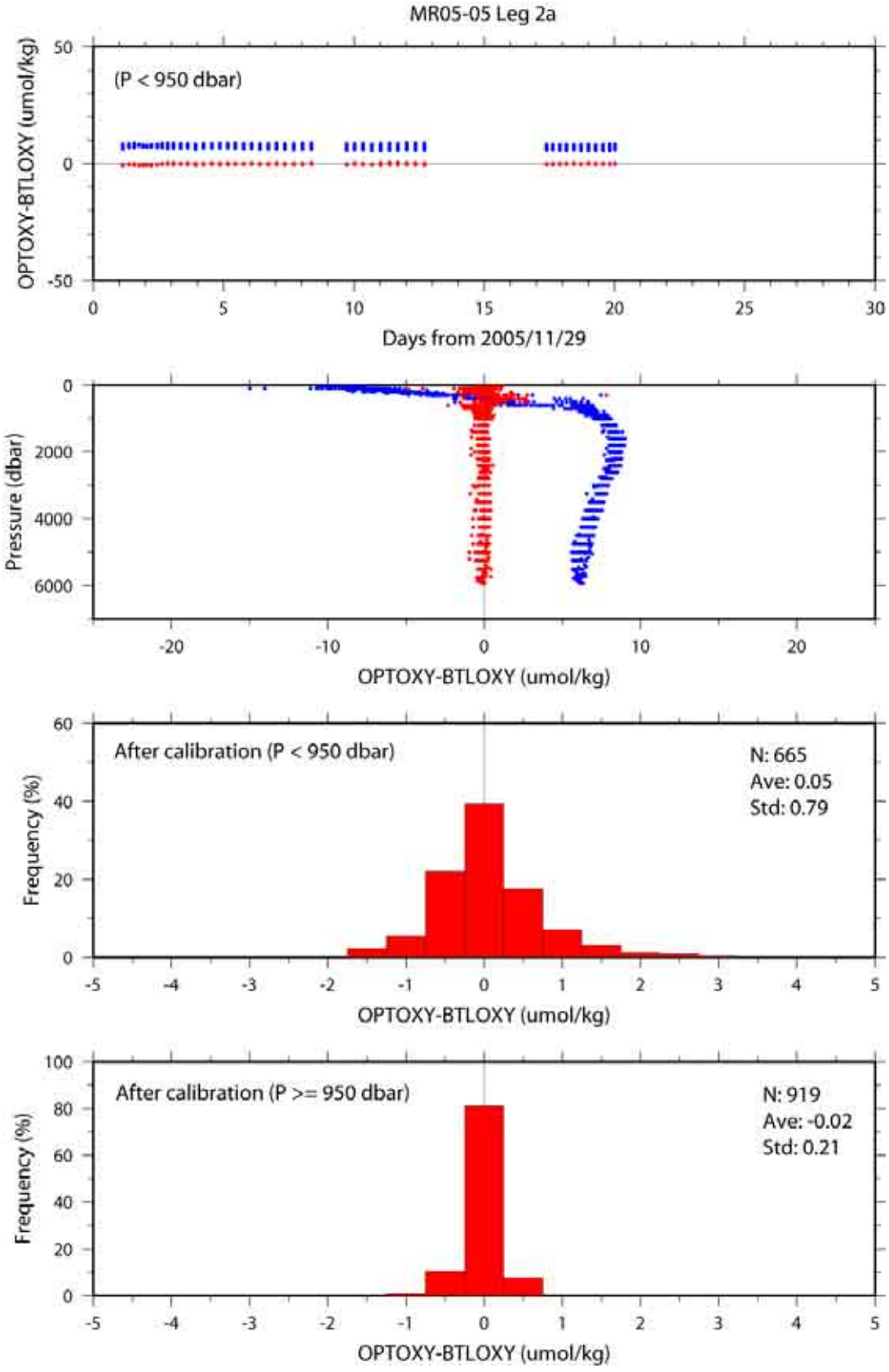


**Figure 3.1.5.21. Same as Figure 3.1.5.20, but for Leg 2a.**

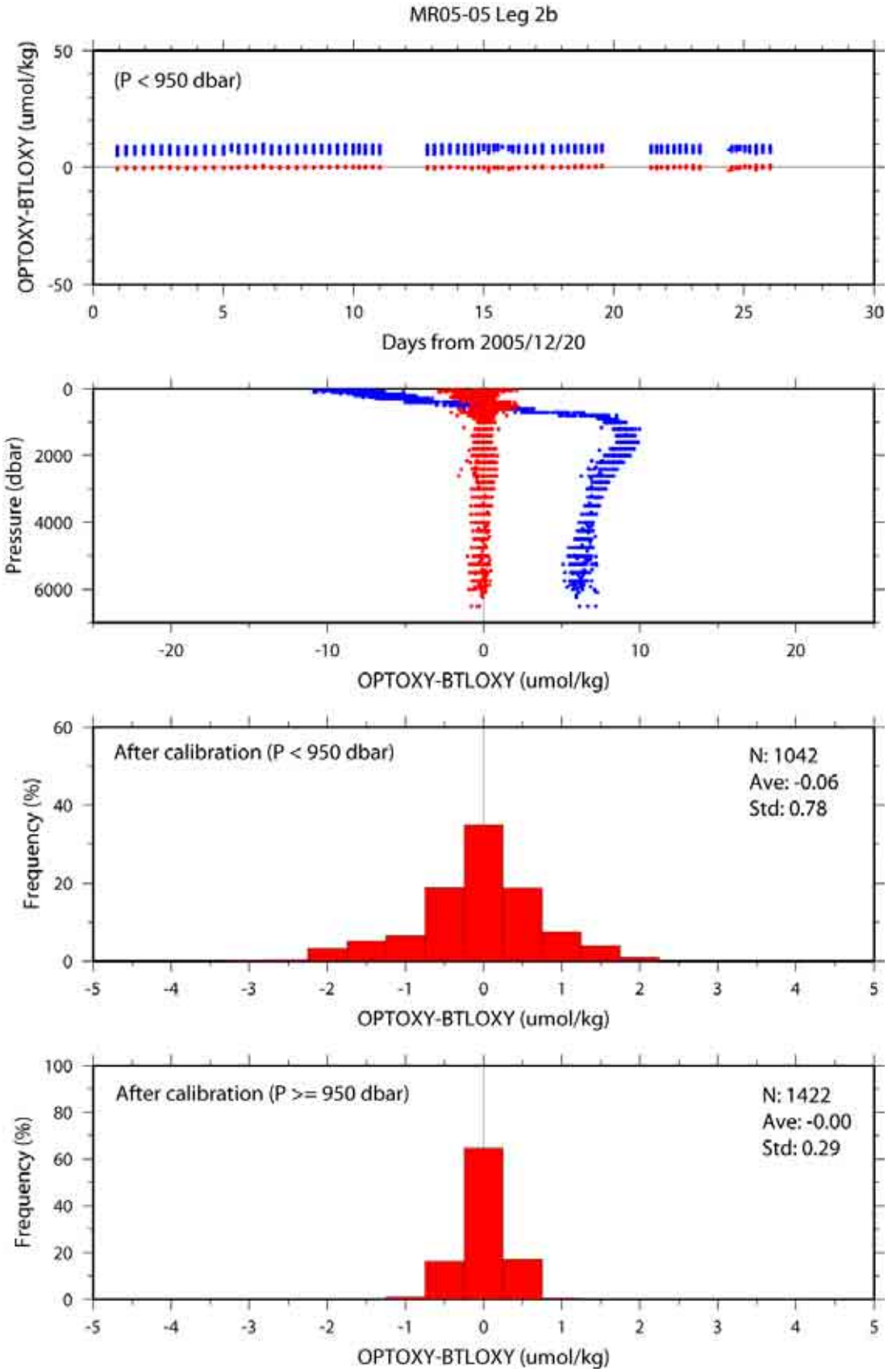


**Figure 3.1.5.22. Same as Figure 3.1.5.20, but for Leg 2b.**

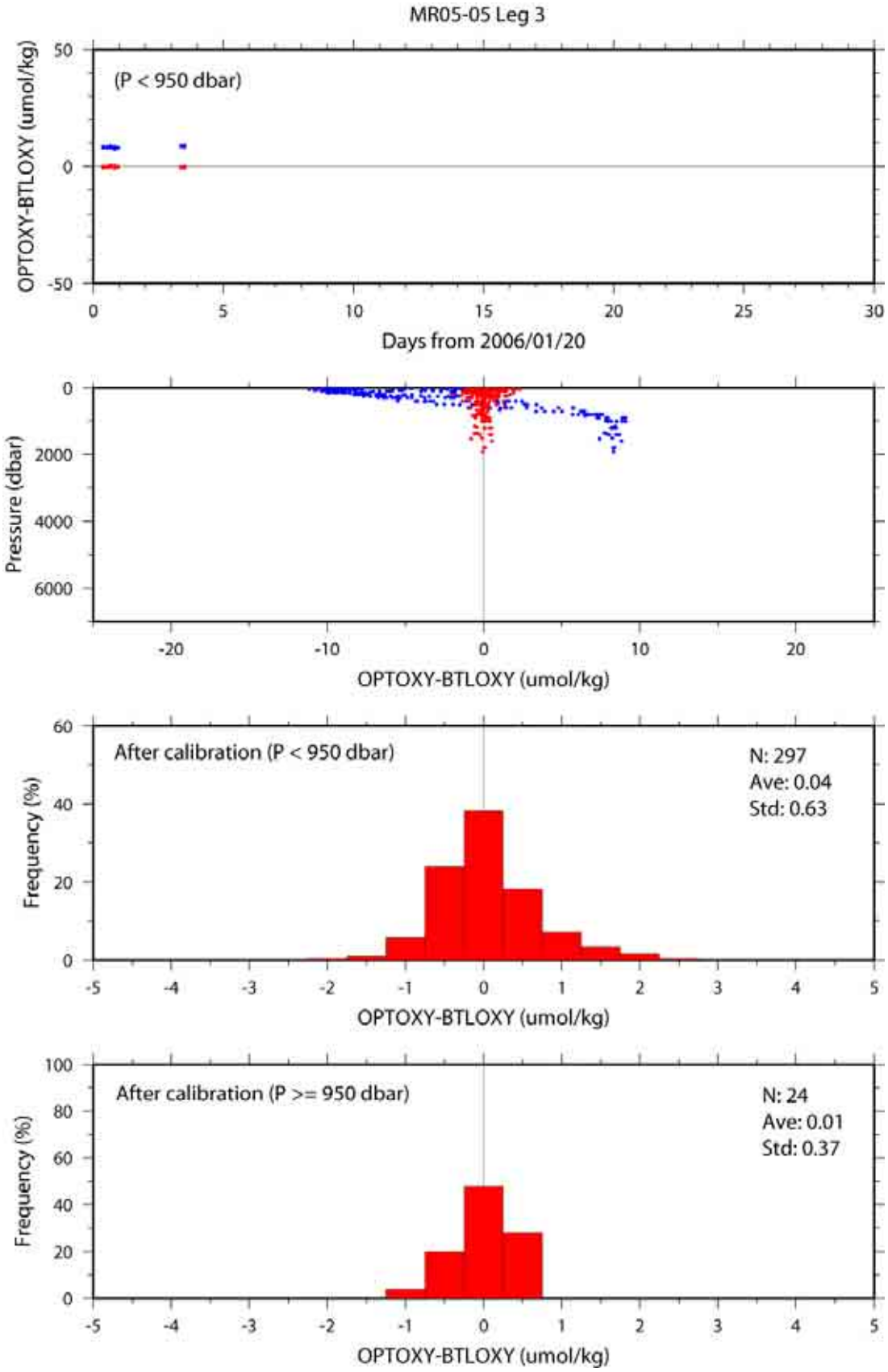


**Figure 3.1.5.23. Same as Figure 3.1.5.20, but for Leg 3.**

**Table 3.1.5.10. Calibration coefficients for the optode oxygen. Number of data (Num) used for the calibration and mean absolute deviation (ADEV) between the optode oxygen and the bottle oxygen are also shown.**

| | | | | |
|---|---|---|---|---|
| Leg 1 | Num | = 2332, | ADEV | = 0.40 µmol/kg |
| | $C0Coef_0$ | = 3199.8217 | | |
| | $C0Coef_1$ | = –111.19786 | | |
| | $C0Coef_2$ | = 2.4186136 | | |
| | $C1Coef_0$ | = –176.28602 | | |
| | $C1Coef_1$ | = 5.4809667 | | |
| | $C2Coef_0$ | = 3.9606075 | | |
| | $CT_0$ | = –1.5721006 | | |
| | $CT_1$ | = 3.3048347e–3 | | |
| Leg 2a | Num | = 1584, | ADEV | = 0.31 µmol/kg |
| | $C0Coef_0$ | = 3199.8059 | | |
| | $C0Coef_1$ | = –111.10240 | | |
| | $C0Coef_2$ | = 2.4059520 | | |
| | $C1Coef_0$ | = –176.28043 | | |
| | $C1Coef_1$ | = 5.4834482 | | |
| | $C2Coef_0$ | = 3.9596793 | | |
| | $CT_0$ | = –0.46492214 | | |
| | $CT_1$ | = 4.8849136e–6 | | |
| Leg 2b | Num | = 2464, | ADEV | = 0.37 µmol/kg |
| | $C0Coef_0$ | = 3199.7833 | | |
| | $C0Coef_1$ | = –112.02933 | | |
| | $C0Coef_2$ | = 2.4177352 | | |
| | $C1Coef_0$ | = –176.35378 | | |
| | $C1Coef_1$ | = 5.5073815 | | |
| | $C2Coef_0$ | = 3.9597133 | | |
| | $CT_0$ | = –0.57695299 | | |
| | $CT_1$ | = –2.3759767e–4 | | |
| Leg 3 | Num | = 321, | ADEV | = 0.45 µmol/kg |
| | $C0Coef_0$ | = 3199.9202 | | |
| | $C0Coef_1$ | = –106.62837 | | |
| | $C0Coef_2$ | = 2.3589462 | | |
| | $C1Coef_0$ | = –174.52350 | | |
| | $C1Coef_1$ | = 5.3716927 | | |
| | $C2Coef_0$ | = 3.9321255 | | |
| | $CT_0$ | = 1.3551441 | | |
| | $CT_1$ | = –3.9945829e–4 | | |

**References**

Budeus, G. and W. Schneider (1998): In-situ temperature calibration: A remark on instruments and methods, *Intl. WOCE Newsletter*, 30, 16-18.

Lagarias, J.C., J.A. Reeds, M.H. Wright and P. E. Wright (1998): Convergence properties of the Nelder-Mead simplex method in low dimensions, *SIAM Journal of Optimization*, 9, 112-147.

Larson, N. and A. Pederson (1996): Temperature measurements in flowing water: Viscous heating of sensor tips, 1st IGHEM Meeting, Montreal, Canada.
(http://www.seabird.com/technical_references/paperindex.htm)

## 3.2 Bottle Salinity

***Takeshi Kawano (JAMSTEC)***
***Fujio Kobayashi (MWJ)***
***Naoko Takahashi(MWJ)***
***Tatsuya Tanaka (MWJ)***

### 3.2.1. Objectives

Bottle salinities were measured in order to be compared with CTD salinities to identify leaking bottles and calibrate CTD salinities.

### 3.2.2. Instrument and Method

#### 3.2.2.1. Salinity Sample Collection

The bottles in which the salinity samples are collected and stored are 250 ml Phoenix brown glass bottles with screw caps. Each bottle was rinsed three times with sample water and was filled to the shoulder of the bottle. The caps were also thoroughly rinsed. Salinity samples were stored more than 12 hours in the same laboratory as the salinity measurement was made.

#### 3.2.2.2. Instruments and Method

The salinity analysis was carried out on Guildline Autosal salinometer model 8400B (S/N 62556), which was modified by addition of an Ocean Science International peristaltic-type sample intake pump and two Guildline platinum thermometers model 9450. One thermometer monitored an ambient temperature and the other monitored a bath temperature. The resolution of the thermometers was 0.001 deg C. The measurement system was almost same as Aoyama et al (2003). The salinometer was operated in the air-conditioned ship's laboratory at a bath temperature of 24 deg C.

An ambient temperature varied from approximately 19 deg C to 24 deg C, while a bath temperature is very stable and varied within +/- 0.002 deg C on rare occasion. A measure of a double conductivity ratio of a sample is taken as a median of thirty-one reading. Data collection was started after 5 seconds and it took about 10 seconds to collect 31 readings by a personal computer. Data were sampled for the sixth and the seventh filling of the cell for Leg.1 and eighth and ninth filling for Leg.2 and Leg.3. In case the difference between the double conductivity ratio of this two fillings is smaller than 0.00002, the average value of the two double conductivity ratios was used to calculate the bottle salinity with the algorithm for practical salinity scale, 1978 (UNESCO, 1981). If

the difference was grater than or equal to the 0.0003, we measured one more additional filling of the cell. In case the double conductivity ratio of the additional filling did not satisfy the criteria above, we measured two more filling of the cell and the median of the double conductivity ratios of five fillings are used to calculate the bottle salinity.

The measurement was conducted about from 10 to 18 hours per day (typically from 3:00 to 17:00) and the cell was cleaned with ethanol or soap or both after the measurement of the day. We measured more than 8,000 samples in total.

### 3.2.3. Preliminary Result

#### 3.2.3.1. Stand Seawater

**(1) Leg.1**

Standardization control was set to 501 and all the measurements were done by this setting. STNBY was 5517 +/- 0001 and ZERO was 0.00001 +/- 0.00001. We used IAPSO Standard Seawater batch P145 whose conductivity ratio was 0.99981 (double conductivity ratio is 1.99962) as the standard for salinity. We measured 117 bottles of P145 during routine measurement. There were 5 bad bottles which conductivities are extremely high. Data of these 5 bottles are not taken into consideration hereafter.

Fig.3.2.1 shows the history of double conductivity ratio of the Standard Seawater batch P145.

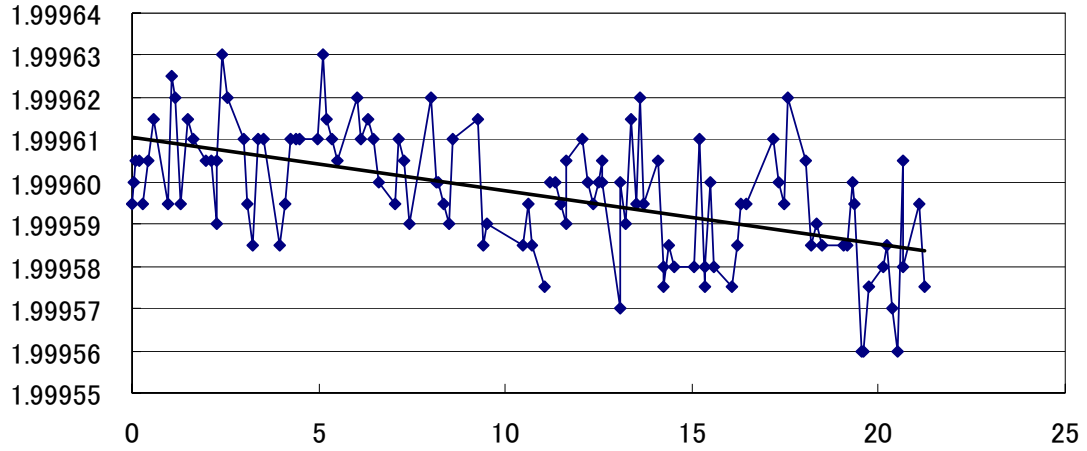


**Fig.3.2.1 History of Double conductivity ratio of P145 during Leg.1. X and Y axes represent time (Julian day) and double conductivity ratio, respectively.**

Drifts were calculated by fitting data from P145 to the equation obtained by the least square method (solid lines). Correction for the double conductivity ratio of the sample was made to compensate the drift (Fig.3.2.2). After correction, the average of double conductivity ratio became 1.99961 and the standard deviation was 0.00012, which is equivalent to 0.0002 in salinity. We added 0.00001 to the corrected measured double conductivity ratio.

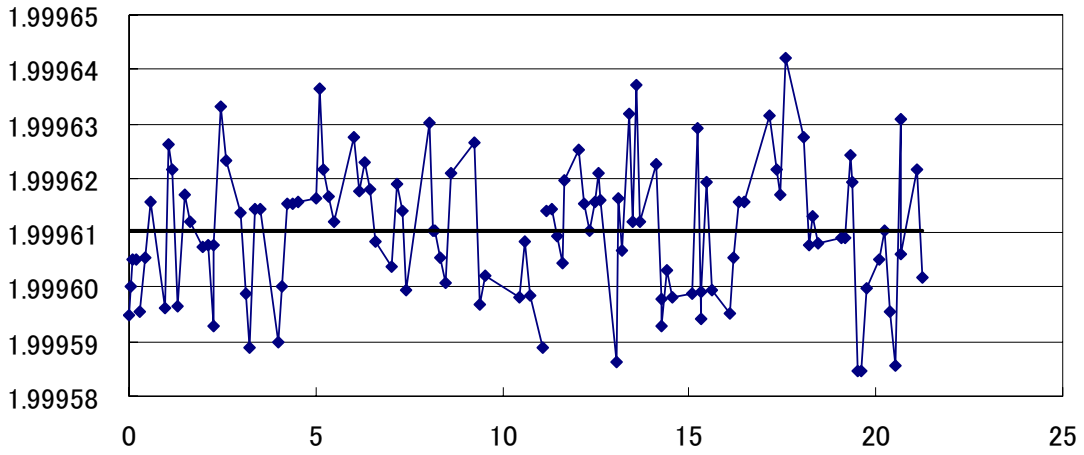


**Fig.3.2.2 History of Double conductivity ratio of P145 during Leg.1. X and Y axes represent time (Julian day) and double conductivity ratio, respectively. (after correction)**

**(2) Leg.2**

Standardization control was set to 474 before WIPE (Wake Islands passage Flux Experiment). STNBY was 5498 +/- 0001 and ZERO was 0.00001 +/- 0.00001. We removed the conductivity cell and wash thoroughly by soap . Then standardization control was changed to 479. STNBY became 5501 +/- 0001 and ZERO was 0.00001 +/- 0.00001.

We used IAPSO Standard Seawater batch P145 whose conductivity ratio was 0.99981 (double conductivity ratio is 1.99962) as the standard for salinity. We measured 54 bottles of P145 during routine measurement before WIPE and 109 bottles after WIPE. There were 2 bad bottles whose conductivities are extremely high. Data of these 2 bottles are not taken into consideration hereafter.

Fig.3.2.3 shows the history of double conductivity ratio of the Standard Seawater batch P145. Drifts were calculated by fitting data from P145 to the equation obtained by the least square method (solid lines). Correction for the double conductivity ration of the sample was made to compensate for the drift (Fig.3.2.4). After correction, the average of double conductivity ratio became 1.99962 and the standard deviation was 0.00012 before WIPE and 0.00011 after WIPE, those are equivalent to 0.0002 in salinity. We add 0.000021 before WIPE and 0.000012 after WIPE to the corrected measured double conductivity ratio.

**(3) Leg.3**

Standardization control was set to 484 and all the measurements were done by this setting. STNBY was 5505 +/- 0001 and ZERO was 0.00001 +/- 0.00001. We used IAPSO Standard Seawater batch P145 whose conductivity ratio was 0.99981 (double conductivity ratio is 1.99962) as the standard for salinity. We measured 25 bottles of P145 during routine measurement.

Fig.3.2.5 shows the history of double conductivity ratio of the Standard Seawater batch P145. Drifts were calculated by fitting data from P145 to the equation obtained by the least square method (solid lines). Correction for the double conductivity ration of the sample was made to compensate for the drift (Fig.3.2.6). After correction, the average of double conductivity ratio became 1.99962 and the standard deviation was 0.00014, which is equivalent to 0.0003 in salinity.

We add 0.000004 to the corrected measured double conductivity ratio.

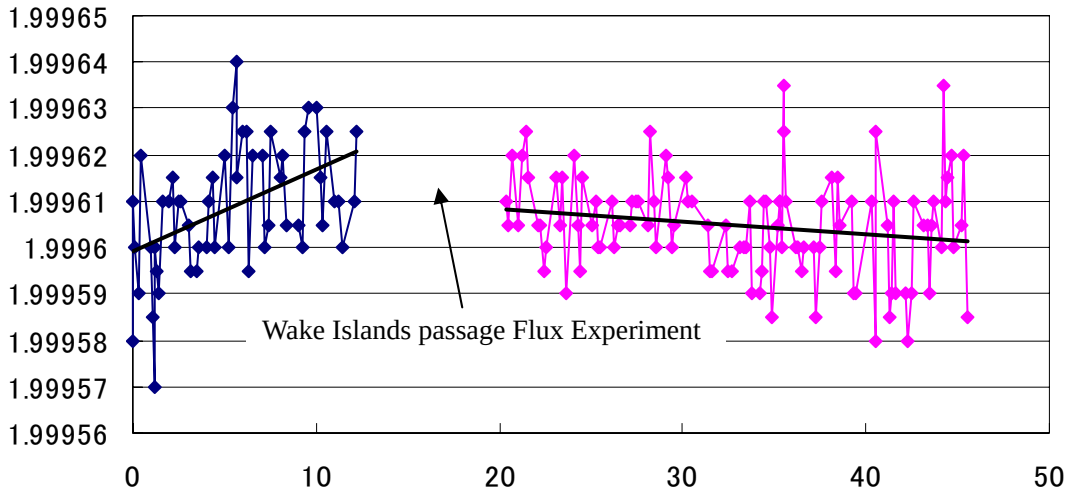


**Fig.3.2.3 History of Double conductivity ratio of P145 during Leg.2. X and Y axes represent time (Julian day) and double conductivity ratio, respectively.**

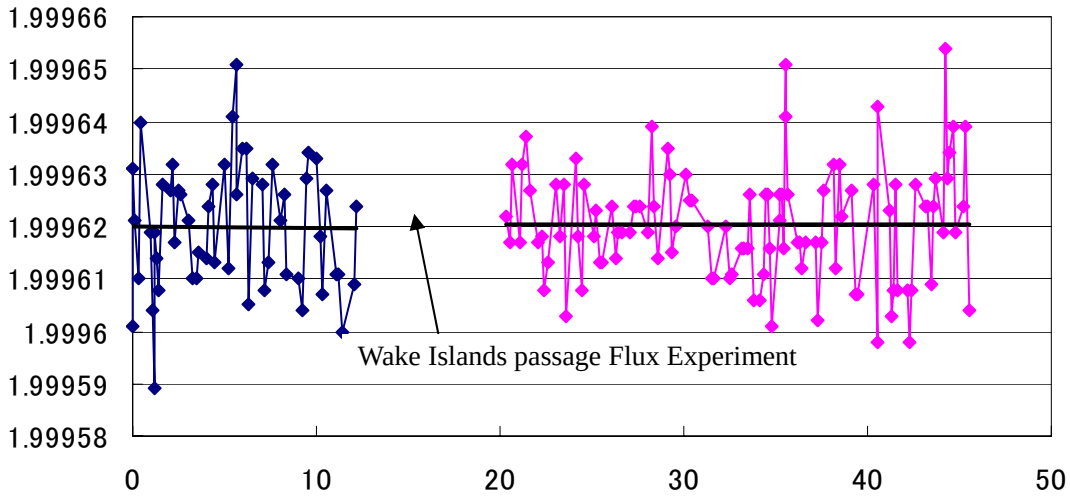


**Fig.3.2.4 History of Double conductivity ratio of P145 during Leg.2. X and Y axes represent time (Julian day) and double conductivity ratio, respectively. (after correction)**

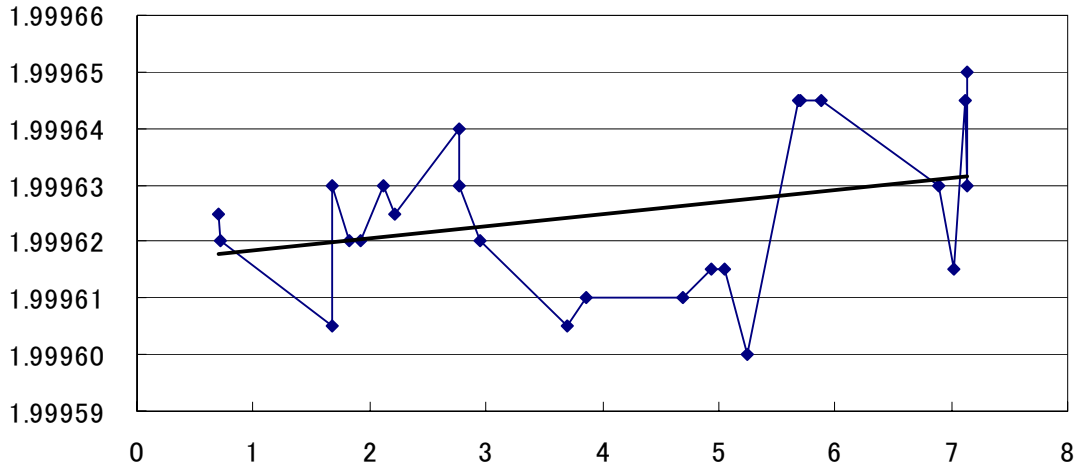


**Fig.3.2.5 History of Double conductivity ratio of P145 during Leg.3. X and Y axes represent time (Julian day) and double conductivity ratio, respectively.**

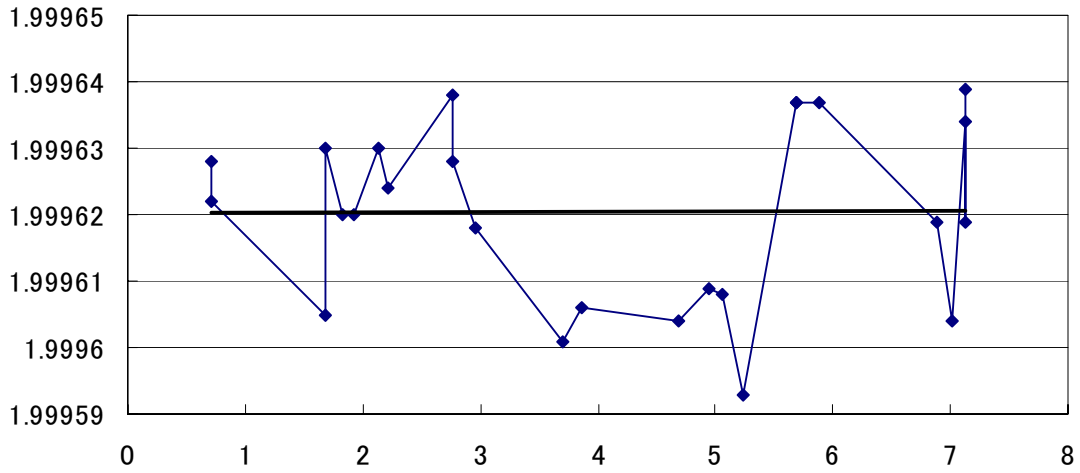


**Fig.3.2.6 History of Double conductivity ratio of P145 during Leg.3. X and Y axes represent time (Julian day) and double conductivity ratio, respectively. (after correction)**

**3.2.3.2. Sub-Standard Seawater**

We also used sub-standard seawater which was deep-sea water filtered by pore size of 0.45 micrometer and stored in a 20 liter cubitainer made of polyethylene and stirred for at least 24 hours before measuring. It was measured every six samples in order to check possible sudden drift of the salinometer. During the whole measurements, there was no detectable sudden drift of the salinometer.

### 2.3.3. Replicate and Duplicate Samples

**(1) Leg.1**

We took 435 pairs of replicate and 27 pairs of duplicate samples. Fig.3.3.7 (a) and (b) show the histogram of the absolute difference between replicate samples and duplicate samples, respectively. There were 2 bad measurements of replicate samples. As these measurements, one of the pair is extremely high (more than 0.01in salinity). Excluding these bad measurements, the standard deviation of the absolute deference of 433 pairs of replicate samples was 0.00017 in salinity and that of 27 pairs of duplicate samples was 0.00032 in salinity.

**(2) Leg.2**

We took 668 pairs of replicate and 20 pairs of duplicate samples. Fig.3.3.8 (a) and (b) show the histogram of the absolute difference between replicate samples and duplicate samples, respectively. There were 3 questionable measurements of replicate samples. Excluding these questionable measurements, the standard deviation of the absolute deference of 665 pairs of replicate samples was 0.00017 in salinity and that of 20 pairs of duplicate samples was 0.00025 in salinity.

**(3) Leg.3**

We took 48 pairs of replicate and 3 pairs of duplicate samples. Fig.3.3.9 shows the histogram of the absolute difference between replicate samples. There was one bad (miss-trip) sample for duplicates. The standard deviation of the absolute deference of 48 pairs of replicate samples was 0.00011 in salinity. The absolute differences of 2 duplicate samples were 0.0002 and 0.0007 in salinity.

### 3.2.3. Further data quality check

All the data will be checked once again in detail with other parameters such as dissolved oxygen and nutrients.

### 3.2.4 Reference

Aoyama, M., T. Joyce, T. Kawano and Y. Takatsuki : Standard seawater comparison up to P129. Deep-Sea Research, I, Vol. 49, 1103～1114, 2002

UNESCO : Tenth report of the Joint Panel on Oceanographic Tables and Standards. UNESCO Tech. Papers in Mar. Sci., 36, 25 pp., 198

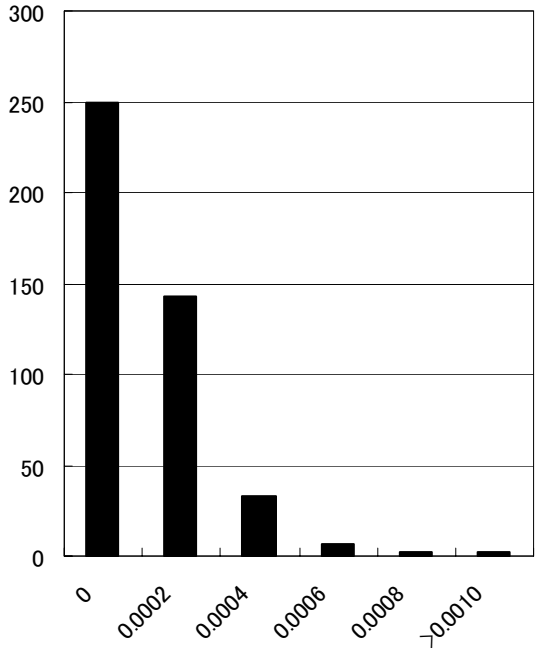


**Fig.3.2.7 (a) The histogram of the absolute difference between replicate samples in Leg.1.**

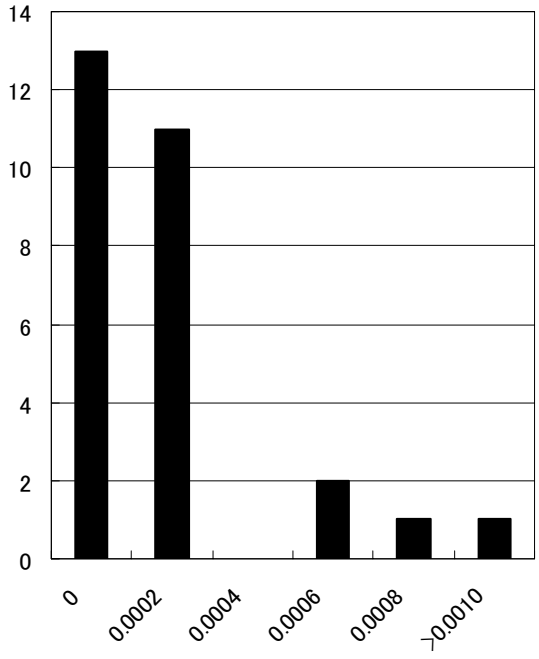


**Fig.3.2.7 (b) The histogram of the absolute samples between duplicate samples in Leg.1.**

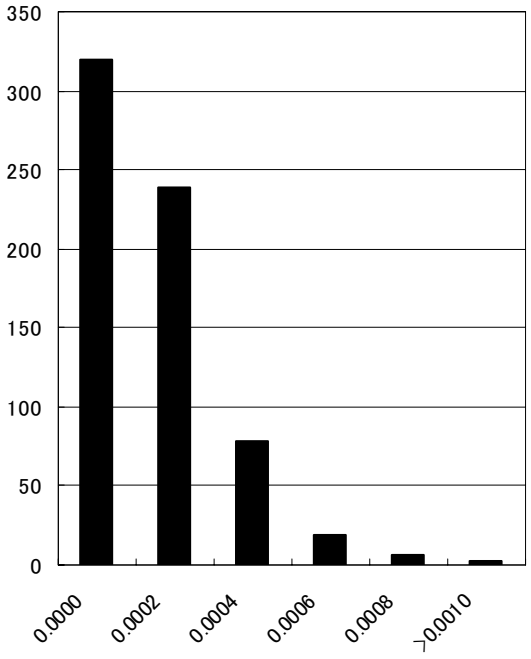


**Fig.3.2.8 (a) The histogram of the absolute difference between replicate samples in Leg.2**

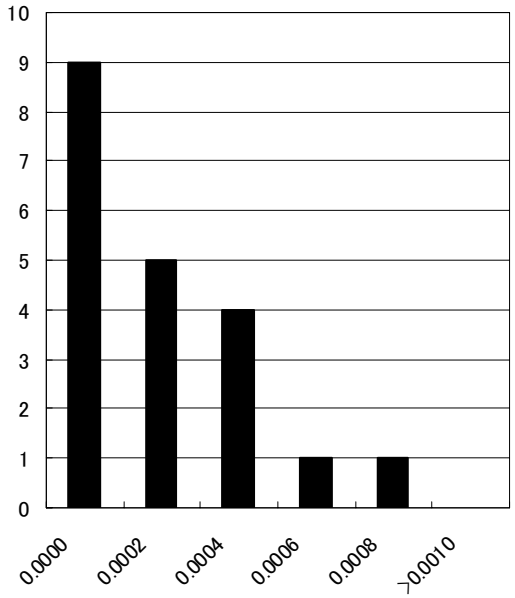


**Fig.3.2.8 (b) The histogram of the absolute samples between duplicate samples in Leg.2.**

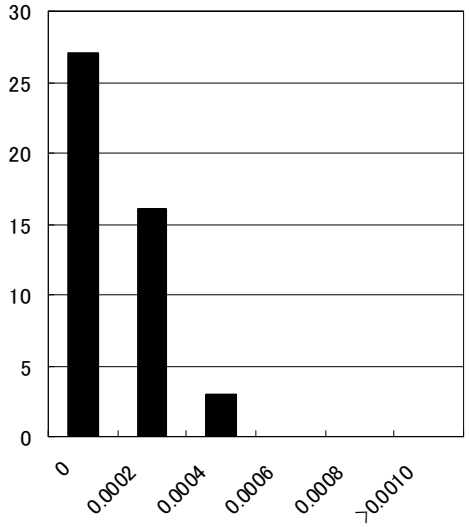


**Fig.3.2.9 The histogram of the absolute difference between replicate samples in Leg.3.**

## 3.3 Bottle Oxygen

30-Jan-2006

### 3.3.1 Personnel

Yuichiro KUMAMOTO [1)], Ikuo KANEKO [1)], Takayoshi SEIKE [2)], Keisuke WATAKI [2)], Kimiko NISHIJIMA [2)], and Takuhei SHIOZAKI [2)]

1) Japan Agency for Marine Earth Science and Technology

2) Marine Works Japan Co. Ltd

### 3.3.2 Objectives

Dissolved oxygen is one of significant tracers for the ocean circulation study. Recent studies in the subarctic North Pacific indicated that dissolved oxygen concentration in intermediate layers decreased in basin wide scale during the past decades. The causes of the decrease, however, are still unclear. During MR05-05 Leg-1 (from 31-Oct-05 to 24-Nov-05), Leg-2 (from 27-Nov-05 to 17-Jan-06), and Leg-3 (from 20-Jan-06 to 30-Jan-06), we measured dissolved oxygen concentration from surface to bottom layers at all the hydrocast stations. The stations along around 24 $^{o}$N reoccupied the WHP P03 stations in 1985. Our purpose is to evaluate decadal change of dissolved oxygen in the subtropical North Pacific.

### 3.3.3 Reagents

Pickling Reagent I: Manganous chloride solution (3M)

Pickling Reagent II: Sodium hydroxide (8M) / sodium iodide solution (4M)

Sulfuric acid solution (5M)

Sodium thiosulfate (0.025M)

Potassium iodate (0.001667M)

CSK standard of potassium iodate: Lot ASE8281, Wako Pure Chemical Industries Ltd., 0.0100N

### 3.3.4 Instruments

Burette for sodium thiosulfate;

APB-510 manufactured by Kyoto Electronic Co. Ltd. / 10 $cm^3$ of titration vessel

Burette for potassium iodate;

APB-410 manufactured by Kyoto Electronic Co. Ltd. / 20 $cm^3$ of titration vessel

Detector; Automatic photometric titrator manufactured, Kimoto Electronic Co. Ltd.

### 3.3.5 Seawater sampling

Following procedure is based on a determination method in the WHP Operations Manual (Dickson, 1996). Seawater samples were collected from Niskin sampler bottles attached to the CTD-system. Seawater for bottle oxygen measurement was transferred from the Niskin sampler bottle to a volume calibrated glass flask (ca. 100 $cm^3$). Three times volume of the flask of seawater was overflowed. Sample temperature was measured by a thermometer during the overflowing. Then two reagent solutions (Reagent I, II) of 0.5 $cm^3$ each were added immediately into the sample flask and the stopper was inserted carefully into the flask. The sample flask was then shaken vigorously to mix the contents and to disperse the precipitate finely throughout. After the precipitate has settled at least halfway down the flask, the flask was shaken again vigorously to disperse the precipitate. The sample flasks containing pickled samples were stored in a laboratory until they were titrated.

### 3.3.6 Sample measurement

At least two hours after the re-shaking, the pickled samples were measured on board. A magnetic stirrer bar and 1 $cm^3$ sulfuric acid solution were added into the sample flask and stirring began. Samples were titrated by sodium thiosulfate solution whose molarity was determined by potassium iodate solution (section 3.3.7). Temperature of sodium thiosulfate during titration was recorded by a thermometer. We measured dissolved oxygen concentration using two sets of the titration apparatus, named DOT-1 and DOT-3. Dissolved oxygen concentration (μmol $kg^{-1}$) was calculated by the sample temperature during the sampling, CTD salinity, flask volume, and titrated volume of the sodium thiosulfate solution.

### 3.3.7 Standardization

Concentration of sodium thiosulfate titrant (ca. 0.025M) was determined by potassium iodate solution. Pure potassium iodate was dried in an oven at 130 $^oC$. 1.7835 g potassium iodate weighed out accurately was dissolved in deionized water and diluted to final volume of 5 $dm^3$ in a calibrated volumetric flask (0.001667M). 10 $cm^3$ of the standard potassium iodate solution was added to a flask using a volume-calibrated dispenser. Then 90 $cm^3$ of deionized water, 1 $cm^3$ of sulfuric acid solution, and 0.5 $cm^3$ of pickling reagent solution II and I were added into the flask in order. Amount of titrated volume of sodium thiosulfate (usually 5 times measurements average) gave the molarity of the sodium thiosulfate titrant. Table 3.3-1 shows result of the standardization during this cruise. Average of the standardization error (C.V.) was 0.02±0.01 %.

### 3.3.8 Determination of the blank

The oxygen in the pickling reagents I (0.5 $cm^3$) and II (0.5 $cm^3$) was assumed to be 3.8 x $10^{-8}$ mol

(Dickson, 1996). The blank from the presence of redox species apart from oxygen in the reagents (the pickling reagents I, II, and the sulfuric acid solution) was determined as follows. 1 and 2 $cm^3$ of the standard potassium iodate solutions were added to two flasks respectively. Then 100 $cm^3$ of deionized water, 1 $cm^3$ of sulfuric acid solution, and 0.5 $cm^3$ of pickling reagent solution II and I each were added into the two flasks in order. The blank was determined by difference between the two times of the first (1 $cm^3$ of $KIO_3$) titrated volume of the sodium thiosulfate and the second (2 $cm^3$ of $KIO_3$) one. The results of 3 times blank determinations were averaged (Table 3.3-1). The averaged blank of DOT-1 and DOT-3 during the whole legs were -0.009 and -0.005 $cm^3$, respectively.

Table 3.3-1 Results of the standardization and the blank determinations during MR05-05.

| Date | $KIO_3$ | | DOT-1 ($cm^3$) | | | DOT-3 ($cm^3$) | | | Samples |
|---|---|---|---|---|---|---|---|---|---|
| (UTC) | # | bottle | $Na_2S_2O_3$ | E.P. | blank | $Na_2S_2O_3$ | E.P. | blank | (Stations) |
| 2005/10/30 | 1 | 20050829-25 | 20051028-3 | 3.960 | -0.010 | 20051028-4 | 3.961 | -0.005 | 1-16 |
| 2005/11/02 | | 20050829-26 | 20051028-3 | 3.961 | -0.010 | 20051028-4 | 3.959 | -0.004 | 18-26 |
| 2005/11/03 | | 20050829-27 | 20051031-1 | 3.960 | -0.011 | 20051031-2 | 3.961 | -0.005 | 28-34 |
| 2005/11/04 | | 20050829-28 | 20051031-1 | 3.960 | -0.009 | 20051031-2 | 3.959 | 0.000 | 36-44 |
| 2005/11/06 | | 20050829-29 | 20051031-3 | 3.960 | -0.011 | 20051031-4 | 3.960 | -0.008 | 46-53 |
| 2005/11/07 | | 20050829-30 | 20051031-3 | 3.958 | -0.008 | 20051031-4 | 3.958 | -0.004 | 55-58,X17,62 |
| 2005/11/09 | | 20050829-31 | 20051105-1 | 3.960 | -0.012 | 20051105-2 | 3.960 | -0.006 | 64-73 |
| 2005/11/11 | 2 | 20050829-37 | 20051105-3 | 3.960 | -0.011 | 20051105-4 | 3.963 | -0.004 | 74-81 |
| 2005/11/12 | | 20050829-38 | 20051105-3 | 3.960 | -0.010 | 20051105-4 | 3.960 | -0.008 | 83-90 |
| 2005/11/14 | | 20050829-39 | 20051112-1 | 3.962 | -0.009 | 20051112-2 | 3.964 | -0.005 | 92-100 |
| 2005/11/15 | | 20050829-40 | 20051112-1 | 3.960 | -0.010 | 20051112-2 | 3.963 | -0.004 | X16,104-110 |
| 2005/11/17 | | 20050829-41 | 20051112-3 | 3.963 | -0.010 | 20051112-4 | 3.963 | -0.006 | 112-120 |
| 2005/11/18 | | 20050829-42 | 20051112-3 | 3.963 | -0.009 | 20051112-4 | 3.964 | -0.004 | 122-130 |
| 2005/11/20 | | 20050829-43 | 20051116-1 | 3.957 | -0.010 | 20051116-2 | 3.958 | -0.007 | 132-140 |
| 2005/11/21 | | 20050829-44 | 20051116-1 | 3.957 | -0.009 | 20051116-2 | 3.959 | -0.005 | 142-146 |
| 2005/11/30 | 3 | 20050830-49 | 20051128-1 | 3.960 | -0.011 | 20051128-2 | 3.961 | -0.005 | 146(2)-153 |
| 2005/12/01 | | 20050829-50 | 20051128-1 | 3.959 | -0.010 | 20051128-2 | 3.958 | -0.005 | 154-163 |
| 2005/12/02 | | 20050829-51 | 20051128-3 | 3.961 | -0.009 | 20051128-4 | 3.961 | -0.006 | 165-173 |
| 2005/12/03 | | 20050829-52 | 20051128-3 | 3.959 | -0.010 | 20051128-4 | 3.959 | -0.005 | 175-183 |
| 2005/12/05 | | 20050829-53 | 20051203-1 | 3.960 | -0.010 | 20051203-2 | 3.960 | -0.008 | 185-193 |
| 2005/12/07 | | 20050829-54 | 20051203-1 | 3.960 | -0.009 | 20051203-2 | 3.960 | -0.006 | 195,197,X14, 201,203 |
| 2005/12/09 | | 20050829-55 | 20051203-3 | 3.959 | -0.010 | 20051203-4 | 3.960 | -0.005 | 205-213 |
| 2005/12/11 | | 20050829-56 | 20051203-3 | 3.961 | -0.010 | 20051203-4 | 3.960 | -0.004 | 215,217 |
| 2005/12/16 | 4 | 20050829-61 | 20051211-1 | 3.963 | -0.009 | 20051211-2 | 3.966 | -0.005 | WC0-WC4 |
| 2005/12/17 | | 20050829-62 | 20051211-1 | 3.962 | -0.008 | 20051211-2 | 3.960 | -0.007 | WC5-WC10 |
| 2005/12/20 | | 20050829-63 | 20051211-3 | 3.961 | -0.010 | 20051211-4 | 3.962 | -0.003 | 217(2)-225 |
| 2005/12/22 | | 20050829-64 | 20051211-3 | 3.964 | -0.010 | 20051211-4 | 3.964 | -0.006 | 227-233,X13 |
| 2005/12/24 | | 20050829-65 | 20051223-1 | 3.964 | -0.008 | 20051223-2 | 3.963 | -0.005 | 237-245 |
| 2005/12/25 | | 20050829-66 | 20051223-1 | 3.964 | -0.009 | 20051223-2 | 3.963 | -0.004 | 247-253 |
| 2005/12/27 | | 20050829-67 | 20051223-3 | 3.965 | -0.011 | 20051223-4 | 3.965 | -0.005 | 255-263 |
| 2005/12/28 | | 20050829-68 | 20051223-3 | 3.963 | -0.007 | 20051223-4 | 3.964 | -0.003 | 265-273 |

# Batch number of the $KIO_3$ standard solution.

Table 3.3-1 continued.

| Date | $KIO_3$ | | DOT-1 ($cm^3$) | | | DOT-3 ($cm^3$) | | | Samples |
|---|---|---|---|---|---|---|---|---|---|
| (UTC) | # | bottle | $Na_2S_2O_3$ | E.P. | blank | $Na_2S_2O_3$ | E.P. | blank | (Stations) |
| 2005/12/30 | 5 | 20050829-73 | 20051229-1 | 3.964 | -0.010 | 20051229-2 | 3.964 | -0.006 | X10,275-279 |
| 2006/01/01 | | 20050829-74 | 20051229-1 | 3.964 | -0.007 | 20051229-2 | 3.965 | -0.005 | 281-289 |
| 2006/01/03 | | 20050829-75 | 20051229-3 | 3.965 | -0.010 | 20051229-4 | 3.963 | -0.007 | 291-299 |
| 2006/01/04 | | 20050829-76 | 20051229-3 | 3.966 | -0.010 | 20051229-4 | 3.966 | -0.006 | 301-312 |
| 2006/01/05 | | 20050829-77 | 20060105-1 | 3.961 | -0.007 | 20060105-2 | 3.961 | -0.004 | 314-318,X09,322 |
| 2006/01/07 | | 20050829-78 | 20060105-1 | 3.961 | -0.009 | 20060105-2 | 3.961 | -0.002 | 324-333 |
| 2006/01/10 | | 20050829-79 | 20060105-3 | 3.959 | -0.008 | 20060105-4 | 3.960 | -0.005 | 335-343 |
| 2006/01/11 | | 20050829-80 | 20060105-3 | 3.962 | -0.009 | 20060105-4 | 3.962 | -0.005 | 345-351 |
| 2006/01/12 | 6 | 20050829-85 | 20060112-1 | 3.965 | -0.011 | 20060112-2 | 3.966 | -0.005 | 369-355 |
| 2006/01/14 | | 20050829-86 | 20060112-1 | 3.963 | -0.009 | 20060112-2 | 3.966 | -0.004 | 353,351(2) |
| 2006/01/20 | 6 | 20050829-88 | 20060112-3 | 3.968 | -0.009 | 20060112-4 | 3.970 | -0.004 | 370-389 |
| 2006/01/23 | | 20050829-89 | 20060112-3 | 3.967 | -0.006 | 20060112-4 | 3.967 | -0.006 | 390-408 |
| 2006/01/25 | | 20050829-90 | 20060120-1 | 3.964 | -0.008 | 20060120-2 | 3.969 | -0.001 | TS7- TS1 |

# Batch number of the $KIO_3$ standard solution.

### 3.3.9 Reagent blank

The blank determined in section 3.3.8, pure water blank ($V_{blk, dw}$) can be represented by equation 1,

$$V_{blk, dw} = V_{blk, ep} + V_{blk, reg} \quad (1)$$

where

$V_{blk, ep}$ = blank due to differences between the measured end-point and the equivalence point;

$V_{blk, reg}$ = blank due to oxidants or reductants in the reagent.

Here, the reagent blank ($V_{blk, reg}$) was determined by following procedure. 1 $cm^3$ of the standard potassium iodate solution and 100 $cm^3$ of deionized water were added to two flasks each. 1 $cm^3$ of sulfuric acid solution, and 0.5 $cm^3$ of pickling reagent solution II and I each were added into the first flask in order. Then into the second flask, two times volume of the reagents (2 $cm^3$ of sulfuric acid solution, and 1.0 $cm^3$ of pickling reagent solution II and I each) was added. The reagent blank was determined by difference between the first (2 $cm^3$ of the total reagent volume added) titrated volume of the sodium thiosulfate and the second (4 $cm^3$ of the total reagent volume added) one. We also carried out experiments for three and four times volume of the reagents. The results are shown in Figure 3.3-1.

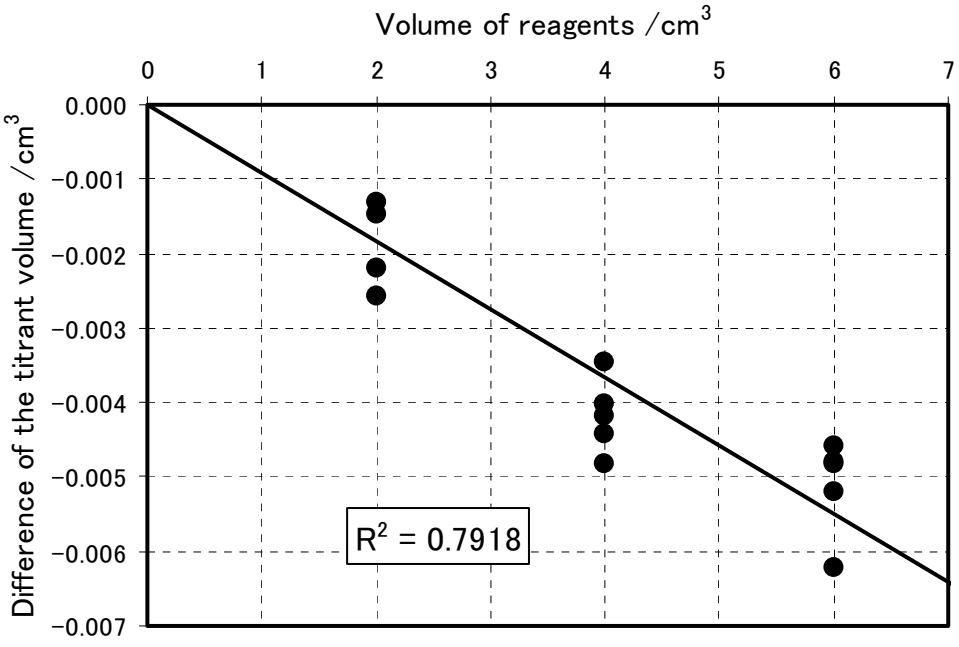


Figure 3.3-1 Blank ($cm^3$) due to redox species apart from oxygen in the reagents

The relation between difference of the titrant ($Na_2S_2O_3$) volume and the volume of the reagents added ($V_{reagent}$) is expressed by equation 2,

$$\text{Difference of the titrant volume} = -0.0009\ V_{reagent} \quad (2).$$

There was no significant difference between the results of DOT-1 and DOT-3. $V_{blk,\ reg}$ for was estimated to be about -0.002 $cm^3$, suggesting that about 0.01 μmol of reductants was contained in every 2 $cm^3$ of the reagents added. In other words, the difference of the pure water blank ($V_{blk,\ dw}$) between DOT-1 and DOT-3, determined in the section 3.3.8, was due to the difference of the end-point blank ($V_{blk,\ ep}$) between the two titration apparatus (-0.007 and -0.003 $cm^3$ for DOT-1 and DOT-3, respectively).

### 3.3.10 Sample blank

Blank due to redox species other than oxygen in the sample ($V_{blk,\ spl}$) can be a potential source of measurement error. The total blank during the seawater measurement, the seawater blank ($V_{blk,\ sw}$) can be represented by equation 3,

$$V_{blk,\ sw} = V_{blk,\ spl} + V_{blk,\ dw} \quad (3).$$

If the pure water blank ($V_{blk,\ dw}$) that is determined in section 3.3.8 is identical both in pure water and in seawater, the difference between the seawater blank and the pure water one gives the sample blank ($V_{blk,\ spl}$).

Here $V_{blk,\ spl}$ was determined by following procedure. Seawater sample was collected in the volume calibrated glass flask (ca. 100 $cm^3$) without the pickling. Then 1 $cm^3$ of the standard

potassium iodate solution, 1 $cm^3$ of sulfuric acid solution, and 0.5 $cm^3$ of pickling reagent solution II and I each were added into the flask in order. Additionally a flask contained 1 $cm^3$ of the standard potassium iodate solution, 100 $cm^3$ of deionized water, 1 $cm^3$ of sulfuric acid solution, and 0.5 $cm^3$ of pickling reagent solution II and I was prepared. The difference of the titrant volumes of the seawater flask and the deionized water one gave the sample blank ($V_{blk, spl}$).

We measured vertical profiles of the sample blank at four stations (Table 3.3-2) using DOT-1 system. The sample blank ranged from 0.4 to 0.8 μmol $kg^{-1}$ and its vertical and horizontal variations are small. Our results agree with reported values ranged from 0.4 to 0.8 μmol $kg^{-1}$ (Culberson *et al.*, 1991) and our previous results obtained in the western North Pacific, reoccupation of WHP-P10 in 2005. Ignoring of the sample blank will introduce systematic errors into the oxygen calculations, but these errors are expected to be the same for all investigators and not to affect the comparison of results from different investigators (Culberson, 1994).

Table 3.3-2 Results of the sample blank determinations during MR05-05.

| Station: P03-006 32.5°N / 118.0°W | | Station: P03-031 29.1°N / 123.9°W | | Station: P03-136 25.5°N / 164.3°W | | Station: P03-215 24.2°N / 172.8°E | |
|---|---|---|---|---|---|---|---|
| CTD Pres. dbar | Sample blank μmol $kg^{-1}$ | CTD Pres. dbar | Sample blank μmol $kg^{-1}$ | CTD Pres. dbar | Sample blank μmol $kg^{-1}$ | CTD Pres. dbar | Sample blank μmol $kg^{-1}$ |
| 9 | 0.48 | 10 | 0.45 | 9 | 0.38 | 10 | 0.39 |
| 149 | 0.71 | 51 | 0.50 | 48 | 0.38 | 50 | 0.40 |
| 249 | 0.68 | 101 | 0.56 | 100 | 0.51 | 100 | 0.48 |
| 400 | 0.63 | 152 | 0.56 | 150 | 0.57 | 150 | 0.53 |
| 600 | 0.74 | 501 | 0.63 | 200 | 0.64 | 200 | 0.63 |
| 800 | 0.70 | 1001 | 0.70 | 600 | 0.59 | 502 | 0.76 |
| 1003 | 0.76 | 2003 | 0.66 | 1201 | 0.52 | 1003 | 0.66 |
| 1403 | 0.69 | 3001 | 0.68 | 2201 | 0.60 | 2000 | 0.69 |
| 1801 | 0.70 | 4249 | 0.73 | 3251 | 0.60 | 3500 | 0.71 |
| 1867 | 0.78 | 4459 | 0.72 | 3751 | 0.62 | 5002 | 0.72 |

### 3.3.11 Replicate sample measurement

Replicate samples were taken from every CTD cast. Total amount of the replicate sample pairs in good measurement (flag=2) was 837. The standard deviation of the replicate measurement was 0.08 μmol $kg^{-1}$ and there was no significant difference between DOT-1 and DOT-3 measurements. The standard deviation was calculated by a procedure (SOP23) in DOE (1994). The difference of the replicate sample pairs did not depend on sampling pressure (Figure 3.3-2) and measurement date (Figure 3.3-3). The standard deviations during Leg-1, Leg-2, and Leg-3 were 0.083 (n=299) and 0.083 (n=493), and 0.085 μmol $kg^{-1}$ (n=45), respectively.

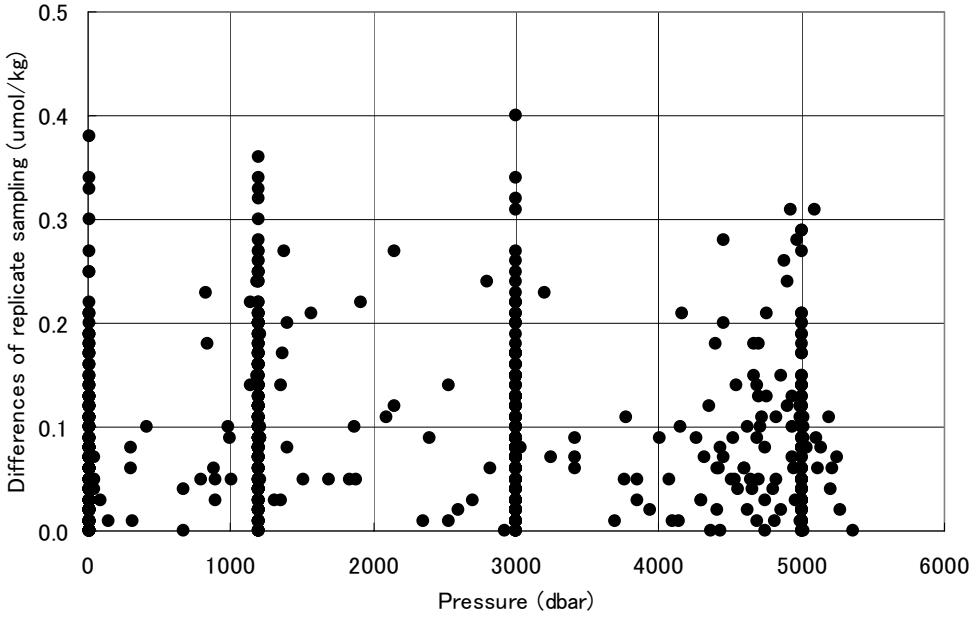


Figure 3.3-2 Differences in the replicate measurements against sampling pressure.

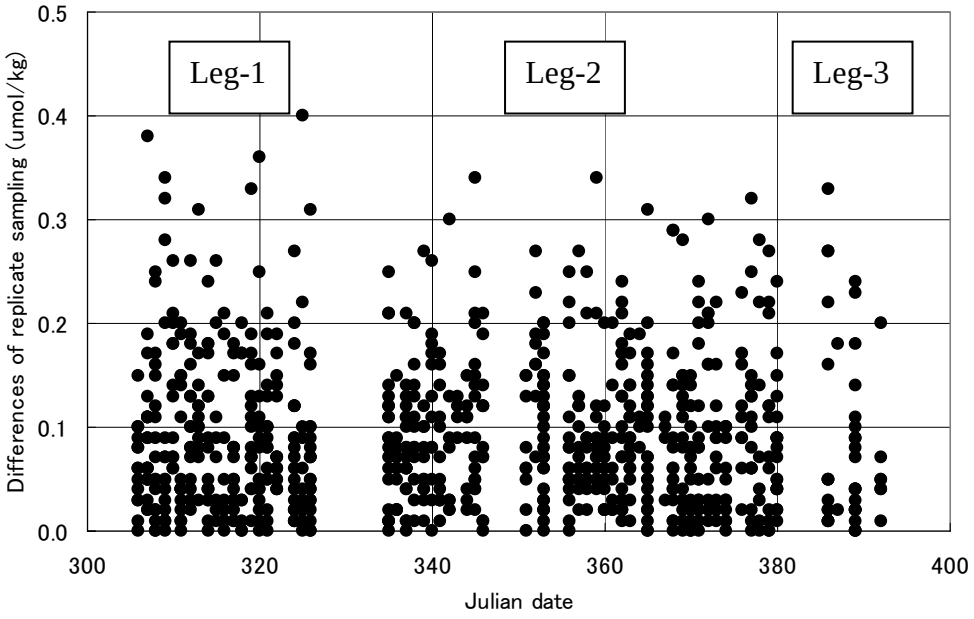


Figure 3.3-3 Differences in the replicate measurements against measurement date (Julian date).

### 3.3.12 Duplicate sample measurement

We also collected seawater samples from two Niskin samplers that were collected at the same depth (duplicate sampling). Total 50 pairs of the duplicate samples were taken in deep layers below 800 dbar during all the legs. The standard deviation of the total duplicate measurement was 0.10 μmol $kg^{-1}$. We concluded that total measurement error of bottle oxygen was 0.10 μmol $kg^{-1}$ during MR05-05 cruise.

### 3.3.13 CSK standard measurements

The CSK standard solution is commercial potassium iodate solution (0.0100 N) for analysis of oxygen in seawater. During the cruises, we measured concentration of the CSK standard solution (Lot ASE8281) against our $KIO_3$ standard in order to confirm accuracy of our oxygen measurement on board (Table 3.3-3). Averaged values of DOT-1 and DOT-3 were 0.009999±0.000016 and 0.009999±0.000025 normal (N) respectively, which indicate that there was no systematic difference between DOT-1 and DOT-3 measurements. The averaged value of the CSK standard solution was so close to the certified value (0.0100 N) that we did not correct sample measurements results using the CSK standard results. Additionally, we also measured the same lots of the CSK standard solution during our last cruise in 2005 (MR05-02). Results of the CSK measurements in the both cruises agreed well within the errors, suggesting there was no systematic difference between our oxygen measurements between MR05-02 and MR05-05 cruises.

Table 3.3-3 Results of the CSK standard measurements.

| Date (UTC) | $KIO_3$ batch# | DOT-1 | | DOT-3 | |
|---|---|---|---|---|---|
| | | Conc. (N) | error (N) | Conc. (N) | error (N) |
| 2005/11/07 | ASE8281-1 | 0.010005 | 0.000005 | 0.010006 | 0.000003 |
| 2005/11/18 | ASE8281-2 | 0.009998 | 0.000003 | 0.009993 | 0.000017 |
| 2005/12/07 | ASE8281-3 | 0.010004 | 0.000007 | 0.010001 | 0.000007 |
| 2005/12/25 | ASE8281-4 | 0.010001 | 0.000004 | 0.010005 | 0.000007 |
| 2006/01/11 | ASE8281-5 | 0.009997 | 0.000006 | 0.009998 | 0.000011 |
| 2006/01/14 | ASE8281-6 | 0.009998 | 0.000008 | 0.009997 | 0.000009 |
| 2006/01/26 | ASE8281-7 | 0.009989 | 0.000006 | 0.009990 | 0.000005 |
| | | | | | |
| Average | | 0.009999 | 0.000016 | 0.009999 | 0.000025 |
| | | | | | |
| Date (UTC) | $KIO_3$ batch# | DOT-1 | | DOT-2 | |
| | | Conc. (N) | error (N) | Conc. (N) | error (N) |
| 2005/6/21 | ASE8281-0 | 0.010005 | 0.000010 | 0.010002 | 0.000006 |

### 3.3.14 Quality control flag assignment

Quality flag values were assigned to oxygen measurements using the code defined in Table 0.2 of WHP Office Report WHPO 91-1 Rev.2 section 4.5.2 (Joyce *et al*., 1994). Measurement flags of 2, 3, 4, and 5 have been assigned (Table 3.3-4). For the choice between 2 (good), 3 (questionable) or 4 (bad), we basically followed a flagging procedure as listed below:

a. Bottle oxygen and difference between bottle oxygen and CTD oxygen at the sampling time were plotted against CTD pressure. Any points not lying on a generally smooth trend were noted.

b. Dissolved oxygen was then plotted against potential temperature or sigma-theta. If a datum deviated from a group of plots, it was flagged 3 or 4.

c. Vertical sections against pressure and potential density were drawn. If a datum was anomalous on the section plots, datum flag was degraded from 2 to 3, or from 3 to 4.

d. If the bottle flag was 4 (did not trip correctly), a datum was noted and flagged 4. In case of the bottle flag 3 (leaking) or 5 (unknown problem), a datum was flagged based on steps a, b, and c.

Table 3.3-4 Summary of assigned quality control flags.

| Flag | Definition | |
|---|---|---|
| 2 | Good | 6,702 |
| 3 | Questionable | 5 |
| 4 | Bad | 10 |
| 5 | Not report (missing) | 4 |
| | Total | 6,721 |

### 3.3.15 Preliminary results

We compared our oxygen data and those of WHP P03 in 1985 and found "offset" between the two datasets. Below 2000 m depth where seasonal and annual-decadal changes of dissolved oxygen are not significant, WHP P03 oxygen concentration is systematically higher than our results by 2.2±1.7 μmol $kg^{-1}$ on average. This offset between the two cruises should be corrected carefully for further comparison of the datasets. We here just compare uncorrected oxygen data between 1985 and 2005/2006 in order to overview decadal change of dissolved oxygen in intermediate layer shallow than 1,000 m depth. Figure 3.3-4 shows distribution of oxygen difference (2005/2006 data minus 1985 data, μmol $kg^{-1}$) against water density (sigma theta) from 24.0 to 27.5 (approximately from 100 to 1200 m depth). We found a significant decrease of dissolved oxygen at the eastern end where oxygen concentration was relatively low. This decrease may be due to variability of local upwelling. Oxygen increase around 130°W centered 26.2 sigma theta implies variation of mesoscale eddies. From 160°W to the International Date Line, around 26.8 sigma theta dissolved oxygen slightly decreased, which is similar to the intermediate oxygen decrease in the subarctic regions. The oxygen change along 24°N, however, is smaller than that found in the northern North Pacific.

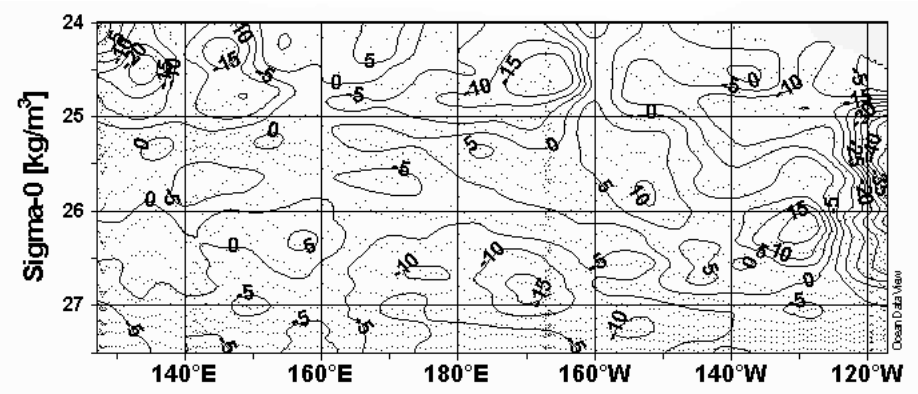


Figure 3.3-4 Oxygen difference (2005/2006 data minus 1985 data, μmol $kg^{-1}$) against water density (sigma theta).

References

Culberson, A.H. (1994) Dissolved oxygen, in WHPO Pub. 91-1 Rev. 1, November 1994, Woods Hole, Mass., USA.

Culberson, A.H., G. Knapp, M.C. Stalcup, R.T. Williams, F. Zemlyak (1991) A comparison of methods for the determination of dissolved oxygen in seawater, WHPO Pub. 91-2, August 1991, Woods Hole, Mass., USA.

Dickson, A. (1996) Determination of dissolved oxygen in sea water by Winkler titration, in WHPO Pub. 91-1 Rev. 1, November 1994, Woods Hole, Mass., USA.

DOE (1994) Handbook of methods for the analysis of the various parameters of the carbon dioxide system in sea water; version 2. A.G. Dickson and C. Goyet (eds), ORNL/CDIAC-74.

Joyce, T., and C. Corry, eds., C. Corry, A. Dessier, A. Dickson, T. Joyce, M. Kenny, R. Key, D. Legler, R. Millard, R. Onken, P. Saunders, M. Stalcup, contrib. (1994) Requirements for WOCE Hydrographic Programme Data Reporting, WHPO Pub. 90-1 Rev. 2, May 1994 Woods Hole, Mass., USA.

## 3.4 Nutrients

*draft as of 7 March, 2006*

***Michio AOYAMA (Meteorological Research Institute***
***/ Japan Meteorological Agency, Principal Investigator)***

***Leg 1***
***Kenichiro SATO (Department of Marine Science, Marine Works Japan Ltd.)***
***Ayumi TAKEUCHI (Department of Marine Science, Marine Works Japan Ltd.)***
***Junji MATSUSHITA (Department of Marine Science, Marine Works Japan Ltd.)***

***Leg 2***
***Junko HAMANAKA(Department of Marine Science, Marine Works Japan Ltd.)***
***Ayumi TAKEUCHI (Department of Marine Science, Marine Works Japan Ltd.)***
***Kohei MIURA (Marine Works Japan Ltd.)***

***Leg 3***
***Junko HAMANAKA(Department of Marine Science, Marine Works Japan Ltd.)***
***Junji MATSUSHITA (Department of Marine Science, Marine Works Japan Ltd.)***
***Kohei MIURA (Marine Works Japan Ltd.)***

### 3.4.1 Objectives

The objectives of nutrients analyses during the R/V Mirai MR05-05 cruise along 24N line in the Western North Pacific are as follows;

Describe the present status of nutrients in good traceability.

The target nutrients are nitrate, nitrite, phosphate and silicate (Although silicic acid is correct, we use silicate because a term of silicate is widely used in oceanographic community.)

Study the temporal and spatial variation of nutrients based on the previous high quality experiments data of WOCE, GOESECS, IGY and so on.

Study the temporal and spatial variation of nitrate: phosphate ratio, so called Redfield ratio.

Obtain more accurate estimation of total amount of nitrate, phosphate and silicate in the interested area.

Provide more accurate nutrients data for physical oceanographers to use as tracers of water mass movement.

### 3.4.2 Equipment and techniques

#### 3.4.2.1 Analytical detail using TRAACS 800 systems (BRAN+LUEBBE)

The phosphate analysis is a modification of the procedure of Murphy and Riley (1962).

Molybdic acid is added to seawater sample to form phosphomolybdic acid which is in turn reduced to phosphomolybdous acid using L-ascorbic acid as a reductant.

Nitrate + nitrite and nitrite are analyzed according to the modification method of Grasshoff (1970).

The sample nitrate is reduced to nitrite in a cadmium tube inside of which is coated with metallic copper. The sample stream with its equivalent nitrite is treated with an acidic, sulfanilamide reagent and the nitrite forms nitrous acid which reacts with the sulfanilamide to produce a diazonium ion. N1-Naphthylethylene-diamine added to the sample stream then couples with the diazonium ion to produce a red, azo dye. With reduction of the nitrate to nitrite, both nitrate and nitrite reacts and are measured; without reduction, only nitrite reacts. Thus, for the nitrite analysis, no reduction is performed and the alkaline buffer is not necessary. Nitrate is computed by difference.

The silicate method is analogous to that described for phosphate. The method used is essentially that of Grasshoff et al. (1983), wherein silicomolybdic acid is first formed from the silicic acid in the sample and added molybdic acid; then the silicomolybdic acid is reduced to silicomolybdous acid, or "molybdenum blue," using ascorbic acid as a reductant.

The flow diagrams and regents for each parameter are shown in Figures 3.4.1-3.4.4.

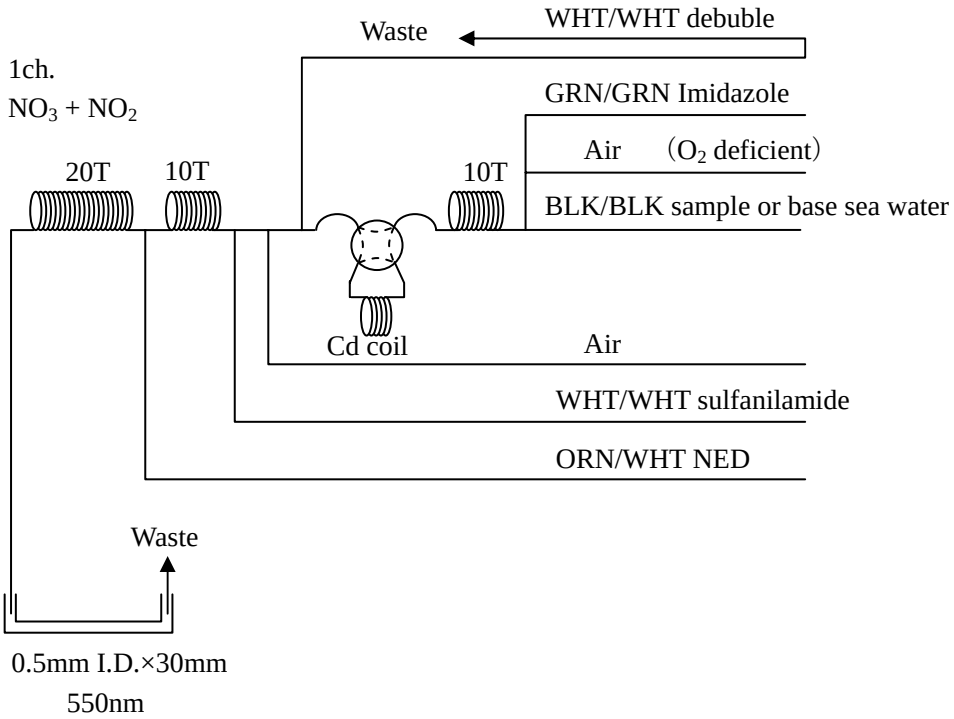


Figure3.4.1: 1ch. ($NO_3$+$NO_2$) Flow diagram.

---

## Nitrate Reagents

Imidazole (buffer), 0.06M (0.4% w/v)
Dissolve 4g imidazole, $C_3H_4N_2$, in ca. 900ml DIW; add 2ml concentrated HCl; make up to 1000ml with DIW. After mixing, 1ml Triton(R)X-100 (50% solution in ethanol) is added.

Sulfanilamide, 0.06M (1% w/v) in 1.2M HCl
Dissolve 10g sulfanilamide, 4-$NH_2C_6H_4SO_3H$, in 1000ml of 1.2M (10%) HCl. After mixing, 1ml Triton(R)X-100 (50% solution in ethanol) is added.

N-1-Napthylethylene-diamine dihydrochloride, 0.004 M (0.1% w/v)
Dissolve 1 g NEDA, C10H7NHCH2CH2NH2・2HCl, in 1000ml of DIW; containing 10ml concentrated HCl. Stored in a dark bottle.

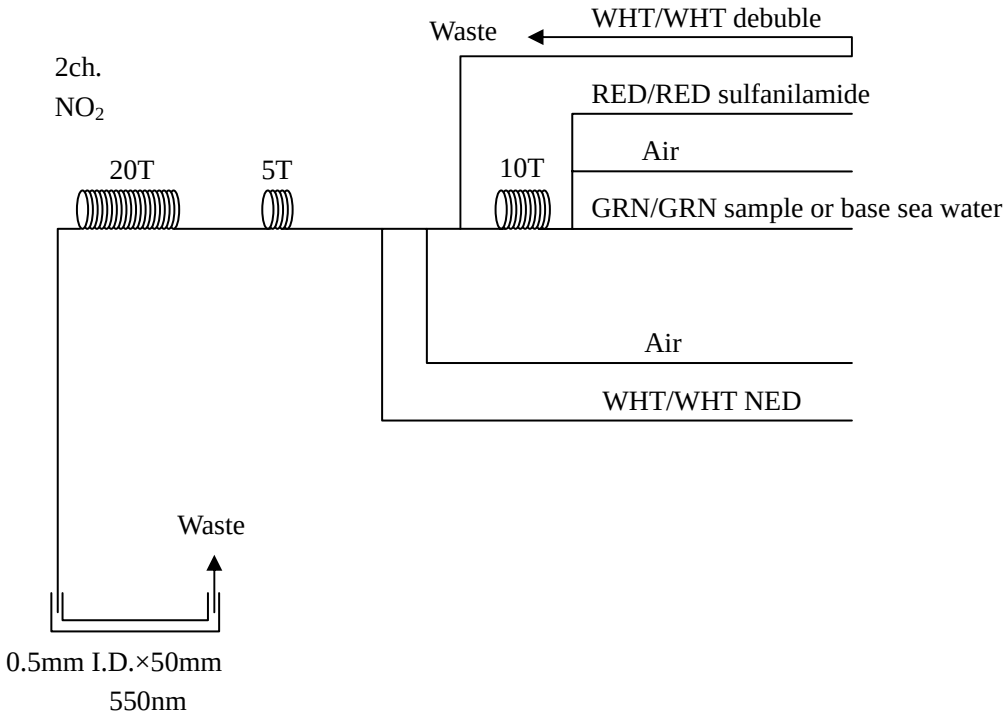


Figure 3.4.2: 2ch. ($NO_2$) Flow diagram.

## Nitrite Reagents

Sulfanilamide, 0.06M (1% w/v) in 1.2M HCl
Dissolve 10g sulfanilamide, 4-$NH_2C_6H_4SO_3H$, in 1000ml of 1.2M (10%) HCl. After mixing, 1ml Triton(R)X-100 (50% solution in ethanol) is added.

N-1-Napthylethylene-diamine dihydrochloride , 0.004 M (0.1% w/v)
Dissolve 1 g NEDA, C10H7NHCH2CH2NH2・2HCl, in 1000ml of DIW; containing 10ml concentrated HCl. Stored in a dark bottle.

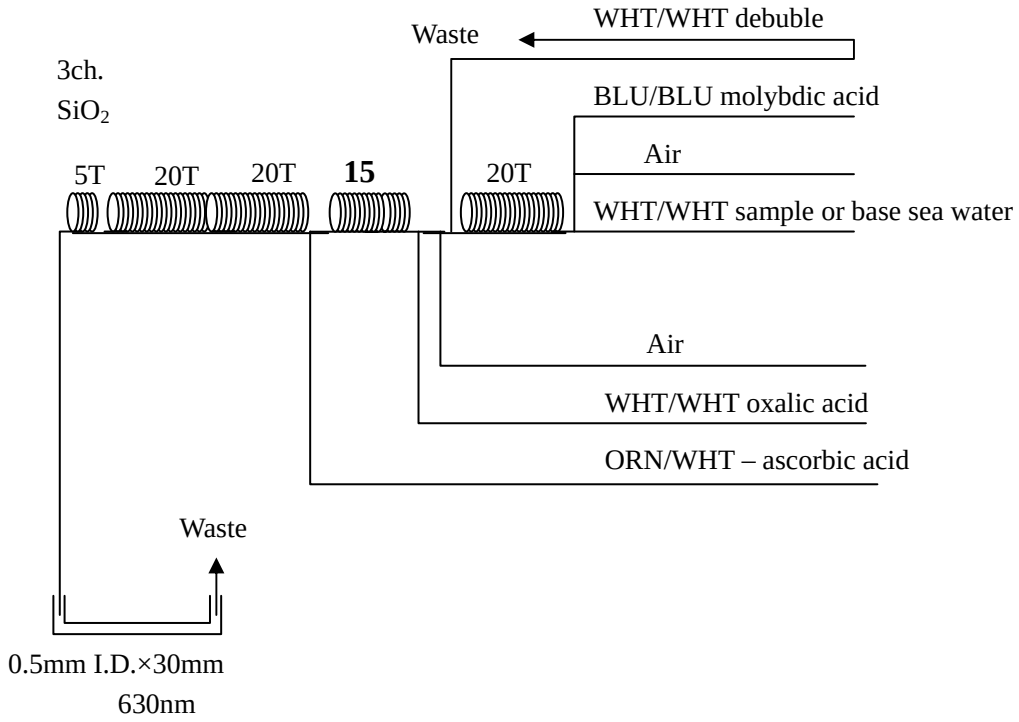


Figure 3.4.3: 3ch. ($SiO_2$) Flow diagram.

---

## Silicic Acid Reagents

Molybdic acid, 0.06M (2% w/v)
Dissolve 15g Disodium Molybdate(VI) Dihydrate, $Na_2MoO_4 \cdot 2H_2O$, in 1000ml DIW containing 6ml $H_2SO_4$. After mixing, 20ml sodium dodecyl sulphate (15% solution in water) is added.

Oxalic acid, 0.6M (5% w/v)
Dissolve 50g Oxalic Acid Anhydrous, HOOC: COOH, in 1000ml of DIW.

Ascorbic acid, 0.01M (3% w/v)
Dissolve 2.5g L (+)-Ascorbic Acid, C6H8O6, in 100ml of DIW. Stored in a dark bottle and freshly prepared before every measurement.

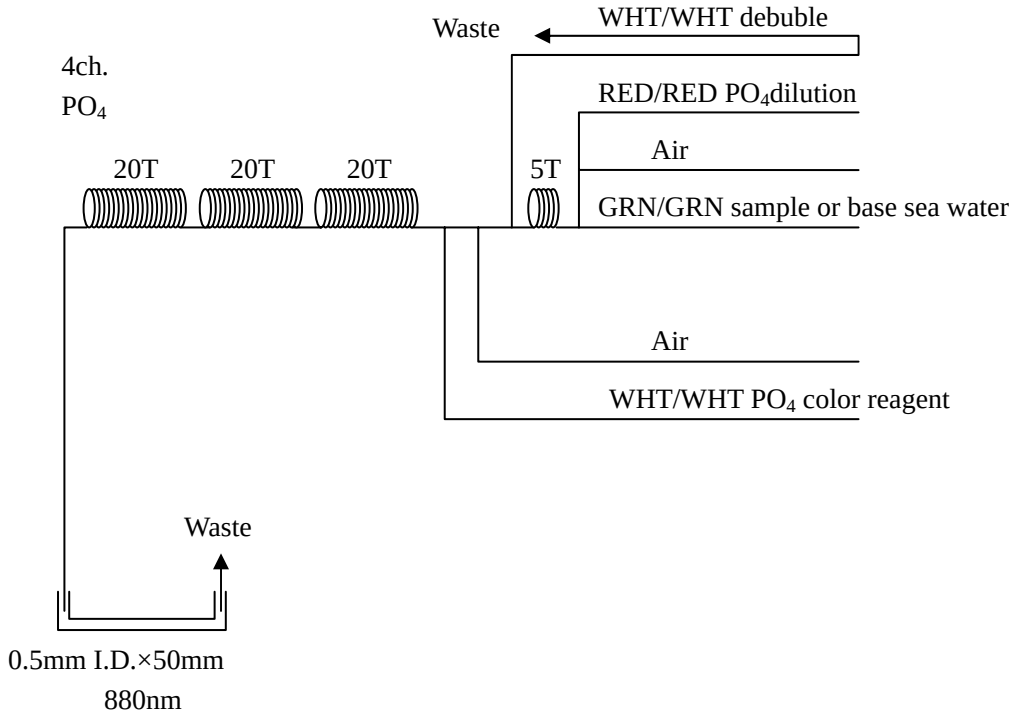


Figure 3.4.4: 4ch. ($PO_4$) Flow diagram.

---

## Phosphate Reagents

Stock molybdate solution, 0.03M (0.8% w/v)
Dissolve 8g Disodium Molybdate(VI) Dihydrate, $Na_2MoO_4 \cdot 2H_2O$, and 0.17g Antimony Potassium Tartrate, $C_8H_4K_2O_{12}Sb_2 \cdot 3H_2O$, in 1000ml of DIW containing 50ml concentrated $H_2SO_4$.

Mixed Reagent
Dissolve 0.8g L (+)-Ascorbic Acid, $C_6H_8O_6$, in 100ml of stock molybdate solution. After mixing, 2ml sodium dodecyl sulphate (15% solution in water) is added. Stored in a dark bottle and freshly prepared before every measurement.

PO4 dilution
Dissolve Sodium Hydrate, NaCl, 10g in ca. 900ml, add 50ml Acetone and 4ml concentrated $H_2SO_4$, make up to 1000ml. After mixing, 5ml sodium dodecyl sulphate (15% solution in water) is added.

#### 3.4.2.2 Sampling procedures

Sampling of nutrients followed that of oxygen, trace gases and salinity. Samples were drawn into two of virgin 10 ml polyacrylates vials without sample drawing tubes. These were rinsed three times before filling and vials were caped immediately after the drawing. The vials are put into water bath at 25 +-1deg. C in 10 minutes before use to stabilize the temperature of samples.

No transfer was made and the vials were set an auto sampler tray directly. Samples were analyzed after collection basically within 17 hours.

#### 3.4.2.3 Data processing.

Raw data from TRAACS800 were treated as follows;

Check baseline shift.

Check the shape of each peak and positions of peak values taken, and then change the positions of peak values taken if necessary.

Carryover correction and baseline drift correction were applied to peak heights of each samples followed by sensitivity correction.

Baseline correction and sensitivity correction were done basically using liner regression.

Load pressure and salinity from CTD data to calculate density of seawater.

Calibration curves to get nutrients concentration were assumed second order equations.

### 3.4.3 Nutrients standards

#### 3.4.3.1 In-house standards

**(i) Volumetric Laboratory Ware.**

All volumetric glass- and plastic (PMP)-ware used were gravimetrically calibrated. Plastic volumetric flasks were gravimetrically calibrated at the temperature of the use within 2-3 K.

**Volumetric flasks.**

Volumetric flasks of Class quality (Class A) are used because their nominal tolerances are 0.05% or less over the size ranges likely to be used in this work. Class A flasks are made of borosilicate glass, and the standard solutions were transferred to plastic bottles as quickly as possible after they are made up to volume and well mixed in order to prevent excessive dissolution of silicic acid from the glass. High quality plastic (polymethylpentene, PMP, or polypropylene) volumetric flasks were gravimetrically calibrated and used only within 3-4 K of the calibration temperature.

The computation of volume contained by glass flasks at various temperatures besides those at the calibration temperatures were done by using the coefficient of linear expansion of borosilicate crown glass.

Because of their larger temperature coefficients of cubical expansion and lack of tables constructed for these materials, the plastic volumetric flasks were gravimetrically calibrated over the temperature range of intended use and used at the temperature of calibration within 3-4 K. The weights obtained in the calibration weightings were corrected for the density of water and air buoyancy.

**Pipettes and pipettors.**

All pipettes have nominal calibration tolerances of 0.1% or better. These were gravimetrically calibrated in order to verify and improve upon this nominal tolerance.

**(ii) REAGENTS, GENERAL CONSIDERATIONS**

**General Specifications.**

All reagents were of very high purity such as "Analytical Grade," "Analyzed Reagent Grade" and others. And assay of nitrite was determined according JISK8019 and assays of nitrite salts were 98.9%. We use that value to adjust the weights taken.

For the silicate standards solution, we use commercial available silicon standard solution for atomic absorption spectrometry of 1000mg $L^{-1}$. Since this solution is alkaline solution of 0.5 M KOH, an aliquot of 40ml solution were diluted to 500ml as B standard together with an aliquot of 20ml of 1M HCl. Then the pH of B standard for silicate prepared to be 6.9.

**Ultra pure water.**

Ultra pure water (MilliQ water) freshly drawn was used for preparation of reagents, higher concentration standards and for measurement of reagent and system blanks.

**Low-Nutrient Seawater (LNSW).**

Surface water having low nutrient concentration was taken and filtered using 0.45 μm pore size membrane filter. This water is stored in 20 liter cubitainer with paper box. The concentrations of nutrient of this water were measured carefully in March 2005.

**(iii) Concentrations of nutrients for A, B and C standards**

Concentrations of nutrients for A, B and C standards are set as shown in Table 3.4.1. The C standard is prepared according to recipes as shown in Table 3.4.2. All volumetric laboratory tools were calibrated prior to the cruise as stated in chapter (i). Then the actual concentration of nutrients in each fresh standard was calculated based on the ambient, solution temperature and determined factors of volumetric lab. wares.

**Table 3.4.1: Nominal concentrations of nutrients for A, B and C standards**

| | A | B | B’ | C-1 | C-2 | C-3 | C-4 | C-5 | C-6 | C-7 | C-8 |
|---|---|---|---|---|---|---|---|---|---|---|---|
| $NO_3$(μM) | 45000 | 900 | 900 | 0 | BA | AY | AX | AV | BC | 55.0 | 55.0 |
| $NO_2$(μM) | 4000 | 20 | 20 | 0 | BA | AY | AX | AV | BC | 1.2 | 1.2 |
| $SiO_2$(μM) | 36000 | 2880 | 3240 | 0 | BA | AY | AX | AV | BC | 172.8 | 194.4 |
| $PO_4$(μM) | 3000 | 60 | 60 | 0 | BA | AY | AX | AV | BC | 3.6 | 3.6 |

**Table 3.4.2: Working calibration standard recipes**

| C-STD | B-1 STD | B-1’ STD | B-2 STD |
|---|---|---|---|
| C-7 | 30 ml | 0 ml | 30 ml |
| C-8 | 0 ml | 30 ml | 30 ml |

B-1 STD: Mixture of nitrate, silicate and phosphate

B-1’ STD: Mixture of nitrate, silicate and phosphate

B-2 STD: Nitrite

**(iv) Renewal of in-house standard solutions.**

In-house standard solutions as stated in (iii) were renewed as shown in Table 3.4.3.

**Table 3.4.3: Timing of renewal of in-house standards.**

| $NO_3$, $NO_2$, $SiO_2$, $PO_4$ | Renewal |
|---|---|
| A-1 Std. ($NO_3$) | maximum 1 month |
| A-2 Std. ($NO_2$) | maximum 1 month |
| A-3 Std. ($SiO_2$) | commercial prepared solution |
| A-4 Std. ($PO_4$) | maximum 1 month |
| B-1 Std. and B-1' Std. (mixture of $NO_3$, $SiO_2$, $PO_4$) | 8 days |
| B-2 Std. ($NO_2$) | 8 days |

| C Std | Renewal |
|---|---|
| C-7～C-8 Std ( mixture of B1 (B1') and B2 Std.) | 24 hours |

| Reduction estimation | Renewal |
|---|---|
| D-1 Std. | when A-1renewed |
| 43μM $NO_3$ | when C-std renewed |
| 47μM $NO_2$ | when C-std renewed |

### 3.4.3.2 RMNS

To get more accurate and high quality nutrients data to achieve the objectives stated above, huge numbers of the bottles of the reference material of nutrients in seawater (hereafter RMNS) are prepared (Aoyama et al., submitted). In the previous world wide expeditions, such as WOCE cruises, the higher reproducibility and precision of nutrients measurements were required (Joyce and Corry, 1994). Since no standards were available for the measurement of nutrients in seawater at that time, the requirements were described in term of reproducibility. The required reproducibility was 1%, 1-2%, 1-3% for nitrate, phosphate and silicate, respectively. Although nutrient data from the WOCE one-time survey was of unprecedented quality and coverage due to much care in sampling and measurements, the differences of nutrients concentration at crossover points are still found among the expeditions (Aoyama and Joyce, 1996, Mordy et al., 2000, Gouretski and Jancke, 2001). For instance, the mean offset of nitrate concentration at deep waters was 0.5 μmol $kg^{-1}$ for 345 crossovers at the world oceans, though the maximum was 1.7 μmol $kg^{-1}$ (Gouretski and Jancke, 2001). At the 31 crossover points in the Pacific WHP one-time lines, the WOCE standard of reproducibility for nitrate of 1% was fulfilled at about half of the crossover points and the maximum difference was 7% at deeper layers below 1.6 deg. C in potential temperature (Aoyama and Joyce,

1996).

**(i) RMNS preparation**

**RMNS preparation and homogeneity for previous lots.**

The study on reference material for nutrients in seawater (RMNS) on the seawater base has been carried out to establish traceability on nutrient analyses in seawater since 1994 in Japan. Autoclaving to produce RMNS has been studied (Aminot and Kerouel, 1991, 1995) and autoclaving was used to stabilize the samples for the 5th intercompariosn exercise in 1992/1993 (Aminot and Kirkwood, 1995). Aminot and Kerouel (1995) concluded that nitrate and nitrite were extremely stable throughout their 27 months storage experiment with overall standard deviations lower than 0.3% (range 5-50 μmol $l^{-1}$) and 0.8% (range 0.5-5 μmol $l^{-1}$), respectively. For phosphate, slight increase by 0.02-0.07 μmol $l^{-1}$ per year was observed due to the leaching from the container glass. The main source of nutrient variation in seawater is believed to be microorganism activity, hence, production of RMNS depends on biological inactivation of samples. In this point of view, previous study showed that autoclaving to inactivate the biological activity is acceptable to RMNS preparation.

In the R/V Mirai BEAGLE2003 cruise, which was the world around cruise along ca. 30 deg. S conducted in 2003 and 2004, RMNS was analyzed at about 500 stations throughout cruises. The results of BEAGLE2003 cruise will be available soon. (Databook of BEAGLE2003, in press)

The seawater for RMNS production was sampled in the North Pacific Ocean at the depths of surface where the nutrients are almost depleted and at the depth of 1500-2000 meters where the nutrients concentrations are the maximum. The seawater was gravity-filtered through a membrane filter with a pore size of 0.45 μm (Millipore HA). The latest procedure of autoclaving for RMNS preparation is that the seawater in a stainless steel container of 40 liters was autoclaved at 120 deg. C, 2 hours, two times during two days. The filling procedure of autoclaved seawater was basically same throughout our study. Following cooling at room temperature in two days, polypropylene bottle of 100 ml capacity were filled by the autoclaved seawater of 90 ml through a membrane filter with a pore size of 0.2 μm (Millipore HA) at a clean bench in a clean room. The polypropylene caps were immediately and tightly screwed on and a label identifying lot number and serial number of the bottle was attached on all of the bottles. Then the bottles were vacuum-sealed to aviod potential contamination from the environment.

**RMNSs for this cruise**

RMNS lots BC,AV,AX,AY and BA, which cover full range of nutrients concentrations in the western North Pacific are prepared as packages. These packages were renewed daily and analyzed every 2 runs on the same day. 250 bottles of RMNS lot AZ are prepared to use every analysis at every hydrographic station. These RMNS assignment were completely done based on random number. The RMNS bottles were stored at a room, REGENT STORE, where the temperature was maintained around 24-26 deg. C.

**Assigned concentration for RMNSs**

We assigned nutrients concentrations for RMNS lots BC,AV,AX,AY and BA.

**Table 3.4.4 Assigned concentration of RMNSs**

| | Nitrate | Phosphate | Silicate |
|---|---|---|---|
| RMNS-BA | 0.1 ± 0.0 | 0.06 ± 0.01 | 1.6 ± 0.1 |
| RMNS-AY | 5.6 ± 0.0 | 0.52 ± 0.01 | 30.1 ± 0.1 |
| RMNS-AX | 21.4 ± 0.1 | 1.61 ± 0.01 | 59.5 ± 0.1 |
| RMNS-AV | 33.4 ± 0.1 | 2.52 ± 0.01 | 157.9 ± 0.2 |
| RMNS-BC | 40.7 ± 0.1 | 2.78 ± 0.01 | 160.0 ± 0.2 |
| RMNS-AZ | 42.3 ± 0.1 | 3.02 ± 0.01 | 137.2 ± 0.2 |

**(ii) The homogeneity of RMNSs**

The homogeneity of lot BC and analytical precisions are shown in Table 3.4.4. These are used for the assessment of the magnitude of homogeneity of the RMNS bottles those are used during the cruise. As shown in Table3.4.5, the homogeneity of RMNS lot BC for nitrate and silicate are the same magnitude as the analytical precision derived from fresh raw seawater. The homogeneity for phosphate, however, exceeded the analytical precision at some extent.

**Table 3.4.5: Homogeneity of lot BC and previous lots derived from simultaneous 30 samples measurements and analytical precision onboard R/V Mirai in May 2005.**

| | **Nitrate CV%** | **Phosphate CV%** | **Silicate CV%** |
|---|---|---|---|
| **BC** | **0.22** | **0.32** | **0.19** |
| **(AH)** | **(0.39%)** | **(0.83%)** | **(0.13)** |
| **(K)** | **(0.3%)** | **(1.0%)** | **(0.2%)** |
| **Precision** | **0.22%** | **0.22%** | **0.12%** |

Note: N=30 x 2

### 3.4.4 Quality control

#### 3.4.4.1 Precision of nutrients analyses during the cruise

Precision of nutrients analyses during the cruise was evaluated based on the 12 measurements, which are measured every 12 samples, during a run at the concentration of C-7. We also evaluated the reproducibility based on the replicate analyses of five samples in each run. Summary of

precisions are shown in Table 3.4.6. As shown in Table 3.4.6 and Figures 3.4.5-3.4.7, the precisions for each parameter are generally good considering the analytical precisions estimated from the simultaneous analyses of 60 samples in May 2005. Analytical precisions previously evaluated were 0.22% for phosphate, 0.22% for nitrate and 0.12% for silicate, respectively. During this cruise, analytical precisions were 0.08% for phosphate, 0.07% for nitrate and 0.08% for silicate in terms of median of precision, respectively. Thus we can conclude that the analytical precisions for phosphate, nitrate and silicate were maintained throughout this cruise or better than that of the pre-cruise evaluations. The time series of precision are shown in Figures 3.4.5-3.4.7.

Table 3.4.6: Summary of precision based on the replicate analyses of 12 samples in each run through out cruise.

| | Nitrate CV% | Phosphate CV% | Silicate CV% |
|---|---|---|---|
| Median | 0.07 | 0.07 | 0.09 |
| Mean | 0.076 | 0.072 | 0.087 |
| Maximum | 0.17 | 0.19 | 0.17 |
| Minimum | 0.03 | 0.03 | 0.02 |
| N | 277 | 277 | 277 |

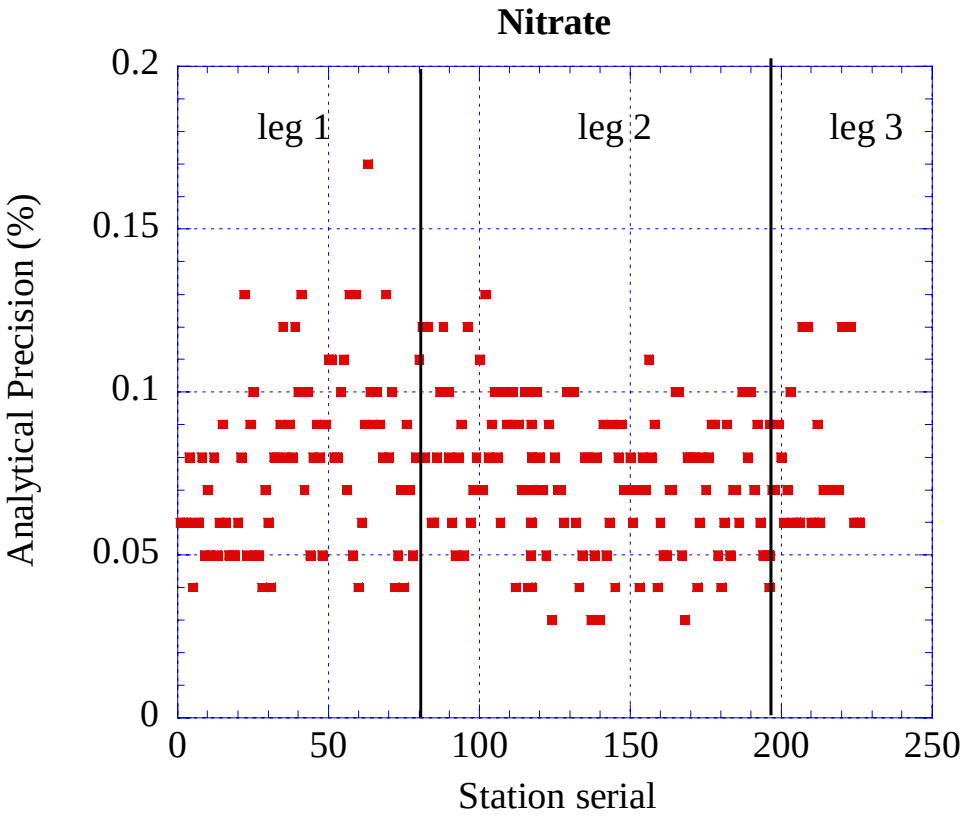


**Figure: 3.4.5 Time series of precision of nitrate**

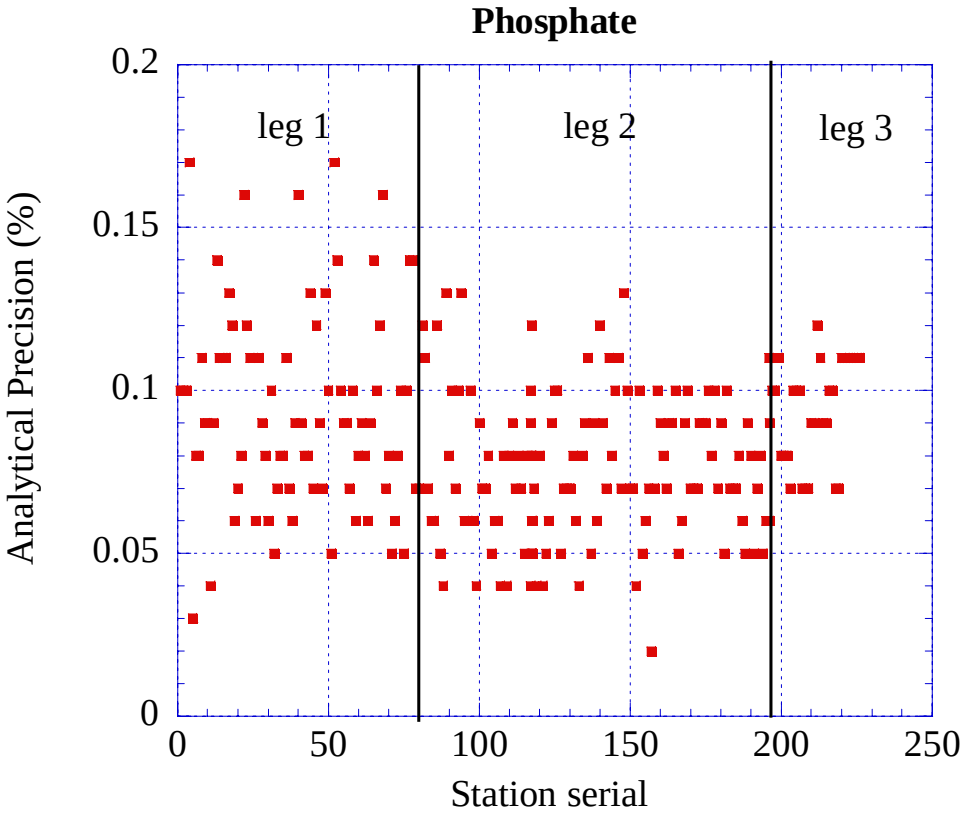


**Figure: 3.4.6 Time series of precision of phosphate**

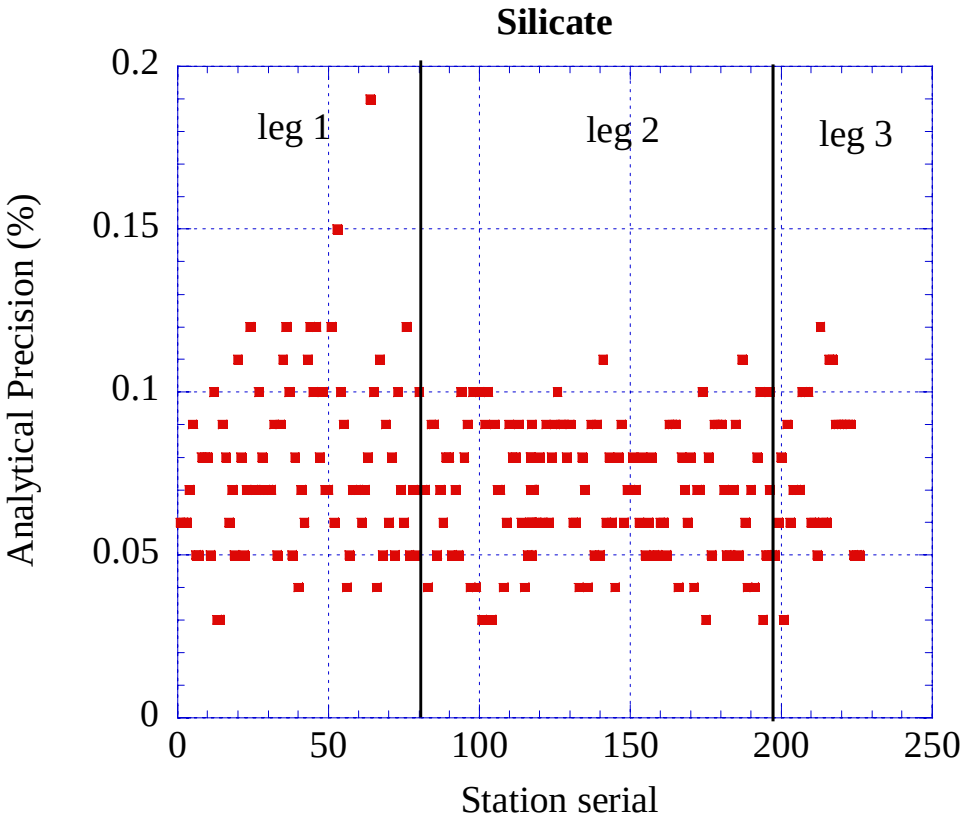


**Figure: 3.4.7 Time series of precision of silicate**

#### 3.4.4.2 Carryover

We can also summarize the magnitudes of carryover throughout the cruise. These are small enough within acceptable levels as shown in Table 3.4.7.

Table 3.4.7: Summary of carry over through out cruise.

| | Nitrate % | Phosphate % | Silicate % |
|---|---|---|---|
| Median | 0.21 | 0.20 | 0.24 |
| Mean | 0.21 | 0.20 | 0.23 |
| Maximum | 0.42 | 0.40 | 0.43 |
| Minimum | 0.01 | 0 | 0.05 |
| N | 277 | 277 | 277 |

### 3.4.5 Evaluation of Z-scores of RMNSs

Since we used RMNSs throughout the cruise, we can evaluate the trueness of our analysis in terms of Z-score of RMNSs.
Z-score for each analysis of RMNS is defined as follws;

$$Zpar = ABS((Cpar - Cnominal)/Ppar) \quad (1)$$

Where
Zpar is Z-score for an analysis
Cpar is obtained concentration of a RMNS for interested parameter, nitrate, phosphate or silicate.
Cnominal is assigned concentration of RMNS for interested parameter, nitrate, phosphate or silicate.
Ppar is analytical precision at the concentration of RMNS for interested parameter, nitrate, phosphate or silicate.

Averages of these Z-scores were obtained for three parameters, nitrate, phosphate and silicate based on Z-scores for 7 RMNSs used at each run and shown in figure 3.4.8. Means of Z-score based on the Z-score of three parameters were also obtained and shown in figure 3.4.9.
These Z-scores were less than 0.5 in general and indicating that our analyses were in excellent traceability throughout the cruise.

**Figure 3.4.8. Z-score of nitrate, silicate and phosphate**

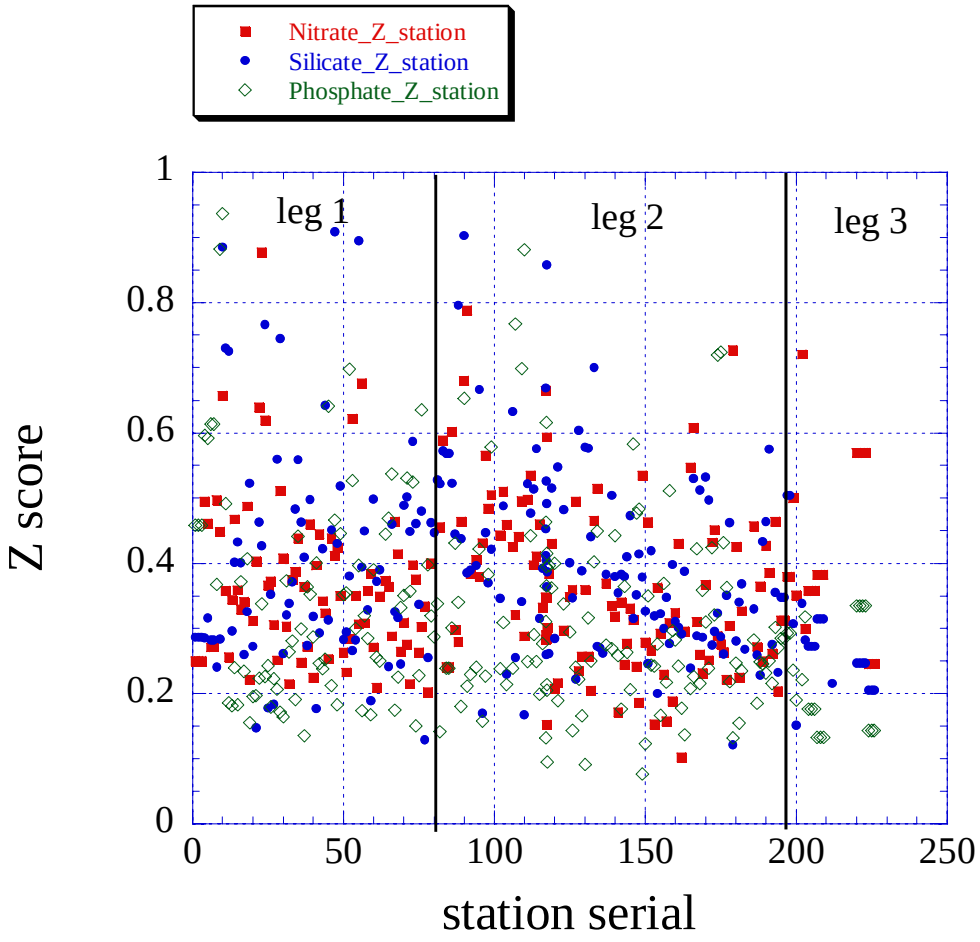

**Figure 3.4.9. Means of Z-score at the stations**

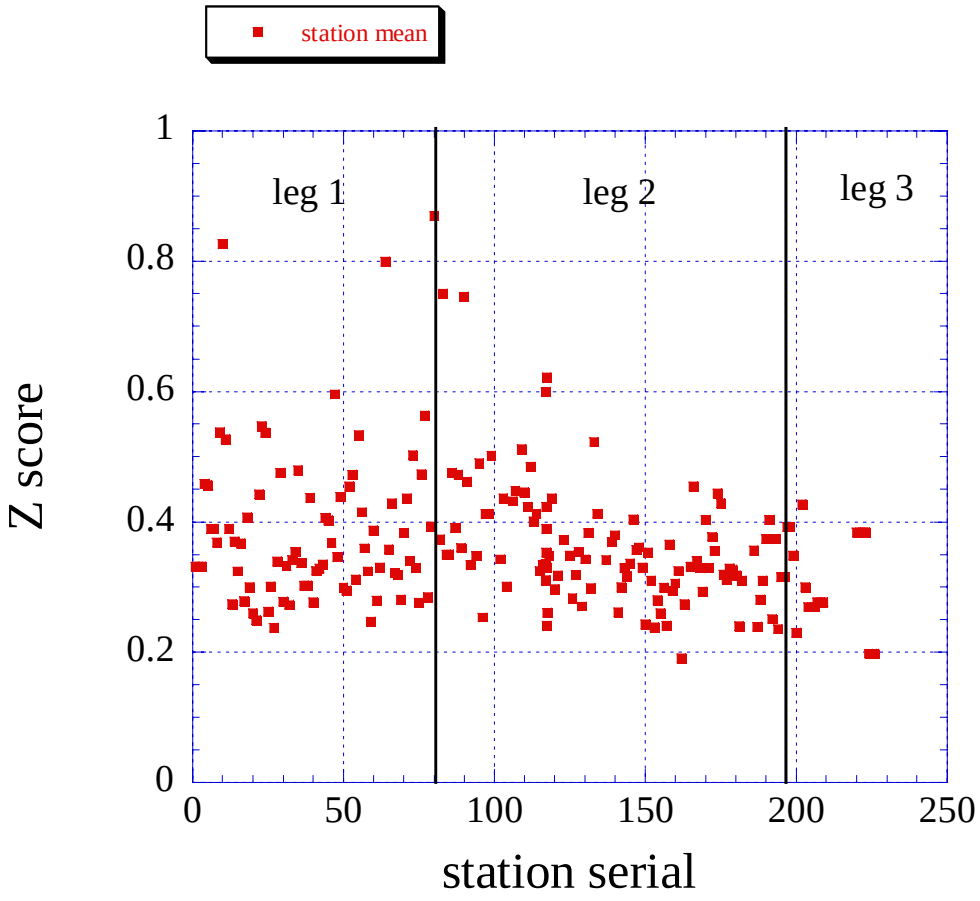

### 3.4.7 Problems/improvements occurred and solutions.

Nothing occurred during the cruise.

## Reference


Aminot, A. and Kerouel, R. 1991. Autoclaved seawater as a reference material for the determination of nitrate and phosphate in seawater. Anal. Chim. Acta, 248: 277-283.

Aminot, A. and Kirkwood, D.S. 1995. Report on the results of the fifth ICES intercomparison exercise for nutrients in sea water, ICES coop. Res. Rep. Ser., 213.

Aminot, A. and Kerouel, R. 1995. Reference material for nutrients in seawater: stability of nitrate, nitrite, ammonia and phosphate in autoclaved samples. Mar. Chem., 49: 221-232.

Aoyama M., and Joyce T.M. 1996, WHP property comparisons from crossing lines in North Pacific. In Abstracts, 1996 WOCE Pacific Workshop, Newport Beach, California.

Aoyama, M., Ota, H., Iwano, S., Kamiya, H., Kimura, M., Masuda, S., Nagai, N., Saito, K., Tubota, H. 2004. Reference material for nutrients in seawater in a seawater matrix, Mar. Chem., submitted.

Grasshoff, K., Ehrhardt, M., Kremling K. et al. 1983. Methods of seawater anylysis. 2nd rev. Weinheim: Verlag Chemie, Germany, West.

JAMSTEC, BEAGLE2003 DATA BOOK, 2005 in press

Joyce, T. and Corry, C. 1994. Requirements for WOCE hydrographic programmed data reporting. WHPO Publication, 90-1, Revision 2, WOCE Report No. 67/91.

Kirkwood, D.S. 1992. Stability of solutions of nutrient salts during storage. Mar. Chem., 38 : 151-164.

Kirkwood, D.S. Aminot, A. and Perttila, M. 1991. Report on the results of the ICES fourth intercomparison exercise for nutrients in sea water. ICES coop. Res. Rep. Ser., 174.

Mordy, C.W., Aoyama, M., Gordon, L.I., Johnson, G.C., Key, R.M., Ross, A.A., Jennings, J.C. and Wilson. J. 2000. Deep water comparison studies of the Pacific WOCE nutrient data set. Eos Trans-American Geophysical Union. 80 (supplement), OS43.

Murphy, J., and Riley, J.P. 1962. Analytica chim. Acta 27, 31-36.

Gouretski, V.V. and Jancke, K. 2001. Systematic errors as the cause for an apparent deep water property variability: global analysis of the WOCE and historical hydrographic data・REVIEW ARTICLE, Progress In Oceanography, 48: Issue 4, 337-402.

## 3.5 Chlorofluorocarbons

***Ken'ichi SASAKI[1)], Masahide WAKITA[1)], Katsunori SAGISHIMA[2)], Yuichi SONOYAMA[2)], Hideki YAMAMOTO[2)], Keisuke WATAKI[2)] and Masanori ENOKI[2)]***

1) Mutsu Institute for Oceanography, Japan Agency for Marine - Earth Science and Technology

2) Marine Works Japan Co. Ltd

### 3.5.1 Objectives

Chlorofluorocarbons (hereafter CFCs) are chemically and biologically stable gases that have been artificially synthesized since 1930's or later. The atmospheric CFCs can slightly dissolve in sea surface water and then spread into the ocean interior. Three chemical species of CFCs, namely CFC-11 (CCl3F), CFC-12 (CCl2F2) and CFC-113 (C2Cl3F3), can be used as transient tracers for decadal scale circulation of the ocean. We determined these CFCs concentrations in seawater on board.

### 3.5.2 Apparatuses

Dissolved CFCs are measured by an electron capture detector (ECD) – gas chromatograph attached with a purging & trapping system.

Table 3-5-1 Instruments

| | |
|---|---|
| Gas Chromatograph: | GC-14B (Shimadzu Ltd.) |
| Detector: | ECD-14 (Shimadzu Ltd) |
| Analytical Column: | |
| Pre-column: | Silica Plot capillary columns [i.d.: 0.53mm, length: 4m, thick: 0.25μm] |
| Main column: | Connected two capillary columns (Pola Bond-Q [i.d.: 0.53mm, length: 13 m, thick: 6.0μm] followed by Silica Plot [i. d.: 0.53mm, length: 30m, thick: 0.25μm]) |
| Purging & trapping: | Automated valve switching system. Trap column are 1/8" SUS packed column (Porapak T) |

### 3.5.3 Procedures

#### 3.5.3.1 Sampling

Seawater sub-samples for CFCs measurement were collected from 12 litter Niskin bottles to 300ml glass bottle. The bottle was filled by nitrogen gas before sampling. Two times of the bottle volumes of seawater sample were overflowed. The bottles filled by seawater sample were kept in water bathes roughly controlled on sample temperature. The CFCs concentrations were determined as soon as possible after sampling. These procedures were needed in order to minimize contamination from atmospheric CFCs.

Air samples for CFCs measurement were collected to 100ml glass cylinder attached magnesium perchlorate dryer tube at the navigation deck on R/V "MIRAI".

#### 3.5.3.2 Analysis

The CFCs analytical system is modified from the original design of Bullister and Weiss (1988). Constant volume of sample water (50ml) is taken into the purging and trapping system. Dissolved

CFCs are de-gassed by N2 gas purge and concentrated in a trap column cooled to -40 degree centigrade. The CFCs are desorbed by electrically heating the trap column to 140 degree centigrade within 1.5 minutes, and lead into the pre-column. CFCs and other compounds are roughly separated in the pre-column and the compounds having earlier retention time than CFC-113 are sent to main analytical column. And then the pre-column is flushed buck by counter flow of pure nitrogen gas (Back flush system). The back flush system prevents to enter any compounds that have higher retention time than CFC-113 into main analytical column and permits short time analysis. CFCs which are sent into main column are separated further and detected by an electron capture detector (ECD). Retention time of each CFC is around 1.5, 4.2 and 10.5 minutes for CFC-12, CFC-11 and CFC-113, respectively. The analytical conditions are listed in Table 3-5-2.

Table 3-5-2 Analytical conditions of dissolved CFCs in seawater.

| | |
|---|---|
| Temperature | |
| Analytical Column: | 95 deg-C |
| Detector (ECD): | 240 deg-C |
| Trap column: | -45 deg-C (at adsorbing) & 140 deg-C (at desorbing) |
| Mass flow rate of nitrogen gas (99.9999%) | |
| Carrier gas: | 20 ml/min |
| Detector make-up gas: | 17 ml/min |
| Back flush gas: | 20 ml/min |
| Sample purge gas: | 150 ml/min |

All nitrogen gases through one or two gas purifier tubes containing Molecular Sieve 13X (MS-13X). The gas purifiers are re-activated by heating to 260 deg C for 24 hr under nitrogen flow every constant interval.

Standard gas (Japan Fine Products co. ltd.)

| | | | |
|---|---|---|---|
| Leg1: CFC-11: 300 pptv; | CFC-12: 160 pptv; | CFC-113: 30 pptv; | Base gas: Nitrogen |
| Leg2: CFC-11: 300 pptv; | CFC-12: 160 pptv; | CFC-113: 50 pptv; | Base gas: Nitrogen |

### 3.5.3.3 Performances

The analytical precisions are estimated from replicate sample analyses. The replicate samples are collected from #31 and #25 of Niskin bottle (250 and 800 m depth, respectively) in Leg1 and Leg2. In Leg3, the replicate samples are collected from other Niskin bottles because many stations have too shallow depth to collect them from Niskin #31 and 25. The precisions were estimated by two methods. One (A) is arithmetic mean of absolute value of difference between two concentrations Another (B) is estimated by following equation, $s= (\Sigma (x_1-x_2)^2/(2n-1))^{0.5}$. Estimated precisions are listed in Table 3-5-3.

There are unknown peaks interfering analysis of CFC-113 in chromatograms for surface 200 m samples. Data flag “4” was given the CFC-113 data influenced by the interference substance. When CFC-113 peak was completely covered by the interference peak, CFC-113 was no data and data flag was “5”.

Table 3-5-3. Analytical precisions of dissolved CFCs in seawater.

| | | | | |
|---|---|---|---|---|
| Leg1 | | | | |
| Niskin #31 | | | | |
| | Mean (± SD) | (A) | (B) | n |
| CFC-11 | 2.742 (±0.575) | 0.015 (±0.016) | 0.016 | 73 |
| CFC-12 | 1.436 (±0.313) | 0.008 (±0.008) | 0.008 | 73 |
| CFC-113 | 0.100 (±0.037) | 0.005 (±0.006) | 0.006 | 73 |
| Niskin #25 | | | | |
| | Mean (± SD) | (A) | (B) | n |
| CFC-11 | 0.064 (±0.087) | 0.004 (±0.004) | 0.004 | 70 |
| CFC-12 | 0.032 (±0.043) | 0.003 (±0.002) | 0.002 | 70 |
| CFC-113 | 0.003 (±0.006) | 0.000 (±0.001) | 0.001 | 70 |
| Leg2 | | | | |
| Niskin #31 | | | | |
| | Mean (± SD) | (A) | (B) | n |
| CFC-11 | 2.407 (±0.428) | 0.008 (±0.010) | 0.009 | 105 |
| CFC-12 | 1.320 (±0.242) | 0.006 (±0.007) | 0.006 | 105 |
| CFC-113 | 0.083 (±0.046) | 0.008 (±0.013) | 0.011 | 103 |
| Niskin #25 | | | | |
| | Mean (± SD) | (A) | (B) | n |
| CFC-11 | 0.573 (±0.144) | 0.005 (±0.009) | 0.007 | 103 |
| CFC-12 | 0.276 (±0.070) | 0.004 (±0.005) | 0.005 | 101 |
| CFC-113 | 0.022 (±0.009) | 0.004 (±0.004) | 0.004 | 103 |
| Leg3 | | | | |
| | Mean (± SD) | (A) | (B) | n |
| CFC-11 | 2.013 (±0.811) | 0.008 (±0.008) | 0.008 | 37 |
| CFC-12 | 1.080 (±0.447) | 0.005 (±0.005) | 0.005 | 37 |
| CFC-113 | 0.093 (±0.090) | 0.008 (±0.010) | 0.009 | 20 |

### 3.5.4 Preliminary Results

Penetration depth of CFC-12 is deepens from eastern to western part of this transect. Maximum concentration could be found 250 – 700 m depth. We found the maximum concentration to be smaller on western part than that on eastern part. That would indicate difference of ventilation age of intermediate water between western and eastern North Pacific. We detected significant increase in CFCs around 250 – 700 m in last two decades (Fig 3-5-1). Shape of CFC-11 distribution is similar to that of CFC-12. We found significant maximum of CFC-113 profiles around 500m depth. The feature has been also found in MR05-02 cruise (WHP P10 revisit observation). The result would give information about formation rate of North Pacific Intermediate water (figures not shown here).

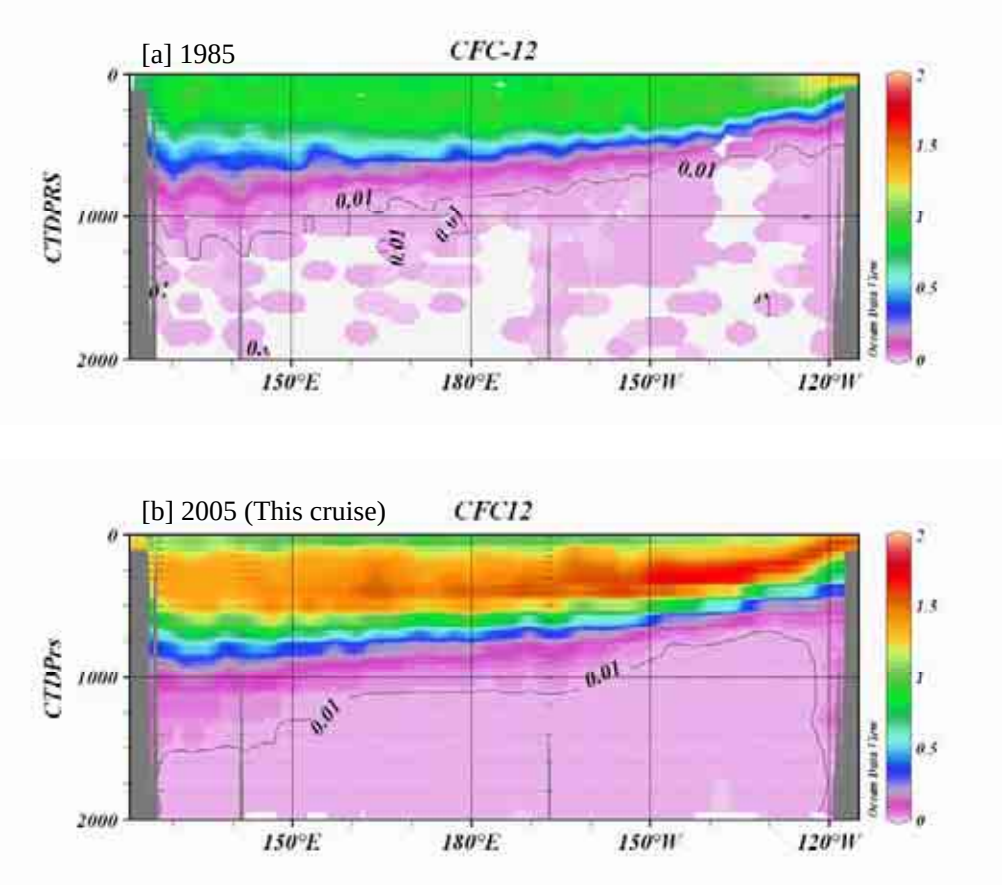


Fig. 3-5-1 Comparison between CFC-12 distributions in 1985 (WOCE P3 data, [a]) and in 2005 (this cruise, [b]) for shallower depth (<2000 m). CFCs concentrations were less than detection limit for deeper layer than 2000 m depth and not shown in the figures. Contour line of 0.01 pmol/kg are given by a solid line. Sampling depths are mark with black small dots.

### 3.5.5 Data archive

All data will be submitted to JAMSTEC Data Management office (DMO) and under its control.

### 3.5.6 References

Bullister, J.L and Weiss R.F. 1988. Determination of CCl3F and CCl2F2 in seawater and air. Deep Sea Research, 35, 839-853.

## 3.6 Carbon Items

***Akihiko Murata (JAMSTEC)***
***Fuyuki Shibata (MWJ)***
***Mikio Kitada (MWJ)***
***Minoru Kamata (MWJ)***
***Taeko Ohama (MWJ)***
***Masaki Moro (MWJ)***
***Yoshiko Ishikawa (MWJ)***

### 3.6.1 Objectives

Concentrations of $CO_2$ in the atmosphere are now increasing at a rate of 1.5 ppmv $y^{-1}$ owing to human activities such as burning of fossil fuels, deforestation, and cement production. It is an urgent task to estimate the absorption capacity of the oceans against the increased atmospheric $CO_2$ as accurately as possible, and to clarify the mechanism of the $CO_2$ absorption, because the magnitude of the anticipated global warming depends on the levels of $CO_2$ in the atmosphere, and because the ocean currently absorbs 1/3 of the 6 Gt of carbon emitted into the atmosphere each year by human activities.

In this cruise, we aimed at quantifying how much anthropogenic $CO_2$ is absorbed in the North Pacific Ocean, especially in North Pacific Intermediate Water. For the purpose, we measured $CO_2$-system parameters such as dissolved inorganic carbon ($C_T$), total alkalinity ($A_T$) and pH.

### 3.6.2 Apparatus

(1) $C_T$

Measurements of $C_T$ was made with two total $CO_2$ measuring systems (systems A and B; Nippon ANS, Inc.), which are slightly different from each other. The systems comprise of a sea water dispensing system, a $CO_2$ extraction system and a coulometer (Model 5012, UIC Inc.).

The seawater dispensing system has an auto-sampler (6 ports), which takes seawater into a 300 ml borosilicate glass bottle and dispenses the seawater to a pipette of nominal 20 ml (system A) and 26ml (system B) volume PC control. The pipette was kept at 20 °C by a water jacket, in which water from a water bath set at 20 °C is circulated.

$CO_2$ dissolved in a seawater sample is extracted in a stripping chamber of the $CO_2$ extraction system by adding phosphoric acid (10 % v/v). The stripping chamber is made approx. 25 cm long and has a fine frit at the bottom. To degas $CO_2$ as quickly as possible, a heating wire kept at 40 °C is rolled from the bottom to a 1/3 height of the stripping chamber. The acid is added to the stripping chamber from the bottom of the chamber by pressurizing an acid bottle for a given time to push out the right amount of acid. The pressurizing is made with nitrogen gas (99.9999 %). After the acid is transferred to the stripping chamber, a seawater sample kept in a pipette is introduced to the stripping chamber by the same method as that for adding an acid. The seawater reacted with phosphoric acid is stripped of $CO_2$ by bubbling the nitrogen gas through a fine frit at the bottom of the stripping chamber. The $CO_2$ stripped in the chamber is carried by the nitrogen gas (flow rates of 140ml $min^{-1}$ for systems A and B, respectively) to the coulometer through a dehydrating module. For system A, the module consists of two electric dehumidifiers (kept at 1 – 2 °C) and a chemical desiccant ($Mg(ClO_4)_2$). For system B, it consists of three electric dehumidifiers with a chemical desiccant.

The measurement sequence such as system blank (phosphoric acid blank), 2 % $CO_2$ gas in a

nitrogen base, and seawater samples (6) was programmed to repeat. The measurement of 2 % $CO_2$ gas was made to monitor response of coulometer solutions (from UIC, Inc.).

(2) $A_T$

Measurement of $A_T$ was made by using a titration system (Nippon ANS, Inc.). The system comprise of a water dispensing unit, an auto-burette (Metrohm), a pH meter (Thermo Electron), and a pair of electrodes (Reference electrode: REF201 (Rodiometer), Glass pH Electrode: pHG201-7 (Radiometer)), or combination electrodes (ROSS 8102BN: Thermo Electron Corporation), which is automatically controlled by a PC.

A seawater of approx. 40 ml is transferred from a sample bottle (brosilicate glass bottle; 130 ml) into a water-jacketed (25 °C), and is introduced into a water-jacketed (25 °C) titration cell. The seawaters are titrated by a acid titrant, which was 0.05 M HCl in 0.65 M NaCl in this cruise.

Calibration of the acid titrant was made by measuring $A_T$ of 5 solutions of $Na_2CO_3$ in 0.7 M NaCl solutions. The computed $A_T$s were approx. 0, 100, 1000, 2000 and 2500 μmol $kg^{-1}$. The measured values of $A_T$ (calculated by assuming 0.05 M) should be a linear function of the $A_T$ contributed by the $Na_2CO_3$. The line was fitted by the method of least squares. Theoretically, the slope should be unity. If the measured slope is not equal to one, the acid normality should be adjusted by dividing initial normality by the slope, and the whole set of calculations is repeated until the slope = 1

Calculation of $A_T$ was made based on a modified Gran approach.

(3) pH

Measurement of pH was made by a pH measuring system (Nippon ANS, Inc.), which adopts a method for the spectrophotometric determination. The system comprises of a water dispensing unit and a spectrophotometer (Carry 50 Scan, Varian). For an indicator, *m*-cresol purple (2 mM) was used.

Seawater is transferred from borosilicate glass bottle (300 ml) to a sample cell in the spectrophotometer. The length and volume of the cell are 8 cm and 13 ml, respectively, and the sample cell is kept at 25.00 ± 0.05 °C in a thermostated compartment. First, absorbances of the seawater only are measured at three wavelengths (730, 578 and 434 nm). Then the indicator is injected and circulated for about 3 or 3.5 minutes. to mix the indicator and seawater sufficiently. After the pump is stopped, the absorbances of seawater + indicator is measured at the same wavelengths. The pH was calculated based on the following equation (Clayton and Byrne, 1993):

$$pH' = pK_2 + \log\left(\frac{A_1 / A_2 - 0.00691}{2.2220 - 0.1331(A_1 / A_2)}\right)$$

where $A_1$ and $A_2$ indicate absorbances at 578 and 434 nm, respectively, and $pK_2$ is calculated as a function of water temperature and salinity.

**Reference**

Clayton T.D. & R.H. Byrne (1993) Spectrophotometric seawater pH measurements: total hydrogen ion concentrtaion scale calibration of m-cresol purple and at-sea results. Deep-Sea Research 40, 2115-2129.

### 3.6.3 Performances

(1) $C_T$

The two systems had worked well during the leg without a major malfunction. Replicate analysis was made for 3 – 4 pair samples at each water column. The repeatabilities for systems A and B during leg 1were estimated to be 0.9 ± 0.8 (n = 80 pairs) and 1.5 ± 1.4 (n = 46 pairs) μmol $kg^{-1}$, respectively. The combined result was 1.1 ± 1.1 μmol $kg^{-1}$ (n = 126 pairs).

During leg 2, the repeatabilities for systems A and B were estimated to be 1.0 ± 0.9 (n = 123 pairs) and 1.2 ± 1.1 (n = 72 pairs) μmol $kg^{-1}$, respectively. The combined result was 1.0 ± 1.0 μmol $kg^{-1}$ (n = 195 pairs).

During leg 3, only the system A was used for measurement of $C_T$. The repeatability was estimated to be 0.5 ± 0.5 (n = 21 pairs).

(2) $A_T$

The systems conducted a high speed titration (5 - 6 min.) compared to systems used in previous studies. A few replicate samples were taken on every station. The repeatability was estimated to be 2.1 ± 1.9 μmol $kg^{-1}$ (n = 124 pairs) during leg 1. It became 2.0 ± 1.8 (n = 204) and 2.2 ± 0.7 (n = 150) duirng legs 2 and 3, respectively.

(3) pH

The system had worked well with no considerable troubles. The average of absolute differences between replicate samples was 0.0007 pH unit (n = 166 pairs) during leg 1. It became 0.0007 and 0.0009 during legs 2 and 3, respectively.

### 3.6.4 Results

Cross sections of $C_T$, $A_T$ and pH along the observation line in legs 1, 2 and 3 are illustrated in Figs. 1, 2 and 3, respectively.

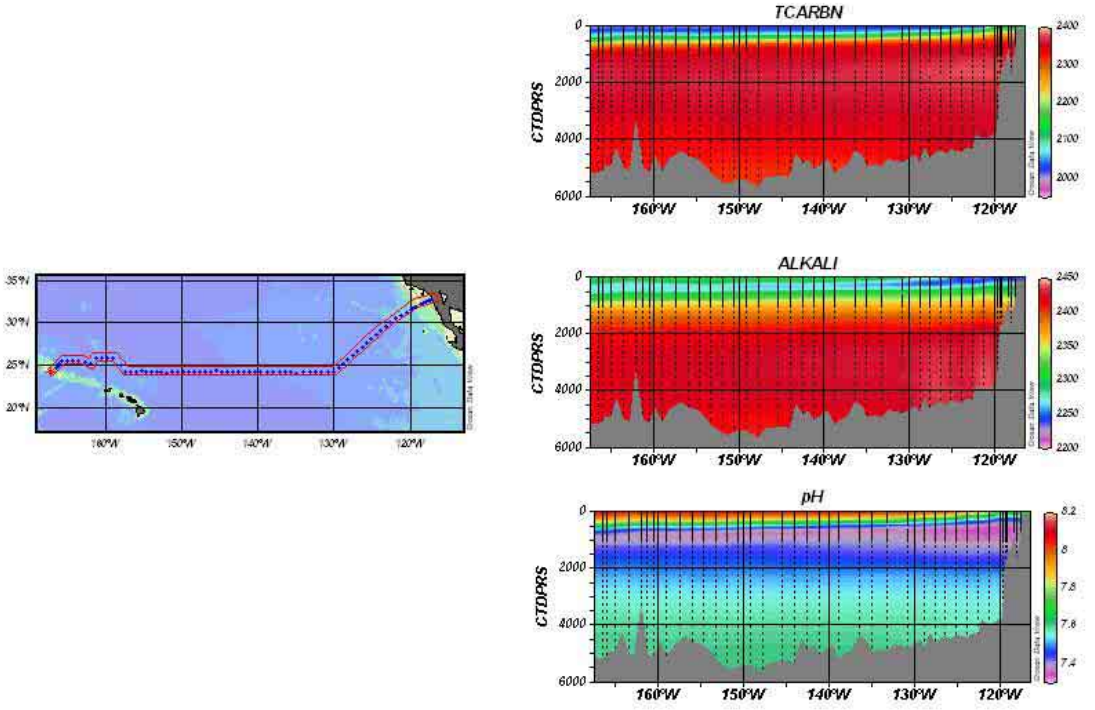


**Fig. 1. Distributions of $C_T$, $A_T$ and pH along the observation line in leg 1.**

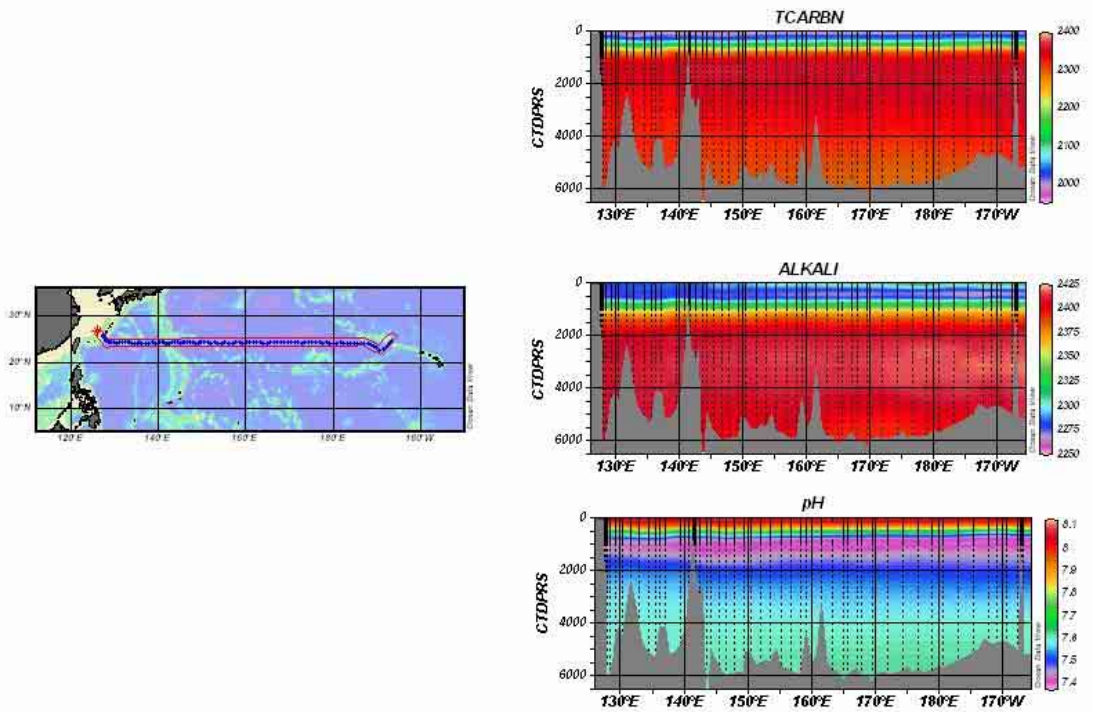


**Fig. 2. Distributions of $C_T$, $A_T$ and pH along the observation line in leg 2.**

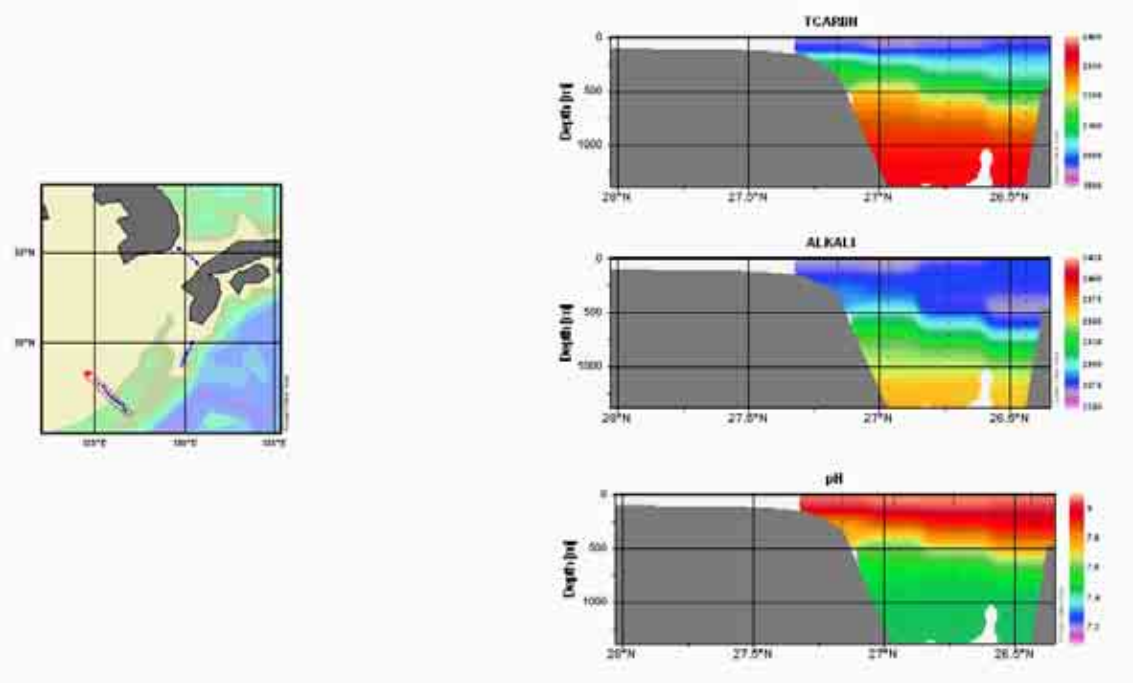


**Fig. 3a. Distributions of $C_T$, $A_T$ and pH along the observation line in leg 3 (East China Sea).**

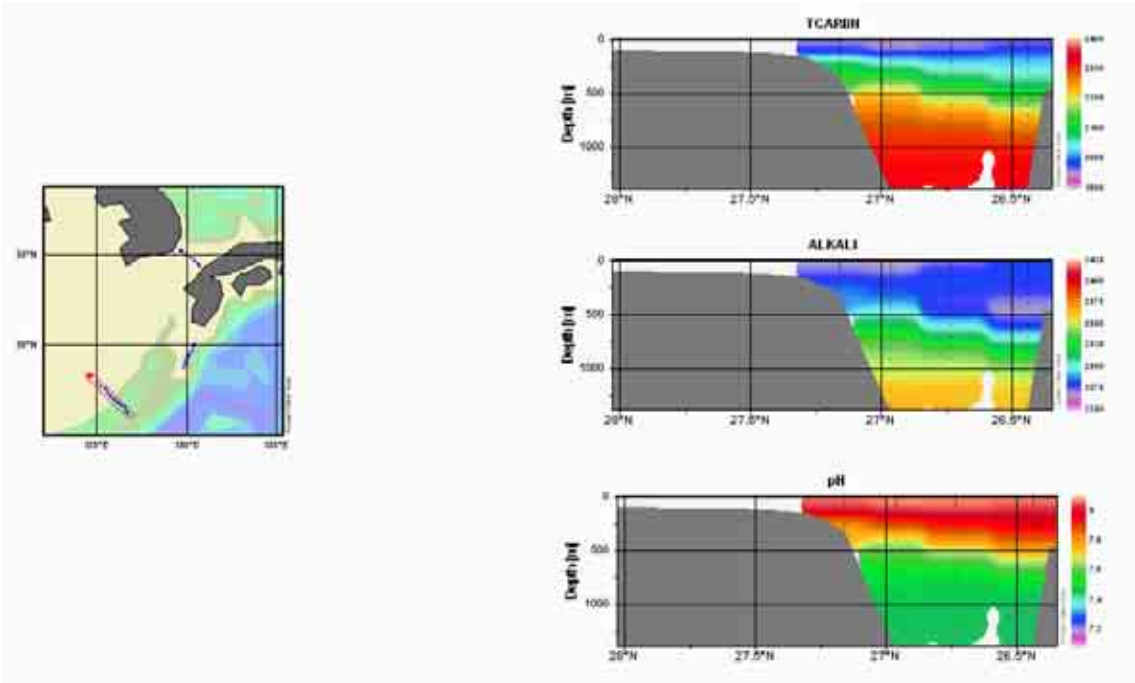


**Fig. 3b. Distributions of $C_T$, $A_T$ and pH along the observation line in leg 3 (Tokara Strait).**

## 3.7 Samples taken for other chemical measurement

### 3.7.1 Carbon-14, carbon-13

30-Jan.-2006

#### 3.7.1.1 Personnel

Yuichiro KUMAMOTO

Japan Agency for Marine Earth Science and Technology

#### 3.7.1.2 Objective

In order to investigate water circulation and carbon cycle in the North Pacific, seawater for carbon-14 (radiocarbon) and carbon-13 (stable carbon isotope) of total dissolved inorganic carbon (TDIC) was collected by hydrocasts from surface to bottom during MR05-05 cruise.

#### 3.7.1.3 Sample collection

The sampling stations and number of samples are summarized in Table 3.7.1-1. All samples for carbon isotope ratios were collected at 23 stations using 12 liter Niskin-X bottles. The seawater sample was siphoned into a 250 $cm^3$ glass bottle with enough seawater to fill the glass bottle three times. Immediately after sampling, 10 $cm^3$ of seawater was removed from the bottle and poisoned by 0.1 $cm^3$ µl of saturated $HgCl_2$ solution. Then the bottle was sealed with a glass stopper with Apiezon grease M and stored in a cool and dark space on board.

#### 3.7.1.4 Sample preparation and measurements

In our laboratory, dissolved inorganic carbon in the seawater samples will be stripped cryogenically and split into three aliquots: radiocarbon measurement (about 200 µmol), carbon-13 measurement (about 100 µmol), and archive (about 200 µmol). The extracted $CO_2$ gas for radiocarbon will be then converted to graphite catalytically on iron powder with pure hydrogen gas. The carbon-13 of the extracted $CO_2$ gas will be measured using Finnigan MAT252 mass spectrometer. The carbon-14 in the graphite sample will be measured by Accelerator Mass Spectrometry (AMS).

Table 3.7.1-1. The sampling stations and number of samples for carbon isotope ratios.

| Station | No. samples | No. replicate samples | Max. sampling pressure /db |
|---|---|---|---|
| P03-024 | 28 | 2 | 4007.5 |
| P03-038 | 30 | 2 | 4403.0 |
| P03-051 | 31 | 2 | 4820.6 |
| P03-X17 | 32 | 2 | 4927.2 |
| P03-074 | 33 | 2 | 5066.1 |

| | | | |
|---|---|---|---|
| P03-090 | 35 | 2 | 5666.1 |
| P03-X16 | 34 | 2 | 5531.8 |
| P03-114 | 31 | 2 | 4602.3 |
| P03-126 | 33 | 2 | 5161.0 |
| P03-138 | 32 | 2 | 4956.0 |
| P03-173 | 31 | 2 | 4742.4 |
| P03-189 | 34 | 2 | 5431.3 |
| P03-X14 | 35 | 2 | 5836.6 |
| P03-211 | 36 | 2 | 5827.9 |
| P03-223 | 36 | 2 | 6242.2 |
| P03-233 | 36 | 2 | 6076.8 |
| P03-247 | 35 | 2 | 5602.4 |
| P03-259 | 35 | 2 | 5675.4 |
| P03-X10 | 36 | 2 | 5865.6 |
| P03-293 | 36 | 2 | 6505.3 |
| P03-X09 | 29 | 2 | 4165.6 |
| P03-341 | 31 | 2 | 4596.0 |
| P03-376 | 21 | 1 | 1911.4 |
| Total | 750 | 45 | |

## 3.7.2 Radionuclides

*draft as of 24 Jan., 2006*

***Michio Aoyama (Meteorological Research Institute / Japan Meteorological Agency, Principal Investigator)***

### 3.7.2.1 Objectives

1) Study more about present distribution of $^{137}$Cs in the subtropical gyre originated mainly from atmospheric nuclear weapons tests conducted in the 1960s.
2) Provide detailed artificial radionuclides database for general circulation model validation

### 3.7.2.2 Target radionuclides

Main target radionuclides are $^{137}$Cs, and Pu..

### 3.7.2.3 Sampling procedures

Sampling of seawater samples of radionuclides in water column was done followed that all parameters. Some additional bottles were available by chance, then, the samples volumes for water column varied from 6 liter to 20 liter. Samples were drawn into 10 or 20 liter cubitainers from the

Niskin bottles. Concentrated Nitric Acid was added to the samples to keep pH1.6.
Surface water samples were drawn through intake pump several meters below the surface. Seawater of 80 liter were collected for $^{137}$Cs and Pu.

**3.7.2.4 Samples accomplished during the cruise**

A total of 20 samples were collected for surface sample.
At the 20 stations, a total of 290 samples were collected for water column.

**3.7.2.5 Problem occurred and solutions.**

No problem occurred.

**3.7.2.6 Sampling summary**

| station # | | Lat. | | | Long. | | | Number of layers |
|---|---|---|---|---|---|---|---|---|
| P03 | 22 | 31 | 14.1 | N | 120 | 33.1 | W | 14 |
| P03 | 36 | 27 | 35.8 | N | 125 | 45.7 | W | 14 |
| P03 | 50 | 24 | 15.4 | N | 130 | 1.9 | W | 14 |
| P03 | 73 | 24 | 14.1 | N | 140 | 21.4 | W | 16 |
| P03 | 88 | 24 | 13.9 | N | 146 | 56 | W | 16 |
| P03 | 112 | 24 | 17 | N | 155 | 16.6 | W | 15 |
| P03 | 124 | 24 | 28.1 | N | 159 | 46.8 | W | 14 |
| P03 | 136 | 25 | 30.5 | N | 164 | 18.5 | W | 15 |
| P03 | 171 | 23 | 4.5 | N | 170 | 2 | W | 15 |
| P03 | 187 | 24 | 14.1 | N | 176 | 1.4 | W | 16 |
| P03 | 197 | 24 | 14.2 | N | 179 | 59.3 | W | 17 |
| P03 | 209 | 24 | 15 | N | 175 | 10 | E | 17 |
| P03 | 221 | 24 | 15.2 | N | 170 | 21.1 | E | 18 |
| P03 | 231 | 24 | 14.9 | N | 166 | 28.6 | E | 18 |
| P03 | 245 | 24 | 16 | N | 160 | 50.4 | E | 16 |
| P03 | 257 | 24 | 14.3 | N | 156 | 4.2 | E | 17 |
| P03 | 273 | 24 | 15.9 | N | 149 | 39.8 | E | 16 |
| P03 | 295 | 24 | 15 | N | 143 | 13.7 | E | 15 |
| P03 | 318 | 24 | 14.7 | N | 137 | 48.2 | E | 15 |
| P03 | 339 | 24 | 15.7 | N | 130 | 59.9 | E | 12 |

## 3.7.3 Nitrous oxide ($N_2O$) and Methane ($CH_4$)

### 1. Personnel

Osamu YOSHIDA,[1,2] Narin BOONTANON,[3] Ayako FUJII,[1] and Naohiro YOSHIDA[1,2,3,4]

[1]Interdisciplinary Graduate School of Science and Engineering, Tokyo Institute of Technology

[2]Japan Society for the Promotion of Science

[3]Solution Oriented Research for Science and Technology, Japan Science and Technology Agency

[4]Frontier Collaborative Research Center, Tokyo Institute of Technology

### 2. Sampling elements

All sampling elements of Tokyo Institute of Technology group (Yoshida's Lab) at hydrographic stations are listed below.

**Table 1**. Parameters and hydrographic station number for samples collection.

| Parameters | Hydrographic station Numbers (Indicated by *R/V Mirai*) |
|---|---|
| $N_2O$ air-sea flux | 3 times a day |
| Dissolved $N_2O$ (concentration and isotope ratios) and $CH_4$ (concentration) | 3, 28, 42, 56, 69, 77, 94, 106, 118, 134, 163, 183, 195, 205, 217, 227, 239, 251, 263, 279, 291, 314, 333, 349, 365, 372, 382, 389, 390, 396, 402, 408, TS7, TS4, TS1 |
| Dissolved $CH_4$ (carbon isotope ratios) | 3, 28, 42, 69, 94, 118, 163, 195, 217, 239, 263, 291, 333, 365, 372, 382, 389 390, 396, 402, 408, TS7, TS4, TS1 |
| Dissolved $CH_4$ (hydrogen isotope ratios) *shallower than 500 m | 3, 28, 42, 69, 94, 118, 163, 195, 217, 239, 263, 291, 333 |
| Air samples for air-sea flux of $CH_4$ | 28, 42, 69, 94, 118, 163, 195, 217, 239, 263, 291, 333, 382, 402, TS4 |
| POM (isotope ratios) | 3, 42, 71, 96, 120, 163, 195, 219, 241, 265, 291, 333 |
| Chlorophyll *a* *at 150, 200, and 250 m | 71, 120 |
| $NO_3^-$ (isotope ratios) | 28, 56, 77, 106, 134, 183, 205, 227, 251, 279, 314, 349 |
| On-board incubation experiments ($N_2O$) | 3, 28, 42, 71, 96, 120, 134, 183, 205, 227, 251, 279, 314, 349 |
| On-board incubation experiments ($CH_4$) | 3, 28, 42, 71, 96 |
| On-board incubation experiments with tracers | 3, 28, 42, 96 |

### 3. Nitrous oxide and related substances

Production, consumptions and air-sea flux of $N_2O$ in the Central North Pacific region

Narin BOONTANON, Ayako FUJII, Osamu YOSHIDA and Naohiro YOSHIDA

Tokyo Institute of Technology Team (Yoshida's Lab)

*3.1. Introduction*

Recently considerable attention has been focused on emission of biogenic trace gases from ecosystems, since the gases contain a significant amount of greenhouse gases such as carbon dioxide ($CO_2$), methane ($CH_4$) and nitrous oxide ($N_2O$). Isotopic signatures of these gases are well recognized to provide constraints for relative source strength and information on reaction dynamics concerning their formation and biological pathways. Nitrous oxide is a very effective heat-trapping gas in the atmosphere because it absorbs outgoing radiant heat in infrared wavelengths that are not captured by the other major greenhouse gases, such as water vapor and $CO_2$. The annual input of $N_2O$ into the atmosphere is

estimated to be about 16.4 Tg $N_2O$-N $yr^{-1}$, and the oceans are believed to contribute more than 17% of the total annual input (IPCC, 2001).

$N_2O$ is produced by the biological processes of nitrification and denitrification (Dore *et al.*, 1998; Knowles *et al.*, 1981; Rysgaard *et al.*, 1993; Svensson, 1998; Ueda *et al.*, 1993). Depending on the redox conditions, $N_2O$ is produced from inorganic nitrogenous compounds ($NH_3$ or $NO_3^-$), with subsequently different isotopic fractionation factors. The isotopic signatures of $N_2O$ confer constraints on the relative source strength, and the reaction dynamics of $N_2O$ biological production pathways are currently under investigation. Furthermore, isotopomers of $N_2O$ contain more easily interpretable biogeochemical information as to their sources than obtained from conventional bulk $^{15}N$ and $^{18}O$ measurements (Yoshida and Toyoda, 2000).

The Pacific Ocean is the largest of the world's five oceans (followed by the Atlantic Ocean, Indian Ocean, Southern Ocean, and Arctic Ocean) (CIA, www) and expected to be important for the biogeochemical and biological cycles. Thus, the study of $N_2O$ production and nutrients dynamics are very important to examine the origins of $N_2O$ in seawater and to estimate the inventory of $N_2O$ from this region with respect to the troposphere.

### *3.2. Materials and methods*

Samples were collected in the framework of MR05-05 research expedition on the *R/V Mirai* from October 31, 2005 to January 30, 2006. The purpose of the expedition was to study on the heat and material transports and their variability of the general ocean circulation and a study on chemical environment and its changes in the ocean. The production and consumption of dissolved $N_2O$ in Central North Pacific region, East China Sea and Tsushima Strait ecosystems was investigated by collecting seawater samples (35 stations), particulate organic matter (POM) (12 stations), samples for nitrate isotope ratios (12 stations), on-board incubation experiments (12 stations) and on-board incubation experiments with tracer (4 stations) as shown in Table 1. The air-sea fluxes measurements were also done along the expedition (3 times a day).

#### *3.2.1 Air-sea flux measurement*

Concentration of $N_2O$ at the surface water and ambient air were conducted using Purge & Trap gas extraction manifold connected to an electron capture detector (ECD) gas chromatograph (Boontanon, 1996). The collections were done three times a day during the expedition.

#### *3.2.2 $N_2O$ concentration and isotope analyses*

Water samplings were carried out at the indicated depths using a CTD water sampler (SBE 32 36x12-L Carousel Water Sampler). For $N_2O$ analyses, water samples were introduced into 225-ml glass vial and then sterilized with mercury chloride (1 ml saturated $HgCl_2$ solution per vial). The vial was then sealed with a butyl-rubber septum and an aluminum cap, taking care to avoid bubble formation, and then brought back to the laboratory and stored at 4˚C until the analyses were conducted. Dissolved $N_2O$ concentrations and its isotopic compositions will be measured by using GC/IRMS.

#### *3.2.3 Isotope ratios of POM*

POM for isotope measurements was collected by filtrated seawater samples (at least 2 L) at the depth 150, 200 and 250 m after passing through the plankton net to prevent the contaminations of the zooplankton and phytoplankton. Collected samples on the filter were treated with 0.05N hydrochloric

acid, washed with Milli-Q water and then dried at 60˚C for 48 hrs. Isotope ratios of POM will be measured by using EA/IRMS.

*3.2.4 Isotope ratios of $NO_3^-$*

For isotopic measurement of $NO_3^-$, water samples were collected in the same depth as $N_2O$ concentration and isotope analyses. The water samples were filtrated using pre-combustion GF/F filter then collected in 100 ml polypropylene bottles and kept frozen until isotopic analyses. Isotope ratios of $NO_3^-$ will be measured by using the chemical reduction method (Boontanon and Yoshida, 2004) and GC/IRMS.

*3.2.5 On-board incubation experiment*

The water samples for on-board incubation experiments were collected at 150, 200 and 250m depth which expected for the highest $N_2O$ production (related to the maximum chl. *a* concentration layer, Campbell *et al*., 1997). Two kinds of experiment were done by using filtrated and not filtrated seawater to compare the difference of $N_2O$ production potential. Water samples were introduced into 225-ml glass vial by passing and not passing through 0.7 μm GF/F filter and then sealed with a butyl-rubber septum and an aluminum cap. After 48 and 96 hrs at *in situ* temperature, the sample was then sterilized with mercury chloride and stored at 4˚C until the analyses were conducted. Dissolved $N_2O$ concentrations and its isotopic compositions will be measured by using GC/IRMS.

*3.2.6 On-board incubation experiment with tracers*

The water samples for on-board incubation experiments (tracer studies) were collected at surface and oxycline (within euphotic zone), which also expected for the highest $N_2O$ production (Cohen and Gordon, 1997).

Three kinds of experiment were done with addition $^{15}N\text{-}NaNO_2^-$ or $^{15}N\text{-}NaNO_3^-$ as tracers and no addition any tracer (natural seawater, as a control) to estimate $N_2O$ production rate and to reveal the pathway of $N_2O$ production. Water samples were introduced into 225-ml glass vial and sealed with a butyl-rubber septum and an aluminum cap, and then $^{15}N\text{-}NaNO_2^-$ or $^{15}N\text{-}NaNO_3^-$ were injected into the vials for tracer experiments. After 48 and 96 hrs at *in situ* temperature, the sample was then sterilized with mercury chloride and stored at 4˚C until the analyses were conducted. Dissolved $N_2O$ concentrations and its isotopic compositions will be measured by using GC/IRMS.

*3.3 Expected results*

In the surface layer, $N_2O$ concentration of water affects the sea-air flux directly (Dore *et al.*, 1998). However the pathway of $N_2O$ production in surface layer is also still unresolved. Usually $N_2O$ production in surface layer is predominantly carried out nitrification, but denitrification also occurs in the case of oxygen concentration is low (Maribeb and Laura, 2004). Moreover it was reported that $N_2O$ production by nitrification has photoinhibition (Olson, 1981). Therefore, this study is expected to reveal the pathway of $N_2O$ production and $N_2O$ production rate in the surface layer (especially euphotic zone).

In deeper layer during the settling particles or fecal pellets which may produce from phytoplankton or zooplankton, either directly or indirectly. In such pattern, $N_2O$ could be produced through *in situ* biological processes of settling particles in subsurface layer and the maximum concentrations could be observed. Consequently, the isotopic measurement of these gases becomes a useful parameter for determining the origin and the production pathway of $N_2O$ under investigation.

Additionally, the Pacific Ocean expected to be the large site of $N_2O$ source to the troposphere. And at least three factors could control the $N_2O$ concentration and its isotopic compositions in these study areas are:

(i) The isotopic compositions of dissolved $N_2O$ were governed through the gas exchange with the atmospheric $N_2O$ in the surface layer.

(ii) The $N_2O$ production in subsurface layer through *in situ* biological processes and it should related to the isotopic compositions of POM and $NO_3^-$.

(iii) The well mixing of $N_2O$ in the deeper part may occur due to the transportation from upper layer or the transportation of $N_2O$ from the other area by the occurrence of ocean current.

(iv) The isotopic and isotopomeric compositions of surface and oxycline $N_2O$ (tracer studies) could provide an information of $N_2O$ production pathway especially in euphotic zone, and could be estimate for those $N_2O$ production rate.

Furthermore, the relationship between the POM, $N_2O$ production as well as $N_2O$ isotope ratios and oxygen concentration in the surrounding water may be critically important for $N_2O$ metabolism through nitrification, denitrification and coupling of nitrification-denitrification, because the $O_2$ gradient within the particle is likely to be regulated by the size of POM. Thus, the incubation experiment may provide information of $N_2O$ production/consumptions in this ocean region.

*3.4 References*


Boontanon, N., 1996. Nitrous oxide gas in Outer Songkla Lake by gas chromatography/Purge & Trap technique. M.Sc. Thesis. Prince of Songkla Univ., Songkla, Thailand.

Boontanon, N. and Yoshida, N., 2004. Nitrogen and oxygen isotopic determination of nitrate by chemical reduction. *In* Proceedings of 2nd International Symposium on Isotopomers, Stresa, Italy, pp.208-211.

Campbell, L., Hongbin, L., Hector, A.N. and Vaulot, D., 1997. Annual variability of phytoplankton and bacteria in the subtropical North Pacific Ocean at station ALOHA during the 1991-1994 ENSO event. *Deep-Sea Research I* **44**, 167-192.

Cohen, Y. and Gordon, L.I., 1978. Nitrous oxide in the oxygen minimum of the eastern tropical North Pacific: evidence for its consumption during denitrification and possible mechanisms for its production. Deep Sea Research **25**, 509-524

Dore, J.E., Popp, B.N., Karl, D.M. and Sansone, F.J., 1998. A large source of atmospheric nitrous oxide from subtropical North Pacific surface water. *Nature* **396**, 63-66.

Intergovernmental Panel on Climate Change 2001. *Climate Change 2001: The Scientific Basis. Contribution of Working Group I to the Third Assessment Report of the Intergovernmental Panel on Climate Change (IPCC).* Cambridge Univ. Press, New York.

Knowles, R., Lean, D.R.S. and Chan, Y.K., 1981. Nitrous oxide concentrations in lakes: variations with depth and time. *Limnology and Oceanography* **26**, 855-866.

Maribeb, C.-G. and Laura, F., 2004. $N_2O$ cycling at the core of the oxygen minimum zone off northern Chile. Marine Ecology Progress Series **280**, 1-11.

Olson, R.J., 1981. Differential photoinhibition of marine nitrifying bacteria: a possible mechanism for the formation of the primary nitrite maximum. Journal of Marine Research **39:** 227-238.

Rysgaard, S., Risgaard-Petersen, N., Nielsen, L.P. and Revsbech, N.P., 1993. Nitrification and denitrification in lake and estuarine sediments measured by the $^{15}N$ dilution technique and isotope pairing. *Applied and Environmental Microbiology* **59**, 2093-2098.

Svensson, J.M., 1998. Emission of $N_2O$, nitrification and denitrification in a eutrophic lake sediment bioturbated by *Chironomus plumosus*. *Aquatic Microbial Ecology* **14**, 289-299.

Ueda, S., Ogura, N. and Yoshinari, T., 1993. Accumulation of nitrous oxide in aerobic ground water. *Water Research* **27**, 1787-1792.

www.cia.gov/cia/publications/factbook/geos/zn.html

Yoshida, N. and Toyoda, S., 2000. Constraining the atmospheric $N_2O$ budget from intramolecular site preference in $N_2O$ isotopomers. *Nature* **405**, 330-334.

## 4. Methane

### Methane concentration and stable isotopic distribution as indicators of biogenic methane dynamics in the central North Pacific and East Chine Sea

Osamu YOSHIDA, Narin BOONTANON, Ayako FUJII, and Naohiro YOSHIDA
Tokyo Institute of Technology Group (Yoshida's Lab)

*4.1. Introduction*

Atmospheric methane ($CH_4$) is a trace gas playing an important role in the global carbon cycle as a greenhouse gas. Its concentration has increased by about 1050 ppbv from 700 ppbv since the pre-industrial era (IPCC, 1995). In order to understand the current global methane cycle, it is necessary to quantify its sources and sinks. At present, there remain large uncertainties in the estimated methane fluxes from sources to sinks. The ocean's source strength for atmospheric methane should be examined in more detail, even though it might be a relatively minor source, previously reported to be 0.005 to 3% of the total input to the atmosphere (Cicerone and Oremland, 1988; Bange et al., 1994).

To estimate an accurate amount of the methane exchange from the ocean to the atmosphere, it is necessary to explore widely and vertically. Distribution of dissolved methane in surface waters from diverse locations in the world ocean is often reported as a characteristic subsurface maximum representing a supersaturation of several folds (Yoshida et al., 2004). Although the origin of the subsurface methane maximum is not clear, some suggestions include advection and/or diffusion from local anoxic environment nearby sources in shelf sediments, and in situ production by methanogenic bacteria, presumably in association with suspended particulate materials (Karl and Tilbrook, 1994). These bacteria are thought to probably live in the anaerobic microenvironments supplied by organic particles or guts of zooplankton (Alldredge and Cohen, 1987).

So, this study investigates in detail profile of methane concentration and stable isotopic distribution in the water column in the central North Pacific as open ocean and the East China Sea as coastal region to clarify methane dynamics and estimate the flux of methane to the atmosphere.

*4.2. Materials and methods*

Seawater samples are taken by CTD-CAROUSEL system attached Niskin samplers of 12 L at 5-25 layers and surface layer taken by plastic bucket at 13-35 hydrographic stations as shown in Table 1. Each sample was carefully subsampled into 30, 125, 600 mL glass vials to avoid air contamination for analysis of methane concentration, carbon isotope ratio, and hydrogen isotope ratio respectively. The seawater samples were poisoned by 20 μL (30 and 125 mL vials) or 100 μL (600 mL vial) of mercuric chloride solution (Tilbrook and Karl, 1995; Watanabe et al., 1995), and were closed with rubber and aluminum caps. These were stored in a dark and cool place until we got to land, where we conducted gas

chromatographic analysis of methane concentration and mass spectrometric analysis of carbon and hydrogen isotopic composition at the laboratory.

The analytical method briefly described here: The system consists of a purge and trap unit, a desiccant unit, rotary valves, a gas chromatograph equipped with a flame ionization detector for concentration of methane, GC/C/IRMS for carbon isotope ratio of methane, GC/TC/IRMS for hydrogen isotope ratio of methane, and data acquisition units. The entire volume of seawater in each glass vial was processed all at once to avoid contamination and loss of methane. Precision obtained from replicate determinations of methane concentration was estimated to be better than 5% for the usual concentration of methane in seawater.

Seawater samples for incubation experiment of methane are taken at 10, 150, 200, 250 m depths which expected as subsurface maxima related to in situ methane production at hydrographic station 3, 28, 42, 71, 96. To address the effect of the methane produced within particles, one was subsampled into 125 mL glass vial directly to avoid air contamination, another was through the filter. The samples were closed with rubber and aluminum caps and stored in a dark and cool place for 2-6 days. After finished the incubation, the samples were poisoned by 20 μL of mercuric chloride solution, closed caps, and stored as well as bottle sampling.

*4.3. Expected results*

Subsurface maximum concentrations of methane (>3 nmol $kg^{-1}$) were expected to be observed in the central North Pacific. A commonly-encountered distribution in the upper ocean with a methane peak within the pycnocline (e.g., Ward et al., 1987; Owens et al., 1991; Watanabe et al., 1995). Karl and Tilbrook (1994) suggested the suboxic conditions would further aid the development of microenvironments within particles in which methane could be produced. The organic particles are accumulated in the pycnocline, and methane produced in the micro reducing environment by methanogenic bacteria. Moreover, in situ microbial methane production in the guts of zooplankton can be expected (e.g., Owens et al., 1991; de Angelis and Lee, 1994; Oudot et al., 2002). Watanabe et al. (1995) pointed out that the diffusive flux of methane from subsurface maxima to air-sea interface is sufficient to account for its emission flux to the atmosphere. In the mixed layer above its boundary, the methane is formed and discharged into the atmosphere in part, in the below its boundary, methane diffused to the bottom vertically. By using concentration and isotopic composition of methane and hydrographic parameters for vertical water samples and incubation experiment, it is possible to clarify its dynamics such as production and/or consumption in the water column.

Kelley and Jeffrey (2002) observed in the equatorial upwelling region of 10 and 20% supersaturated methane. Rehder et al. (2002) reported that the enhancement of methane fluxes to the atmosphere in regions of coastal upwelling is likely to occur on a global scale. In this study, the combination of in situ methane production and coastal upwelling result in the property distributions and large methane flux in the eastern North Pacific can be expected.

Tsurushima et al. (1996) reported that methane flux in the East China Sea was somewhat larger than the oceanic usual values. Remarkable supersaturation in coastal regions, including continental shelf zones, has been expected related to biological productivity, advection from nearby sources in shelf sediments, and diffusion and/or advection from local anoxic environments.

*4.4. References*

Alldredge, A. A., Y. Cohen, Can microscale chemical patches persist in the sea? Microelectrode study of

marine snow, fecal pellets, Science, 235, 689-691, 1987.
Bange, H. W., U. H. Bartell, S. Rapsomanikis, and M. O. Andreae, Methane in the Baltic and the North seas and a reassessment of the marine emissions of methane, Global Biogeochem. Cycles, 8, 465–480, 1994.
Cicerone, R. J., and R. S. Oremland, Biogeochemical aspects of atmospheric methane, Global Biogeochem. Cycles, 2, 299–327, 1988.
de Angelis, M. A., and C. Lee, Methane production during zooplankton grazing on marine phytoplankton, Limnol. Oceanogr., 39, 1298-1308, 1994.
IPCC (Intergovernmental Panel on Climate Change), Climate Change 1995, in The Science of Climate Change, edited by J. T. Houghton, L. G. M. Filho, B. A. Callander, N. Harris, A. Kattenberg, and K. Maskell, Cambridge Univ. Press, New York, 1995.
Karl, D. M., and B. D. Tilbrook, Production and transport of methane in oceanic particulate organic matter, Nature, 368, 732–734, 1994.
Kelley C. A. and Jeffrey, W. H. 2002. Dissolved methane concentration profiles and air-sea fluxes from 41S to 27N. Global. Biogeochem. Cycle, 16, No.3, 10.1029/2001GB001809.
Oudot, C., P. Jean-Baptiste, E. Fourre, C. Mormiche, M. Guevel, J-F. Ternon, and P. L. Corre, Transatlantic equatorial distribution of nitrous oxide and methane, Deep-Sea Res., Part I 49, 1175–1193, 2002.
Owens, N. J. P., C. S. Law, R. F. C. Mantoura, P. H. Burkill, and C. A. Llewellyn, Methane flux to the atmosphere from the Arabian Sea, Nature, 354, 293–296, 1991.
Rehder, G., R. W. Collier, K. Heeschen, P. M. Kosro, J. Barth, and E. Suess, Enhanced marine CH4 emissions to the atmosphere off Oregon caused by coastal upwelling, Global Biogeochem. Cycles, 16, 10.1029/2000GB001391, 2002.
Tilbrook, B. D., and D. M. Karl, Methane sources, distributions and sinks from California coastal waters to the oligotrophic North Pacific gyre, Mar. Chem., 49, 51–64, 1995.
Tsurushima, N., S. Watanabe, N. Higashitani, and S. Tsunogai, Methane in the East China Sea water, J. Oceanogr., 52, 221–233, 1996.
Ward, B. B., K. A. Kilpatrick, P. C. Novelli, and M. I. Scranton, Methane oxidation and methane fluxes in the ocean surface layer and deep anoxic waters, Nature, 327, 226–229, 1987.
Watanabe, S., N. Higashitani, N. Tsurushima, and S. Tsunogai, Methane in the western North Pacific, J. Oceanogr., 51, 39–60, 1995.
Yoshida, O., H. Y. Inoue , S. Watanabe, S. Noriki, M. Wakatsuchi, Methane in the western part of the Sea of Okhotsk in 1998-2000, J. Geophys. Res., 109, C09S12, doi:10.1029/2003JC001910, 2004.

### 3.7.4 Volatile Organic Compounds

(1) Personnel

Yoko Yokouchi (National Institute for Environmental Studies)

(2) Objectives

To know the distribution of volatile organic compounds emitted from marine biota.

(3) Measured compounds

- Bromoform
- Dibromomethane
- Methyl iodide
- Methyl chloride
- Methyl bromide
- Dimethyl sulfide
- Carbonyl sulfide
- Isoprene

(4) Methods

Air samples are taken on board forward of any potential contamination from the stack, at the front of the uppermost deck on the Mirai. Samples are collected once a day (during the daytime). Evacuated 6-L stainless steel canisters with inert surfaces were used for the collection.

Samples will be analyzed using a preconcentration/capillary gas chromatographic/mass spectrometer (GC/MS) after the cruise.

**Sampling Time and Position**

| Time (UTC) | | Latitude | Longitude |
|---|---|---|---|
| 2005/10/31 | 22:55 | 32°36.47'N | 117°32.46'W |
| 2005/11/1 | 22:17 | 32°07.15'N | 118°47.96'W |
| 2005/11/2 | 22:12 | 31°05.71'N | 120°47,90'W |
| 2005/11/3 | 21:50 | 29°29.76'N | 123°18.68'W |
| 2005/11/4 | 22:29 | 27°33.67'N | 125°49.78'W |
| 2005/11/5 | 2:56 | 25°41.36'N | 128°12.76'W |
| 2005/11/6 | 22:12 | 24°15.32'N | 130°36.36'W |
| 2005/11/7 | 22:25 | 24°14.74'N | 133°26.51'W |
| 2005/11/8 | 22:37 | 24°14.82'N | 136°27.46'W |
| 2005/11/9 | 23:38 | 24°14.73'N | 139°37.42'W |
| 2005/11/10 | 23:06 | 24°12.87'N | 140°44.18'W |
| 2005/11/11 | 23:09 | 24°16.43'N | 141°52.06'W |
| 2005/11/12 | 22:35 | 24°14.64'N | 144°48.26'W |
| 2005/11/13 | 23:38 | 24°15.51'N | 147°41.78'W |
| 2005/11/14 | 22:48 | 24°15.96'N | 149°54.21'W |
| 2005/11/15 | 23:22 | 24°16.31'N | 152°38.34'W |
| 2005/11/16 | 22:34 | 24°17.26'N | 155°16.69'W |
| 2005/11/17 | 22:16 | 24°36.84'N | 157°43.75'W |
| 2005/11/18 | 21:52 | 25°50.09'N | 160°26.07'W |
| 2005/11/19 | 22:46 | 25°08.43'N | 161°59.92'W |
| 2005/11/20 | 21:46 | 25°29.93'N | 164°16.31'W |
| 2005/11/21 | 23:49 | 24°40.67'N | 166°33.59'W |
| 2005/11/22 | 23:13 | 22°18.32'N | 165°17.27'W |
| 2005/11/23 | 21:36 | 20°37.03'N | 161°10.17'W |
| 2005/11/30 | 0:19 | 24°39.48'N | 166°19.81'W |
| 2005/12/1 | 0:12 | 24°16.06'N | 167°1.8'W |
| 2005/12/2 | 0:19 | 23°39.5'N | 167°34.58'W |
| 2005/12/2 | 23:31 | 22°45.4'N | 169°19.39'W |
| 2005/12/4 | 0:18 | 23°50.28'N | 171°41.88'W |
| 2005/12/5 | 0:16 | 24°14.49'N | 174°20.96'W |
| 2005/12/6 | 0:32 | 24°14.38'N | 176°45.57'W |
| 2005/12/7 | 0:24 | 24°14.38'N | 179°9.53'W |
| 2005/12/8 | 0:19 | 24°7.77'N | 179°27'E |
| 2005/12/9 | 0:57 | 24°14.71'N | 178°23.22'E |
| 2005/12/10 | 1:02 | 24°15.28'N | 175°59.64'E |
| 2005/12/11 | 1:17 | 24°14.89'N | 173°33.7'E |
| 2005/12/13 | 0:39 | 18°46.87'N | 172°42.04'E |
| 2005/12/14 | 1:08 | 16°11.08'N | 171°59.1'E |
| 2005/12/15 | 0:37 | 14°43.91'N | 170°58.72'E |
| 2005/12/16 | 1:03 | 13°10.24'N | 170°23.96'E |

## 3.7.5 Colon Bacillus and General Bacteria

27-Jan.-2006

### 3.7.1.1 Personnel

Masaaki TAMAYAMA [1)], Kunihiko WATANUKI [2)], Shinya KAKUTA [3)]

1) Japan Macro-Engineers' Society (JAMES)

2) Rissho University

3) Japan Agency for Marine Earth Science and Technology

### 3.7.1.2 Objective and Methods

Seawater was sampled by CTD and surface pump onboard R/V MIRAI MR05-05-Leg3 in January 20 to 28, 2006. Numbers of samples of CTD and surface pump are 315 and 33, respectively. Nothing was sampled in the Korean EEZ.

The purpose of this study is to investigate distributions of colon bacillus and general bacteria or various kinds of minor germs in seawater. The origin of the idea came from our study on pollution of the Yellow River in China. The river is well polluted from the upper to down stream. The fact is reported in the official annual report by Chinese Agency of Environment. We have being discussed to find a rather simple method to reveal polluted state of river water than COD or BOD analysis. We tried a method developed for the food industry by Nippon Bacteria Analysis Co., Ltd for our purpose and found that it might be applicable and useful.

Part of our study is shown in the following table (Table 3.7.5-1). Locations in the table is listed from upper to down stream. According to eye observation the stream of Qin irrigation duct is clean and clear. The duct was built in the era of Qin Dynasty in the 3$^{rd}$ century BC and people still use it. It shows least distributions of Colon bacillus and general bacteria. On the other hand, the final outlet duct built in the 20$^{th}$ century in the northern edge of Hetao plain is worst ever and its data reflects that condition. We might see and understand such distributions in seawater to some extents.

The analytical method is simple but time required for colon bacillus and general bacteria is 24 and 48 hours, respectively. It is shorter than BOD analysis.

We plan to report a short note at the BLUE EARTH Symposium 2006 on February 22 and 23, 2006. We have a limited time for sample analysis, so consider to analyze running surface samples that cover a wide span of the leg3 rather than those obtained by the CTD sampler.

Table 3.7.5-1 Distributions of Colon Bacillus and General Bacteria along with the Yellow River, Ningxiahuizu to Neimenggu Zizhiqu in September 2004

| River | Location | Colon bacillus Number/gram | General bacteria Number/gram |
|---|---|---|---|
| Yellow River | Zhongwei Shi | 55 | 9000 |
| Yellow River | Qindongxia Shi | 0 | 17000 |
| Qin irrigation duct | Yinchuan Shi | 0 | 4000 |
| Tanglai irrigation duct | Yinchuan Shi | 15 | 5100 |
| Yellow River | Shizishan Shi | 555 | 14400 |
| Yellow River | Sanshenggong dam | 25 | 4900 |
| Final outlet duct | Linhe Shi | 10 | More than 155000 |
| Wuliangsuhai (Lake) | Bayannaoer Shi | 30 | More than 80000 |
| Yellow River | Baotou Bridge | 35 | 8700 |

Acknowledgement

My appreciation shall be extended to all staff of the research crew onboard. Their sampling is excellent, steady and reliable.

## 3.8 LADCP(Lowered Acoustic Doppler Current Profiler)

### 3.8.1 Personnel

***Shinya Kouketsu***

***Ikuo Kaneko***

***Shuichi Watanabe***

***Hiroshi Uchida***

***Takayoshi Seike***

### 3.8.2 Instrument and method

Direct flow measurement from sea surface to the bottom was carried out using a lowered acoustic Doppler current profiler (LADCP). The instrument was the RDI Workhorse Monitor 307.2kHz unit (RD Instruments, USA). The instrument was attached on the CTD/RMS frame, orientating downward. The CPU firmware version was 16.27.

One ping raw data were recorded. From St. 1 to St. 48, a bin length was set to 16m. The bin length of 8m was used from St. 50. A total of 79, 126 and 31 operations were made with the CTD observations in Leg 1 from San Diego to Honolulu, Leg2 from Honolulu to Nakagusuku, and Leg3 from Nakagusuku to Sekinehama respectively. Since the pressure resistance of the instrument is 6500dbar, the instrument was detached on the CTD/RMS frame at St. 223, 293, 353 and 357 where the depth was deeper than about 6000dbar. The performance of the LADCP instrument was not good from St. 1 to St. 110 in Leg1. The data near bottom were often missed. We changed the instruments from Serial Number (SN) 2553 to SN 1512 from St. 112. The performance was improved. Profiles were obtained over 100m distance from LADCP in shallow depth and almost 60m in deeper depth.

Echo intensity was weak from station 351 to 367. Backscatters might be especially too few in this section.

### 3.8.3 Preliminary results

An inversion method of processing LADCP data in Visbeck (2002) was adopted. GPS navigation data and bottom-track velocities were used for the calculation of constraints. CTD data were used for the sound speed and depth calculation. Shipboard ADCP data are not included in the calculation.

Figures from 3.8.1 to 3.8.6 show the cross-section (left) and error velocity (right) fields for Leg1, Leg2, the Wake passage, the Okinawa trough, Tokara strait, and Tsushima strait respectively. There are not intense currents in Leg1 and Leg2. Error velocities estimated by the inversion are small values of 0.05 – 0.2m/s, but the typical value of the surface currents is about 0.2m/s in this section. It may be difficult to describe the detailed structure of currents. In Leg3 (Okinawa trough, Tokara strait, and Tsushima strait cross sections), small error velocities (less than 10cm/s) are estimated.

Velocities using bottom tracks are shown in Figures 3.8.7 (Leg1) and 3.8.8 (Leg2). Typical values of the bottom current were 5 – 10cm/s. The large bottom flow of about 15cm/s was observed near

the shore of the United States. The errors of 0.5 - 2 cm/s are quite small. It is sufficient to detect the bottom current. The velocities near the bottom are not shown in Leg3, since the depths are shallow and the inversion errors are sufficient small all through the water columns.

**Reference**

Visbeck, M. (2002): Deep velocity profiling using Lowered Acoustic Doppler Current Profilers: Bottom track and inverse solutions. *J. Atmos. Oceanic Technol.*, 19, 794-807.

**Figure 3.8.1**

Leg1

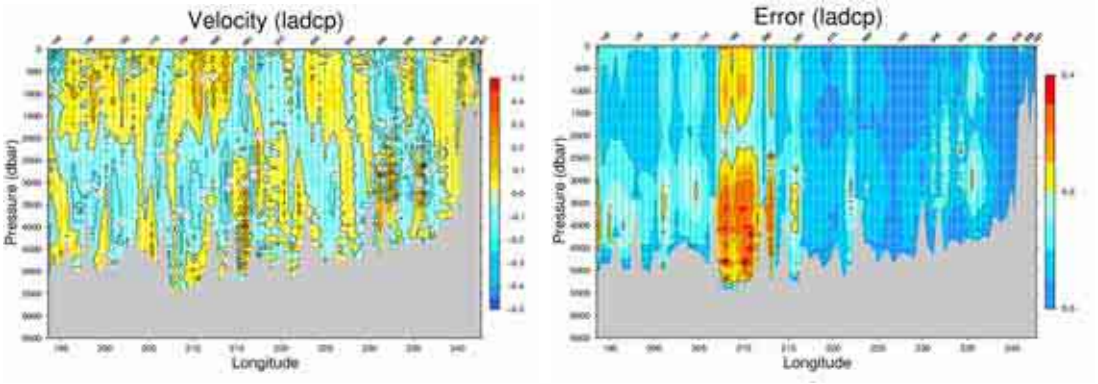


**Figure 3.8.2**

Leg2

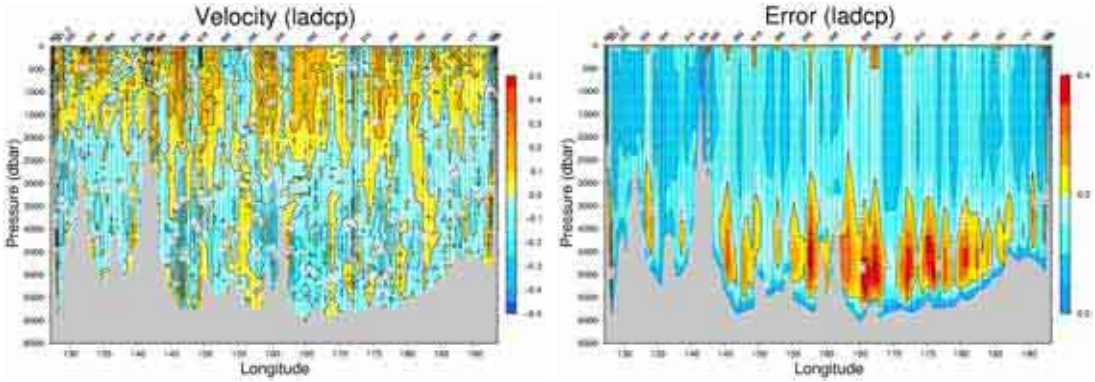


**Figure 3.8.3**

Wake Passage

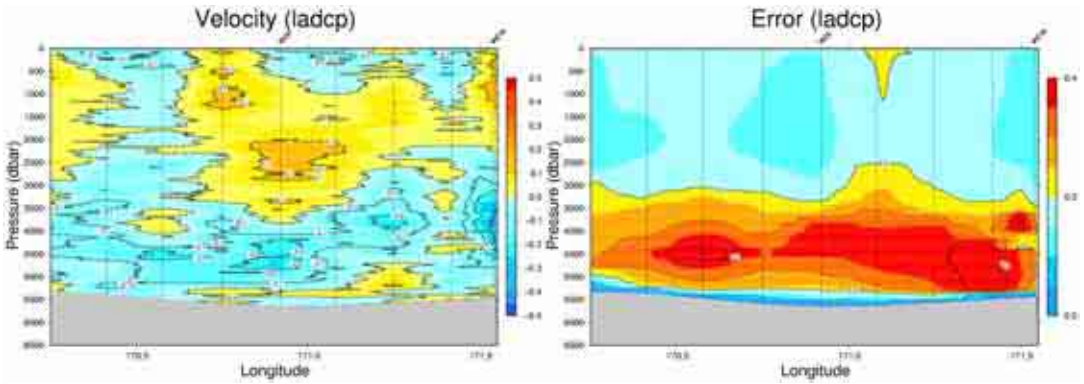

**Figure 3.8.4**

Okinawa Trough

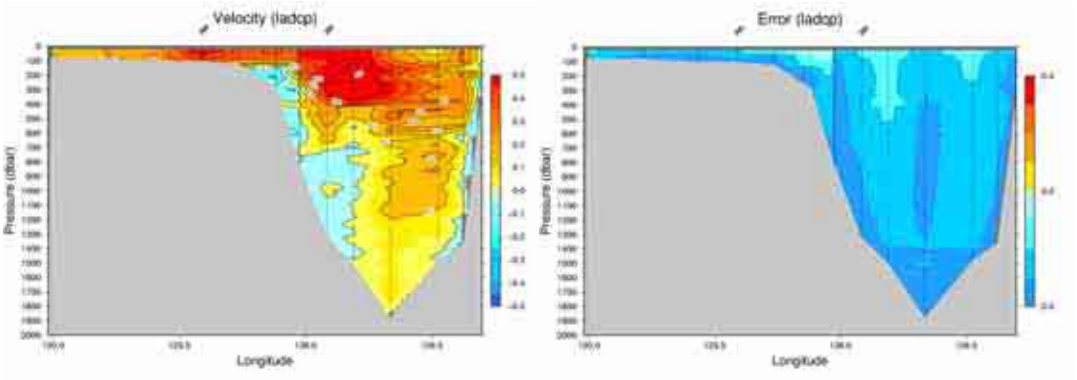


**Figure 3.8.5**

Tokara strait

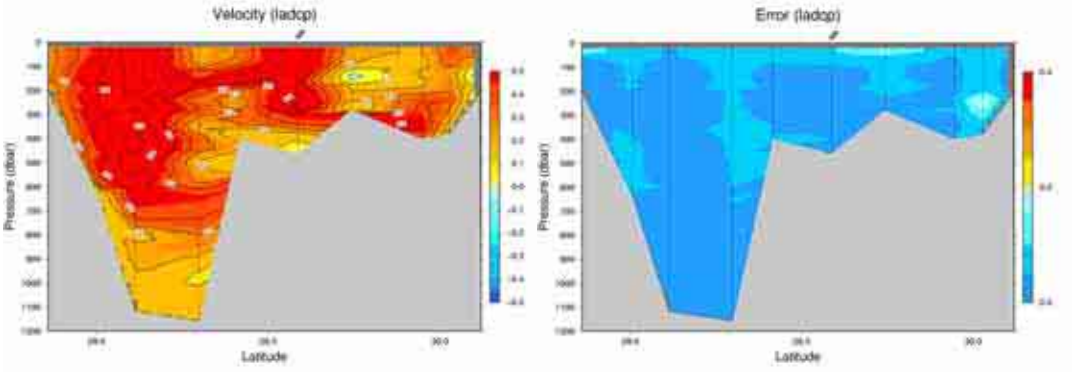


**Figure 3.8.6**

Tsushima strait

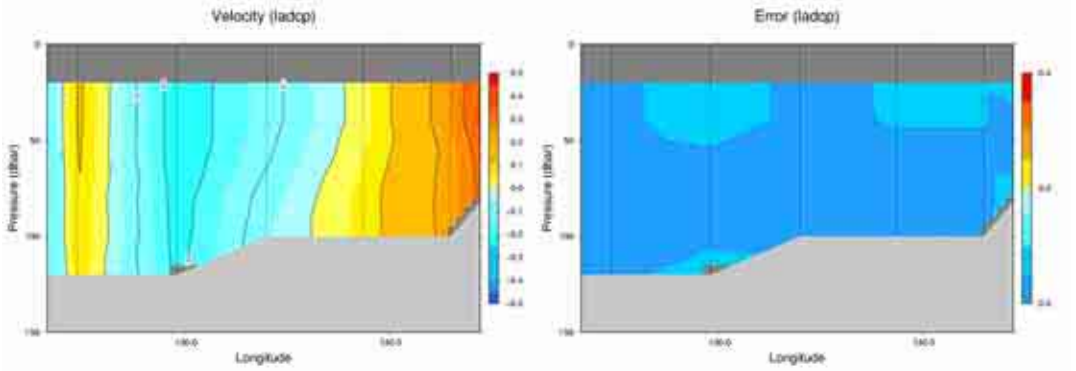

**Figure 3.8.7**

Leg1

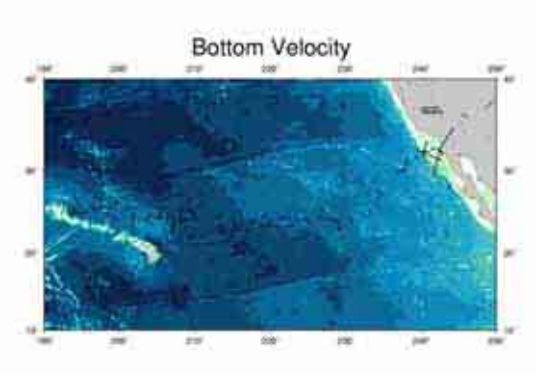


**Figure 3.8.8**

Leg2

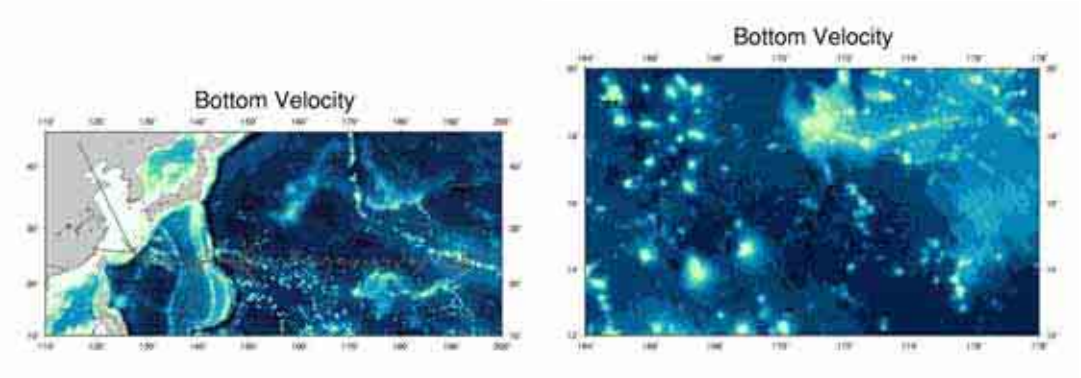

## 4.1 Argo floats

### 4.1.1 Personnel

| | |
|---|---|
| ***Nobuyuki Shikama*** | (IORGC): Principal Investigator (not on board) |
| ***Hiromichi Ueno*** | (IORGC): not on board |
| ***Mizue Hirano*** | (IORGC): not on board |
| ***Satoshi Ozawa*** | (MWJ): Technical Staff |

### 4.1.2 Objectives

The objective of deployment is to clarify the structure and temporal/spatial variability of water masses in the North Pacific such as the North Pacific Tropical Water.

The profiling floats launched in this cruise measure vertical profiles of temperature and salinity automatically every ten days. The data from the floats will enable us to understand the phenomenon mentioned above with time/spatial scales much smaller than in previous studies.

### 4.1.3 Parameters

- water temperature, salinity, and pressure

### 4.1.4 Methods

#### 4.1.4.1 Profiling float deployment

We launched an APEX float manufactured by Webb Research Ltd. These floats are equipped with an SBE41 CTD sensor manufactured by Sea-Bird Electronics Inc.

The floats usually drift at a depth of 1000 dbar (called the parking depth), diving to a depth of 2000 dbar and rising up to the sea surface by decreasing and increasing their volume and thus changing the buoyancy in ten-day cycles. During the ascent, they measure temperature, salinity, and pressure. They stay at the sea surface for approximately nine hours, transmitting the CTD data to the land via the ARGOS system, and then return to the parking depth by decreasing volume. The status of floats and their launches are shown in Table 4.1-1.

### 4.1.5 Data archive

The real-time data are provided to meteorological organizations, research institutes, and universities via Global Data Assembly Center (GDAC: http://www.usgodae.org/argo/argo.html, http://www.coriolis.eu.org/) and Global Telecommunication System (GTS), and utilized for analysis and forecasts of sea conditions.

Table 4.1-1 Status of floats and their launches
Float

| | |
|---|---|
| Float Type | APEX floats manufactured by Webb Research Ltd. |
| CTD sensor | SBE41 manufactured by Sea-Bird Electronics Inc. |
| Cycle | 10 days (approximately 9 hours at the sea surface) |
| ARGOS transmit interval | 30 sec |
| Target Parking Pressure | 1000 dbar |
| Sampling layers | 110 (1950, 1900, 1850, 1800, 1750, 1700, 1650, 1600, 1550, 1500, 1450, 1400, 1350, 1300, 1250, 1200, 1150, 1100, 1050, 1000, 975, 950, 925, 900, 875, 850, 825, 800, 775, 750, 725, 700, 675, 650, 625, 600, 580, 560, 540, 520, 500, 490, 480, 470, 460, 450, 440, 430, 420, 410, 400, 390, 380, 370, 360, 350, 340, 330, 320, 310, 300, 290, 280, 270, 260, 250, 240, 230, 220, 210, 200, 195, 190, 185, 180, 175, 170, 165, 160, 155, 150, 145, 140, 135, 130, 125, 120, 115, 110, 105, 100, 95, 90, 85, 80, 75, 70, 65, 60, 55, 50, 45, 40, 35, 30, 25, 20, 15, 10, 4 dbar) |

Launches

| Float S/N | ARGOS PTT ID | Date and Time of Reset (UTC) | Date and Time of Launch (UTC) | Location of Launch | CTD St. No. |
|---|---|---|---|---|---|
| 2296 | 60094 | 2006/01/03 07:32 | 2006/01/03 09:22 | 24-14.25N 144-12.65E | P03-291 |

# 4.2 Moorings

## Wake Island passage Flux Experiment *(17 February 2006)*

***Hiroshi Uchida, Hirofumi Yamamoto, Masao Fukasawa, Ikuo Kaneko (JAMSTEC), Satoshi Ozawa, Hirokatsu Uno, Akinori Murata, Hiroki Ushiromura, Shinsuke Toyoda, Tomoyuki Takamori (MWJ), Shinya Okumura, Yasutaka Imai and Ryo Ohyama (GODI)***

### 4.2.1 Mooring observation

Wake Island passage Flux Experiment (WIFE) mooring array was designed to observe Lower Circumpolar Deep Water (LCDW) flowing into the Northwest Pacific Basin from the Central Pacific Basin. Near the Wake Island Passage five deep moorings were placed along a transect of a deep passage (Fig. 4.2.1.1). WIFE started in May 2003. Five moorings were deployed at R/V Mirai cruise MR03-K02 in May 2003 for the first mooring period. The moorings were recovered and re-deployed at R/V Hakuho-maru cruise KH04-4 Leg2 in October 2004 for the second mooring period. The moorings of the second period were recovered in this cruise and WIFE observation was finished.

For temperature and salinity measurements, high-accuracy conductivity and temperature with optional pressure recorders, the SBE 37-SM MicroCAT (Sea-Bird Electronics, Inc., USA), are used. For current measurements, 2 types of current meters are used. For 3,400 and 4,400 m layers, acoustic Doppler current meters, RCM 11 (Aanderaa Instruments, NORWAY), are used. The RCM 11 measure current in the area from 0.4 to 2.2 meters from the instrument which minimizes the effect of marine fouling and local turbulence. For the 5,400 m layer, current meters, RCM 8 (Aanderaa Instruments, NORWAY), are used. The RCM 8 consists of two main parts, the vane assembly and the recording unit

with a rotor.

In order to detect top depth of the mooring line from ship, acoustic transponders, 10-inch XT-6000 (Benthos, Inc., USA), are used. In order to recover the moorings as securely as possible, two (parallel) acoustic releasers, Model L and/or LII (Nichiyu Giken Kogyo Co., Ltd., JAPAN), are used for each mooring. The releaser applies Gas-Generation mechanism to free a hock.

Setup parameters and maximum operating life of the WIFE moored instruments are summarized in Table 4.2.1.1. Operating life time of the Aanderaa's current meter is depend on the storage capacity of the Data Storing Unit (DSU). DSU 2990E (262,100 10-bit words) is used for all RCM-11 and RCM-8.

After recovery of the all moorings high-quality $CTDO_2$/RMS measurements with LADCP were conducted (Fig. 4.2.1.2). Water sampling parameters are salinity, oxygen and nutrients. Detail of the bathymetry along observation line was measured by the multi narrow beam of R/V Mirai (Fig. 4.2.1.2).

Detail of the WIFE mooring system with serial numbers of the instruments is shown in Figure 4.2.1.3.

**Table 4.2.1.1. Setup parameters for the moored instrumetns.**

| ***Instrument*** | ***Sampling Interval*** | ***Sampling Rate (Mode)*** | ***Averaging Time*** | ***Maximum Operating Life*** |
|---|---|---|---|---|
| SBE 37-SM | 30 minutes | one sample | - | > 2.5 years |
| RCM-11 | 60 minutes | 2.5 Hz (Burst) | 60 seconds | 2.3 years |
| RCM-8 | 60 minutes | 50/3600 Hz | 60 minutes | 2.3 years |
| Compact-OPTODE | 60 minutes | 1 Hz (Burst) | 10 seconds | 1.6 years |

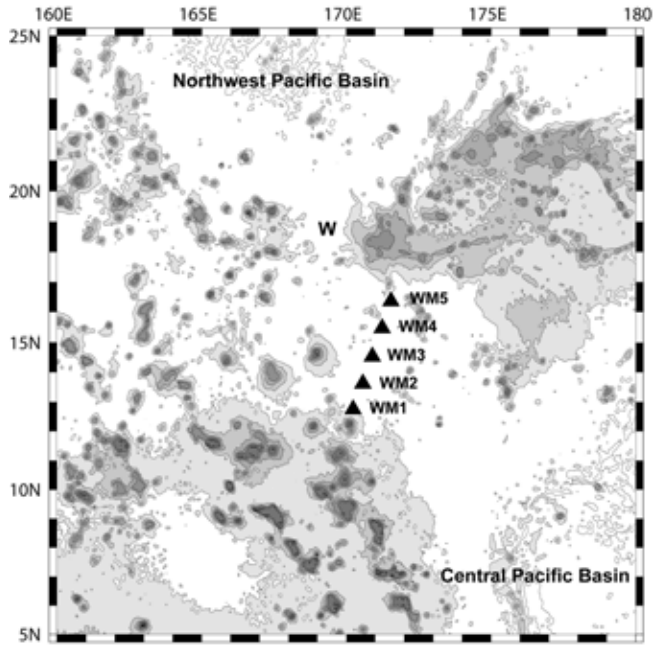


**Figure 4.2.1.1. Mooring station locations with bathymetry. Contour interval of the bathymetry is 1 km and area shallower than 5 km is shaded. A letter "W" shows location of Wake Island deep passage.**

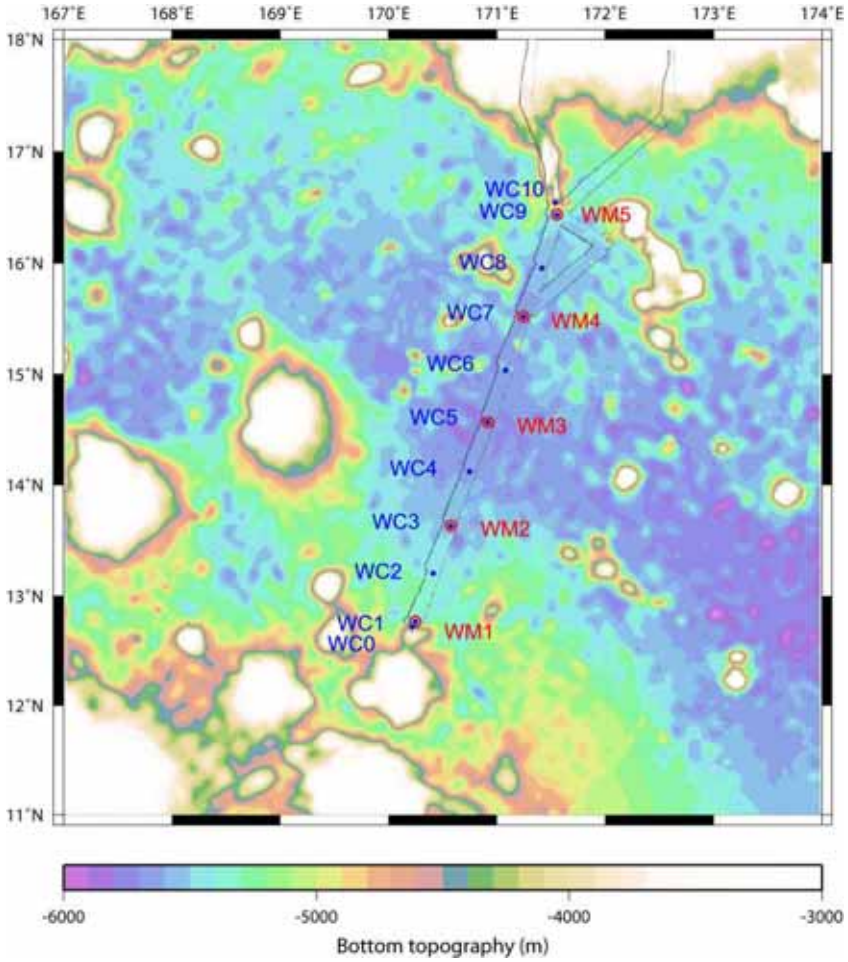


**Figure 4.2.1.2. Detail of bathymetry based on Smith and Sandwell (1997). Bathymetry derived from multi narrow beam data obtained in this cruise is superimposed. Location of mooring stations (WM) and CTD/RMS/LADCP stations (WC) are also shown.**

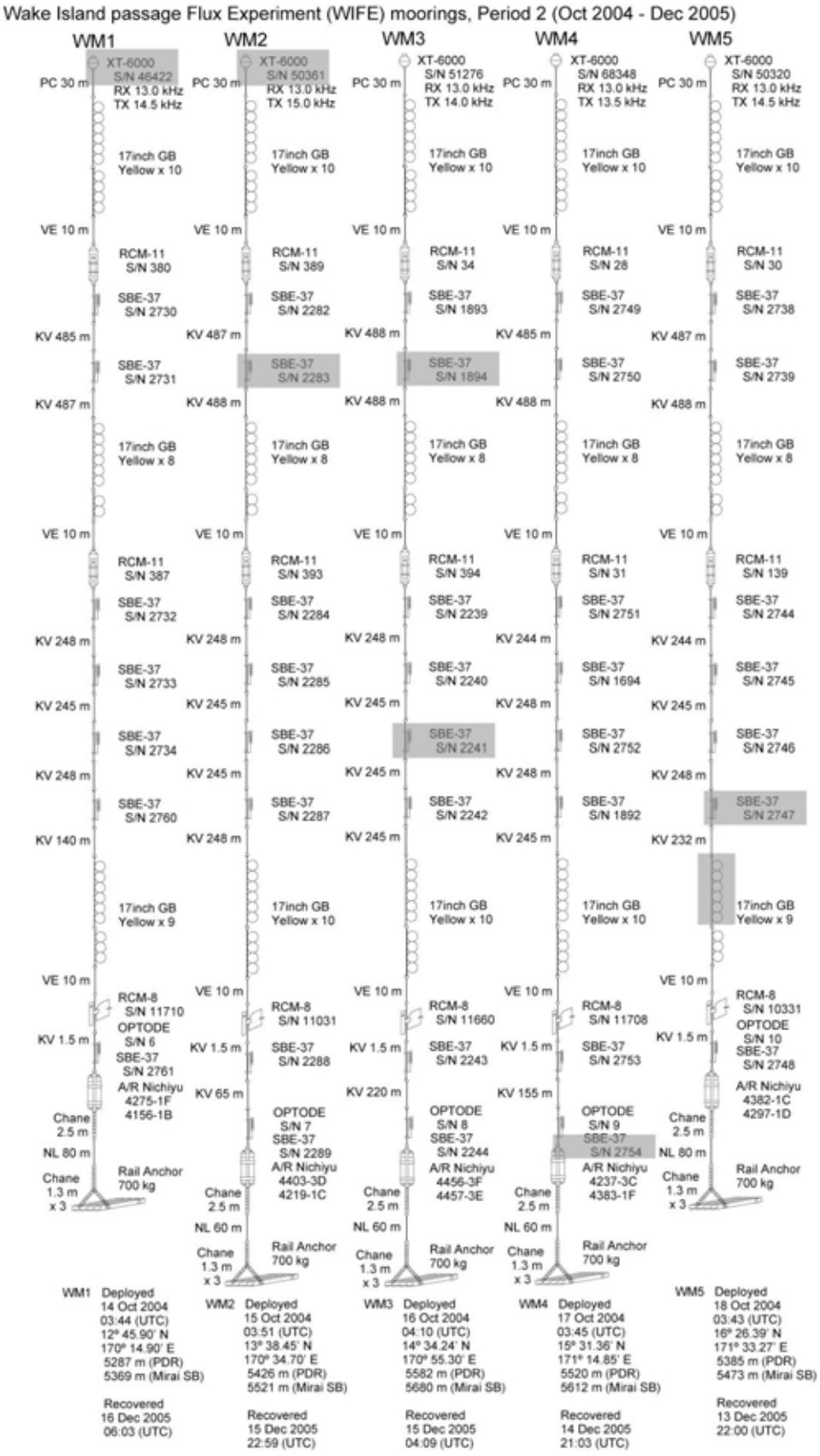


Figure 4.2.1.3. WIFE mooring system. Leaked or broken instruments are shaded.

**4.2.2 Recovery**

The five moorings were recovered safely. Date and time of the recovery are listed in SUM (station summary) file and shown in Figure 4.2.1.3. Before the recovery of the each mooring, the precise location of the mooring was determined by the transponder of the mooring using acoustic navigation system on the R/V Mirai. Determined locations are listed in Table 4.2.2.1. Unfortunately precise location of the mooring WM1 and WM2 could not be determined due to leaking of the transponders.

At station WM5, 6 grass buoys were broken. The buoys were broken at between 20:00 and 20:30, 22 March 2005. The time was estimated from CTD pressure data of WM5.

Five CTDs (S/N 1894, 2241, 2283, 2747 and 2754) shown in Figure 4.2.1.3 leaked and the data could not be recovered from the CTDs. Hole size of the wire guard may not large enough compared to the wire. One CTD (S/N 2282) also leaked a little. After cleaning inside the instrument and replacing the battery, the data could be recovered except for the data of the last 4 hours. After the recovery of the data from S/N 2282, the end cap of the CTD was changed to the end cap of S/N 2748 for in-situ calibration of the CTD.

Fourteen CTDs (S/N 1694, 1892, 1893, 2239, 2240, 2242, 2282, 2284, 2285, 2286, 2289, 2730, 2733 and 2739) suffered from a manufacturing defect of Druck pressure sensor. Conductivity data may be affected by the defect even if the pressure data is replaced to some reliable value.

Six CTDs (S/N 2243, 2244, 2287, 2288, 2738 and 2760) showed large time drift of pressure sensor.

A rotor of RCM-8 current meter S/N 11031 was lost at the recovery of the mooring.

Pressure data were bad for RCM-8 current meter S/N 11031 and RCM-11 current meter S/N 31.

For all oxygen sensors (Compact-OPTODE), measurements were stopped at 23:00, 30 December 2005 due to manufacturing defect of firmware of the Compact-OPTODE.

Table 4.2.2.1. Location of the moorings determined using acoustic navigation system. Locations of WM2 and WM1 could not be determined by acoustic navigation system due to leaking of the transponder. Depth of the location is derived from multi narrow beam bathymetry data obtained in this cruise.

| Station | Latitude | Longitude | Depth (m) |
|---|---|---|---|
| WM5 | 16° 26.18’ N | 171° 33.21’ E | 5477 |
| WM4 | 15° 31.19’ N | 171° 14.69’ E | 5616 |
| WM3 | 14° 34.14’ N | 170° 55.21’ E | 5680 |
| WM2 | (13° 38.45’ N) | (170° 34.70’ E) | 5522 |
| WM1 | (12° 45.90’ N) | (170° 14.90’ E) | 5378 |

### 4.2.3 In-situ calibration of moored instruments

The moored CTDs (SBE-37SM) and moored oxygen sensors (optode) were attached to water sampling frame at a CTD/RMS cast after the recovery for their in-situ calibration (Fig. 4.2.3.1). The CTD/RMS casts for the in-situ calibration are listed in Table 4.2.3.1. By comparing with the in-situ accurate $CTDO_2$ data, the moored CTD and oxygen data are going to be calibrated. For the in-situ calibration, sampling interval of the moored CTD and oxygen sensor was set to 6 seconds and 1 second, respectively.


**Figure 4.2.3.1. Photos of the moored CTDs and oxygen sensors attached to the CTD/RMS frame.**

Table 4.2.3.1. In-situ post-recovery calibration of moored CTDs and oxygen sensors (optode).

| Moored instruments (Station) | In-situ calibration date | CTD station |
|---|---|---|
| *SBE-37SM* | | |
| S/N 2730-2734, 2760, 2761 (WM1) | 16 December 2005 | WC1 |
| S/N 2738, 2739, 2744-2746, 2748 (WM5) | 17 December 2005 | WC3 |
| S/N 1694, 1892, 2749-2753 (WM4) | 17 December 2005 | WC4 |
| S/N 1893, 2239, 2240, 2242-2244 (WM3) | 17 December 2005 | WC5 |
| S/N 2282*, 2284-2289 (WM2) | 18 December 2005 | WC7 |
| *OPTODE* | | |
| S/N 6-10 (WM1-5) | 18 December 2005 | WC8 |

* The in-situ calibration data could not be obtained from S/N 2282 due to leaking during the CTD cast.

### References

Smith, W.H.F. and D.T. Sandwell (1997): Global seafloor topography from satellite altimetry and ship depth soundings, Science, 277, 1956-1962.